CRANFIELD UNIVERSITY
Cranfield Health
Department of Analytical Science and Informatics

Helen Trill

Diagnostic Technologies for Wound Monitoring

Supervisors: S.Setford & S.Saini
This thesis is submitted for the degree of Doctor of Philosophy
March 2006

Abstract

Chronic wound infections represent a worldwide problem, generating high morbidity and medical expense. Failure to control infections such as MRSA in the reparative process of a wound can cause disruption of normal anatomical structure and function, resulting in a chronic wound. Existing approaches to identifying infection largely involve surveying a range of physical parameters, and a limited use of non-invasive technologies. Evaluation is time consuming, and often results in inconsistencies in patient care.

This project researches three possible alternative methodologies/technologies for the monitoring of wounds, by measuring components of wound fluid. Two of the three technologies are designed to be used by physicians and patients, similarly to commercially available home blood glucose test kits, and are based on the measurement of three biomarkers: glucose, ethanol and H_2O_2 in PBS, and in serum as surrogate wound fluid. The first is a voltammetric technique known as dual pulse staircase voltametry (DPSV), which produces peaks characteristic of particular analytes at an electrode. The second is an amperometric biosensor array, based on screen printed three electrode assembies of carbon, rhodinised carbon (glucose biosensor only) and Ag/AgCl reference. The glucose biosensor uses glucose oxidase enzyme as the biorecognition agent, the H_2O_2 biosensor is a mediated system using horseradish peroxidase enzyme and dimethylferrocene mediator, and the ethanol biosensor is a bienzyme mediated system utilising alcohol oxidase enzyme horseradish peroxidase enzyme and coupled dimethylferrocene mediator. Wounds are known to produce characteristic odours, therefore the third technology studied is a single sensor odour analyser with advanced data analysis to detect five commonly occuring wound bacteria, S.aureus, K.pneumoniae, S.pyogenes, E.coli and P.aeruginosa in growth media and surrogate wound fluid. This technology would be used as a 'near patient' monitoring system and is based on machine olfaction similar to that of a commercial electronic nose, but uses a single metal oxide sensor in combination with principle components analysis.

DPSV scans of the individual analytes demonstrated distinctive peaks, exhibiting non-linear relationships with concentration. A great deal of useful information was generated using this technique, however, limitations were discovered regarding repeatability and inter-analyte interference in mixtures. Limits of detection in surrogate wound fluid with the glucose biosensor, hydrogen peroxide biosensor, and ethanol biosensor were as follows: 169.5 µM glucose, 8.43 µM hydrogen peroxide, and 7.94 µM ethanol respectively (all at 99.7% confidence). Direct detection of ethanol from metabolically active S.aureus in surrogate wound fluid yielded a limit of detection of 1.23×10^8 CFU/ml at 99.7% confidence, and 19 µM in terms of ethanol specific response. The single sensor odour analyser demonstrated the ability to detect and discriminate between the three biomarkers, between five bacteria individually, and partial discrimination of paired bacteria (in broth and surrogate wound fluid). It was also found that S.aureus could be detected down to a cell density of 5×10^6CFU/ml in surrogate wound fluid, lower than that found for the biosensor concept.

Acknowledgements

Firstly I'd like to thank Selly Saini for giving me the opportunity of working on this project. Huge thanks to my supervisor Steve Setford for his continuous support and guidance. Thanks also to the project consultants Laurie Ritchie, and Jon Lee-Davey for their assistance, and to the many other staff who have contributed in some way to the success of this project.

Thanks to my family and partner for their endless support during this enduring experience, and to the many friends who have helped make my time at Silsoe memorable.

Contents

List of Figures

List of Tables

Notation

A	Amps
C	Concentration
D	Diffusion coefficient
E	Potential
E_{det}	Measurement potential
E_{ox}	Oxidation potential
E_{red}	Reduction potential
I or i	Current
J	Flux
L	Litre
mM	Millimolar
O or ox	Oxidised
Q	Total charge
R or red	Reduced
t	Time
t_{det}	Detection period
t_{ox}	Oxidation period
t_{red}	Reduction period
U	Units (of enzyme)
µ	Micro
V	Volts
+ve	Positive
-ve	Negative
Ω	Ohms

Abbreviations

ADH	Alcohol dehydrogenase
Ag/AgCl	Silver/silver chloride
AOx	Alcohol oxidase
ATP	Adenine triphosphate
CFU	Colony forming units
CV	Cyclic voltammetry
C-NS	Coagulase negative *staphylococcus aureus*
DMEM	Dulbecco's modified eagle's medium
DMFc	Dimethylferrocene
DNA	Deoxyribonucleic acid
DPSV	Dual pulse staircase voltammetry
ELISA	Enzyme linked immunosorbent assay
FAD	Flavin adenine dinucleotide
FET	Field effect transistor
FIA	Fluorescent immunoassay
FTIR	Fourier transform infrared spectroscopy
GAG	Glycosaminoglycans
GC-MS	Gas chromatography mass spectrometry
GDH	Glucose dehydrogenase
GOx	Glucose oxidase

HPLC	High performance liquid chromatography
HRPx	Horseradish peroxidase
IR	Infrared
LAPS	Light addressable potentiometric sensor
LED	Light emitting diode
LSV	Linear sweep voltametry
MMP	Matrix metalloproteinase
MOS	Metal oxide sensor
MRSA	Methicillin resistant *Staphylococcus aureus*
MSSA	Methicillin susceptible *Staphylococcus aureus*
NA	Nutrient agar
NAD	Nicotinamide adenine dinucleotide
NHE	Normal hydrogen electrode
OHP	Outer Helmholtz plane
O/N	Overnight
PAD	Pulsed amperometric detection
PARC	Pattern recognition engine
PBS	Phosphate buffered saline
PCA	Principle components analysis
PYG	Peptone yeast glucose broth
PZ	Piezoelectric
RNA	Ribonucleic acid
RO	Reverse osmosis
RPM	Revolutions per minute
SAW	Surface acoustic wave
SCFA	Short chain fatty acids
TCA	Trichloroacetic acid
TSB	Tryptone soy broth
UTI	Urinary tract infection
VFA	Volatile fatty acids
VOC	Volatile organic compounds
VRSA	Vancomycin resistant *Staphylococcus aureus*

1. Introduction

1.1 Biochemistry and Physiology of the Skin

1.1.1 Structure of the skin

The skin is a large organ covering every contour of the human body, conforming to the movements of the organism inside. The skin provides the major interphase between the organism and its environment, and is adapted to withstand the desiccation of dry environments, as well as exposure to the many mechanical, chemical and microbial variables. It also contains a vasculature and sweating system to thermally regulate the body, and a neuroreceptor network to report environmental information. The skin is conventionally recognised as having two major layers. The outer layer is a thin stratified epithelium, known as the epidermis, ranging only from 75 to 150 μm in thickness around the body (except palms and soles). Underlying the epidermis is a dense fibroelastic connective tissue called the dermis. Unlike the epidermis, the thickness of the dermis varies considerably throughout regions of the body. The dermis contains the extensive vascular and nerve networks, as well as specialised excretory and secretory glands, and keratinised appendage structures such as hair and nail. Beneath the skin lies the subcutaneous tissue (hypodermis), which is composed of loose areolar connective tissue and fatty connective tissue, and also has substantial variations in its thickness. Fibrous bands run from the dermis through to the subcutaneous tissues, thereby providing attachment of the skin to the fibrous skeletal components (Odland, 1983).

The epidermis is subdivided into (Odland, 1983):

1) A germinative basal cell layer of keratinocytes;
2) Above the germinal layer is the stratum spinosum, comprising several layers of polyhedral cells;
3) Above this is the stratum granulosum, which is a layer of flattened nucleated cells containing distinctive cytoplasmic inclusions, and keratohyalin granules.
4) The stratum granulosum is the transition to the overlying end product, the stratum corneum, consisting of the keratinised lamellae of anucleate, thin flat cells. This final layer ranges from 15 to 20 cellular layers in thickness.

The epidermis is constantly replacing itself, by keratinocyte daughter cells dividing and migrating outward, and transforming to eventually becoming flattened anucleate cells of the stratum corneum. On average, it takes a period ranging from 45 to 75 days for the epidermis to completely renew itself. It is because of the constant renewal of the epidermal cell population that the skin is able to react so diversely to both physiological and pathological stimuli.

In psoriasis, there is a prominent increase in mitotic activity in the epidermis. In hyperproliferative states, cell production can be governed by a reduction in cell cycle, or an increase in the number or proportion of proliferating cells (Holbrook, 1983). The mechanism for this is not yet understood.

1.1.2 Carbohydrate metabolism of epidermis

Glucose is a fuel for energy metabolism and a substrate for biosynthesis of mucopolysaccharides, lipids, glycogen, nucleic acids, and proteins. Glucose circulates freely in the interstitial fluid space of the dermis and epidermis and is thought to diffuse freely across epidermal cell walls. The utilisation of glucose in the epidermis probably differs in basal and upper cell layers (Freinkel, 1983), and is proportional to substrate concentration, except at very high concentrations. The utilisation of glucose increases in proliferative states, and glucose uptake is enhanced during wound repair and psoriatic epidermis (Freinkel, 1983, Im & Hoopes, 1970).

Anaerobic glycolysis produces a high lactic acid content in the skin, far exceeding that of blood by as much as three fold. Lactic acid is the major metabolite of glucose. When glucose is absent, the epidermis oxidises endogenous lipids. This occurs in cornification when exogenous substrate is limited, or as a result of a pathological or physiological increase in circulating fatty acids (i.e. starvation or diabetes) to a level high enough to compete for access to the tricarboxylic acid cycle. The increase in glucose and O_2 utilisation in wound repair is accompanied by a decrease in the formation of lactic acid and CO_2. All of the sugar moieties used to form the carbohydrate components needed by the skin are derived originally from glucose. Glycogen is one of the products of synthesis derived from glucose metabolism in the skin. Except for in foetal epidermis, glycogen is sparse in the human dermis. However, in proliferative responses to physical trauma, such as a wound or exposure to radiation with UV light and X-ray, glycogen accumulates and

probably serves as an added source of energy during repair processes. In psoriasis, the amount of glycogen is four or five times greater than the level in normal epidermis (Freinkel, 1983, Im & Hoopes, 1974). X-ray irradiation also produces an inflammatory reaction, caused by cellular damage, and ultraviolet light causes an increase in acid proteinase in the skin. Healing wounds contain a methionine and valine napthylamide hydrolase, which is different from normal skin enzymes (Frienkel, 1983), and also have increased levels of the serum arylamidase and aminopeptidase activity

1.1.3 Physiology of wound healing

This Section is taken from Gogia (1995). Wound healing is a complex and highly regulated series of biological events. Wounds are categorised on the basis of severity and extent of injury to the dermis. Epidermal wounds extend into the epidermal layer and possibly the superficial layer of the dermis. These are called partial thickness wounds. The wound initially forms a crust of blood and debris particles, and then proceeds to heal by regeneration i.e. re-epithelialisation. The new cells gradually thicken until healing is complete, at which point the crust falls off leaving the proliferated cells to keratinize. It takes 24 to 48 hrs for the epithelial cells to respond to injury, and the wound heals without scar tissue. Dermal wounds extend through the epidermis and dermis to the subcutaneous tissue, and may also involve muscles and bone. These are called full thickness wounds, and heal by three mechanisms resulting in scar formation (Figure 1.1). The first phase is inflammation, which prepares the wound for healing. The second is the fibroplastic phase, which rebuilds damaged structures, and the third is the remodelling phase, which modifies the scar to fit the wound. In normal healing, each phase overlaps.

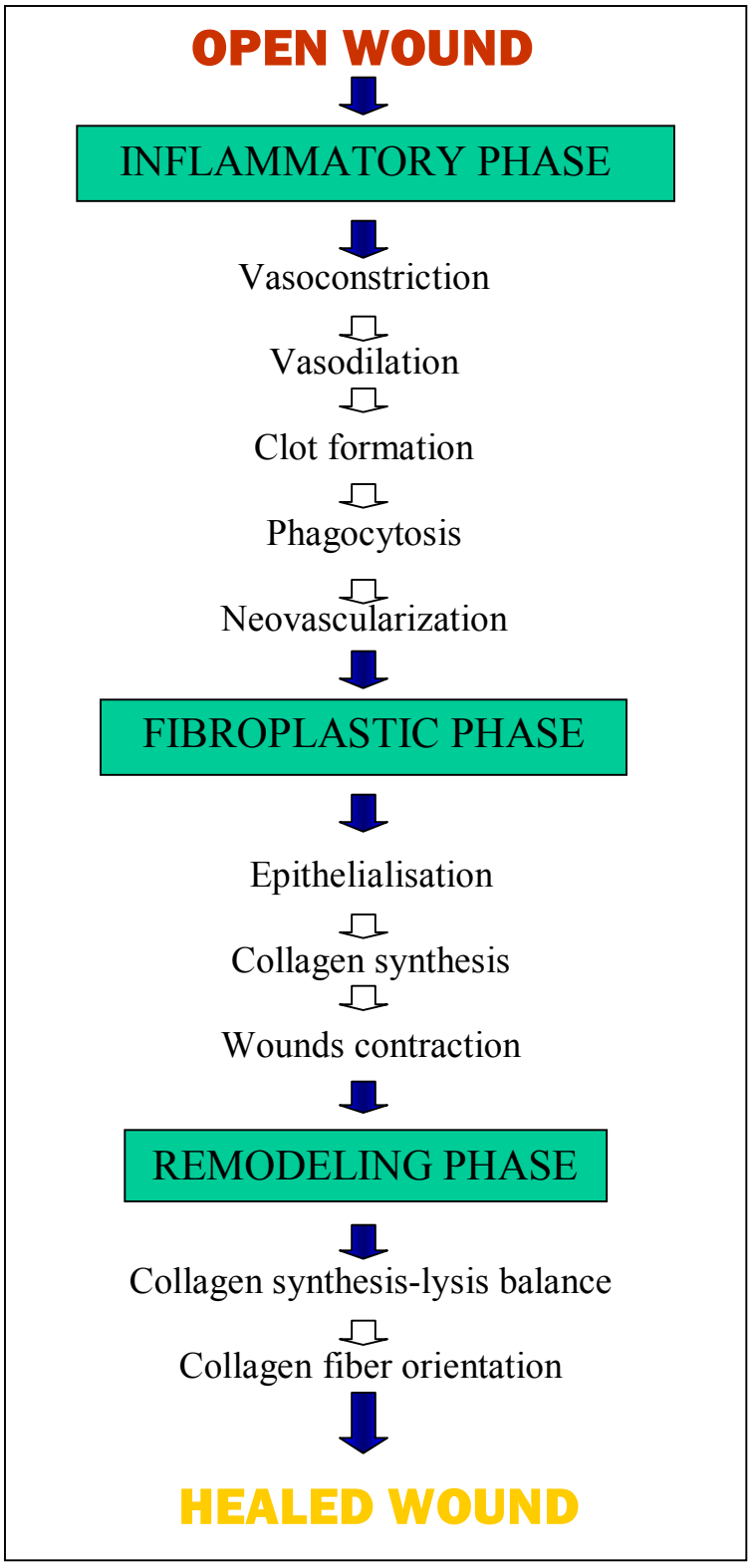

***Figure 1.1**: The phases to scar formation in a full thickness wound (Gogia, 1995).*

1.1.3.1 Inflammatory phase

Inflammation is a prerequisite to wound healing. It is a vascular and cellular response to dispose of bacteria, foreign material, and dead tissue. The first stage is the vasoconstriction of the damaged blood and lymphatic vessels, to slow or stop blood loss. This is achieved through the secretion of norepinephrine by the blood vessels, and serotonin by the platelets and mast cells. The platelets also plug or stop blood loss.

At the same time, leukocytes cluster along the sticky vessel walls, which is known as neutrophilic margination. Following vasoconstriction, the non-injured vessels dilate and increase their permeability in response to the histamine released by the mast cells, and the prostaglandin released by the injured cell membrane. Vasoconstriction lasts for about five to ten minutes, and vasodilation lasts for less than one hour. The increase in vessel permeability allows plasma to leak into the wound area, so that fibrin can block the lymphatic flow and seal off the wound, localise the inflammatory reaction, and prevent the spread of infection. The wound is red, hot, swollen, and painful at this stage of healing.

Leukocytes, erythrocytes and platelets adhere to the dilated blood vessel walls. Polymorphonuclear leukocytes migrate through the capillary pores first, and prevent infection by enzymatically dissolving and digesting debris and foreign material by the process of phagocytosis. When these leukocytes die, they release their intracellular enzymes and debris, which becomes part of the wound exudate. Mononuclear leukocytes move from the capillary into the wound next, where they are transformed into macrophages, the most important cells of the inflammatory stage. The macrophages ingest

the unsolubilised material, engulf leftover polymorphonuclear leukocytes, and ingest microorganisms. The products of digestion of these materials are excreted, i.e., ascorbic acid, hydrogen peroxide, and lactic acid. The hydrogen peroxide released helps to control anaerobic microbial growth. Ascorbic acid and lactic acid accumulate and signal to increase production of macrophages. The macrophage products result in greater pus production, which can impair wound healing. At the end of this phase, fibrinolysin is produced by the blood vessels to dissolve the blood clots, and the lymph channels then open to help reduce wound edema.

1.1.3.2 Fibroplastic phase

This phase is also referred to as the proliferative phase, since rebuilding of the damaged tissue occurs. Repair of the epithelium goes through a sequence of mobilisation, migration, proliferation, and differentiation, and continues until the wound is healed. The epithelial cells migrate into the wound area to form multiple layers beneath the clot. This provides a protective barrier to prevent fluid and electrolyte loss from the wound, and to reduce the chance of infection. The temporary crust loosens and detaches once epithelialisation is completed.

While re-epithelialisation occurs, the wound contracts and is remodelled by mobilisation of the surrounding tissues. The centripetal movement of normal skin, primarily myofibroblasts, decreases the size of the wound by forcing granulation tissue to retract. Contraction begins after five days of wounding and peaks at two weeks. Contraction proceeds at a uniform rate, and is not affected by the size of the wound, though is affected

by the shape. However, if the wound has not closed by two to three weeks, contraction stops.

Fibroblasts are produced by undifferentiated mesenchymal cells, and are stimulated to synthesise collagen tissue by lactic acid, ascorbic acid, and other cofactors. Collagen tissue is necessary to strengthen and stiffen the wound. Collagen molecules cross-link intermolecularly to increase the tensile strength of the wound. A gel-like substance called glycosaminoglycans (GAG) is also produced by fibroblasts, to give lubrication and density to the connective tissue. As the amount of collagen increases, the number of fibroblasts is reduced, marking the end of the fibroblastic phase.

1.1.3.3 Remodelling phase

This phase is also called the maturation phase, and begins after approximately two to four weeks. The enlarged, dense scar formed in the fibroblastic phase is remodelled in form, bulk and strength. New collagen is produced as the old breaks down. If the rate of collagen production exceeds its breakdown, a hypertrophic scar or keloid forms, which is either raised, or extends beyond the normal boundaries of the wound. If collagen breakdown exceeds its production, a softer scar forms.

1.1.3.4 Types of healing wounds

Primary closure / healing by first intention: Occurs when full-thickness surgical incisions or other wounds with minimal skin loss are approximated and sutured together. Healing is completed by re-epithelialisation only.

Secondary closure / healing by secondary intention: Occurs in large, open, full-thickness wounds with soft tissue loss. They heal by collagen deposition, wound contraction, and granulation, followed by epithelialisation. These wounds take longer to heal, and form a scar.

Delayed primary closure / healing by third intention: Occurs in contaminated more extensive wounds, or wounds at risk of infection. By deliberately delaying wound closure, infection can be treated and monitored, without delaying the formation of tensile strength. The wounds are then sutured together and complete healing by re-epithelialisation.

1.1.4 Body composition and body fluid compartments

In an average male, body weight is split as follows (Ganong, 2003):

18% protein and related substances

7% mineral

15% fat

60% water

These values differ with sex, age, and degree of obesity. With age, the percentage of body fat increases, which in turn decreases the percentage of water. Total body fluid is mostly distributed between two compartments: extracellular and intracellular. A third and smaller

compartment is referred to as transcellular, and includes fluid from synovial, peritoneal, pericardial, and intraocular spaces.

The distribution of the ~60% water in body fluid compartments can be divided as follows as a percentage of body weight (Ganong, 2003, Guyton & Hall, 2000) :

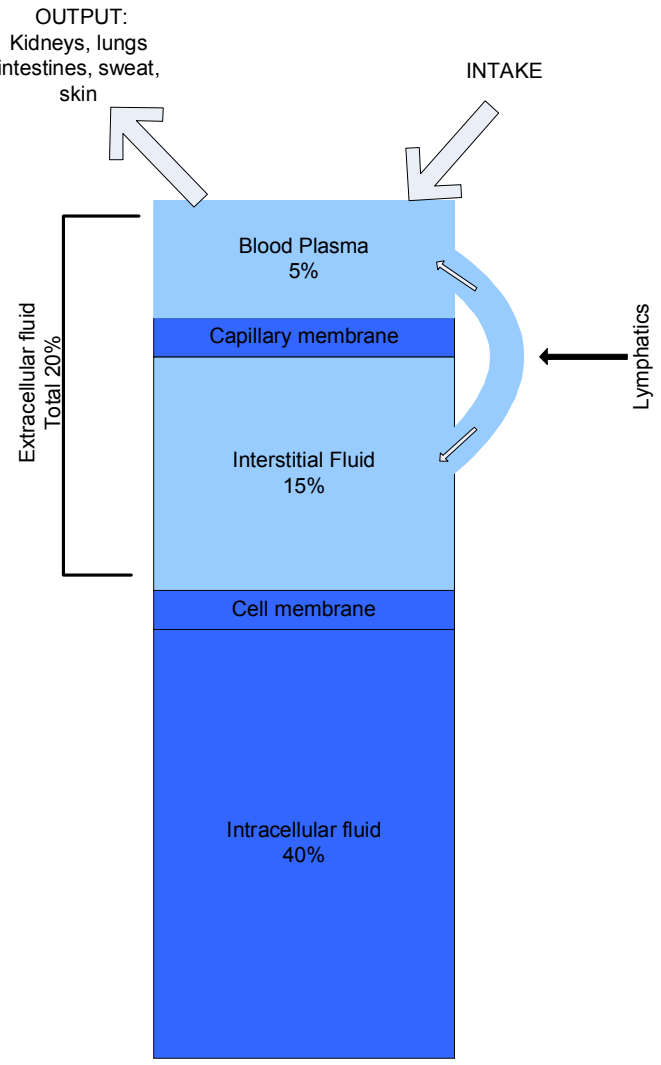

Figure 1.2: *Distribution of water in major body fluid compartments*

The intracellular fluid is inside the cells of the body. The concentration of substances is similar from one cell to another and is therefore considered to be one large fluid compartment. The extracellular fluid is outside the cells and is further divided into blood plasma and interstitial fluid, which is often referred to as a gel phase. Plasma is the noncellular part of blood, and continuously communicates with the interstitial fluid through the pores of the capillary membrane. The extracellular fluids are constantly mixing, and almost all solutes in extracellular fluid can pass though the pores, except for proteins. For this reason, the composition of the two fluids are approximately similar, except for the protein content, which is higher in plasma (Guyton & Hall, 2000). The molecular masses of the major proteins in plasma are (Ganong, 2003):

Albumin	69,000
Haemoglobin	64,450
β_1Globulin	90,000
γ Globulin	156,000
Fibrinogen	340,000

Since the proteins cannot pass through to the interstitial fluid, they exert an osmotic force across the capillary wall that pulls water into the blood. The proteins also provide ~15% of the buffering capacity of blood in an anionic form at the normal plasma pH of 7.4. The normal composition of the major body fluid compartments is listed in Table 1.1, though it should be noted that these values vary slightly from book to book.

Table 1.1: *Composition of major body fluid compartments (Guyton & Hall, 2000).*

Constituent	Plasma (mmol/L)	Interstitial fluid (mmol/L)	Intracellular fluid (mmol/L)
Na^+	142	139	14
K^+	4.2	4.0	140
Ca^{++}	1.3	1.2	0
Mg^+	0.8	0.7	20
Cl^-	108	108	4
HCO_3^-	24	28.3	10
HPO_4^-, $H_2PO_4^-$	2	2	11
SO_4^-	0.5	0.5	1
Amino acids	2	2	8
Creatine	0.2	0.2	9
Lactate	1.2	1.2	1.5
Glucose	5.6	5.6	
Protein	1.2	0.2	4
Urea	4	4	4
Others	4.8	3.9	10

Although blood contains both extracellular fluid and intracellular fluid, it is considered a separate fluid compartment because it is contained within the circulatory system.

1.1.5 Biochemical composition of wound fluid

Wound fluid bathes the tissue undergoing repair and regeneration. When tissue is damaged, a cascade of reactions causes blood to coagulate by converting soluble fibrinogen (the largest plasma protein) into insoluble fibrin. What remains is an exudate of plasma called serum. Serum has the same components as plasma, except that it doesn't contain fibrinogen. The wound fluid may also contain soluble tissue and cell-derived molecules responsible for co-ordinating the healing process (Ganong, 2003, Clough & Noble, 2003).

It is a highly complex biomatrix containing thousands of species at steady state, including essential trace elements of amino acids such as citrate and arginate, and metal ions such as iron, copper and zinc. Proteins and enzymes uptake the metal ions to form metal ion-protein complexes. The protein bound total metal fraction is not known in wound fluid, but can be assumed to be analogous to that of blood plasma.

Jones, Taylor and Williams (2000) investigated the change in levels of these trace elements in wound fluid by Potentiometric Stripping Analysis, a quantitative electro-analytical tool. Wound fluid was sampled from 20 female breast cancer patients, and analysed for total copper and zinc levels on the day of the operation, and each day for 5 days post-op. The copper and zinc levels in blood plasma were also measured 1 day pre-op. Though there were some day to day variations, they found that overall the mean total copper varied little from the first day to the fifth post-op day, and were very similar to the levels measured in blood plasma. The values measured in individual samples ranged from 7.5 μM to 61.2 μM . The same observations were found for zinc, with individual values ranging from 10.1 μM to 65.8 μM.

Recent studies in wound fluid have targeted metabolites such as creatinine, urea, lactate, glucose, serum proteins, proteolytic enzymes and their inhibitors, inflammatory mediators such as prostanoids and cytokines, and growth factors. Both total protein and albumin (serum protein) are present in wound fluid, with total protein levels reaching >40g/l of which ~60% was albumin (Clough & Noble, 2003). James, Hughes, Cherry *et a*l (2000) studied the exudate from the chronic wounds of 12 patients over 8 weeks, and found that exudates from healing wounds had a significantly higher total protein concentration than

that from non-healing wounds. They also found that in wound fluid with albumin levels of <20g/l the wound failed to heal. This is in agreement with Trengove, Langton and Stacey (1996) who studied biochemical changes in paired serum and wound fluid samples from non-healing and healing chronic leg ulcers. Trengrove *et al* (1996) also found that C-reactive protein, a marker of inflammation, decreased in healing wounds, suggesting a decreased inflammatory state in the wound. C-reactive protein is used as a clinical marker of inflammation in disorders such as rheumatoid arthritis, pancreatitis, postoperative complications, appendicitis, and infection. The wide range of other biochemical parameters studied were: sodium, potassium, chloride, urea, creatinine, uric acid, calcium, magnesium, phosphate, bicarbonate, glucose, lactate, LDH, alkaline phosphatase, ALT, AST, GGT, CK, total bilirubin, α-1-globulin, α-2-globulin, β-globulin, γ-globulin, C3, C4, cholesterol, and triglycerides.

The analysis of healing and non-healing wound fluid found that there was a significant increase in six of the biochemical analytes, and a significant decrease in one from the non-healing to healing phase. The values found are tabulated below.

Table 1.2: *Comparison of selected biochemical analytes from non-healing and healing wound fluids (from Trengove, Langton and Stacey, 1996)*

Biochemical	**Non-healing wound**	**Healing wound**	**Units**
Glucose	1.2	2	mM
Biocarbonate	17.5	19	mM
Albumin	19	23	g/L
Total protein	34	41	g/L
Gamma globulin	4.5	6	g/L
Cholesterol	1.6	1.8	mM
C-reactive protein	13	5	g/L

In the comparison between paired wound fluid and serum samples (from blood), no significant difference was found in sodium, magnesium, phosphate, urea, creatinine, potassium, or chloride. Lactate levels were greater and glucose and bicarbonate levels lesser in wound fluid compared to serum. These results are thought to be consistent with the existence of an acidotic, anaerobic environment. In wound fluid, LDH was almost twenty times the value in serum, and albumin, total protein and the globulins were approximately half the levels found in serum. Cholesterol and triglyceride levels were reduced in wound fluid. The levels of C-reactive protein were similar in wound fluid and serum. This study concluded that wound fluid has the electrolyte composition, urea, creatinine levels and osmolarity equivalent to serum and therefore appears to reflect the extracellular environment of the wound.

Earlier studies by Burton, Hohn & Hunt *et al* (1977) found that there is increased consumption of oxygen, oxidation of glucose, and increased generation of hydrogen peroxide and superoxide anion in surgical wounds. This is a result of phagocytosis by mammalian polymorphonuclear leukocytes and monocytes. Hydrogen peroxide and superoxide anions are either directly or indirectly important microbicidal agents, and their generation by the leukocyte oxidase system is a necessary requisite for the killing of many species of microorganisms.

Nanney & Wenczak (1993) investigated the role of growth factor-α and its receptor in epithelial cell proliferation in human burn wounds. By isolating and labelling growth factor-α with proliferating cell nuclear antigen, and using it to treat partial and full

thickness burn wounds 2 to 22 days after injury, they found that both growth factor-α and its receptor are present in proliferating epidermis. The simultaneous intense localisation supports an epidermal growth factor/transforming growth factor-α/epidermal growth factor receptor-mediated growth repair mechanism. Growth factor-α and epidermal growth factor receptor were also found to be present in non-proliferating populations within healing burn wounds, which suggests additional roles for this growth factor pathway during wound repair.

Differences also occur in proteolytic activity in acute and chronic wound environments. During wound repair, many different matrix metalloproteinases (MMPs) are produced which act on protein. Bennett, Buslem & Gibson *et al* (1999) analysed wound fluids from acute surgical and chronic wounds of various types, and found MMP activity was elevated by 30 fold more in chronic wounds than in acute wounds. There was also much higher degradation of epidermal growth factor in chronic wound fluid samples than in acute wound fluid samples. Levels of MMP activity decreased significantly from the non-healing to healing phase in chronic leg ulcers, and therefore a reduction in MMP levels may be required for healing to occur in chronic wounds. Proinflammatory cytokines IL-1 and TNF-α stimulate the production of MMPs. TNF-α, IL-1, IL-6, and IL-8 elevate in chronic wounds, and TNF-α, IL-1, and IL-6 then decrease as healing occurs. Parks (1999) reported that MMPs are typically not expressed in normal, resting, healthy tissue. However, expression occurs in any active cell involved in injury repair or remodelling process of diseased, tumour or inflammatory conditions, and therefore expression of MMP does not necessarily indicate a chronic wound. Though they are assumed to be involved in

remodelling the local extracellular environment, the different distinct functions and actual substrates of the many MMPs are not known, but are likely to serve different functions in different compartments. It is reasonable to assume that a wound that requires a large degree of remodelling would have elevated levels of MMPs. Collagenase-1 is the best understood MMP, and is thought to facilitate cell movement during re-epithelialisation by breaking down matrix barriers that impede cell migration (Parks, 1999).

1.1.6 Factors affecting wound healing

There are many factors, both systemic and local, that affect the normal healing of wounds. General/systemic factors include: age, obesity, malnutrition, endocrine and metabolic disorders, hypoxia, anaemia, malignant disease and immunosuppression. Local factors include: necrotic tissue, foreign bodies, tissue ischaemia, haematoma formation, and poor surgical technique. Microbiological factors: type and virulence of organism, size of bacterial dose, antibiotic resistance. Table 1.3 summarises the most common and important clinical factors, (Gogia, 1995, Surgical-tutor.org., 2002).

1.1.6.1 Bacterial invasion

Skin and mucous membranes are the major protective boundaries between bacterial pathogens and soft tissue. Mucosal membranes are covered with commensal flora that help to prevent infection, and the skin is populated by certain bacteria and fungi. Physical disruption of the body's epithelial barrier physiologically and immunologically compromises the host, and may result in the invasion of microorganisms. Even latent organisms may become activated and invasive. Invading bacteria may translocate from the

Table 1.3: *Factors affecting wound healing (Gogia, 1995).*

FACTOR	AFFECT ON WOUND HEALING
Systemic factors: Nutrition	Balanced nutrition is crucial for normal healing. Deficiency of any nutrient during healing may result in impaired or delayed healing. Protein is one of the most important nutrients since its deficiency impairs the formation of new capillaries, fibroblastic proliferation, proteoglygans and collagen synthesis, and wound remodelling. Deficiencies in vitamins A, E, C and K also adversely affect wound healing. Minerals are also important. Deficiency of zinc and magnesium causes a decreased rate of epithelialisation and collagen synthesis. People with high fat content and poor dietary habits are at risk of delayed healing, and infection.
Vascularity	Arterial insufficiency causes tissue hypoxia and results in chronic, non-healing wounds, which are susceptible to infection. Venous pressure causes leakage of fibrinogen around the capillaries into the dermis. This results in a blockage of tissue oxygenation, nutrient exchange, and waste removal. Venous stasis ulcers are at risk of infection and difficult to heal.
Systemic medications	Steroids decrease tensile strength, rate of epithelialisation and neovascularisation, and inhibit wound contraction. They also suppress the immune system. Other medications such as chemotherapeutic agents and immunosuppressive medications also increase susceptibility to infection, prolong inflammation, and impair the healing process.
Systemic diseases	Diabetes mellitus adversely affects wound healing. Uncontrolled diabetes decreases collagen synthesis and phagocytosis, and increases the risk of infection. It also often causes atherosclerosis, resulting in circulatory deficiency. Acquired immune deficiency syndrome (AIDS), and diseases which reduce the blood supply, make the wound susceptible to infection and affect phagocytosis and collagen synthesis. Renal and liver failure significantly affect wound healing.
Age	With aging, physiological changes occur that cause wounds to heal at a slower rate, and increase the risk of multiple breakdowns.
Local Factors: Local infection	All wounds are contaminated, but not all are infected. A bacterial concentration $>10^5$ organisms/gram of tissue is defined as infection. Approx. 50% of wound complications are due to local wound infection. The highest effect of infection is the reduction of collagen production. The toxicity of bacteria also kills cells needed for healing.
Blood supply	The supply of blood and oxygen to the wound cells is vitally important, since it is depended upon to deliver components for healing. Therefore, wounds with decreased blood supply are at higher risk of infection and impairment.
Local medications	Although topical agents help to prevent infection or promote healing, they have been known to have adverse affects on wound healing. Topical antimicrobials, such as acetic acid or hydrogen peroxide, can affect fibroblast function at certain concentrations. Other antimicrobials can cause slower re-epithelialisation and decreased collagen synthesis.
Dressings	Dressings can facilitate and inhibit wound healing. The choice of dressings is vast, and all have advantages and disadvantages. The right type of dressing should be used for each stage of healing. The wrong choice could have a detrimental effect on the rate of healing.
Nectrotic tissue / Eschar	Eschar, and the presence of necrotic tissue, impairs healing and increase the risk of infection. This results in a chronic, non-healing wound.
Desiccation	Moist wounds heal much faster than dry wounds. A moist environment has a 50% faster rate of epithelialisation.

gut and enter a wound by the slowed capillary blood flow. Bacteria also survive in skin appendages, such as sweat glands and hair follicles, thereby enabling colonisation and invasion by movement upwards, rather than from the surface of large wounds (Smith & Thomson, 1994).

The primary pathogens isolated from wounds include *Staphylococcus aureus* and *Pseudomonas aeruginosa*. Endogenous wound infections are usually caused by more than one organism. Table 1.4 lists the organisms commonly isolated from wounds, their percentage occurrence, the wounds they were isolated from, and the volatiles they are reported to produce. However, quantitative biology alone cannot predict sepsis. The presence of $>10^5$ organisms/g of tissue does not mean infection is present, since the development of infection depends on the nature of the wound and of the organism(s) involved. Attempts to use other systemic microbial indicators, such as endotoxin, have not been successful since they do not cover the entire microbial population. Physiologic indicators such as circulating tissue necrosis factor or other cytokines, do not differentiate injury from sepsis and therefore also cannot predict wound infection or systemic sepsis (Slack & Greenwood, 1992; Smith & Thomson, 1994).

1.1.6.2 Hospital acquired infection

Wounds are acquired in a number of ways. Hospital-acquired wounds, from surgery or intravenous medical devices for example, are surprisingly one of the highest causes of morbidity and medical expense, classified as follows:

***Clean wounds*:** are not inflamed, and less than 1% of the wound has become infected. Also, the wound is not located in a site with a heavy microflora population, and the surgical practice was good.

Clean-contaminated wounds: are located at sites of heavy microflora load, but surgical practice was good. 1 to 5% of the wound is infected.

Contaminated wounds: are located in the bowel, or previously infected areas where pus has accumulated. 10 to 20% of the wound is infected.

***Table 1.4**: Information on common wound pathogens (Barchiesi, D'errico, Del Prete et al, 2000; Murray et al, 1998)*

Bacteria	Characteristics	% occurrence in wounds	Type(s) of wound infected	Metabolic products / volatiles known to be produced
Coagulase -ve *staphylococcus epidermidis*	Facultative anaerobe. Gram +ve. (CoNS) (less invasive than *staph. aureus*, but often present)	20.4	Surgical wounds bloodstream infections, especially patients with weak immune systems.	Acids, alcohols
Enterococcus faecalis	Facultatively anaerobe. Gram +ve cocci. Catalase -ve. Homofermentative, without gas production.	7.1	UTI and intra abdominal and pelvic wound infections, bacteremia, endocarditis.	Pyruvate, lactic acid
Enterobacter species	Facultative anaerobe. Gram –ve rod. Ferment rather than oxidize often with gas production. Catalase +ve, oxidase -ve	6.4	Wounds.	Butanediol, ethanol, CO_2, 3-methyl-1-butanol, ammonia.
Escherichia coli	Gram –ve rod. Heterolactic fermenter often with gas production. Catalase +ve, oxidase -ve	7.8	Pressure sores. Surgical wounds.	Lactic acid, acetic acid, succinic acid, formic acid, ethanol, butanediol.
Klebsiella pneumoniae	Facultative anaerobe. Gram –ve rod. Ferment rather than oxidize often with gas production. Catalase +ve, oxidase -ve	6.1	Surgical wounds	Butanediol, ethanol, CO_2.
Proteus mirabilis	Facultative anaerobe. Gram –ve rod. Ferment rather than oxidize often with gas production. Catalase +ve, oxidase -ve	8.7	U.T infections. Pressure sores, leg ulcers	Lactic acid, acetic acid, succinic acid, formic acid, ethanol, butanediol, isobutylamine, isopentylamine, ethylamine, isobutanol, isopentyl acetate, 1-undecene, methyl ketones
Pseudomonas aeruginosa	Aerobe. Gram –ve rod. Oxidase +ve, catalase +ve. Nutritionally versatile. Chemoheterotrophic.	25.1	Wounds/burns. UT infections, septicaemia. Respiratory system infections. Soft tissue, bone, joint infections.	Pyruvate.
Serratia spp.	Facultative anaerobe. Gram –ve	7.4	Surgical wounds.	Butanediol, ethanol, CO_2, by butanediol fermentation.
Staphylococcus aureus	Facultative anaerobe. Gram +ve cocci. Catalase +ve. Oxidase -ve. Chemoorganotrophic. Coagulase +ve.	28.2	Skin/soft tissue/blood/ pressure sores. Enters through surgical wounds. Leg ulcers. Boils/ TSS. Pneumonia. Passed on easily.	Isobutanol, isopentyl acetate, 1-undecene, methyl ketones, ammonia, ethanol, trimethylamine, 2,5 dimethylpyrazine isoamylamine, 2-methylamine, acetic acid.
Streptococcus spp. E.g. S.pneumoniae and S.pyogenes	Facultative anaerobe. Gram +ve cocci. Oxidase –ve. Catalase -ve. Homolactic fermentative. (Fastidious, growth enhanced by blood or serum).	13.8	Pressure sores, leg ulcers, and causes respiratory infections, meningitis, puerperal sepsis, TSS like symptoms.	Lactic acid, alcohols

In the United States in 1999, two million people with a wound caught bacterial and viral infections in hospital. Ninety thousand of these people died, which made hospital infections the number five killer in the U.S. (Plotkin & Shnayerson, 2002). In England one in ten patients acquire an infection and there is a 10% chance of dying. The economic burden is almost £1 billion a year for the NHS in England (Plowman, 2000). These patients also spend 2.5 times longer in hospital than if they had not contracted a hospital acquired infection. Such patients also often require additional treatment once they have left hospital.

The elderly and persons with spinal cord injury are two groups known to be at risk for pressure ulcer development. A survey revealed the percentage of patients with ulcers to be: 9.2% in multiple acute care hospitals, 3 to 14% for hospitalised patients, and up to 25% in nursing homes (Ablaza & Fisher, 2003). Pressure sores are not only a source of infection and medical expense, but also have a significant impact on a number of quality of life issues, including life satisfaction, mental health, and productive use of time.

The magnitude of the problem of wounds has prompted the development of telemedicine, in which patient hospitalisation is shortened by being discharged to receive home health care. Interactive video and transmission of high-resolution images allows a specialist to review a wound without being present. The patient can then be treated by their local practitioner or by nursing home visits. As well as cutting costs and increasing access to care, home health care also improves psychosocial aspects.

1.1.7 Conventional wound assessment

Conventional identification usually involves morphological evaluation by microscopic methods, and growth tests on selective media under a range of conditions. These tests are time consuming, taking up to 48 hours, manually intensive, and there is no single definitive test for the identification of a particular bacteria. Also, before identification tests can be performed, a series of basic steps, involving pre-enrichment, selective enrichment, biochemical screening and seriological confirmation, must be performed (Bamberg, Sullivan, Conner-Kerr, 2002). To reduce time, API bacterial identification strips are used by bacteriologists throughout the world because they are easy to use, and give good performance. The strips usually contain 20 miniature biochemical tests, the results of which can be checked on a database to give the identity of the microorganism (Biomerieux, 2002). ELISA, gene probes, latex immunofluorescence and latex agglutination all require obligatory and extensive sample preparation, are expensive and require a high competence level.

1.1.8 Wound management

1.1.8.1 Odour and dressings

Many infected wounds produce an unpleasant odour. Malodour and exudate is thought to be a result of the overgrowth of bacteria in damaged tissue. The smell is usually attributed to anaerobic bacteria, although anaerobic bacteria only make up about 50% of bacteria isolated from wounds. Discussions and data specifying the chemical nature and origin of these wound odours are limited and often contradictory.

Since the formation of odour cannot be prevented, dressings have been developed to adsorb the volatile molecules released from the wound responsible for the malodour. There are over 2,000 dressing materials available commercially, which can be organised into eight commonly used dressing categories: gauze dressings; non-adherent dressings; hydrocolloid dressings; semi-permeable films; semi-permeable hydrogels; semi-permeable foams; exudate absorbing dressings; biologic dressings (Cuzzell & Krasner, 1995). Many of the odour absorbing dressings contain activated charcoal or carbon (Fisher, Fram & Thomas *et al* 1999). The idea of integrating a sensor into a dressing to produce a "smart bandage" or "smart plaster" to measure wound biomarkers is attractive. The properties of some commercially available wound dressings are given in Table 1.5.

***Table 1.5**: Properties of some odour absorbing wound dressings (Fisher, Fram & Thomas et al 1999).*

Dressing name	Manufacturer	Properties
Actisorb Plus	Johnson and Johnson	Charcoal cloth of 95-98% carbon and viscose rayon fabric. Fabric is enclosed in a sleeve of spun-bonded non-woven nylon, and sealed. Designed to be placed directly on wound and covered with secondary absorbent layer to remove the odour causing molecules and toxins.
Carboflex	ConvaTec Ltd	Consists of a wound contact layer composed of alginate and carboxymethylcellulose fibres, bonded to a plastic film with perforations for one-way liquid flow. Behind film is charcoal cloth and absorbing layer, followed by a second perforated plastic layer and sealed all around.
Carbonet	Smith and Nephew Medical	Wound contact layer of knitted viscose backed with absorbent fibrous cellulose, bonded to activated charcoal layer between two layers of polyethylene net. Completed with outer layer of polyester fleece.
Lyofoam C	Seton Healthcare	Can be applied directly. Two pieces of polyurethane foam bonded around the perimeter, and enclosing a non-woven fabric with activated carbon granules.

1.1.8.2 Antibiotic Treatment

The most effective way of treating wounds is to prevent or eradicate the infection. In some cases this can be achieved with either antibiotics, or antimicrobial agents. Sensitivity testing is performed on skin and wound cultures to help choose the antibiotic that will be most effective. However, it is not possible to achieve the desired concentration of antibiotic at the site of infection. Also, bacteria are becoming resistant to an increasing number of antibiotics, and therefore wounds often cannot be treated in this way. For example, *Staphylococcus aureus (S.aureus*) was a major killer until 60 years ago, before the advent of Penicillin. However, now that certain strains (such as MRSA252) of *S.aureus* have become resistant to penicillin, *S. aureus* preys on patients with weakened immune systems again, and remains the fastest bacteria to develop resistance to each new antibiotic. *S. aureus* has been resistant to methicillin for some time now. This strain of *S.aureus* is referred to as methicillin resistant *staphylococcus aureus* (MRSA). It is now often found to be resistant to vancomycin (VRSA), one of the few remaining antibiotic defences against bacteria (Dorey, 2005). New antibiotics named Linezoid and Quinupristin are being used to tackle *S. aureus,* but strains resistant to these have already been identified (Pearson, 2002; Huycke, Sahm, Gilmore, 1998).

1.1.8.3 Alternative treatments

There are a vast range of topical medications and pharmacological agents used in wound healing, including: cleansers and antiseptics, antimicrobials, anti-inflammatory agents, anaesthetics and analgesics, debriding enzymes, and tissue glues. In addition, a new alternative hydrogel treatment has been developed called metronidazole. Metronidazole

works by entering the cell where it is reduced and binds to DNA causing interference with replication. This only occurs under a low redox potential. In studies discussed by Hampson (1996), the data suggests that the odour is eradicated within seven days of treatment with metronidazole, although, these studies were not standardised, and lacked adequate controls.

Nabi Biopharmaceuticals (Boca Raton, Fla.) are developing a vaccine called StaphVax to combat *S.aureus*. Vaccines are much harder to develop and also to prove to be effective than antibiotics, but all of nature's obvious antibiotics have been found. Newly sequenced genomes have yielded a number of possible new genetic targets, but it will take years to develop new drugs. Vaccines must be tested more vigorously than antibiotics, since they are given to healthy people and routinely to children. However, a vaccine against these bacteria would have a huge advantage over antibiotics, since it would knock out the bacteria before resistance develops. StaphVax was researched and developed by NIH for 17 years, before it was licensed to Nabi Biopharmaceuticals to try to complete and take it to market. Nabi invested $100 million into the vaccine over the next 8 years, and results showed that the vaccine may protect sick patients for at least a year. Nabi is currently planning Phase III trials for the vaccine (Plotkin & Shnayerson 2002).

1.2 Electroanalytical chemistry

1.2.1 Fundamentals

Electroanalytical chemistry is essential to results Chapters 3 and 4, where a scanning voltametric technique and biosensor array were used to detect biomarkers of wound infection. Therefore, this section covers the fundamental concepts of electroanalytical chemistry. Electroanalytical chemistry is generally accepted as its own branch of analytical chemistry, providing an overlap between physical electrochemistry and chemical analysis, by practically applying the theories of physical electrochemistry to investigate the properties of solutions. An electrode in solution is an ideal transducer between the chemical and electrical domains, whether its role is to monitor species in the solution, or to generate a new species that will interact with the medium, and itself be monitored. In electrochemistry, charge is transported through the electrode by the movement of electrons. Electrodes are typically composed of solid metals such as platinum or gold, liquid metals such as mercury, carbon such as graphite, or semiconductors such as indium-tin oxide. The passage of charge in the electrolyte phase, is carried via the movement of ions, and is typically a liquid solution containing ionic species, such as H^+, Na^+, Cl^-, usually in water.

Electrochemical properties are studied in an electrochemical cell, which commonly consists of three electrodes immersed in an electrolyte phase. Two of these electrodes are typically platinum, gold or carbon, and function as the working and counter electrodes, and the third is a reference electrode, such as the Ag/AgCl reference electrode or the saturated calomel electrode (SCE). The electrolyte phase is usually a liquid phase containing ionic species, for example NaOH or PBS. In an electroactive system, the electric potential generated

between the electrodes can be measured in volts (V), or the resulting current at a particular potential in amps (A). One is most often interested in the reaction at the working (or indicator) electrode, and therefore a reference electrode is necessary to standardise measurement.

1.2.1.1 Reference electrodes

The primary internationally recognised reference electrode is the standard hydrogen electrode, or normal hydrogen electrode (NHE). However, there are several reference electrodes to choose from, and therefore a measured potential is quoted with respect to the reference electrode used. The two other common reference electrodes are the saturated calomel electrode with a potential of 0.242 V vs. NHE, and the silver-silver chloride electrode (Ag/AgCl) with a potential of 0.197 V *vs.* NHE (Bard & Faulkner, 2001).

Since reference electrodes have constant concentration of the complimentary ionic species, and therefore a fixed potential, any changes in the electrochemical cell are attributed to the working electrode. Therefore, the potential of the working electrode is controlled with respect to the reference. If the working electrode is driven at a suitably negative potential, electrons may be donated to ionic species within the supporting solution. This flow of electrons from the working electrode to the electrolyte solution constitutes a reduction current. For example, when a power supply and microammeter are connected across a cell, and the potential at a platinum electrode is held at a sufficiently negative potential with respect to a Ag/AgCl reference electrode, electrons flow from the electrode to ionic species in the solution, i.e. reduction of such species to yield a reduction current. Conventionally,

this is called a cathodic current and is taken as negative (Bard & Faulkner, 2001). For example:

$$2H^+ + 2e^- \rightarrow H_2$$

The reverse of this whole process generates an oxidation or positive anodic current. With a Ag/AgCl reference, the reaction would be:

$$Cl_2 + 2e^- \rightarrow 2Cl^-$$

i.e. the Ag/AgCl is reduced to Ag, and Cl^- is liberated into the solution. The rate of flow of electrons is defined as current, *i*, with units of Amperes (A). By plotting a current vs. potential curve, one can gain information about the nature of the solution, the electrodes, electroactive species and the reactions that occur at the interfaces (Bard & Faulkner, 2001).

1.2.1.2 Faradaic and non-Faradaic currents

The arrangement of the charged species at the electrode interface is often referred to as an electrical double layer, since its structure loosely resembles two layers. The electrode double layer constitutes the non-faradaic current. The layer closest to the electrode, the inner layer (or compact, Hermholtz, or Stern layer), contains solvent molecules and sometimes ions or molecules that have been specifically adsorbed. The centre of the specifically adsorbed ions is called the inner Helmholtz plane. The centre of the nearest solvated ions is called the outer Helmholtz plane (OHP). Since the interactions between the OHP and the charged metal only involve long-range electrostatic forces, their interaction is

essentially independent of the chemical properties of the ions. These ions are therefore non-specifically adsorbed. Thermal agitation in the solution causes the non-specifically adsorbed ions to be distributed in a region called the diffuse layer, from the OHP to the bulk of the solution. The thickness of this diffuse layer depends on the ionic concentration in the solution (concentrations $>10^{-2}$M have a thickness < ~100Å) (Bard & Faulkner, 2001). Sometimes the effect of the non-faradaic double layer is negligible and can be ignored, but at other times the presence of the double-layer capacitance or a charging current is too great to be ignored. Advanced electroanalytical methods aim to reduce the non-faradaic current since it limits analytical detection. Since Faradaic currents are proportional to the concentration of chemical species, and non-faradaic currents are independent of the concentration of species, at low concentrations, the observed current is inaccurate and has limited sensitivity. This is because the non-faradaic current will be greater than that of the faradaic current. The non-faradaic current is also larger at high scan rates (rate of increase in potential with time in voltametric measurements), resulting in distorted electrochemical responses. However, since non-faradaic current decays exponentially with time, one can reduce its contribution to the signal by sampling the current when the non-faradaic current has reached a steady state.

1.2.2 Electroanalytical techniques

To investigate electrochemical behaviour, certain variables of an electrochemical cell are kept constant, and the resulting variation of the other variables (such as current, potential, or concentration) is observed. Electroanalytical techniques are characterised as either static or dynamic. In static methods, no experimental parameters are changed during

measurement of potential differences at zero current. In dynamic techniques, system conditions change during measurement. Dynamic electrochemical techniques are largely controlled by diffusion, which may or may not be coupled with chemical reactions in solution or on the surface. Voltage, current and time variables can be adjusted to obtain maximum information. Within these categories, there are two principle classes depending on whether current or voltage is the controlled variable. Techniques within these classes are often described by an operational nomenclature consisting of an independent-variable part, followed by the dependent-variable part, i.e. (volt-ammetry, chrono-potentiometry). Generally, an electrical excitation signal (often the independent variable) is applied to a system, with particular electrodes, solution composition and geometry, and the response signal is monitored (dependent variable). Together this gives a description of the properties of the system (Heineman & Kissinger, 1984). In a generalised system:

$$O + ne^- \leftrightarrows R$$

where O and R are oxidised and reduced forms of an electroactive species, in a solution containing a relatively high concentration of inert supporting electrolyte, and the heterogeneous electron transfer rate is fast and reversible. In dynamic experiments, the sample is often either completely in the O or R form, whereas in static experiments, both forms are usually present (Heineman & Kissinger, 1984).

1.2.2.1 Diffusion

An important process influencing electrochemistry is diffusion, a factor in almost every analytical measurement. Derivation of Fick's mathematical laws of diffusion uses a collection of inert particles in random motion as its model. In fluid media, a molecule undergoes frequent and continuous collisions with other molecules, which generates randomness to each molecules trajectory. In a closed isotropic system, with no thermal, electromagnetic or concentration gradients, or phase boundaries, the number of molecules moving in a given plane approximate the number moving in alternative planes, and thus there is no net movement of molecules in any given direction. Therefore, the concentration, or chemical potential, of the solute is uniform throughout the system, and at equilibrium. If a dissimilar chemical potential region is created, the solute molecules will temporarily move between regions until a homogeneous condition is restored. This is known as mass transfer. The movement of molecules from a higher to a lower chemical potential is known as diffusion, and is also an example of mass transfer. The driving force for diffusion is to reach the most energetically favourable state, and thus maximise entropy. However, in real systems, the transition between high and low chemical potential regions is not infinitely sharp.

Another important concept is flux (mol/cm^2 s). Flux is defined as the number of molecules passing through a unit area of an imaginary plane per unit of time. As with mass transfer, equilibrium requires the sum of all fluxes in a given system to equal zero. Flux is a measure of the rate of mass transfer at a fixed point, and holds a direct relationship to electrode current.

In an infinite system of pure solvent at equilibrium, we can imagine it divided into a number of thin adjacent slabs of uniform thickness Δx. If a number, N_0, of solute molecules is introduced at time t=0 into the central slab, at the start, the concentration profile exhibits a sharp spike at the centre. The gradient at each boundary of the central slab is a huge negative number, but is a short-lived behaviour. Bombardment by solvent molecules with each other causes the molecules to move randomly from the central slab, the motion of which is no more probable in one direction than the other. Therefore, the fluxes across either boundary are equal at all times. However, the time steps are not evenly spaced. If the distance increments become infinitesimally small ($\Delta x \rightarrow dx$), the distribution will follow the normal curve giving a Gaussian distribution (Figure 1.3) (Heineman & Kissinger, 1984),

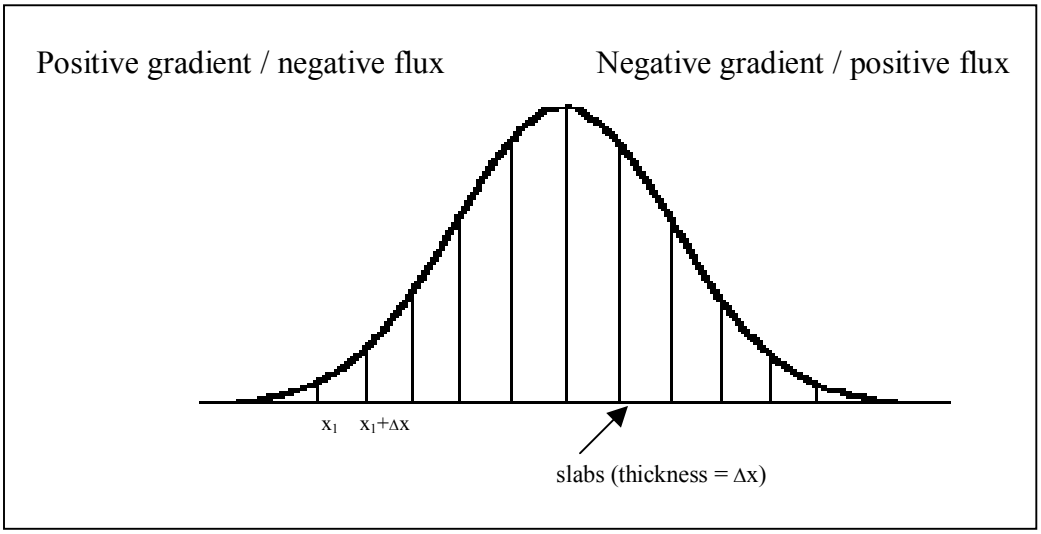

Figure 1.3: *Representation of a Gaussian concentration profile*

1.2.2.2 Chronoamperometry

The Cottrell equation forms the foundation for chronoamperometric techniques. In chronoamperometry, a potential is applied that is sufficient to reduce or oxidise species at

the electrode surface, and the current response is measured as a function of time, hence 'chrono'. This technique is more commonly referred to as amperometry, and is particularly useful for the detection of individual analytes. It has been exploited as a detection method in liquid chromatographic techniques, such as high performance liquid chromatography. Amperometry is also widely used in biosensor applications where the use of biological reagents confers specificity of the sensor, thus allowing individual electroactive species to be determined.

At a favourable potential (the driving force), electrons will be donated to, or accepted from an electrode and a current will flow. An increased potential above the standard electrode potential (an over-potential), may be applied to increase the rate of electron transfer. The magnitude of the current produced depends on two factors:

1) The rate of electron transfer between the electrode and the redox species in the surrounding medium.
2) The rate of mass transfer of electroactive species to the electrode.

Since electroanalytical techniques are controlled by the mass transport of reactants or products to or from the electrode, it is assumed that the rate of electron transfer at the electrode is greater than the rate of mass transfer. The Cottrell equation relates the diffusion limited current (I_D) to the bulk concentration of the species (Heineman & Kissinger, 1984). This equation tells us that the diffusion controlled current is proportional to the bulk concentration of the species of interest.

$$i_D = nFAC_0\sqrt{(D_0/\pi t)}$$

i_D = *Current (Amps, A)*
n = *Number of electrons transferred by molecule (mol/mol)*
F = *Faraday constant ($9.6485x10^4$ C/mol)*
A = *Electrode area (cm^2)*
C_0 = *Concentration of the bulk (mol/cm^3)*
D_0 = *Diffusion coefficient of the reactant (cm/s^2)*
t = *Time (s)*

1.2.2.3 Pulsed amperometric detection

Pulsed amperometric detection (PAD) is a sensitive method which has been used for the detection of many compounds, including carbohydrates following separation by liquid chromatography (Neuburger & Johnson, 1987; Johnson & LaCourse, 1991, 1993), the detection of carbohydrates, amines and sulphur species (Johnson, Dobberpuhl, Roberts *et al*, 1993), detection of thiols and disulfides (Owens & LaCourse, 1997) and more recently for the detection of sulphur containing antibiotics following separation by HPLC (LaCourse & Dasenbrock, 1999), and the detection of sulphur-containing amino acids with disposable gold electrodes (Cheng, Jandik, Avdalovic, 2003). PAD is based on 'the application of triple-step potential waveforms to incorporate amperometric detection with alternated anodic and cathodic polarisations to clean and reactivate electrode surfaces' (Johnson & LaCourse, 1991) (Figure 1.4). These polarisations clean and reactivate the electrode surface, thus improving its sensitivity with respect to fixed potential amperometry.

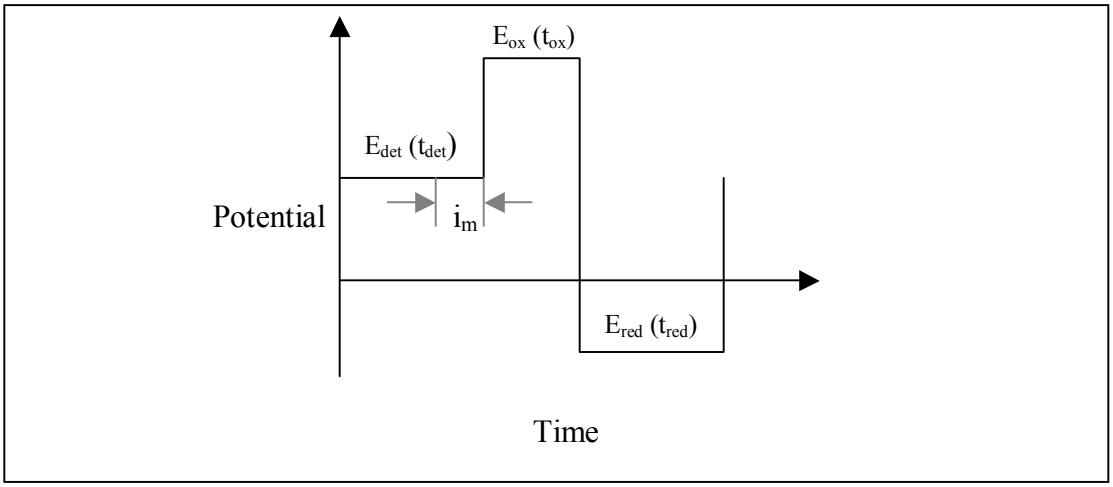

***Figure 1.4**: A single PAD cycle. Current is sampled at i_m. E_{det} is the anodic measuring potential, E_{ox} the oxidative cleaning potential, and E_{red} the cathodic reactivation potential. t_{det}, t_{ox}, and t_{red} are the time periods for E_{det}, E_{ox}, and E_{red} respectively.*

The detection potential (E_{det}) used in the waveform is chosen to suit the particular surface-catalysed reaction of interest, the current of which is sampled during a short time period (t_{det}) after a delay, near the end of the detection period (i_m). After detection, adsorbed species are oxidatively desorbed by an electrolytic process which occurs simultaneously with the anodic formation of surface oxide, by application of a positive step (E_{ox}) in the potential wave-form. Next, a negative step (E_{red}) is applied to regenerate the 'clean' electrode surface by cathodic dissolution of the oxide film prior to the next cycle of the wave-form.

1.2.2.4 Voltammetry

In linear sweep, or staircase voltammetry (LSV), the potential of the working electrode is swept across a potential range in a linear manner and the resultant current recorded. Considering the situation where the potential is increased with time, species are oxidised at the electrode surface at different potentials depending on redox properties of the analyte(s),

producing separate peaks at these potentials, pertaining to the analytes reacted. The current produced is plotted against potential as a voltammogram, and can be used to give information about different species in solution. In cyclic voltammetry (CV), as with LSV, the potential is swept, for example, forward in a linear manner versus time, before the 'direction' of the scan is reversed and sweeps back in a negative manner. The term cyclic arises from the closed loop drawn within the plot (Monk, 2001).

As Figure 1.5 shows, in the presence of a reversible redox species, a peak may be evident in both the positive and negative CV scans. In ideal, fully reversible systems, these peaks are of similar shape, and their peak heights and peak area will be the same. Oxidation occurs in the forward scan, and reduction in the reverse. The magnitude of the current is proportional to concentration. Cyclic voltammetry is a useful technique for identifying the potentials of interest for a species in solution prior to the application of other electrochemical methods (Owens & LaCourse 1997). It is also useful for determining reaction kinetics, diffusion data and the reversibility of a system.

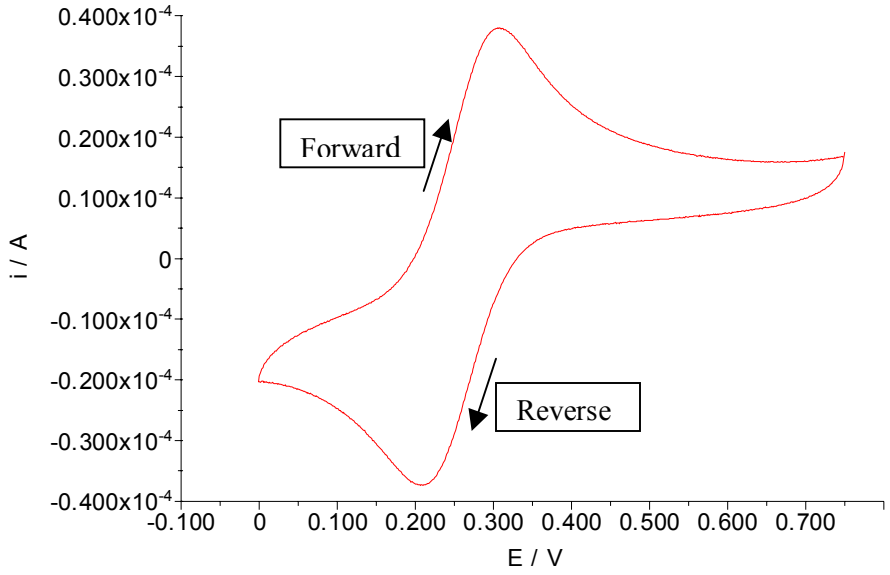

Figure 1.5: *Example of a Cyclic Voltammetry scan of ferricyanide*

1.2.2.5 Dual pulse staircase voltammetry

Dual pulse staircase voltammetry (DPSV) incorporates cleaning pulses to clean and reactivate the electrode, as with PAD. In DPSV, the cleaning phase is applied at the start of the scan, and followed by linear sweep (staircase) voltammetry, increasing in discrete steps to approximate a continuous waveform (Figure 1.6). The scan yields a voltammogram containing current-voltage peaks which correspond to different compounds present in the solution. This technique has been used successfully for the simultaneous voltammetric detection and quantification of glucose and fructose (Fung & Mo, 1995, Bessant & Saini, 1999), the detection of ethanol (Fung & Mo, 1996), and for the measurement of aliphatic compounds (Bessant, 1998). This technique has not yet been incorporated into most

commercially available potentiostats, but its use only requires simple modification of the linear sweep method that is incorporated.

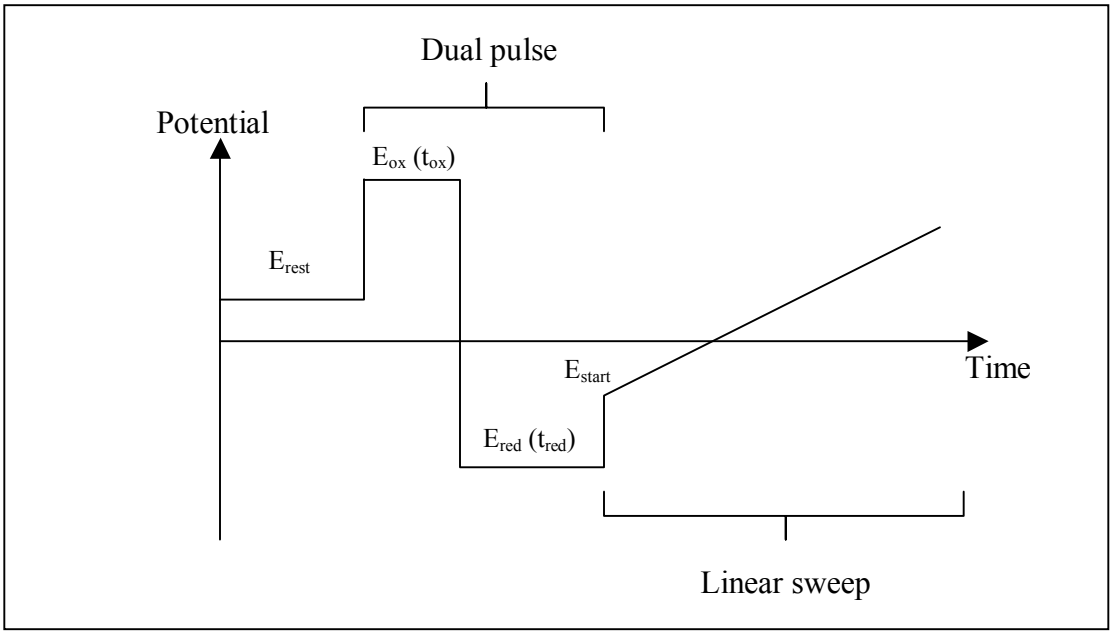

Figure 1.6: *DPSV waveform. E_{rest} is the resting potential, E_{ox} (t_{ox}) is the oxidative cleaning potential and time, E_{red} (t_{red}) is the cathodic reactivation and time. E_{start} is the potential at which the linear staircase sweep starts.*

1.2.3 Electroanalytical detection of H_2O_2

As mentioned, hydrogen peroxide (H_2O_2) is produced in wounds by phagocytosis and is therefore a potential marker of healing. H_2O_2 is also found in the tissues, since substantial amounts of H_2O_2 are present in beverages (coffee), and in urine and exhaled air (Clement, Halliwell & Long, 2000). Electrochemical determination of H_2O_2 is usually performed by oxidation at a platinum electrode, which is often modified by deposition of a film with enhanced electrocatalytic activity (Bertotti, Kosminsky & Matos *et al*, 2003). Detection of H_2O_2 is also important in biosensor construction, because many oxidase enzymes used in

biosensors such as glucose oxidase or alcohol oxidase produce H_2O_2 as an end-product, which can be directly electrochemically determined at the electrode (Gorton, Karyakin & Palleschi *et al*, 2003).

1.3 Biosensors

Biosensors are currently defined as analytical devices incorporating either: a biological material, such as a tissue, microorganism, organelle, cell receptor, enzyme, antibody or nucleic acid; a biologically derived material, for example recombinant antibody, engineered protein or aptamer; a biomimic such as a synthetic catalyst, combinatorial ligand or imprinted polymer. Furthermore, the recognition element should be intimately associated with, or integrated within, a physicochemical transducer or transducing microsystem, which may be optical, electrochemical, thermometric, piezoelectric, magnetic or micromechanical (Turner, 2005). Biosensors usually yield a digital electronic signal which can be related to the concentration of a specific analyte or group of analytes. Biosensors have been developed for use in a wide variety of sectors including medicine, drug discovery, environment, food, process industries, security and defence.

Enzyme based electrochemical biosensors can be classified as (Saxena & Malhotra, 2003):

i) Potentiometric biosensors, which use ion-selective electrodes to determine changes in concentration of chosen ions, for example hydrogen ions.

ii) Amperometric biosensors, which determine the electric current associated with the electrons released during redox processes.

iii) Conductimetric/Impedimetric biosensors, which determine conductance/impedance changes associated with changes in the overall environment.

The next section focuses on amperometric biosensors, since amperometric biosensors were used in this thesis.

1.3.1 Amperometric biosensors

Amperometric biosensors have proven the most commercially successful biosensor devices to date, with applications as diverse as breath alcohol detection and blood glucose monitoring. Biosensors may be operated in a two electrode configuration (a working electrode and joint reference/counter electrode) if currents are low enough to avoid disturbing the reference electrode equilibrium potential, and the *iR* drop through the solution does not significantly alter the applied potential from the potentiostat. To prevent both these problems a three electrode configuration is often adopted using an auxiliary (Counter) electrode through which the current arising from analyte-specific reactions at the working electrode may pass.

Electrode designs are constantly evolving, ranging from the standard solid laboratory electrodes, screen printed electrodes of varying composition, to needle type electrodes for implantable devices. A discussion of the three generations of biosensors, exemplified by the glucose sensor is included in the glucose measurement section that follows.

1.3.1.1 Glucose measurement

Glucose biosensors are by far the most commercially successful biosensors to date, with over 40 home blood glucose meters on the market for those with diabetes (Newman & Turner, 2005). The main share of the market is occupied by Roche Diagnostics, LifeScan, Abbott and Bayer. The most commonly used enzymes in glucose biosensors are glucose oxidase (GOx) and glucose dehydrogenase (GDH). GOx enzymes oxidise ß-D-glucose substrate, accepting electrons at its FAD prosthetic site in the process. GOx is able to transfer these electrons to molecular dioxygen present in the sample, resulting in the production of hydrogen peroxide.

By immobilising GOx close to, or onto a suitable transducer, an amperometric biosensor can be made, monitoring either O_2 depletion of H_2O_2 production, and as such represents an example of a first generation biosensor.

One difficulty in using GOx is the potential problem of dissolved dioxygen limitation. To overcome this, oxygen can be replaced with an artificial mediator (electron acceptor). A mediator is a redox couple that can shuttle electrons between the redox centre of the enzyme and the electrode, and can be electrochemically regenerated at potentials where interference from species such as ascorbic acid (vitamin C) and acetaminophen (paracetamol) are minimised (Newman & Turner, 2005). Commonly employed mediators include hydroquinone, ferrocene, certain redox dyes and ferro/ferricycanide. Mediated enzyme systems represent the second generation of biosensors.

An alternative approach is offered by the so-called 'third generation biosensors'. In this case, the electrode is configured such that it is able to exchange electrons directly with the enzyme active site deeply buried within the protein, thus negating the need for electron shuttle molecules. The difficulty in engendering electrical contact between the active site of the enzyme and the electrode make this a difficult and rarely reported approach (Varma *et al*, 1993), but has been reported by Yang, Lanqun and Takeyoshi, *et al* (2005), Christenson, Dock and Gorton *et al* (2004), Xu & Han (2004) for example.

The first widely-commercially successful glucose biosensor was a mediated device (second generation) based on a screen printed disposable sensor design called the ExacTech device, developed by MediSense in conjunction with the Universities of Cranfield and Oxford. The majority of products today utilise similar technology, i.e. using the basic concept of an amperometric biosensor, employing GOx and electrochemical mediators on a disposable strip format. This type of glucose monitor is based on the measurement of glucose in a blood sample typically taken from the finger using a small lancet.

Since finger pricking is uncomfortable, other sampling sites and methods have been investigated. For example, the GlucoWatch® biographer - a continual, non-invasive, automatic glucose monitor. This device incorporates the use of an amperometric biosensor, which detects glucose in interstitial fluid as it is extracted through intact skin by a process of reverse iontophoresis every 20 minutes, for 12 hours, after a 3 hour warm up period. The amount of glucose extracted within one three minute iontophoresis cycle is estimated to be between 50 – 500 picomol. It is favourable over the finger-prick methods, since it lacks the

discomfort, is convenient, automated, and facilitates intensive glucose control regimes. The GlucoWatch® is a small, wrist-watch device capable of both sampling and detection, contains all necessary circuitry, and a digital display. The operation of the device is controlled by a microprocessor, which also converts the sensor signals into glucose readings. The circuitry includes two independent potentiostat circuits to operate the biosensors, and a galvanostat circuit for the iontophoresis. Temperature fluctuations and perspiration are detected by the incorporation of temperature and skin conductivity sensors. The AutoSensor itself is disposable, and fits into the skin-side of the biographer. It contains two identical biosensors and iontophoresis electrodes, two hydrogel disks which serve as biosensor electrolyte, glucose reservoirs, and also have the glucose oxidase enzyme dissolved into them. The biosensor working electrodes have a screen-printed layer of Pt/C composite ink. The reference and counter electrodes have screen-printed Ag and Ag/AgCl layers. The counter electrode is also used as the iontophoresis electrode. However, the Glucowatch has not been as successful as hoped, due to its high cost compared to other glucose measurement devices available, and problems with skin irritation after prolonged use (Garg, Jovanovic & Potts *et al*, 2000; Panchagnula, Pillai, Nair *et al*, 2000)

For further information on finger prick biosensors, minimally invasive systems and the potential of non-invasive systems such as fluorescence or IR spectroscopy, readers are referred to Newman & Turner (2005) who have reviewed blood glucose biosensors from a commercial perspective.

1.3.1.2 Alcohol measurement

Another major area of biosensor use is for the detection of characteristic odours of alcohol in breath, and alcohol in beverages. Sprules, Hartley, Wedge *et al* (1996) investigated the use of screen printed amperometric biosensors for the measurement of alcohol in beverages for example. Kim, Lee, Lee *et al* (1999) investigated using an amperometric biosensor to determine breath alcohol, and was able to measure over the concentration range 20-800 ppm. The selective, sensitive, and reliable detection of ethanol in the breath of a vehicle driver is essential to determine whether a driver has consumed too much alcohol. This biosensor utilises nicotinamide adenine dinucleotide (NAD^+) cofactor, which is reduced in the presence of ADH and ethanol to NADH (Kim, Lee & Lee *et al,* 1999) which can be subsequently oxidised at an electrode poised at a suitable oxidising potential.

$$CH_3CH_2OH + NAD^+ \xrightarrow{ADH} CH_3CHO + NADH + H^+$$

$$NADH \xrightarrow{Electrode} NAD^+ + H^+ + 2e^-$$

This biosensor consists of an Ag/AgCl reference electrode, an active working electrode containing ADH, and a 'compensator' electrode containing a protein analogue (typically bovine serum albumin) in place of ADH. The differential signal that is produced between the active and inactive electrodes minimises the interference from oxidisable species in a person's breath. Before measurement, the biosensor is hydrated in phosphate buffer at pH 7.4. Ethanol catalysis and stoichiometric levels of NADH are produced by the enzymatic

reaction, with the NADH being subsequently oxidised at the active electrode poised at a potential of +470mV (vs. Ag/AgCl), and compared to the compensator electrode.

There are few commercially available amperometric biosensors based on gas-phase analysis, as opposed to liquid-phase analysis. This is because of the difficulty associated with the use of enzyme electrodes to monitor gaseous samples without aqueous media. For this reason, gas-phase biosensors, like the differential-type amperometric biosensor described above, are pre-hydrated in buffer, which is retained in the enzyme-immobilised gel layers. Small thick-film based sensors can be made cheaply by conventional screen printing technology.

1.3.2 Screen-printed electrodes

Screen-printed electrodes are commonly used instead of the conventional solid-state electrodes because they lend themselves more easily to mass production and commercial use. Layers of speciality inks are deposited sequentially onto an insulating support or substrate. They have certain favourable characteristics that have contributed to their widespread use in environmental, clinical or industrial applications. Benefits include their small size, low cost, simplicity of manufacture and disposability. They have been used as amperometric sensors and/or biosensors, for example in the detection of maltose and glucose (Feng, Zhang & Zhang *et al*, 1998), sulphur-containing amino acids (Cheng, Jandik & Avdalovic 2003), and alcohol in beverages (Sprules, Hartley & Wedge *et al* 1996). Gorton, de Mattos and Ruzgas (1996) have discussed the properties of modified gold and platinum screen printed electrodes for use as sensors and biosensors, and Hart,

Turner & Hopcroft (1996) compared the use of screen- and ink-jet printing to produce electrodes. Alegret, Albareda-Sirvent & Merkoci (2000) have reviewed the configurations used in the designs of screen-printed enzymatic biosensors.

Often, the surface of the screen printed electrode is modified for a particular application. For example, coating the electrode surface with a transition metal such as a hexacyanoferrate (HCF) film, confers additional electrocatalytic properties on the electrode. For example, reduced form Prussian blue (FeHCF) can electrocatalytically reduce H_2O_2 by acting as an electrocatalytic mediator, (Gorton, de Mattos & Ruzgas, 1996; Ricci & Palleschi, 2005; O'Halloran, Pravda and Guilbault, 2001). Certain analytes can be amperometrically detected at low potentials by combination of catalytic materials with oxidase enzymes,

The versatility and simplicity of screen-printing means that designs can be simply and cheaply configured, and sensor and biosensor strips are increasingly being incorporated into small hand held or portable devices.

1.3.3 Direct (label-free) detection of bacteria with biosensors

Most microbiological tests are performed in large centralised laboratories, and require highly trained technical staff. However, the desire for tests to be portable, rapid and sensitive has led to the development of biosensor technologies in the clinical field. Since one aspect of this thesis is concerned with bacterial detection, a summary of the main direct and indirect biosensor technologies reported for bacterial detection follows.

The monitoring of cells at solid-liquid interfaces is generally based on the direct measurement of a biochemical reaction at the transducer surface, for example, changes in: pH, oxygen consumption, ion concentrations, potential difference, current, resistance, or optical properties. For example, certain optical biosensors can detect minute changes in the refractive index when cells bind to immobilised receptors on the transducer surface. An interferometer (Edwards, Hartman & Schneider, 1997) is an optical unit consisting of an LED/filter excitation source, and a photodiode detection system. The increase in CO_2 concentration that can arise from active bacterial metabolism, may be detected by the change in emulsion of the aqueous colorimetric pH indicator, which in turn modulates the fluorescence detected by the photodiode.

Bioiluminescence biosensors

Certain enzymes emit photons as a by-product of their catalytic degradation of substrate molecules, a phenomenon known as bioiluminescence. This phenomenon maybe used to detect the presence and physiological conditions of cells. These systems have been used to detect a wide variety of microorganisms, for example *of Salmonella Newport* and *E.coli* (Blasco, Murphy & Sanders *et al*, 1998). Bacteriophages are used to lyse bacteria, such that the cell content released can be measured by ATP bioluminescence. This is an attractive approach due to its high specificity and ability to distinguish between viable and non-viable cells. However, the assay time is long, and the method is not suitable for determining low bacterial numbers.

Piezoelectric biosensors

These systems may be used for direct label-free detection of bacteria, and other applications, with real-time output. The surface of a PZ sensor is coated with selective ligands, such as antibodies, and placed in a solution containing bacteria. Bacteria of the required specificity will be bound by the antibodies, which results in an increase in the mass of the crystal, and a proportional decrease in the resonant frequency of the crystal. These have been developed for *Vibrio cholerae* (Carter *et al*, 1995) and *Salmonella typhimurium* (Prusak-Sochaczewski *et al*, 1990) for example.

Electrical impedance biosensors

This method is useful in the detection of bacteria in clinical specimens, to monitor quality, detect specific food pathogens, and in industrial microbial process control. Cell density, growth, and long term behaviour of cells on the electrodes cause a change in the impedance of the biosensor. A reusable Bulk Acoustic Wave Impedance Sensor has been developed to continuously detect the growth of *Proteus vulgaris* on the surface of solid medium (Deng *et al* (1996).

1.3.4 Indirect Detection of Bacteria

Fluorescent immunoassay techniques

The immunogenic nature of microorganisms, due to the presence of proteins and polysaccharides in their outer coats, allows the development of fluorescent immunoassay (FIA) techniques for bacterial detection. Fluorochrome molecules are used to label

immunoglobulins, absorb light at a short wavelength, and emit it at a higher wavelength which is detected by fluorescent microscopy. FIA utilises the high degree of specificity inherent in immunological reactions.

Microbial metabolism based biosensors

Microorganisms can transduce their metabolic redox reactions into quantifiable electrical signals by oxidoreductase reactions and a mediator. The microbial content of a sample can be determined by monitoring the microbial metabolism. For example, oxygen consumption could be detected by a transducer. It may also be possible to detect other metabolic products of bacteria.

Electrochemical immunodetection of bacteria

The advantages of electrochemical sensors over optical sensors are that they can operate in turbid media, with comparable instrumental sensitivity, and are also easier to miniaturise. The continuous response of an electrode system also allows on-line control. Light addressable potentiometric sensors (LAPS) based on field effect transistor (FET) technology has been used successfully for the immunoassay of bacteria (Abdel-Hamid, Atanasov & Ivnitski *et al,* 1999).

Further information on biosensors for the detection of pathogenic bacteria can be found in Abdel-Hamid, Atanasov, Ivnitski *et al* (1999) who have reviewed the aforementioned techniques in 1.3.3 and 1.3.4 in detail.

1.4 Electronic Nose

1.4.1 The human olfactory system and odours

The inspiration behind the mechanisms of an electronic nose is that of human olfaction. Therefore, to understand the operation of an electronic nose it is important to first understand the biological act of 'smelling' with the human olfactory system that enables us to characterize an odour (Gardner, Craven & Bartlett, 1996). Therefore, a description of the human olfactory system and the properties of odorous molecules shall follow before discussing the so-called method of 'machine olfaction'.

Humans have three sensory systems which play a part in the sensation of flavour. These are olfaction or sense of smell, gustation or sense of taste and trigeminal sense (response to irritant chemical species). Of these three, smell is the dominant contributor to the sensation of flavour, and has much wider powers of classification than the taste or trigeminal senses. Smell alone can often determine the flavour profile of a product.

Odorant molecules stimulate the human olfactory system located in the human nose. Here, they are drawn into the nasal cavity across the epithelium, which contains a mucous layer and olfactory hairs or cilia leading into olfactory cells. The cilia have G-receptor binding proteins which act as chemosensory receptors. Since there are only a limited number (~100) of receptor proteins, they require partially overlapping sensitivities in order to allow complex smells to be identified. There are ~100 million olfactory cells, which serve as signal amplifiers and generate secondary messengers. These messengers generate signals which travel from the olfactory nerves to ~5000 glomeruli nodes in the olfactory bulb via

axons. In the olfactory bulb, the signals are further processed by ~100,000 mitral cells before they are sent via a granular cell layer to the higher sensory centers in the cerebral cortex of the brain. The receptor cells only live an average of 22 days, and are believed to have a low sensitivity in the ppm range, and low specificity. However, the signal amplification and neural processing that subsequently occur greatly enhance the sensitivity and discrimination between thousands of odours (Gardner & Bartlett, 1994). The perceived intensity of an odour is not linearly related to its concentration, but typically a sigmoidal relationship. A more detailed analysis of each aspect of the human olfactory system can be found in Gardner & Bartlett (1999).

1.4.1.1 Properties of odorous molecules

Many simple odours may arise from single molecular species. Such odorants are typically hydrophobic and polar with a molecular mass of 30-300 Da. However, most natural smells, perfumes and flavours are complex mixtures of chemical species frequently containing hundreds or maybe thousands of constituents. Subtle differences between the relative quantities of these constituents can determine the overall odour of a product. It is essential that the molecules are volatile in order to be carried up into the nose via the nasal passages to the olfactory receptors. Molecules heavier than 300 Da are generally not active odorants at room temperature. However, volatility is not just determined by molecular weight. The strength and type of interactions between molecular species is also important, as is the geometrical shape and charge distribution of the odorant species. Typically, for example, polar molecules are more volatile than non-polar molecules. Odorous molecules generally possess one or two functional groups within the structure which makes them

more polar. Examples of two functional group structures that are associated with odorous molecules are shown below.

Alcohol

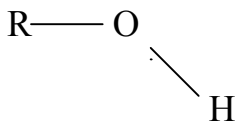

Acid

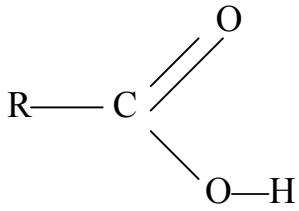

Aromatic molecules are also important in odour chemistry, since they are often highly odorous and are generally chemically stable. This is because they have six delocalized π–electrons involved in the π bonding molecular orbitals localized above and below the plane of the molecules, referred to as aromaticity. A more in depth description of the molecular structure of odour molecules and intermolecular forces can be found in Gardner & Bartlett (1999).

1.4.2 Machine olfaction

In many industries, the human nose is still the main 'instrument' used to evaluate the smell and flavour of products, such as perfumes and foodstuffs. However, this is a costly process, since trained panels of experts are required. Physicochemical properties are measured using conventional analytical equipment, such as gas chromatography-mass spectroscopy (GC-MS). As well as being time consuming, these methods often fail to detect some key flavour constituents since they fall below the capability of the instrument. These factors generated

a demand for electronic instruments that can imitate the human olfactory system, and also provide a low cost, rapid sensory system.

The first reported electronic nose was in 1964 by Wilkins & Hatman, who studied the redox reactions of odorants at an electrode. However, the first report of the concept of an electronic nose as an intelligent chemical array sensory system for odour classification, was not until the early eighties, by Persaud & Dodd (1982) and Ikegami & Kaneyasu (1985). The term 'electronic nose' was first used in the late eighties and appeared at a conference in 1987 in the UK (Gardner, 1987). There are various synonyms for electronic nose such as artificial nose, mechanical nose, odour sensing system, and as yet the term has not been defined. A definition proposed by Gardner & Bartlett (1994) shall be used for the purpose of this thesis: 'An electronic nose is an instrument, which comprises an array of electronic chemical sensors with partial specificity and an appropriate pattern-recognition system, capable of recognizing simple or complex odours.'

As the name 'machine olfaction' suggests, it is an intelligent chemical array sensor system analogous to the human nose. The process of machine olfaction fundamentally consists of three stages: an electronic sensor array, a pre-processor and a pattern recognition engine (PARC). The broadly responsive sensor array imitates the olfactory receptor cells, the pre-processing corresponds to the processes of the olfactory bulb, and the computer based pattern recognition system mimics the cerebral cortex of the brain. The diagram in Figure 1.7 illustrates the basic analogies between human and machine olfaction.

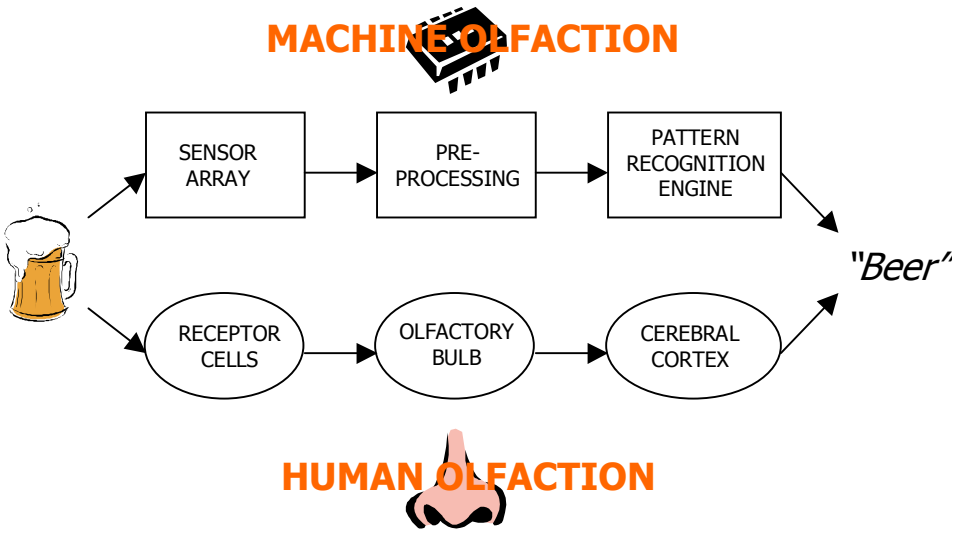

***Figure 1.7**: Diagram showing the analogy between the three basic stages of machine and human olfaction.*

1.4.3 Sensors

The primary requirement of the sensor array is to generate a pattern of responses that is discernibly different for different samples. The sensors in the array of an electronic nose are therefore required to have partial sensitivity to permit response to a broad range of gases or odours, i.e. they should differ but overlap between sensors across the array, in a similar manor to biological olfactory receptors, thereby ensuring that the entire pattern of response across the sensor array is analysed (Gardner & Bartlett, 1999). The sensor array responses are processed by specialised computer software which produces profiles, and thus converts smells into a digital representation, or 'fingerprint' (Gibson, Prosser, Hulbert, 2000). This enables the identification of many odours that may contain hundreds of individual chemical components. This is opposite to the requirements of an ideal gas sensor, which should respond to only one gas.

It is desirable for the sensors to have a reasonable response time and recovery time. It is also important that the individual sensors are reproducible in their response to a given odour, and that the response is reproducible between sensors of nominally the same type. This eliminates the need to fully retrain and recalibrate the system if a sensor needs replacing. Numerous sensor technologies have been utilised in sensor arrays, most notably inorganic semi-conducting materials such as metal-oxide sensors, acoustic wave sensors and conducting polymers.

1.4.3.1 Metal-Oxide Sensors

Metal oxide semi-conductor (MOS) gas sensors are available commercially from suppliers such as Fiagro Engineering (Japan) and Capteur mixed MOS sensors from City Technology (UK), and are the most widely used sensors for construction of arrays for the measurement of odours. The most widely used material in metal oxide sensors is tin-dioxide, SnO_2, doped with small amounts of catalytic metal such as palladium or platinum. Varying the choice of catalyst and operating conditions enables these sensors to be used in a wide range of applications. The construction of each of these sensors is similar, consisting of a ceramic support tube coated with tin oxide (and catalysts), and containing a platinum heater coil (Gardner & Bartlett, 1999).

The gas or odour is sensed by a change in resistance at the semiconductor. As the concentration of adsorbed oxygen at the semiconductor surface changes, the change in resistance proportional to the concentration of the analyte can be measured. At ambient conditions, oxygen adsorbs to the surface of the metal oxide layer and dissociates to form

O-, by extracting electrons from the semiconductor. Semiconductors come in two types, *n* or *p*. The electron extraction will respectively increase or decrease the resistance. For example, if the semiconductor is exposed to a reducing gas, oxygen will be removed from the surface and thus will gain electrons, leading to a positive (*p*) or negative (*n*) change in resistance, depending on semiconductor type (Lee-Davey, 2004). Other factors such as humidity also have an effect on resistance. At low temperatures it is possible that water may form. This complicates the detection of volatile odours (Gibson, Prosser, Hulbert, 2000). However, these sensors are usually operated at elevated temperatures of 100-600 °C which reduce the negative effects of water.

In terms of suitability to the application of wound monitoring, MOS sensors have the advantages of low cost, and fast response times. They are also particularly sensitive to volatiles such as alcohols (0.1-100 ppm) (Ragazzo-Sanchez, Chalier, Chevalier *et al*, 2006; Hansen, Petersen, Byrne, 2005) and are not sensitive to the detection of sulphur- or nitrogen-based odours. The disadvantage of MOS sensors and other chemical sensors is that they are susceptible to baseline drift, defined by D'Amico & Di Natale (2001) as: "a slow unpredictable change of the sensor response, undefined from the statistical point of view, which is superimposed to both the signal and noise levels". Drift is particularly insidious in machine olfaction, since their utility is based upon pattern recognition models developed from particular responses. Therefore it is important that drift behaviour is identified early on and compensated for by the incorporation of a suitable mathematical models.

1.4.3.2 Conducting Polymer Sensors

Organic materials offer a wider choice of sensor materials, and more importantly, can incorporate functional groups that can interact with different classes of odorant molecules. For example, conducting polymers, such as poly(pyrrole), and biological lipid coatings. They can also be operated closer to room temperature (20-60°C). As a result of this, the first commercial electronic noses used conducting polymer gas sensor arrays.

Polymer sensors generate a change in resistance when analyte adsorbs onto the polymer film and induces swelling. However, they are susceptible to changes in humidity, since it affects the baseline structure and swelling behaviour of the polymer (Gardner & Bartlett, 1994, 1999).

1.4.3.3 Acoustic wave sensors

Acoustic wave gas sensors detect the effect of sorbed molecules on the propagation of acoustic waves. The basic device consists of a piezoelectric substrate, usually quartz, coated with a suitable sorbant coating. Sorption of vapour molecules into the sorbant coating is detected by changes in wave velocity, and hence frequency and amplitude of oscillation of the sensor. Acoustic wave sensors operate at ultrasonic frequencies of typically 1 to 500 MHz.

Two main types of acoustic wave sensors exist: bulk acoustic wave (BAW) and surface acoustic wave (SAW). BAW sensors rely upon the application of an electric field to make the quartz crystal oscillate at its resonant frequency. SAW sensors exploit wave

propagation across the sensor surface. Both of these acoustic wave-type sensors require excitation by a.c. voltage.

1.4.4 Signal pre-processing

Figure 1.8 depicts the generic architecture of an electronic nose. Individual sensors *i* produce a time-dependent electrical signal $y_{ij}(t)$ in response to odour (a set of unknown odour samples A, B, C of unknown class *j)*. The rise and decay time of the sensor will depend upon one or more of the following parameters (Gardner & Bartlett, 1994):

1) the flow delivery system that carries the odour from the source to the sensor array e.g., the flow profile and type of carrier gas;
2) the nature of the odour, e.g., type, concentration;
3) the reaction kinetics of the odour and the active material;
4) the diffusion of the odour within the active material;
5) the nature of the sensing material e.g., physical structure, porosity, thermal time-constant;
6) the nature of the substrate supporting the active material e.g., thermal conductivity, acoustic impedance;
7) ambient conditions, e.g., temperature of active material, carrier gas, humidity, pressure.

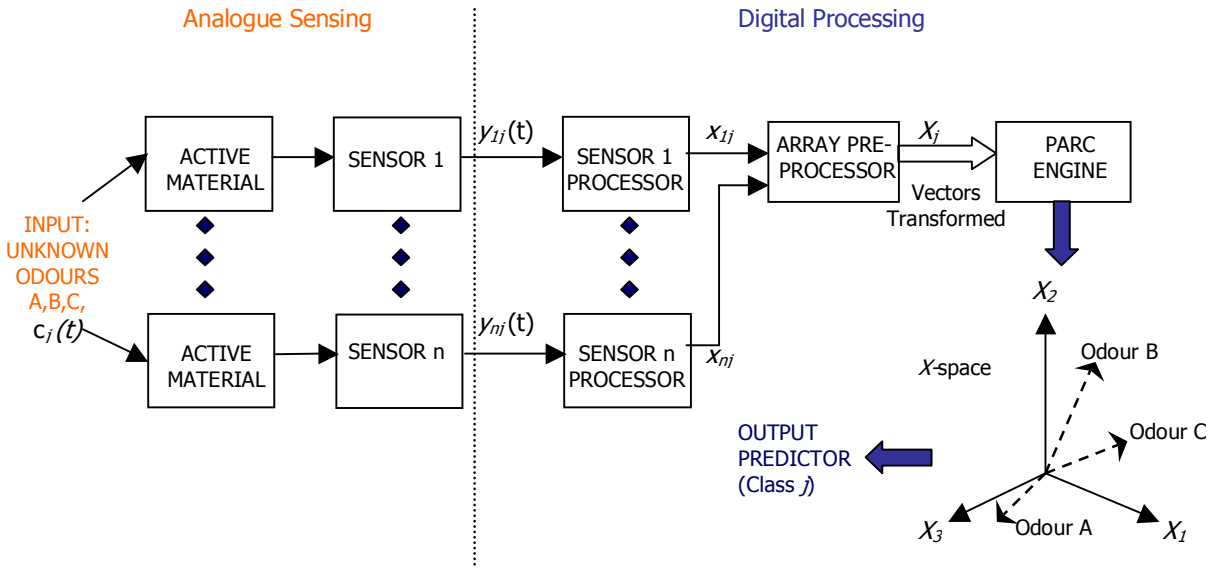

Figure 1.8: *Architecture and processing stages of an electronic nose, including unsupervised learning of unknown odour inputs. The difference between the response vectors x_j are maximized in the transformed vector space, e.g. X-space for eigenvectors in PCA. (Based on Gardner & Bartlett, 1994, 1999).*

An array of *n* sensors gives a response vector X_j. The array response vector may be pre-processed to help the discrimination process. The technique of baseline manipulation relates the sensor response to a constant signal value, the baseline. For example, with MOS sensors, the baseline signal is the sensors response to air. The signal noise can be reduced parametrically or as a specific requirement for the input to a pattern recognition engine. The scale of the response vectors is often normalized so that the output of individual sensors can be visualized within the range. This process conditions the data so that all features in the response vectors are of the same magnitude. Next, the vectors are analysed by a suitable pattern recognition technique.

1.4.5 Pattern recognition techniques

The processing of input odour signals in an electronic nose can essentially be divided into two methods: unsupervised and supervised. The objective of unsupervised learning is to discriminate between unknown odours by enhancing the differences between their related input vectors, while supervised learning aims to classify unknown odours as known ones that have been learnt during earlier training and calibration of the PARC engine.

The pattern recognition technique of supervised learning essentially involves the introduction of known sets of odours to the sensor array, which produce corresponding sets of response vectors. These sets are known as training or calibration sets, and are used to generate a knowledge base. The knowledge base is further extended by incorporating regression coefficients in a parametric model, or a non-parametric model such as a neural network. Once the system has been trained, unknown odours can be analysed with the electronic nose using the knowledge base to assign the most likely class of odour. Artificial neural networks can handle non-linear data, and are tolerant to sensor drift or noise (≈10%). They also produce lower predictive error rates than chemometric techniques (Gardner & Bartlett, 1994; Ciosek & Wroblewski, 2006).

Figure 1.8 also illustrates the spread of signals through an electronic nose using an unsupervised pattern recognition technique. The set of N unknown odour samples produce a corresponding set of N unknown array vector responses (x). The vectors are separated in multidimensional space by maximizing the distances between the vectors. This can lead to a set of p clusters in a feature space of reduced dimensionality, which can be associated

with the known classes of odour (i.e. j takes the value of 1 to p). Techniques such as principle component analysis (PCA) and cluster analysis are useful for displaying the differences of multivariate data in a reduced dimensionality.

1.4.5.1 Principle components analysis

Since PCA was the methodology implemented for the investigation of odour analyser response to imitation wound odour in this thesis, a brief description of this technique follows. Further details of PCA can be found in Gardner & Bartlett (1999), Wold, Esbensen & Geladi (1987), and Massart, Wu & Guo *et al* (2002). PCA is an unsupervised technique (i.e. does not require a training set), multivariate (i.e. can consider many variables simultaneously), non-parametric statistical technique. It is widely used, due to its powerful ability to discriminate between simple and complex datasets, such as array-generated odour profiles. PCA analyses the inter-relationships between a large number of variables and seeks to reduce them to a smaller number of indices, called principle components (X_p), that describe their common underlying dimensions.

Each principle vector accounts for a degree of variance in the data. The principle components are ordered so that the first component, X_1 displays the greatest amount of variance, followed by the second greatest as X_2 and so on. It is typical for a large proportion of the variance in the data to be within the first two principle components. Therefore, a plot of these two principle components can be used to represent a large proportion of the variance in the data, and thus determine any distinct groups of odours. High X_p values show a disciminating sensor, whereas values nearer to zero contribute noise to the score. PCA is

a useful technique to explore the functionality of an electronic nose, by determining differences in multivariate data.

1.4.6 Applications of electronic nose technology

Commercial electronic noses were first launched in the 1990s, for example, from Alpha MOS in 1993, Neotronics and Aromascan in 1994, Bloodhound Sensors and HKR Sensorsysteme in 1995 (Gibson, Hulbert, Prosser, 2000). Commercial odour monitors have been produced for several years, such as the Portable odour monitor by Sensidyne Inc, USA, which can detect the intensity of an odour using only one sensor.

Electronic noses have been used in a variety of applications, mostly to classify the smells of beverages and foods (Schaller, Bosset and Escher, 1998), giving information about the grade or quality of whiskeys, beers, and wines (Lamagna, Reich, Rodriguez, *et al*, 2004; Marti, Busto, Guasch et al, 2005), or freshness of meat and fish (Blixt, Borch, 1999; Olafsdottir, Nesvadba, Di Natale, *et al,* 2004) for example. They have also been reported for use in monitoring cell culture (Bachinger, Riese, Eriksson, *et al*, 2000), the automotive industry (Garrigues, Talou, Nesa, 2004), environmental monitoring (Onkal-Engin, Demir, Engin, 2005; Nake, Dubreuil, Raynaud *et al*, 2005), and the characterisation of perfumes (Penza, Cassano, Tortorella *et al,* 2001; Yang, Yang and Peng *et al*, 2000). Odour analysis is also a promising area of interest in medical diagnostics. Portable, application specific devices could be used for a wide range of diseases, and are likely to become more common and user friendly for the detection and identification of clinical infections in the future.

Magan, Pavlou, McNulty *et al* (2002) have reported the use of an electronic nose for the diagnosis of urinary tract infections (UTIs), by examining the volatile production patterns produced by bacterial contaminants in urine samples. Larsson, Mardh and Odham (2000) have investigated the use of an electronic nose to detect breath alcohol, using ANNs for the prediction of ethanol concentration. Gibson, Prosser, Hulbert, Pavlou (2000) reported a project carried out in 1996 between Bloodhound Sensors Ltd with Oxoid Ltd, investigating selective culturing techniques and subsequent measurement of the odours generated by the organisms. A 4-6 hour incubation time was found to be sufficient to produce characteristic odours. A number of strains of *E.coli, P.mirabilis, P.aeruginosa* and *S.aureus* were used to train a neural network, and were identified with 95% confidence match. Gibson, Prosser, Hulbert *et al* (1997) have also studied the detection and simultaneous identification of 12 different bacteria and 1 yeast using headspace samples from plate cultures using an electronic nose and neural networks with a classification rate of 93.4%. Gardner, Shin and Hines (2000) have investigated the use of an electronic nose system based on an MOS sensors array to diagnose illness from the breath of dairy cows. In 2005 the same group also published a paper on the identification of *Staphylococcus aureus* (MRSA, MSSA and C-NS) from ear, nose and throat infections using an electronic nose. An array of 32 polymer carbon black composite sensors were exposed to swab samples from patients in hospital known to be infected, to produce distinctive response patterns for each vapour. Swabs were cultured for 24 hours before 'sniffing' with the electronic nose. This was followed by a combination of three statistical techniques PCA, self-organising mapping, and fuzzy C means, with the objective of producing clusters of the different bacteria species and prediction with an accuracy of 99.69%.

Although in the aforementioned study culturing time was long, and no attempt was made to determine the limits of detection or the chemical make up of the odours, the results from this and other initial investigations into the use of odour analysis in clinical applications are encouraging and suggest that odour analysis is a worthwhile area of continued investigation for the identification of bacterial species for a range of clinical conditions, such as UTI's, throat infections, lung cancer, diabetes or hospital acquired infection of wounds. Odour analysis has the prospect of supplying answers to medical practitioners by measuring distinct odours characteristic of certain clinical conditions, such as acetone of the breath of diabetics for example. It is hoped that one day odour analysis may also form an integral part of diagnostic medical practice in hospitals, and in the case of this thesis, be used to provide rapid diagnostic information about the nature of a wound environment in an effort to help combat the growing threat of hospital acquired infections such as MRSA.

1.5 Chromatographic techniques and test kits

Chromatography is a widely used standard technique, both for routine analysis and for the validation of new and developing analytical technologies. It is a separation procedure for resolving mixtures and isolating components, based on differential migration, i.e. the selective retardation of solute molecules during passage through a bed of sorbant or porous material (stationary phase). As solvent (mobile phase) flows through the column, the solutes travel at different speeds depending on their relative affinities for the stationary phase. The solutes are separated, and elute from the column at different times. The pattern of solute peaks emerging from a chromatographic column is called a chromatogram.

Chromatographic analysis has been described in detail elsewhere (Kolb & Ettre, 1997) but a brief description of the main chromatography techniques follows.

1.5.1 Liquid chromatography

Liquid chromatography can be classified into three types. In adsorption chromatography, the stationary phase is an adsorbent such as gel, and separation is based on the repeated adsorption and desorption of solute species on the stationary phase. There are two modes for this type: normal and reverse. Normal phase chromatography utilises a more polar stationary bed, with the mobile phase being more non-polar, thus polar species are retained longer. Reverse phase chromatography is the opposite of this. In ion exchange chromatography, ions are held on a porous insoluble solid and are exchanged for ions in a solution that are brought in contact with the solid. Synthetic ion exchange resins are used in applications such as water softening and solution purification. The resins are high-molecular-weight polymers that contain large numbers of an ionic functional group per molecule. Cation-exchange resins contain acidic groups such as sulfonic acid groups, and anion-exchange resins contain basic groups. In size exclusion chromatography, the column is filled with porous material, resulting in separation based on size. Larger molecules that are too large to enter the pores are eluted first, whilst smaller molecules are more able to penetrate the pores and thus take longer to elute. This technique is also often called gel permeation chromatography. In all types, as molecules are eluted from the column, they are detected and a chromatogram is produced (Skoog, West, Holler, 2000).

1.5.2 Gas chromatography

In gas chromatography (GC), the mobile phase is a gas. Gas chromatography is widely used as an analytical tool for separating relatively volatile components such as alcohols, ketones, aldehydes and many other organic and inorganic compounds. In gas chromatography, the sample is vaporized and injected onto a chromatographic column. The sample must be of a suitable volume, and is introduced as a "plug" of vapour. Calibrated microsyringes are used to inject liquid samples through a rubber or silicone diaphragm or septum into a heated sample port located at the head of the column. The sample port is usually about 50 °C above the boiling point of the least volatile component of the sample. Elution is brought about by the flow of an inert gaseous mobile phase, commonly helium. Many changes and developments have occurred in gas chromatographic instruments since their first commercial introduction. Microprocessors are used for automated control of most parameters, such as column temperature, flow rates, and sample injection. Columns have been developed that are capable of separating components of complex mixtures in relatively short times.

Detection devices must be used which are able to respond to minute quantities of solutes as they exit the column. The ideal detector would also have a linear response, stability, and uniform response for a wide variety of chemical species. Several types of detector exist. The effluent from a chromatographic column is often monitored continuously by selective techniques such as spectroscopy or electrochemistry, such as mass spectroscopy (MS) or Fourier Transform IR spectroscopy (FTIR), to give techniques such as GC-MS. These so-called 'hyphenated techniques' are powerful tools for the identification of components of

complex mixtures. Computer-based chromatography instrumentation often incorporate large databases to compare spectra and identify compounds eluting from the chromatographic column.

1.5.3 Applications of Chromatography

1.5.3.1 Chromatographic detection of bacteria

Bartlett, Gorbach & Mayhew *et al* (1976) hypothesized that short-chain fatty acids (SCFA) produced by certain organisms might serve as markers in clinical samples. Table 1.6 summarises this and other reported cases of the use of different chromatographic techniques.

1.5.3.2 GC-MS analysis of urine

GC-MS has been used in many clinical applications, such as in the analysis of urine. The often characteristic odours of a culture often give a clue as to the identification of one or more of the organisms present, and trained microbiologists can often identify a microbial culture by smell alone. Traditionally, volatile species are determined by sample extraction followed by GC-MS analysis. However, this approach requires some knowledge of the molecules involved. Several variables, such as pH, acidity, carbohydrate content, temperature and protein levels, need to be kept within a narrow range.

GC-MS is often used along with the e-nose in research, to provide valuable compositional data and for validation purposes. For example, Evans, Persaud & Pisanelli (1996) used both techniques in a diagnostic study of urine odour of UTI patients. Urine samples were collected over a period of several days, and the urine headspace was analysed by GC-MS

and e-nose. The patterns obtained from the sensor array were captured and stored for further processing. Mathematical treatment of the data enabled differentiation between the normal population and myopathy population. GC-MS analysis found that the composition of urine headspace is markedly different within normal and diseased populations. The key volatile components found in normal urine were 2-heptanone and 4-heptanone. In diseased urine, the amounts of these volatiles increased, and also contained 2(3H)phenanthrene-4-4a, 10-tetrahydro-4a-methyl and phenyl-isopropylphenyl. The GC-MS analysis validated the results obtained from the electronic nose, since the different patterns obtained from the gas sensor apparatus correlated with the different volatiles detected by GC-MS.

Headspace GC-MS (HS-GCMS) was chosen as the standard method with which to compare the electronic nose and generate information on the five bacteria used in this thesis. Though not directly comparable, it was acknowledged to possess the most similarities to the single sensor odour analyser.

Technique	Analysis specifications	Culturing specifications	Sample type	Metabolites detected	Reference
Direct GLC	GC: Packard 419 and Shimadzu GC4BMPF dual-column gas chromatograph with flame ionization detector. Silycated Pyrex column. Temps: inj. and detect. 200°C, oven isothermal 125°C. N_2, H_2 and air flows 30, 30 and 300 ml/min respectively.	Bacteria were incubated anaerobically in PYG, then human ascites fluid for prolonged periods at 37°C . 1 part purulent material:1 part 5% aq H_2SO_4, chilled, then NaCl and diethylether added, then centrifuged at 5°C.	Pus/serous fluid that may contain anaerobic gram negative bacilli.	Bacilli, particularly bacteroides, clostridia, fusobacteria produce SCFA from carbohydrate and protein. Positive response if >0.1µmol/ml isobutyric, butyric, succinic acids. (Note, extraction of acetic and propionic acids poor). Total analysis time: 48hrs+	Bartlett, J.G. *et al* (1976) Rapid diagnosis of anaerobic infections by direct gas liquid chromatography of clinical specimens.
HS-GLC	GC: Perkin-Elmer F45 with auto HS injector, flame ionization detector. Column: 0.4% Carbowax. Temps: Inj. needle temp 150°C, oven temp 115°C, inj. and det. temp 140°C. N_2 carrier pressure 180kPa, H_2 400kPa, air 380kPa. Inj. time 3s, analysis time 1.8min. MS: 30cm radius 60° magnetic deflection instrument.	Specimens cultured 1 part urine:1 part medium in yeast extract peptone medium containing lactose methionine, and analysed after 3 hrs. To increase vapour pressure of volatile compounds, 2ml liquid sample added to 3g potassium carbonate to salt out neutral and alkaline compounds into the HS. Sealed, vortexed, held at 60°C for inj.	Urine samples that may contain enterobacteria $>10^5$ CFU, indicative of urinary tract infection.	Depends on production of ethanol from lactose or arabinose by *E.coli,* and methyl mercaptan which oxidizes to dimethyl disulphide from methionine by *Proteus*. Positive response indicated by: ethanol: 0.22mM, dimethyl disulphide: 0.48mM, methyl mercaptan: 2.4mM. Total analysis time: 4 hrs.	Hayward,N.J. (1983) HS-GLC for the rapid laboratory diagnosis of UTI caused by enterobacteria. Similar described by: Coloe, P.J. (1978) HS-GLC for rapid detection of *E.coli* and *P. mirabilis* in urine.
GC	GC: HP 5751G dual column GC, with hydrogen flame detector and 3mV Servogor span recorder. Column: chromosorb. Columns run isothermally at 200°C. Temps: Inlet 200°C, detector 240°C. N_2 carrier gas 10ml/min H_2 and air optimized. Direct injection.	Anaerobic bacteria grown in glucose broth containing peptone, yeast, glucose, cysteine HCl. Before analysis, sample of culture in broth applied on 1ml packed cation-exchange resin on glass wool in a Pasteur pipette. Drained fluid collected and directly analysed by GC for acids.	Glucose broth containing anaerobic bacteria.	Acetate, propionate, isobutyrate, butyrate, propionate, pyruvate, isovalerate, lactate, valerate, caproate, fumarate, succinate, lactic acid, pyruvic acid, succinic acid. Total analysis time undisclosed: estimate 48hrs	Carlsson,J. (1973) Simplified gas chromatographic procedure for identification of bacterial metabolic products.

HS-GC	HS-GC: Perkin-Elmer F45 with auto inj. device and flame ionization detector. Column: 16m glass capillary column, with SP1000 as stationary phase. Temps: column 100°C, inj. needle 150°C, detector 150°C. Split ratio 1:20. Inj. period 4s. N_2 carrier gas 2ml/min.	Cultures inoculated on PYG medium and incubated for 3 days anaerobically. Broth and pus acidified to pH2 using dilute H_2SO_4. 1ml sample added to HD vial containing 2g Na_2SO_4, crimp sealed, and analysed by HS-GC. Vials kept at 75°C for 20min before analysis.	Anaerobes in pus and peptone yeast extract medium.	Isovaleric acid, butyric acid, alcohols. (Note: Unable to analyse compounds of low volatility e.g. lactic acid and succinic acid produced by many anaerobes.)	Larsson,L. *et al* (1981) HS-GC as a tool in the identification of anaerobic bacteria and diagnosis of anaerobic infections.
HS-GC-MS	HS-GC: Unacon 810B automated headspace concentration-gas chromatograph with two adsorption traps and flame ionization detector. Trap one packed with Tenax. Trapped organics desorbed at 200-220°C and back flushed to the column for separation. Column: CPWAX-57CB Temps: oven 60 °C for 4mins, then rising 6°C/min from 60-180°C.	*Proteus mirabilis, Klebsiella pneumoniae, pseudomonas aeruginosa,* and *staphylococcus aureus* grown in TSB for 24hrs in a stirred flask fitted with a one hole plug. Flask swept with nitrogen for 20mins at 60ml/min and trapped organics automatically adsorbed at connection to instrument.	Clinical isolates of pathogenic bacteria.	Isobutanol, isopentanol, acetoin prominently produced, and also butanol, undecane, undecene, butanol with differing profiles for each bacteria.	Aldringer,S. *et al* (1986) Characterisation of pathogenic bacteria by automated headspace concentration-gas chromatography.

Nb: SCFA: Short chain fatty acids / VFA: volatile fatty acids

Table 1.6: *Summary of the reported uses of chromatographic techniques to detect bacteria*

1.5.4 Test kits

Test kits are also often used to validate a new or emerging technology. For example, Draeger Ltd (Blyth, UK) produce gas detection systems, such as their 'Accuro' pump. These are used in combination with a detection tube, specific to the analyte of interest, e.g. alcohol, carbon monoxide, carbon dioxide, hydrogen sulphide, benzene, giving a colorimetric chemical sensor. The pump pulls the sample through the detector tube at a precisely defined volume. Direct reading is based on the chemical reaction of the measured substance with the chemicals in the tube, which leads to a discoloration in the detector tube. The length of this discoloration indicates the concentration of the reacting gas (Draeger, 1992). This system is typically used for the measurement of emissions or for air investigation in the workplace. However, such a system may be used to support the finding of work involving analysis of volatile gaseous samples, e.g. HS GC-MS and machine olfaction.

Lovibond (Amesbury, UK) produce a number of test kits, which are designed for water analysis e.g. washing water, ground and raw water, wastewater and effluents, industrial processes, and swimming pools, but can be used for other applications. The 'Checkit' range contains a range of test kits, including for hydrogen peroxide, ammonia, aluminium, chlorine, copper, and pH. Under the action of appropriate chemical reagents, samples develop a specific colour that reveals the presence and concentration of the substance being tested.

A number of other colorimetric tests are available for validation of research data. For example, BioAssay Systems (Hayward, USA) manufacture a range of 'QuantiChrom' assay kits, based on enzymatic colorimetric detection using standard 96 well plates and a plate

reader. A number of assay kits are available, such as for measurement of glucose, calcium, magnesium, haemoglobin and uric acid, in blood, serum and urine.

1.6 Project objectives

Chronic wound infections, often acquired in hospital and caused by bacteria such as MRSA, represent a worldwide problem generating high morbidity and medical expense. If a wound becomes infected during the reparative process, the wound does not heal properly and may result in a chronic wound, which may also lead to the bacterial infection spreading beyond the initial site of infection. Existing approaches to identifying infection largely involve surveying a range of physical parameters, and a limited use of non-invasive technologies. Evaluation is time consuming, and often results in inconsistencies in patient care. Also, by the time a bacterial infection has been identified, it is difficult to treat.

It is therefore preferable to detect a non-healing wound as early as possible. It is proposed that this could be achieved by monitoring the wound environment with either: a small, portable handheld device incorporating an array of single use disposable sensors; and/or a simple and fast 'near-patient' monitoring system. For both of these a sample would need to be taken and analysed at regular intervals, giving almost instantaneous results.

Three possible monitoring concepts have been identified for investigation, the objectives of which are listed below:

1) Identify a suitable model for wound fluid, and determine how best to produce it
2) Identify biomarkers indicative of healing/non-healing wounds

3) Identify key bacteria commonly isolated from wound infections
4) Investigate the feasability of using the scanning voltametric technique Dual Pulse Staircase Voltametry to monitor wounds.
5) Construct and optimise a biosensor array (to measure each of the selected biomarkers) and determine suitability for monitoring wounds
6) Investigate a single sensor odour analyser for its suitability as a near patient wound monitoring system, by 'sniffing' surrogate wound samples containing pathogenic bacteria commonly isolated from wounds
7) Use headspace GC-MS as a standard laboratory technique to identify bacterial metabolites. Use Draeger tubes to further verify findings.
8) Use enzyme based colorimetric test kits to validate biosensor measurements.

2. Standard methods

2.1 Bacteria, biomarkers and surrogate wound fluid

From the extensive literature search, it was decided to use the following bacteria to interrogate the discriminatory powers of the odour analyser: *Staphylococcus aureus; Streptococcus pyogenes; Klebsiella pneumoniae; Pseudomonus aeruginosa; Escherichia coli.* These bacteria were selected for their high occurrence in a range of wound infections, as summarized in Table 1.4.

Three biomarkers indicative of healing/non-healing were selected though the literature search (see Section 1.1.5 on the biochemical composition of wound fluid). Glucose was selected because it has been reported to increase from the non-healing to healing phase of a wound (Trengove, Langton and Stacey, 1996). H_2O_2 generation has been reported to increase in surgical wounds as a result of phagocytosis by mammalian polymorphonuclear leukocytes and monocytes. This is because hydrogen peroxide and superoxide anions are either directly or indirectly important microbicidal agents, and their generation by the leukocyte oxidase system is a necessary requisite for the killing of many species of microorganisms (Burton, Hohn & Hunt *et al* (1977)). Ethanol was selected because it is produced metabolically by certain pathogenic bacteria commonly isolated from wounds (Barchiesi, D'errico, Del Prete *et al,* 2000*;* Murray *et al,* 1998 - Table 1.4), and could thus indicate an increase or decrease in bacterial numbers in the wound environment.

As a proof of concept study, a surrogate wound fluid was required which represented 'real' wound fluid as closely as possible. Wound fluid bathes the tissue undergoing repair and regeneration. When tissue is damaged, a cascade of reactions causes blood to coagulate by converting soluble fibrinogen (the largest plasma protein) into insoluble fibrin, leaving an exudate of plasma called serum (Ganong, 2003, Clough & Noble, 2003). A study by (Trengove, Langton and Stacey, 1996) concluded that wound fluid has the electrolyte composition, urea, creatinine levels and osmolarity equivalent to serum and therefore appears to reflect the extracellular environment of the wound (Section 1.1.5). Given these findings, serum was considered to be a suitable choice of surrogate wound fluid.

2.1.1 Introduction

The aim of this chapter is to provide information on the bacteria used in this thesis to investigate the use of sensor technologies to monitor wounds. The five commonly occurring wound bacteria: *S.aureus, S.pyogenes, K.pneumoniae, E.coli, P.aeruginosa* were chosen for investigation in this thesis (see Table 1.4). Each of the 3 sensor technologies investigated in this thesis were examined with respect to their ability to detect and possibly discriminate between these bacteria in a model wound environment. Were such an approach to be successful it is possible that such an approach would provide *in situ* information on the pathogenic state of a wound. It is envisaged that wound fluid would be sampled for analysis in a 'real' situation, but at this early investigative stage, serum was chosen as a model, or surrogate, for wound fluid, since this is the major component of wound fluid. Bacteria could then be grown to the desired cell density in a controlled environment.

In order to obtain information on the cell densities of a bacterial population at a given time in a given growth medium, it was necessary to construct growth curves for the five bacteria selected in each of the selected media. This is a standard microbiological technique, described in Section 2.2.5. Controlling cell density enabled comparison of data within and across experiments.

In the development of new technology, it is important to also use a standard technique to provide a basis for comparison and validation. Headspace GC-MS (HS GC-MS) was selected as the standard method to investigate the presence of volatiles in the headspace of the five chosen bacteria. Although an off-line technique, gas chromatography (GC) has been used for the analysis of fatty acids present in glucose-containing culture media. However, HS GC-MS is also suitable for the study of acidic, neutral and alkaline compounds, including fatty acids up to octanoic acid, alcohols up to octanol and amines up to decylamine (Larsson, Mardh & Odham, 1981) and is thus a more preferable technique. HS GC-MS is particularly suited to the detection of relatively volatile early eluting compounds such as alcohols, which are commonly produced by bacteria. A Draeger tube system for alcohol detection was also used for further verification of bacterial headspace content. Glucose and hydrogen peroxide test kits were chosen to validate the detection of the biomarkers glucose and hydrogen peroxide by the biosensor array investigated in Chapter 4.

2.2 Materials and Methods

2.2.1 Bacteria, growth media and equipment

Five laboratory strains of bacterial cultures were obtained from NCIMB Ltd, Aberdeen, UK, freeze dried in vacuum sealed ampoules. These were: *Escherichia coli* (NCIMB 11943), *Klebsiella pneumoniae* subsp. *pneumoniae* (NCIMB 13281), *Pseudomonas aeruginosa* (NCIMB 8295), *Staphylococcus aureus* subsp. *aureus* (NCIMB 13062), *Streptococcus pyogenes* (NCIMB 11841).

Agar and broth powders were dissolved in RO water at appropriate concentrations, and sterilized by autoclaving. The growth mediums nutrient agar (NA), brain-heart infusion agar from (BHI) and tryptone-soya broth (TSB) were supplied by Fisher, Loughborough, UK. 28 ml capacity universal glass media vials, 500 ml Pyrex bottles, sterile disposable Petri dishes, 10 µl inoculation loops, Bunsen burner, isopropanol, Laylette pipettes and tips were also from Fisher, Loughborough, UK. 10 ml quantities of broth were made up in 28 ml universal bottles for sub-culturing, and 5 ml quantities in 20 ml HS GC-MS vials (Sigma, Poole, UK) for HS GC-MS experiments, and autoclaved. The NA and BHI agar were autoclaved in 500 ml Pyrex bottles, then poured into sterile Petri dishes in a laminar flow cabinet, and left to set. Plates and broths were stored at 4 ˚C in a constant temperature room.

2.2.2 Revival of freeze dried bacteria

Revival of the vacuum packed freeze dried cultures was carried out with aseptic technique in a type II laminar flow cabinet. A file cut was made around the diameter of the vial at the

mid-point of the cotton wool plug inside the vial and then cracked open. The cotton plug was removed and the open end of the vial flamed in a Bunsen burner. 0.5 ml of growth media was added and mixed with a pipette. The suspension was sub-cultured onto pre-labelled nutrient agar plates and tryptone soya broth, and incubated at 37 ˚C to grow. The organisms were sub-cultured at least twice before use in experiments, since resuscitated freeze-dried cultures exhibit a lengthened lag period.

2.2.3 Cryopreservation of bacterial cultures

As a precautionary method (in case of culture attenuation, death, suspected contamination or cross contamination) after revival and subculture of the freeze dried culture, each bacterial species was also cryopreserved with a cryopreservation kit from Sigma, Loughborough, UK. This is a commonly used method for the long term preservation of bacteria. Before preservation, each strain was grown up on NA plates for about 10 hours. Under aseptic conditions in a type II laminar flow cabinet, individual colonies were picked off plates of a particular culture using a sterile inoculation loop, and placed into duplicate cryopreservation tubes which were supplied containing beads and liquid. This process was repeated until a visibly dense suspension was formed. The caps were put onto the tubes, and shaken a little to distribute the colonies amongst the beads before freezing. This was repeated for each bacterial culture before freezing at -20 ˚C. Therefore, when required, a tube of a given bacteria could be removed from the freezer, and using aseptic technique, a bead removed from the tube and placed into broth where the bacteria bound to the bead formed a ‘fresh’ bacterial suspension.

2.2.4 Blood collection and separation

To imitate wound fluid, serum was the model chosen for the reasons given in Section 2.1. After obtaining ethical approval from The Cranfield Biomedical Ethics Committee (Cranfield University, Cranfield, UK), blood samples were collected from volunteers within the Faculty of Medicine and Biosciences by trained medical personnel. Volunteers were asked to fast overnight before donating approximately 50 ml of blood early morning. Blood was collected in Sarstedt (Nümbrecht, Germany), S-monovette 9 ml serum gel tubes with multifly needle and adapter, which form a closed blood collection system. After collection, the serum gel tubes were centrifuged at 3500 rpm for 20 minutes in a Jouan B4i bench-top centrifuge. This separated the serum from the blood with a gel layer in-between the two, to reduce the chance of contamination of the serum with red blood cells. Serum was removed and transferred to new centrifuge tubes, and either placed in the refrigerator for immediate use, or stored in the freezer. The blood collection tubes and remaining blood content were treated with a 1% Virkon solution for 48 hours before being autoclaved and discarded.

To produce imitation interstitial fluid, protein reduced plasma was produced, since the only significant difference between plasma and interstitial fluid is the high protein content of plasma (see Section 1.1.4). Blood was collected in S-monovette plasma gel tubes (instead of serum), and centrifuged to separate the plasma. The plasma was transferred to Vivaspin 2 concentrator tubes (Sartorious, Epsom, UK) with a molecular weight cut off of 10,000. The Vivaspin tubes could hold a 2 ml volume of plasma. Six tubes were used to remove protein from a volume of 12 ml of plasma, by centrifugation at 4,700rpm for 1 hour. Build

up of protein occurred at the PES vertical membrane in the Vivaspin tube preventing all the plasma from being filtered through. Therefore, the plasma that had not filtered through was transferred to a fresh Vivaspin tube and the cycle repeated until filtration was complete. The filtrate produced was a clear colour due to the protein removal, and thus considered a reasonable representation of interstitial fluid. A discussion of the differences between interstitial fluid, serum and plasma can be found in Sections 1.1.4 and 1.1.5.

2.2.5 Bacterial calibration curves

In order to gain an understanding of the growth rates of each of the five bacteria used in this study, it was necessary to establish growth curves. This also facilitated the control of bacterial cell densities in later experiments. Therefore growth curves were constructed for each bacteria in each of the media they were grown in. The methodology employed for the construction of the growth curves follows.

9 ml of growth media (TSB, YPD, or serum + DMEM) was inoculated with 1 ml of bacterial suspension and incubated overnight (O/N) at 37 ˚C. The following morning, 1 ml of medium was removed from the O/N broth and used to inoculate 9ml of fresh growth media. The optical density was measured at 600nm with a Beckman DU-640 spectrophotometer immediately after inoculation, representing time zero. Non-inoculated growth media was used as the blank for optical density readings. The freshly inoculated broth and blank were incubated at 37 ˚C in a Gallenkamp Orbital Incubator at 140 rev/min. After every 1 hour, 1 ml of broth was removed, and its optical density measured. This was followed by serial dilutions of the broth from 10^{-1} to 10^{-6} in sterile RO water. 10 µl of

dilutions 10^{-2}, 10^{-3}, 10^{-4}, 10^{-5}, 10^{-6} and blank were spotted and spread onto NA plates in pre-marked 1/6 sections, as illustrated in Figure 2.1. Plates were allowed to dry near a Bunsen flame, and then inverted and incubated at 37 ˚C overnight. These steps were repeated for each culture, and performed in triplicate.

Absorbance versus time values were plotted, illustrating the standard phases of growth: lag, exponential and stationary, (death not recorded). The following morning, the colonies for each dilution in each of the 1/6 sections of the plates were counted. The most appropriate (countable) dilution was converted into colony forming units per ml (CFU/ml) and plotted against absorbance. When growing bacteria in the studies that follow it was therefore possible to approximate what time the bacteria would reach a particular cell density, and to check this by measuring the optical density and referral to the relevant graphs.

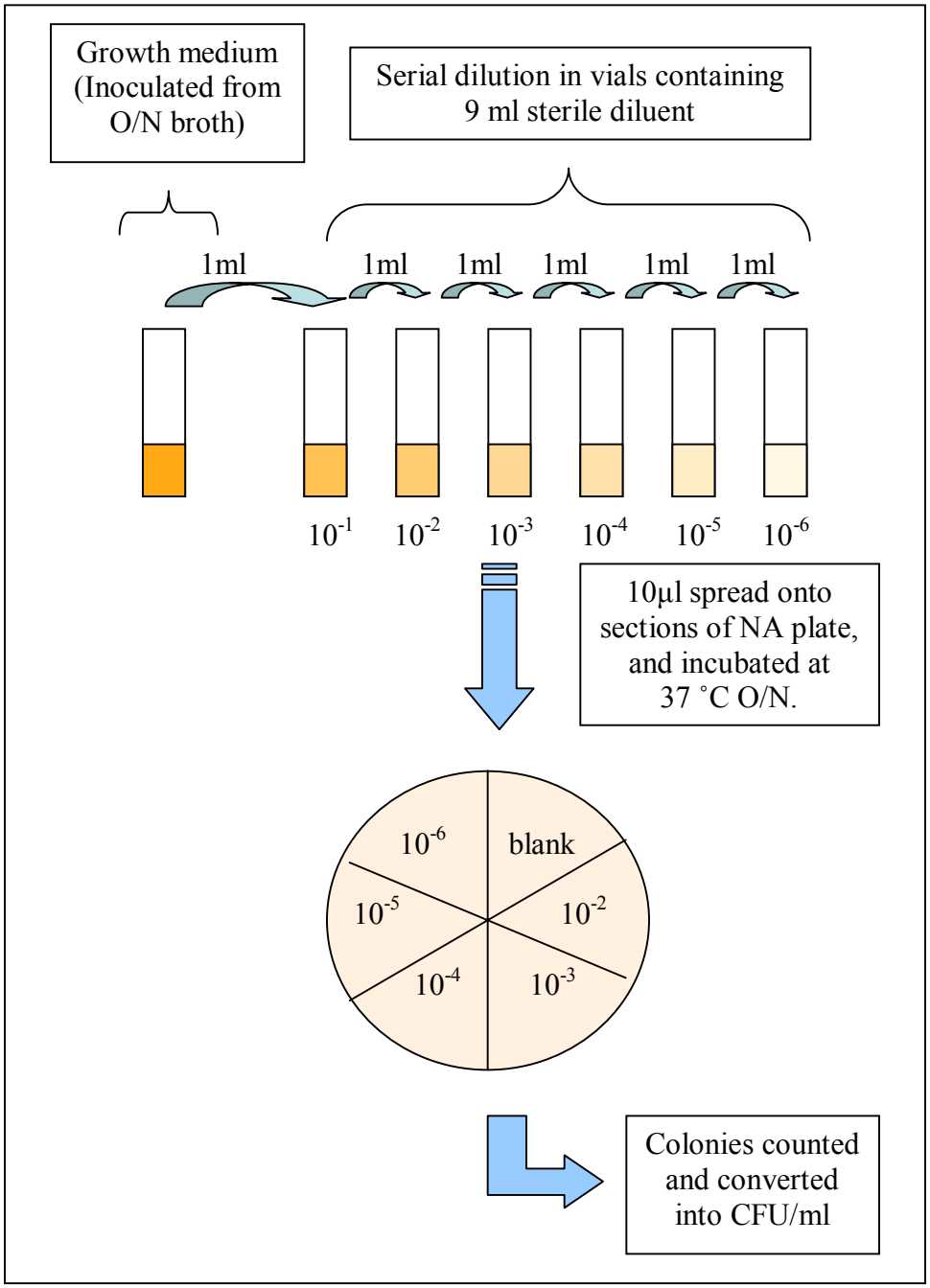

Figure 2.1: *Serial dilution and plating layout for production of bacterial growth curves*

2.2.6 Headspace GC-MS

Standards and bacterial samples were run on a Perkin Elmer (Wellesley, MA, USA) Autosystem XL gas chromatograph, linked to a Turbomass mass spectrometer and Turbomatrix 16 headspace sampler. A Perkin Elmer Elite FFAP GC column (30m x 0.25mm x 0.25µm) was used, the stationary phase being nitroterephthalic acid modified polyethylene glycol, and features high polarity, a broad temperature range of 40°C to 260°C, and is especially suited for organic acids, free fatty acids and alcohols. The headspace GC-MS hardware was operated via a Dell Optiplex GX110 PC, running Turbomass version 4.1.1, Turbomatrix, and the National Institute of Standards and Technology (NIST) mass spectral database. Glass sample vials (20 ml), aluminium caps, starsprings, PTFE Butyl rubber septa, and hand crimper were also from Perkin Elmer.

The methods for the Turbomatrix, GC and MS follow:

Turbomatrix

Temperatures (°C)		***Times (min)***		***Pressure (psi)***	
Vial oven:	75	Thermostat:	15	Column:	35
Needle temp:	80	Pressurise:	3		
Transfer line temp:	85	Withdraw:	0.2		

GC
Equilibration 0.5 min
35 °C for 6 min
200 °C for 3 min increasing at 8 °C/min
Total run time 29.63 min

MS
Scan masses (m/z) 33 to 350
Retention window 1 to 29.63 min

2.2.7 Test kits

To validate the biosensor data in this thesis, test kits were used. A Lovibond (Amesbury, UK) 'Checkit' hydrogen peroxide test kit based on colorimetric observation was supplied by Fisher. The hydrogen peroxide kit involved adding and crushing a tablet supplied with the kit to a 10 ml test sample (H_2O_2 in 0.1M PBS) transferred to the test compartment, inverting and waiting for two minutes. The colour produced was then compared against standards colours on the kit. It was not possible to use this kit to test the serum samples because serum has an inherent colour similar to that generated by the kit. Only clear samples, such as PBS, could be tested.

The glucose test kit selected was a BioAssay Systems (Hayward, USA) Quantichrom glucose test kit. This assay was also based on colorimetric detection, but using 96 well plates and a plate reader (Dynex Technologies MRX Revelation Micro Plate Reader) rather than the eye. This kit is designed to be used with serum or plasma samples. Standards were prepared and 5 µl added to centrifuge tubes, and 500 µl 'reagent' added (supplied by kit). The tubes were heated in boiling water for 8 minutes, and cooled for 4 minutes in cool water. 200 µl of the standards were transferred to a 96 well plate, and the optical density measured at 630nm. Optical density values were blank subtracted and plotted against glucose concentration.

To support the findings of HS GC-MS, a Draeger short-term gas detector pump called an 'Accuro' pump was used with short term alcohol measurement tubes from Draeger Ltd, Blyth, UK (also refer to Section 1.5.4). By connecting the Draeger pump with an alcohol

detector tube to a compressible bag, as illustrated in Figure 2.2 (b), it was possible to measure the alcohol content of the headspace of bacteria, although it should be noted that Draeger pumps and tubes are not designed for this application, and the tube does not differentiate between different alcohols. Bacteria were grown up as normal to 5 x10^8 CFU/ml, and 5 ml transferred to a compressible bag. The bag was inflated using a pump, and kept compressed by closing the clamp located around the tubing. The tubing was then attached to the end of the Draeger tube, and the tubing clamp opened. The Accuro was pumped 10x, and the change in colour over part of the alcohol tube was read off as alcohol in ppm.

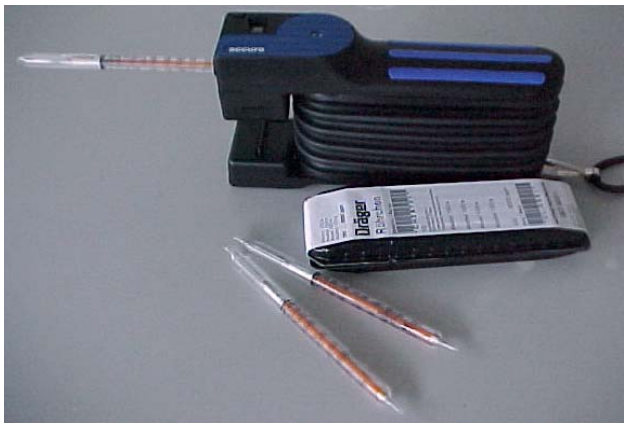

(a)

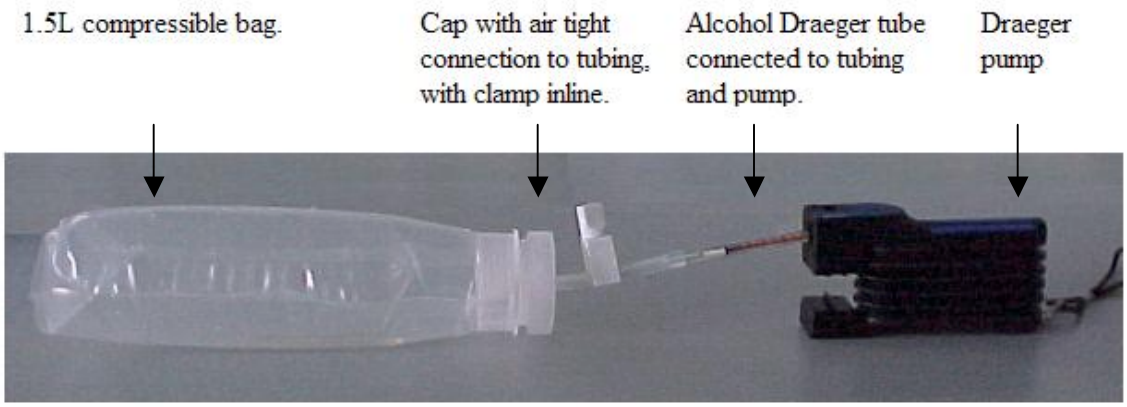

(b)

Figure 2.2: *(a) Draeger Accuro pump and tubes, (b) experimental setup for the measurement of alcohol content of five bacteria in the headspace of a compressible bag.*

2.3 Results and discussion

2.3.1 Bacterial growth curves

The calibration growth curves for each of the bacteria grown in TSB are shown in Figure 2.3. The three phases: lag, exponential and stationary can be seen, more obviously for *S.aureus* and *S.pyogenes* than for others. *P.aeruginosa* appears to have had the smallest overall change in absorbance, while *E.coli* has had the greatest, and all have grown successfully. Figure 2.4 illustrates the calibration plot for these five bacteria in TSB. The bacterial inoculation procedure was such that the curves produced were for bacterial numbers of $x10^8$ CFU/ml. The reasons for this are two fold: firstly, to consider instrument sensitivity, i.e. levels below this are not detected; secondly, to save time.

In order to move one step closer to that of a 'real' wound environment, bacteria were later grown in a variation of Eagles medium, a minimal medium called Dulbecco's modified Eagles medium, which itself has many variations. Figure 2.5 shows the calibration plots for the bacteria grown in DMEM. After successful initial investigations with the odour analyser using DMEM (see Chapter 5), the bacteria were grown in serum as the surrogate wound fluid. However, it was found that only *S.aureus* would grow in serum, therefore it was necessary to supplement the serum with DMEM. It was found that 90:10 v/v serum:DMEM was enough for the bacteria to grow, illustrated in Figure 2.6.

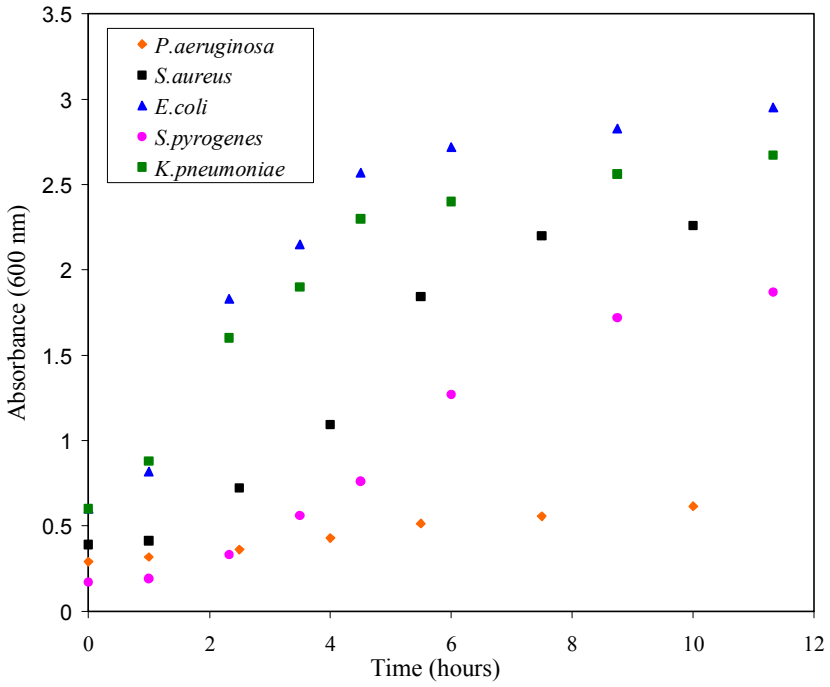

Figure 2.3: *Growth curves of five bacteria grown in TSB*

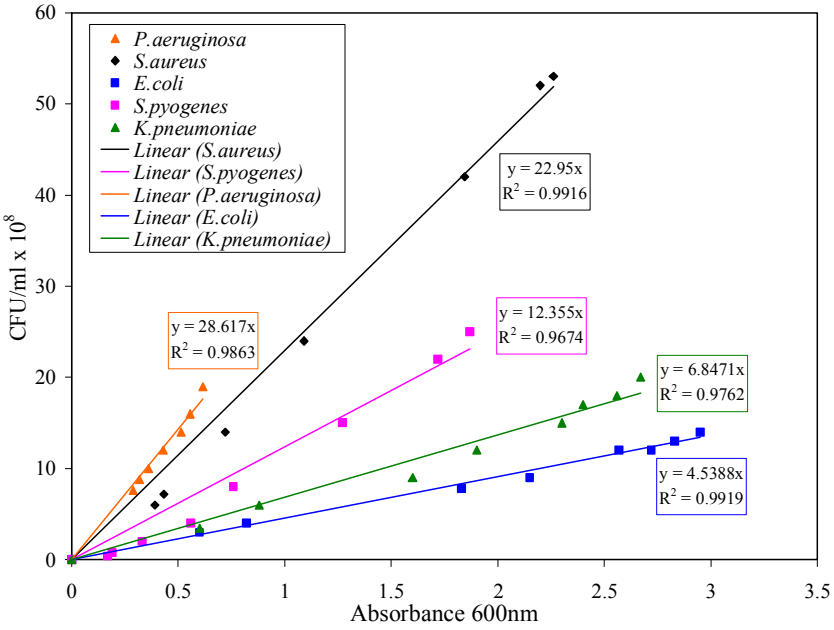

Figure 2.4: *Calibration plots for five bacteria grown in TSB.*

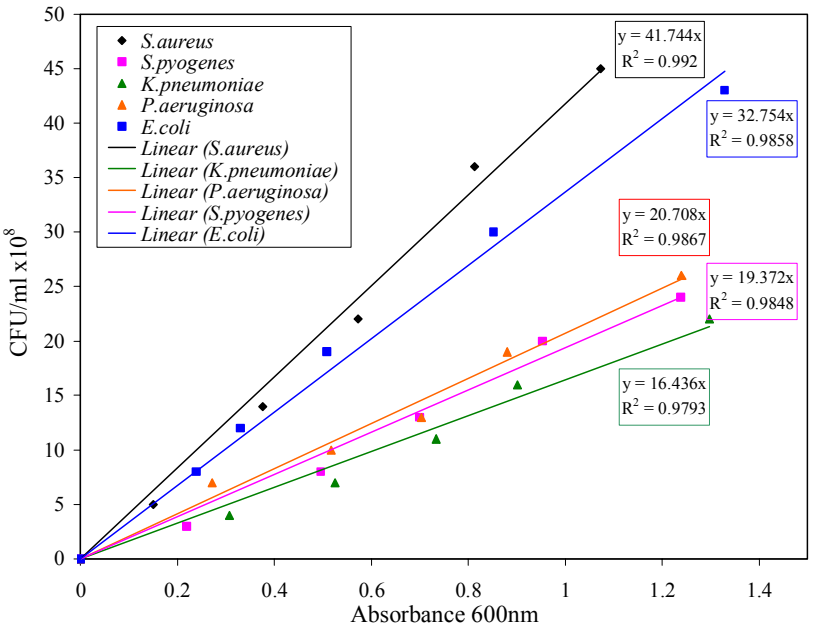

Figure 2.5: *Calibration plots for five bacteria grown in DMEM.*

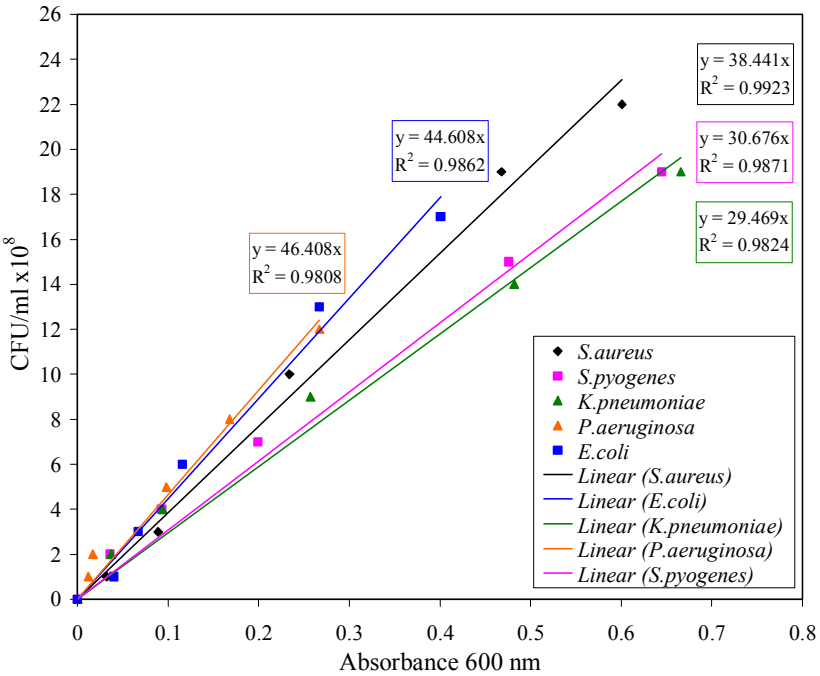

Figure 2.6: *Calibration plots for five bacteria grown in 90:10 v/v serum:DMEM.*

Figure 2.7 demonstrates the large differences in cell densities produced by growing *S.aureus* in serum, 90:10 v/v serum:DMEM, and protein reduced plasma. Although protein reduced plasma was not used in the studies in this thesis, it was considered, since some interstitial fluid may also be present in wounds, and may well be more of a major component than serum in superficial wounds to the skin, and could be an area to investigate in the future. It can be seen that *S.aureus* grown in serum reached much higher cell densities than when grown in protein reduced plasma, and when grown in 90:10 v/v serum: DMEM higher still densities were achieved.

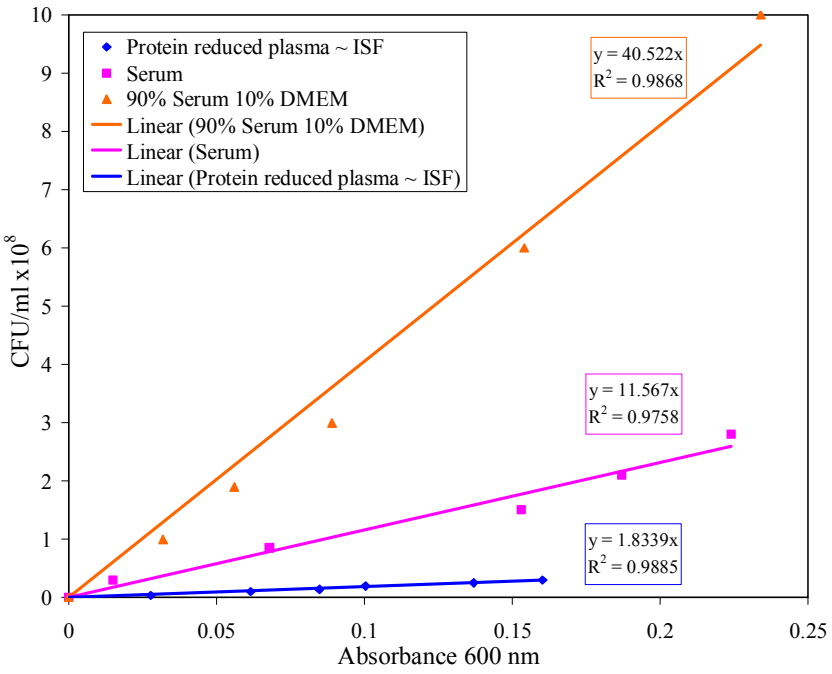

Figure 2.7: *Comparison of calibration plots for S.aureus grown in protein reduced plasma, serum, and 90:10 v/v serum:DMEM.*

2.3.2 Detection of ethanol by headspace GC-MS

Information related to the detection of bacterial volatiles by chromatographic methods or otherwise was limited. However, it was known that ethanol is the major metabolic product of many bacteria, and it was known that ethanol could be detected by HS GC-MS (Hayward *et al* 1977, 1983, Coloe, 1978).

100 ppm aqueous ethanol was used to optimise the Turbomatrix (headspace sampler) and GC methods by varying the oven temperatures, temperature gradients, sample and injection volumes pressures and temperatures to produce peaks of acceptable resolution and size. To enable quantification of the concentrations of ethanol in the bacterial samples analysed, it was necessary to produce a standard calibration curve for ethanol. Therefore, ethanol standards were run and analysed. Figure 2.8 illustrates the process of converting the chromatogram produced into appropriate quantitative information. Within the Turbomass software it was possible to integrate the area of a peak, in this case ethanol. A value for the area was also displayed. The peaks were confirmed as ethanol by using the peak information to search the NIST database, which produced a list of possible matches, each scored out of 1000 for probability of a match to the data.

Figure 2.9 (a) depicts the increase in ethanol peak size with increase in ethanol concentration, and (b) the calibration graph generated from the integrated peak area data. A clear linear relationship is present with an R^2 value of 0.9826. This graph was used to quantify the bacterial ethanol data

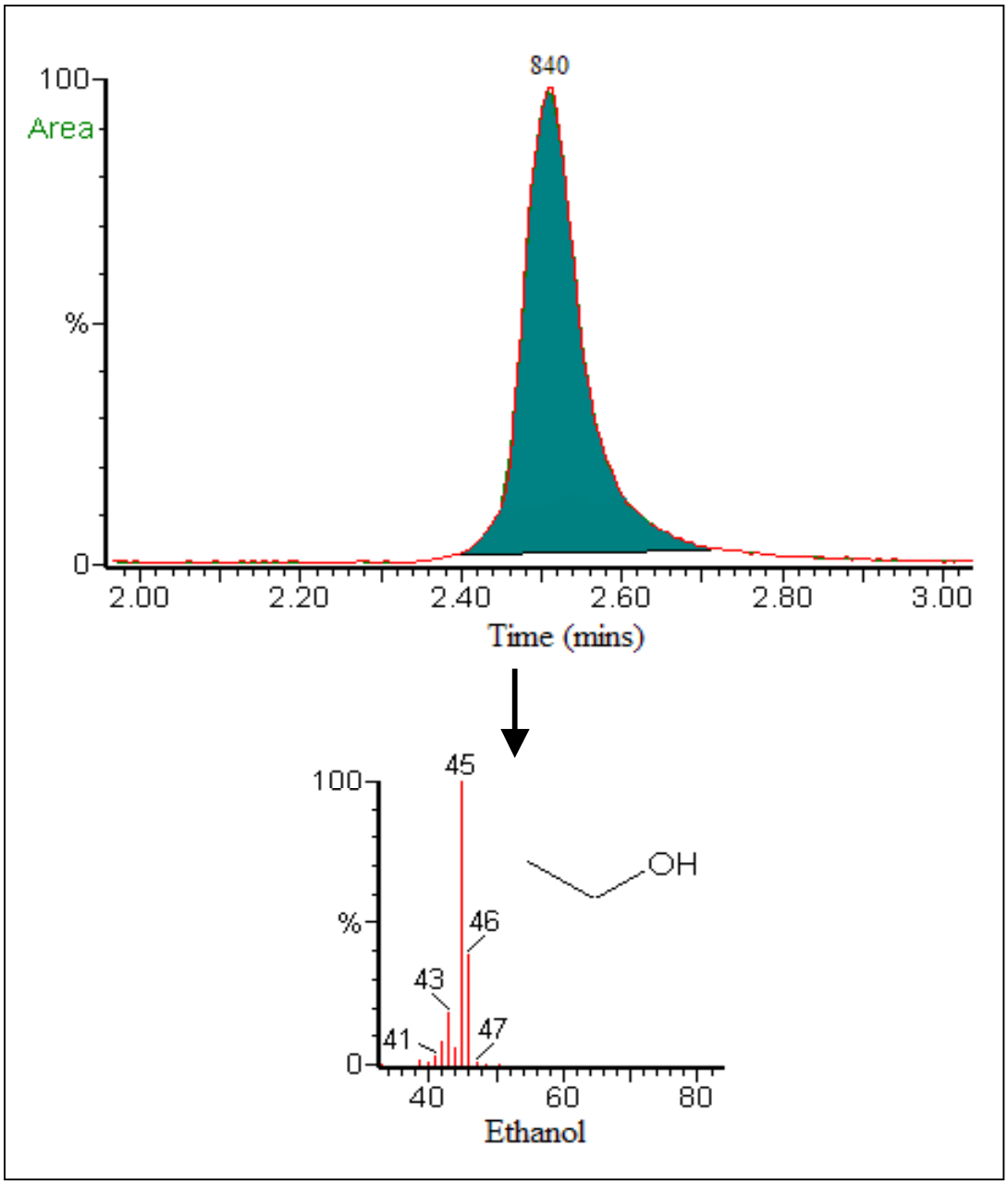

Figure 2.8: *Headspace GC-MS detection of ethanol standards – example peak area integration and identification.*

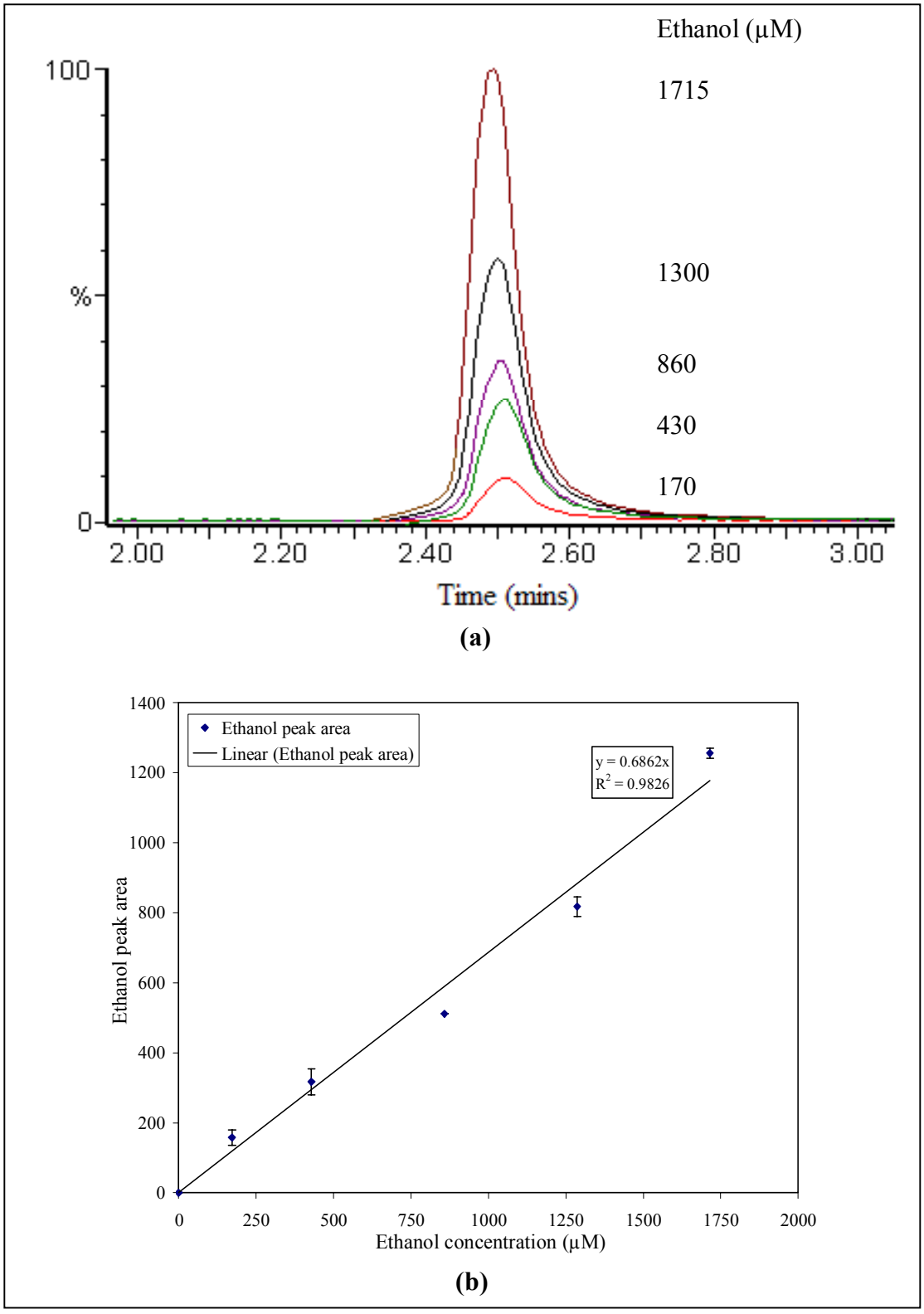

Figure 2.9: *Headspace GC-MS detection of ethanol standards – (a)Ethanol peaks, (b) Calibration plot.*

2.3.3 Detection of bacteria by headspace GC-MS

The headspace of the five bacteria: *S.aureus, K.pneumoniae, E.coli, S.pyogenes,* and *P.aeruginosa* was analysed by HSGC-MS. The bacteria were grown as normal to three different cell densities: $0.5x10^9$, $1.0x10^9$, $1.5x10^9$ CFU/ml in duplicate in 90:10 v/v serum: DMEM. 1 ml samples were pipetted into headspace vials, sealed and the headspace analysed.

Selection of a peak revealed the molecular weights that made up the peak. The peaks produced were verified as ethanol by removing background noise (Figure 2.10) and importing the peak information into the NIST database. Following this, integrating the peak yielded a value for the area. Figure 2.10 also illustrates the process of integration. It can be seen that some small 'peaks' (red line) that do not exist before integration (green line) are generated in this process. This is simply the programs interpretation of the data, i.e. three points increasing/decreasing in number is interpreted as a peak, however small. This process could be manipulated within the program and the same parameters were used for each bacterial sample peak integration.

It was hoped that other metabolic products would also be detected such as lactic acid, however, it was found that in this instance, it was only possible to detect ethanol. It is assumed other compounds produced were at levels too low to be detected by this method, perhaps because of the minimal nature of the medium the bacteria were growing in.

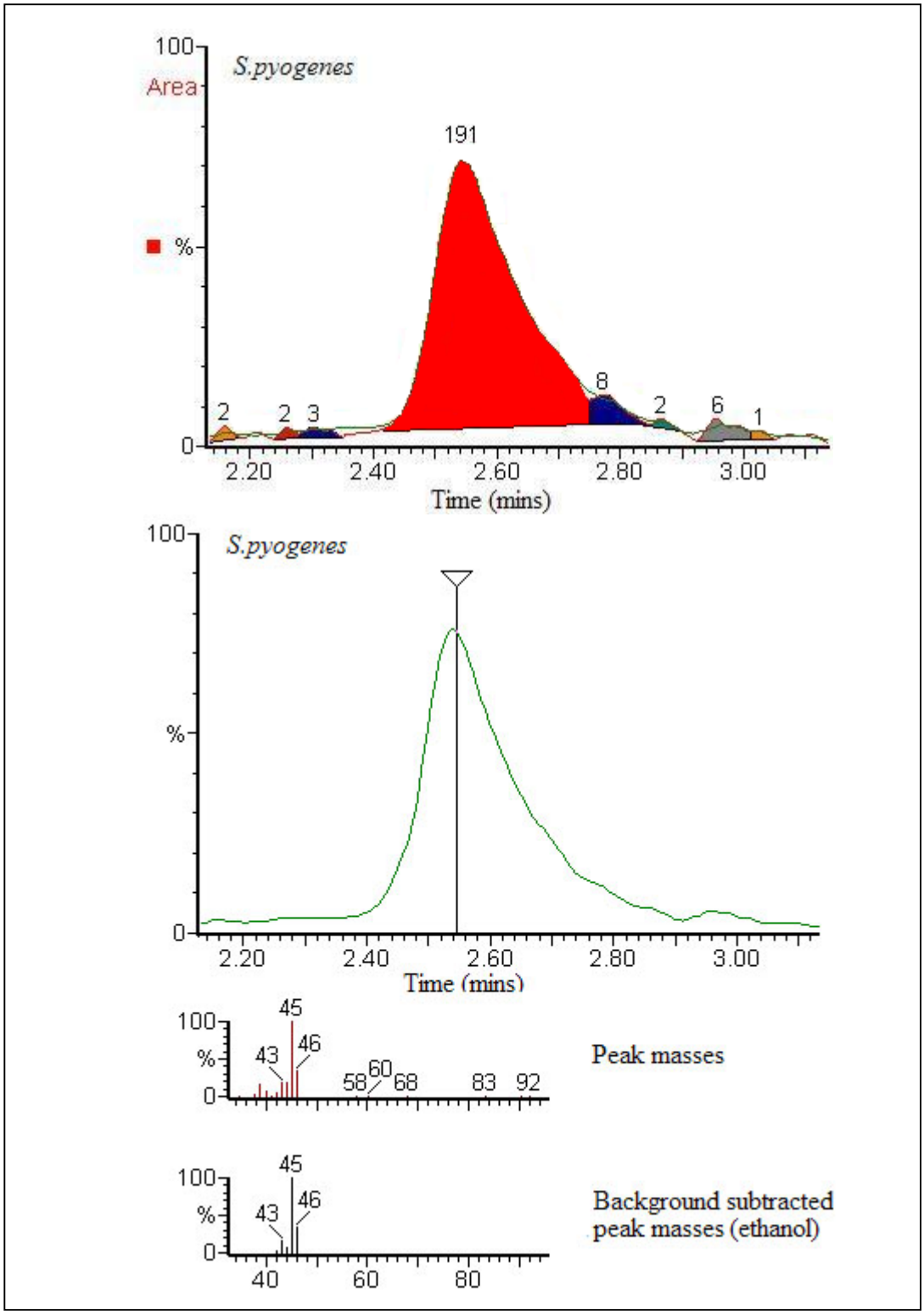

Figure 2.10: *Headspace GC-MS detection of bacteria – S.pyogenes example – Peak area integration and identification as ethanol.*

The peak areas, which are the average of duplicate runs, are recorded in Table 2.1. Using the ethanol calibration graph the peak areas were converted to ethanol concentration, shown in Figure 2.11. The concentration increased with cell density for all bacteria. The most ethanol was produced by *S.aureus*, closely followed by *S.pyogenes* in the region of 325 μM at a cell density of $1.5x10^9$ CFU/ml. *K.pneumoniae, E.coli,* and *P.aeruginosa* produced similar concentrations of ethanol to each other at all three cell densities.

The data generated does reveal the limitations of a technique such as HS GC-MS. One ethanol peak produced for each bacteria is not enough to be able to use a discriminatory technique such as principle components analysis, and hence it may not be possible to use this technique as a diagnostic tool with wound fluid samples containing unknown bacteria. Development work beyond the scope of this project may improve the range of bacterial metabolites detected. However, this data was useful, as it confirmed the metabolic production of ethanol by the five bacteria, and that the concentrations produced were in a range that could potentially be detected by other means with more diagnostic potential, such as by electrochemical methods (Chapter 3), biosensors (Chapter 4), or by odour analysis (Chapter 5). It has previously been shown that machine olfaction based instruments, and more specifically the single sensor odour analyser developed by Lee-Davey (2004) are particularly suited to detecting volatiles such as ethanol.

Table 2.1: *Integrated ethanol peak area values for headspace GC-MS of bacteria grown in 90% serum 10% DMEM.*

	Integrated peak area				
CFU/ml	*S.aureus*	*K.pneumoniae*	*P.aeruginosa*	*S.pyogenes*	*E.Coli*
$1.5x10^9$	224	156	144	219	138
$1.0x10^9$	145	56	53	65	51
$0.5x10^9$	52	6	19	13	26
0	0	0	1	0	1

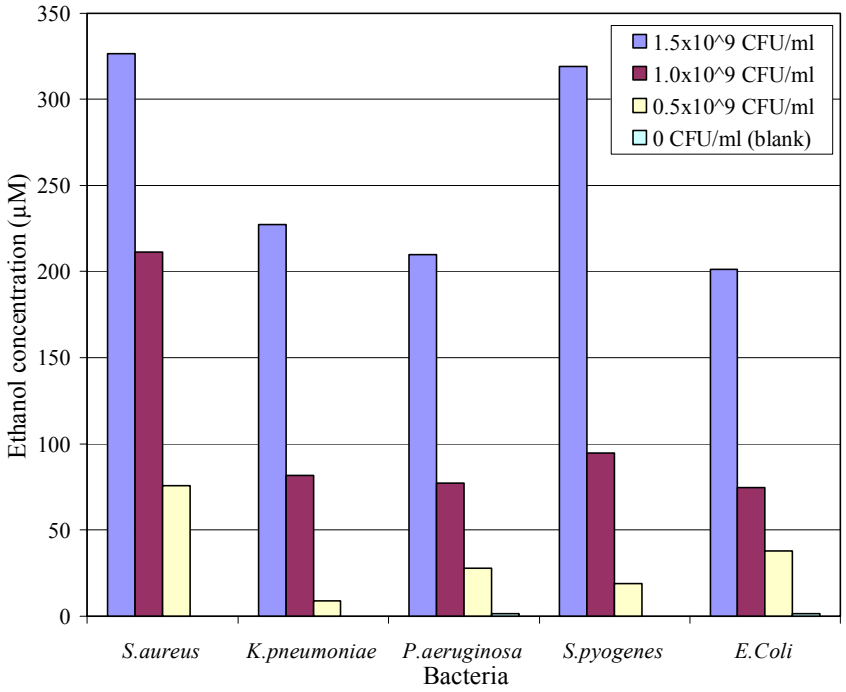

Figure 2.11: *Ethanol concentrations detected by headspace GC-MS analysis of bacteria grown in 90:10 v/v serum:DMEM*

2.3.4 Detection of mixed bacteria by headspace GC-MS

It is normal for more than one bacteria to be seriologically confirmed as present in a sample taken from a wound. Therefore paired combinations of the five bacteria, and one combined sample of all five bacteria were analysed by headspace GC-MS. Two cell densities, $1.0x10^9$

and $1.5x10^9$ CFU/ml were analysed in duplicate. Bacteria were grown separately in 90:10 v/v serum:DMEM as normal to the required densities, and added together to form the combinations listed in Table 2.2. Minor adjustments to densities were made using blank 90:10 v/v serum:DMEM to produce the desired final numbers of CFU/ml.

Ethanol peaks were integrated as described for the individual bacterial populations in Section 2.3.3, giving the values recorded in Table 2.3. These were converted into ethanol values displayed in Figure 2.12. The letters refer to those allocated in Table 2.2 for the particular bacterial combinations studied.

Table 2.2: *Bacteria combinations analysed by headspace GC-MS.*

Symbol	**Bacteria**
A	*S.aureus* + *S.pyogenes* + *E.coli* + *K.pneumoniae* + *P.aeruginosa*
B	*S.aureus* + *S.pyogenes*
C	*K.pneumoniae* + *P.aeruginosa*
D	*S.aureus* + *E.coli*
E	*P.aeruginosa* + *S.pyogenes*
F	*K.pneumoniae* + *S.pyogenes*
G	*K.pneumoniae* + *E.coli*
H	*S.aureus* + *K.pneumoniae*
I	*P.aeruginosa* + *E.coli*
J	*S.pyogenes* + *E.coli*
K	*S.aureus* + *P.aeruginosa*

Table 2.3*: Integrated ethanol peak area values for headspace GC-MS of combinations of bacteria grown in 90:10 v/v serum:DMEM*

	Integrated peak areas										
CFU/ml	A	B	C	D	E	F	G	H	I	J	K
1.5×10^9	222	283	89	182	80	76	377	292	74	353	522
1.0×10^9	82	105	53	64	42	34	124	110	38	103	179
0	1	0	1	0	0	0	1	2	0	0	1

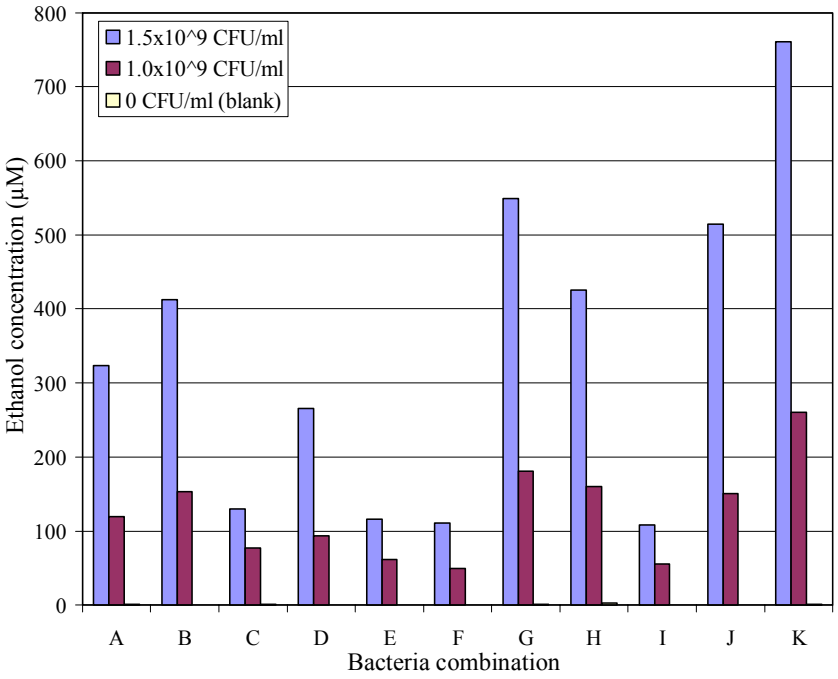

Figure 2.12: *Ethanol concentrations detected by headspace GC-MS analysis of bacteria combinations grown in 90:10 v/v serum:DMEM*

As found with the individual bacteria, ethanol concentration increased with cell density, and negligible amounts of ethanol were detected in the blanks. The amount of ethanol produced for different combinations varied from 49.5 to 261 µM for $1.0x10^9$ CFU/ml, and from 111 to 761 µM for $1.5x10^9$ CFU/ml. Combination K (*S.aureus* + *P.aeruginosa*) produced the most ethanol at both densities. There does not appear to be a relationship between the results for the combinations of bacteria and the individual bacteria.

2.3.5 Alcohol Draeger tube test

Further authentication of the presence of ethanol in bacterial headspace was provided by detection using an alcohol Draeger tube, as described in Section 2.2.7. The levels detected are shown in Table 2.4. The values are lower than those detected by HS GC-MS, but as already mentioned, the Draeger pump and tubes are not designed for this application, and

therefore care must be taken in interrogating these results. They do however suggest the presence of ethanol at slightly higher levels in the headspace of *S.aureus* and *S.pyogenes* than in *P.aeruginosa*, *E.coli* and *K.pneumoniae*, as found by HSGC-MS.

Table 2.4: *Alcohol levels detected by Draeger tubes*

Bacteria	**Alcohol (µM)**
P.aeruginosa	431
E.coli	431
S.pyogenes	517
K.pneumoniae	431
S.aureus	517
Blank	86

2.3.6 Glucose BioAssay

The calibration graph generated from the QuantiChrom glucose BioAssay is displayed in Figure 2.13. A clear linear relationship was present with an R^2 value of 0.9975 for the range 0 to 16 mM glucose.

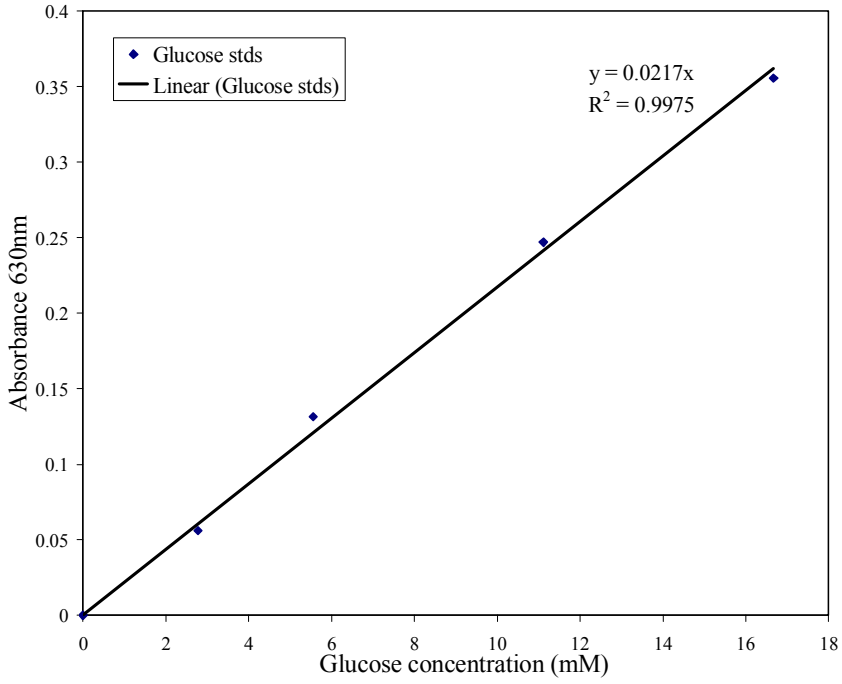

Figure 2.13: *Glucose BioAssay standards*

2.3.7 H_2O_2 'Checkit' test kit

Standards tested produced colours matching those displayed on the Lovibond 'Checkit' kit box.

2.4 Overall Chapter Conclusions

A suitable surrogate wound fluid (serum) was identified and produced successfully. It was found that S.aureus was able to grow in serum alone, and that by supplementing the serum so that it contained 90:10 v/v serum: DMEM, all five selected wound bacteria could grow and be used for odour analysis. Growth curves and calibration plots were produced for the five bacteria grown in TSB, DMEM, and 90:10 v/v serum: DMEM, providing useful information on the growth cycles and cell densities of the bacteria, which will be used in the studies on odour analysis that follow in Chapter 5. HS GC-MS and a Draeger pump and tube system was used to detect volatiles in the headspace of five bacteria grown in 90:10 serum: DMEM, verifying the presence of ethanol, and that it is produced at a level measurable by other means, such as by an alcohol biosensor. Standard calibrations were produced for the glucose test kit, which is referred to in Chapter 4, to validate the biosensor data.

3. Detection Using Dual Pulse Staircase Voltammetry

3.1 Introduction

This chapter investigates the first of three possible monitoring technologies, the electrochemical technique of dual pulse staircase voltammetry (DPSV) described in Section 1.2.2.5. This technique was identified as an appropriate technique, due to its rapidity and ability to produce information rich voltammograms while also cleaning the electrode surface of fouling agents. Using a standard three electrode system, this technique has been reported to produce characteristic peaks for different analytes allowing both qualitative and quantitative determination of analytes in solution (Bessant, 1998; Fung & Mo, 1995). and may present an alternative to the more common approach of using amperometric biosensors for such measurements. If successful, this approach would offer the benefits of reduced cost of sensor fabrication, and it is possible that a single sensor may be used to measure several components, rather than the necessity of using a biosensor array to determine individual components, as investigated in Chapter 4. However, reports using the technique of DPSV are limited, and there are none relating to its use in a complex matrix such as a biological fluid, and therefore this study was undertaken to establish the feasibility of this technique for wound monitoring.

Amperometric detection was not investigated for the monitoring of wounds, since it lacks specificity in mixtures, however, cleaning pulses are common to the techniques of pulsed amperometric detection (PAD) and DPSV. Therefore, for illustrative purposes, PAD was compared with amperometry to demonstrate the functionality of the cleaning pulses for the removal of fouling agents. Following this, gold and platinum solid electrode materials were

compared. The suitability of two screen printed electrodes for use in DPSV were tested, since ultimately, if the technique was successful, it is envisioned that a portable device using disposable electrodes would be produced. Work was carried out initially referring to the work of Bessant (1998) to establish the system (using NaOH). Once established, PBS was used as it is known to have similar electrolyte composition as serum. Each of the three biomarkers identified (Section 2.1): ethanol, glucose and H_2O_2, were investigated individually and in mixtures, and corresponding voltammograms produced. The influence of a number of possible electrochemical interferents such as paracetamol (acetaminophen) and vitamin C (ascorbic acid) that may be present in 'real' (i.e. clinical) samples was also investigated.

3.2 Materials and Methods

3.2.1 Reagents

Solutions of NaOH and NaCl (both Sigma, Poole, UK) were prepared in reverse osmosis water. Ethanol (99.9% denatured HPLC grade) was from Aldrich (Poole, UK). 4-Acetomidophenol, salicylic acid, L-ascorbic acid, bilirubin, distilled water, cholesterol, cysteine and creatinine, methanol, propanol, acetone, glucose, trichloroacetic acid, glutathione, dopamine were from Fisher (Loughborough, UK). Hydrogen peroxide (31.3% v/v assay ACS reagent), fructose, gentisic acid, levo-dopa, tetracycline, tolazamide, and tolbutamide were from Sigma (Poole, UK).

3.2.2 Instrumentation

Electrochemical measurements were made using a PGSTAT10 multichannel (4 channels) Autolab (Eco Chemie, Utrecht, The Netherlands), which was operated by GPES (version 4.9) software under PC control.

A Chemlab SS3 stirrer was used during all amperometric experiments with an 8x6mm magnetic follower (Fisher, Loughborough, UK). The electrochemical cell was a 10 ml glass beaker (Fisher, Loughborough, UK). A standard laboratory clamp stand and clamps were used to hold beakers and three electrode configuration with Autolab connections in position (Figure 3.1). Screen printed electrodes were connected to the Autolab using connectors made in house from standard components from Maplins, UK. The connectors are known as FFC (Flat Flexible Cable) Connectors, using a 1.25mm pitch (Molex, part number 39-51-3084). They are mounted onto 'Veroboard', and then connect via 4mm plugs and sockets to the potentiostat. The wires were protected by heat shrink rubber, and the circuit board by PVC tape.

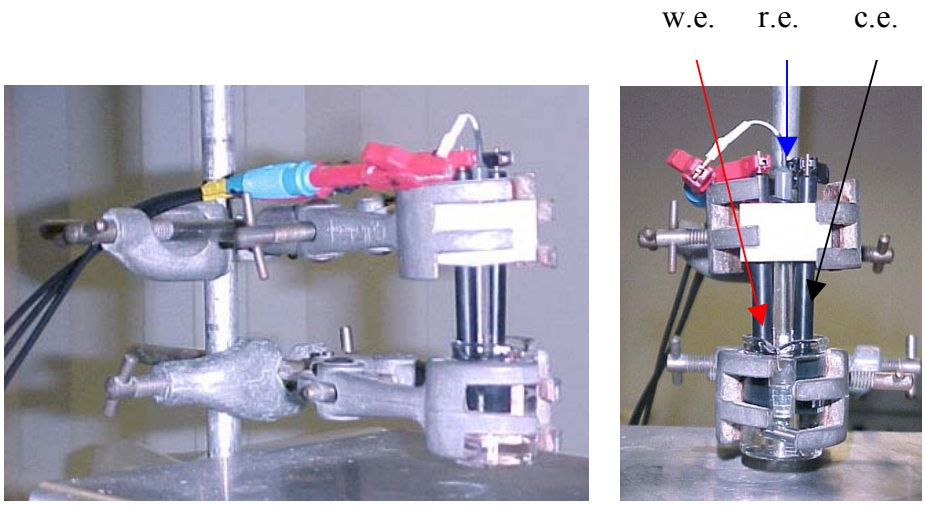

Figure 3.1: *Assembly of solid electrodes (working (w.e.), reference (r.e.), counter (c.e.)).*

3.2.3 Electrode materials

Gold and platinum solid-state electrodes and the Ag/AgCl solid-state reference electrode were from Bioanalytical Systems (BAS), West Lafayette, USA. The reference electrode is internally saturated with KCl to maintain a constant Cl^- ion activity, and maintains its own internal redox potential. The Ag/AgCl reference was stored in 3 M NaCl when not in use. The screen printed three electrode assembly of carbon, carbon, and Ag/AgCl were made in house. The carbon ink base layer 145R and Ag/AgCl reference electrode layer was from MCA Services Ltd., Melbourn, UK, and the insulation layer – 242-SB epoxy-based blue protective coating ink was from Agmet ESL, Reading UK. A further description of the screen printing process is given in Section 4.2.4. The screen printed electrodes with gold working electrode (w.e.), carbon counter (c.e.) and Ag/AgCl reference (r.e.) were from an existing in-house design and fabricated by Dupont (Bristol, UK). These two screen printed sensors are shown in Figure 3.2.

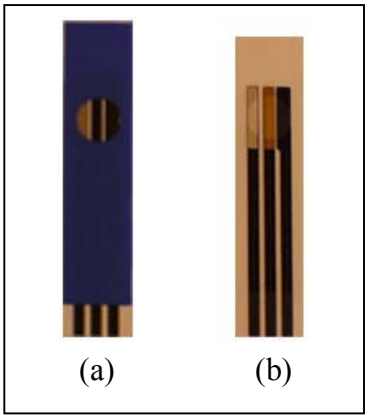

Figure 3.2*: Screen printed three electrode assembly electrodes*
(a) carbon (w.e.), carbon (c.e.) Ag/AgCl (r.e.), (b) gold (w.e.), carbon (c.e.), Ag/AgCl (r.e.).

To remove electroactive agents from the solid-state electrodes between measurements, they were first polished with 0.05 μm alumina (Sigma) in reverse osmosis water and a polishing pad, secondly washed with acetone, and thirdly, ultrasonicated in a beaker of acetone to remove remaining alumina, and allowed to air dry.

3.2.4 Electrochemical techniques

In pulsed amperometric detection (PAD), the cleaning and detection parameters were as follows: E_{ox} = 0.8 V, E_{red} = -0.2 V, E_{det} = 0.2 V, t_{ox} = 0.2 s, t_{red} = 0.4 s, t_{det}=0.2 s (Bessant, 1998 - refer to Section 1.2.2.2).

The technique of dual pulse staircase voltammetry (DPSV), described in Section 1.2.2.5, consisted of two electrode cleaning pulses, (the first a 3 s pulse at +0.7 V (vs. Ag/AgCl reference electrode), the second a 2 s pulse at -0.9 V) to clean the electrode surface, followed by detection typically scanning the potential range - 0.9 V to +0.8 V, following the work of Bessant (1998). A response was registered even before the addition of analyte, due to electrode effects and the electrochemical activity of the buffer solution. This response took time to reach steady state, and therefore no analyte was added until steady state had been reached i.e. a scan of the blank (0.1 M NaOH or 0.1 M PBS as stated) was repeatable, typically requiring 8 to 10 scans. This also allowed the option of blank subtraction, since, in this study, the response of a system was taken as a summation of the blank response and the response of the analyte. After each addition of analyte, the cell was stirred for 10 s before being scanned until a repeatable response was obtained. Detection

was performed in 10 ml of either 0.1 M NaOH, 0.1 M HCl or 0.1M PBS as indicated for each result.

3.3 Results and Discussion

3.3.1 Comparison of amperometry and pulsed amperometric detection

Although DPSV is the technique being investigated here, the effectiveness of the cleaning pulses can be illustrated by comparing fixed potential amperometry with pulsed amperometric detection. Figure 3.3 compares these two techniques for the detection of 64 mM increases in ethanol concentration in 0.1 M NaOH buffer at a gold working electrode. It can be seen that PAD gives significantly higher current values with each step increase in ethanol concentration when compared to fixed potential amperometry, therefore illustrating that the cleaning pulses employed in PAD are effective. In fixed amperometry, the lower sensitivity is thought to be due to the organic residue of the dehydrogenation reaction remaining strongly adsorbed to the electrode surface, and therefore hindering further adsorption of molecules from the bulk of the solution. The application of the three step waveform aims to maintain a uniform electrode activity. After measurement, the anodic polarisation step oxidatively degrades the adsorbed organic material to CO_2 simultaneously with the formation of the oxide layer. The cathodic polarisation step that follows reduces the PtO and regenerates the active platinum electrode (Hughes, Meschi and Johnson, 1981; Johnson & LaCourse, 1990; LaCourse, Johnson, Rey, *et al*, 1991; Tarnowski & Korzeniewski, 1996).

Repeating this study for glucose at a platinum electrode found that as glucose concentration was increased, the sensitivity of the platinum electrode was reduced, due to fouling. Sensitivity to glucose was better with PAD than fixed-potential amperometry, but the difference was far smaller than for ethanol. This may mean that glucose has less of a fouling effect than ethanol, and therefore the effect of the desorption and regeneration cleaning pulses of PAD would not be as significant. Further information on the use of PAD to detect carbohydrates can be found in: Cai, Liu, Shi (2005); Neuburger & Johnson (1987); Johnson & LaCourse (1991); Johnson, Dobberpuhl, Roberts, *et al* (1993).

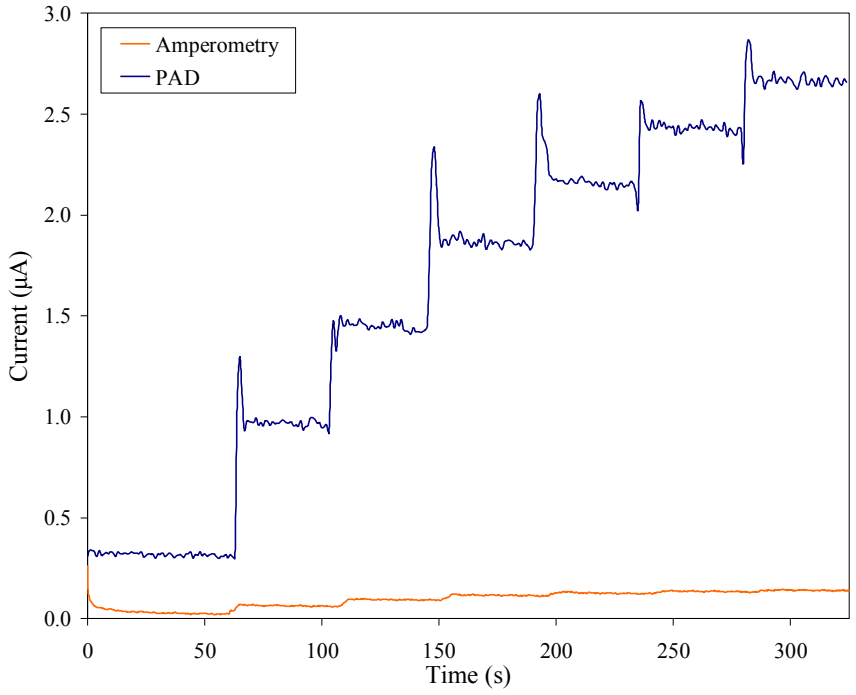

Figure 3.3: *Comparison of fixed-potential amperometric and pulsed amperometric detection (PAD) to 64 mM increases in ethanol concentration in 0.1M NaOH, at a gold working electrode with Ag/AgCl reference.*

3.3.2 Comparison of gold and platinum electrodes

Figure 3.4 compares the responses of platinum and gold working electrodes in PAD. The responses are similar in shape, and in magnitude of current, and both electrode materials

show a decrease in sensitivity at higher concentrations, characterized by smaller increases in current. This is due to adsorption of ethanol oxidation products to the electrode surface (Tarnowski & Korzeniewski, 1996). Although this effect is less significant when performing PAD due to the potential cleaning pulses applied, at higher concentrations, the accumulation of adsorbed ethanol reduces the electrode catalytic surface activity, thus resulting in lower sensitivity (Johnson, Dobberpuhl & Roberts *et al*, 1993).

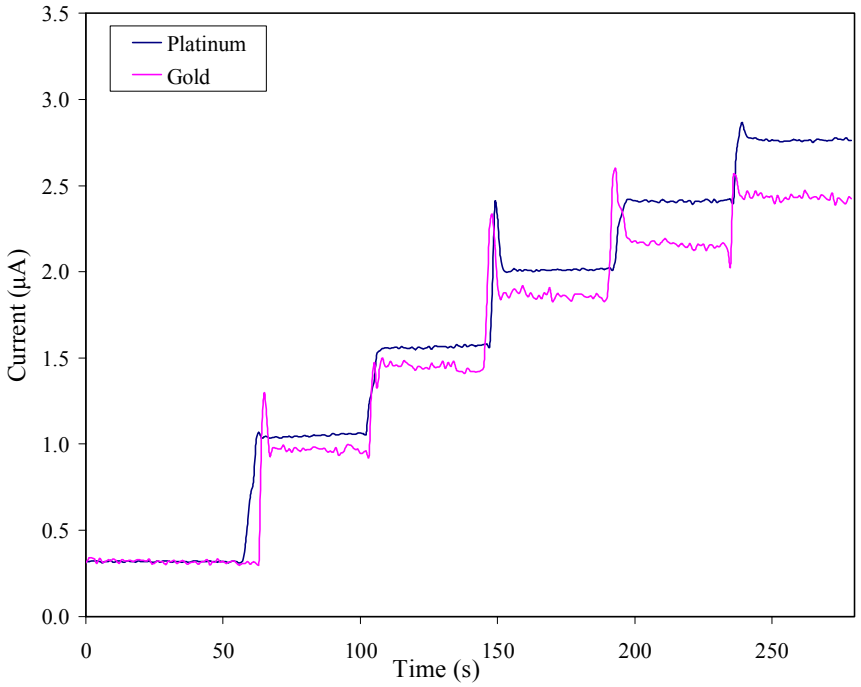

Figure 3.4: *Comparison of platinum and gold working electrode vs. Ag/AgCl reference, for determination of 64mM increases in ethanol by pulsed amperometric detection (PAD). (PAD [platinum]:0.6 V (detection), 1.2 V (oxidation), 0.2 V (reduction); PAD [gold]: 0.2 V (detection), 0.8 V (oxidation), -0.2 V (reduction)).*

3.3.3 Dual pulse staircase voltammetry

Despite PAD being a good aliphatic determination method, its use in a system to monitor the wound environment is not practical, since it lacks selectivity for samples containing more than one electrochemically active species, and therefore the sample would ideally

require some form of pre-treatment, such as fractionation, by HPLC for example. However, the cleaning parameters employed in PAD that are used to regenerate the surface of a working electrode, can be used in combination with the greater selectivity of staircase voltammetry to create the potentially useful method of DPSV. Voltammetry, incorporating *in situ* cleaning reduces losses in electrode activity, a common phenomenon when using solid, nobel metal electrodes for voltammetric measurements. Fung & Mo (1996) have also shown that ethanol can be detected by DPSV over a large linear range (0.01 – 10 mM), a useful characteristic in the context of this work.

Initial validation of the DPSV method was performed by repeating earlier studies performed in this laboratory. Since the determination of glucose and ethanol are of interest here, data first presented in a paper by Bessant & Saini (1999) was reproduced using the system described in this Chapter (Figure 3.5). The potentials of the peaks in Figure 3.5 are similar for glucose and fructose, though interestingly glucose gives a higher response in the first peak (-0.7 V), and fructose the second peak (-0.14 V). The potential of the second ethanol peak (-0.2 V) is slightly lower than that of glucose and fructose (-0.14 V) and the peak is also broader. With regards to glucose and fructose, the peaks around -0.7 V were due to hydrogen oxidation and reduction, and the oxidation peak around -0.14 was due to the oxidation of the carbonyl group present in both fructose and glucose (Fung & Mo, 1995). Figure 3.6 and 3.7 show DPSV responses to increasing concentrations of glucose and ethanol respectively in 0.1 M NaOH.

As observed for the two sugars studied, it is possible that other alcohols may produce similar DPSV curves to ethanol. Therefore, DPSV of methanol and 1-propanol was carried out. Figure 3.8 compares the DPSV responses of 64 mM ethanol, 64 mM methanol and 64 mM 1-propanol. The shape of the methanol response curve is similar to ethanol, but a much lower current is observed. 1-Propanol produced less distinguishable peaks, similar to that of the blank. Therefore, it seems that in the case of these three alcohols, there is the possibility of inter-analyte interference, but with greater selectivity towards ethanol.

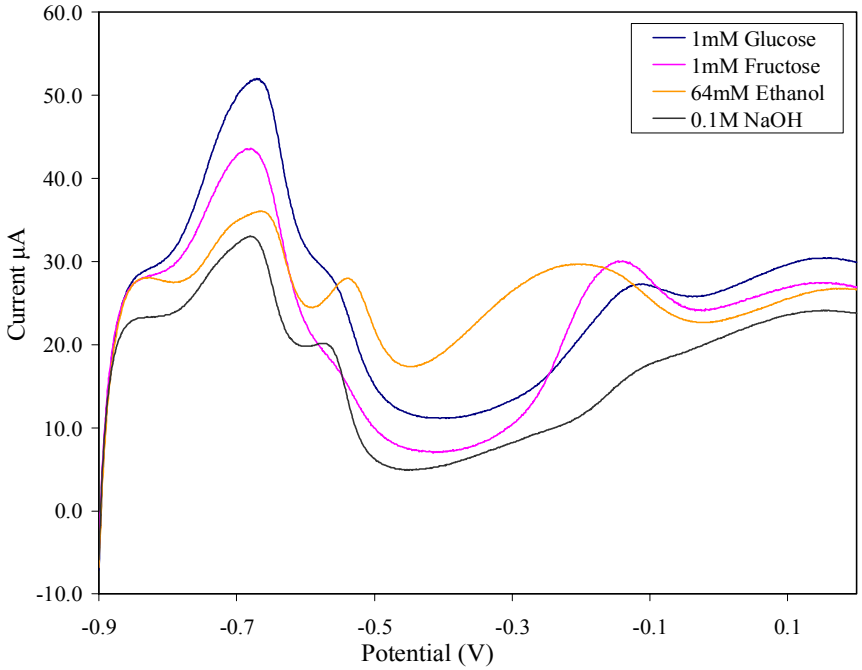

***Figure 3.5**: DPSV responses for 1 mM glucose, 1 mM fructose, and 64 mM ethanol in 0.1 M NaOH at a platinum working electrode vs. Ag/AgCl.*

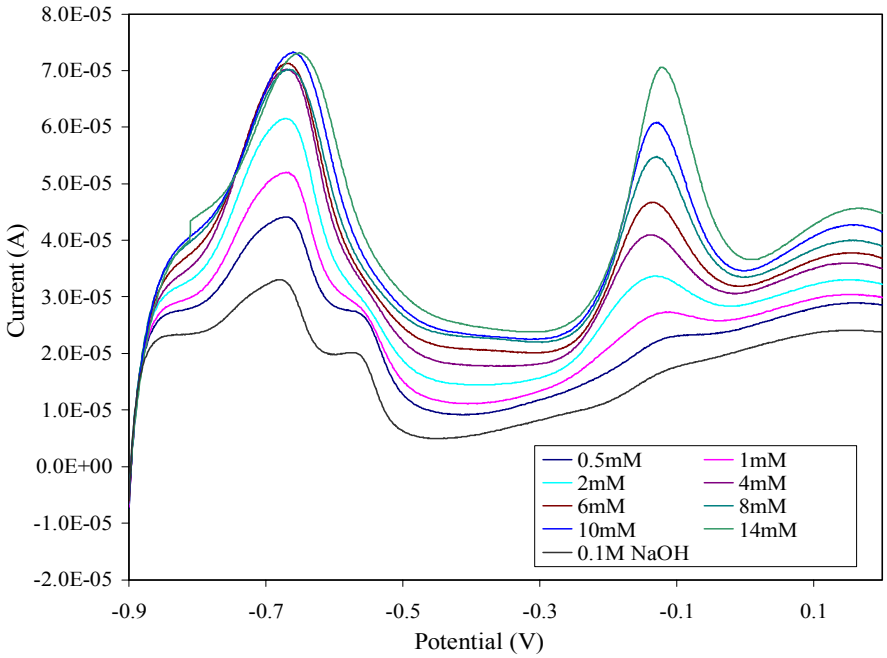

***Figure 3.6**: DPSV responses for different concentrations of glucose in 0.1M NaOH, at a platinum working electrode with Ag/AgCl reference.*

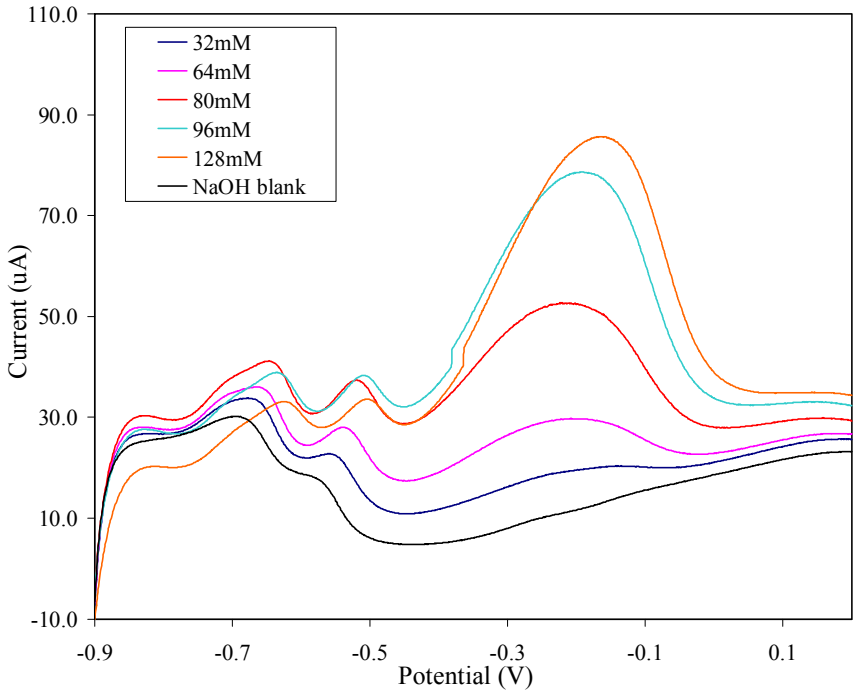

***Figure 3.7:** DPSV responses for different concentrations of ethanol in 0.1M NaOH, at a platinum working electrode with Ag/AgCl reference.*

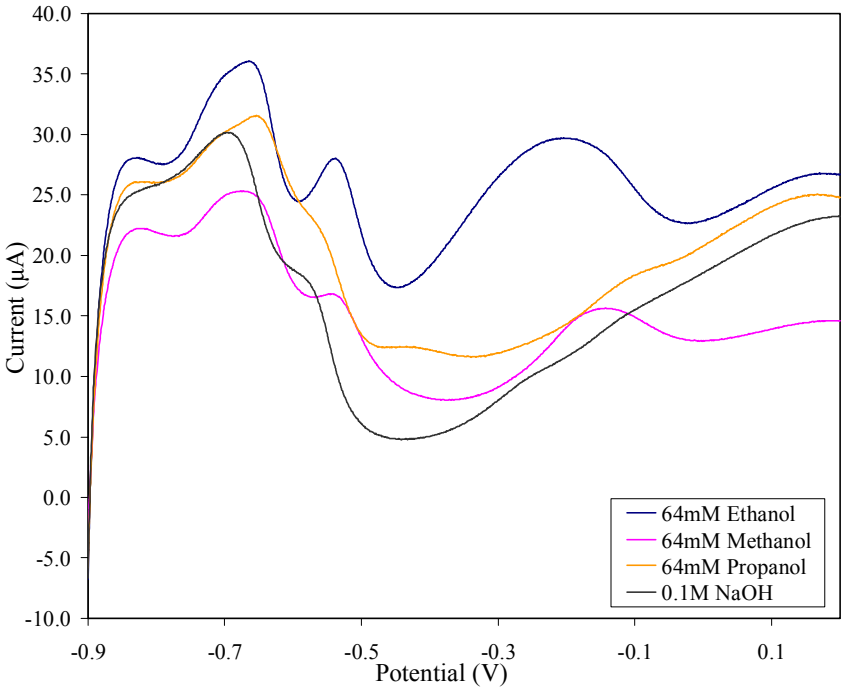

Figure 3.8: *DPSV responses to 64 mM Ethanol, 64mM Propanol, and 64 mM Methanol, at a platinum electrode, in 0.1 M NaOH, with Ag/AgCl reference.*

3.3.4 Comparison of platinum and gold solid electrodes for DPSV

Typically, platinum electrodes are only chosen when the sensitivity of gold electrodes is not sufficient, such as in the detection of low-molecular-mass *n*-alcohols and glycols, which can be detected at platinum electrodes with high sensitivity (Johnson, Dobberpuhl, Roberts *et al*, 1993). Since platinum and gold are both known to be excellent solid-state working electrodes, the sensitivities of both of these were compared. Figure 3.9 compares the DPSV responses of platinum and gold working electrodes to 5 mM ethanol in 0.1 M NaOH, where it can be seen that the platinum displays a slightly superior response curve to gold. Therefore platinum would seem a preferable choice to gold as a solid working electrode for the measurement of ethanol.

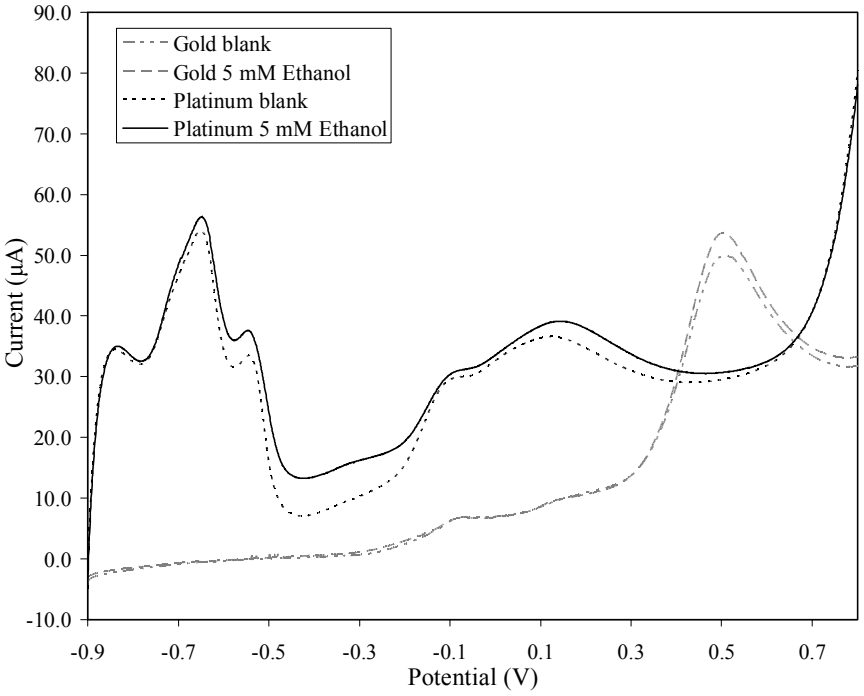

Figure 3.9**:** *Comparison of blank subtracted DPSV responses to 64 mM ethanol at platinum and gold working electrodes in 0.1 M NaOH, with Ag/AgCl reference.*

3.3.5 Investigation of interferents

A common problem in the development of new sensor technologies is that of interfering species i.e. chemicals present in the sample that yield an electrochemical signal that conflicts with that of the analyte of interest, thereby reducing the effectiveness of the sensor measurement. The most commonly problematic interferents in sensor/biosensor construction with respect to clinical samples are ascorbic acid (vitamin C) and acetaminophen (paracetamol). It was therefore of interest to determine whether a range of possible interferents were electroactive in the potential regions of those peaks produced by DPSV for the analytes of interest in this study. The potential interferents were measured electrochemically in 0.1 M NaOH at clinically valid levels (Table 3.1) at a platinum electrode vs. Ag/AgCl.

Table 3.1: *Concentrations of possible interferents found in blood*

Interferents	**Chemical Name**	**Molecular weight**	**Concentration**	
			from: (mM/l)	***to: (mM/l)***
Acetominophen	4-acetomidophenol	151	0.33	1.32
Ascorbic acid	L-ascorbic acid	176.13	0.04	0.17
Bilirubin	Bilirubin	584.67	0.17	0.68
Cholesterol	Cholesterol	386.65	4.53	18.10
Creatinine	Creatinine	113.12	0.66	2.65
Cysteine	Cysteine	121.11	0.05	1.00
Dopamine	3-hydroxytyramine-hydrochloride	189.64	0.17	0.69
Gentisic acid	2,5-dihydroxybenzoic acid	154.12	0.81	3.24
Glutathione	(y-GLU-CYS-GLY;GSH)	307.19	0.0081	0.032
Levo-dopa	3-3,4-dihydroxyphenyl-L-alanine	197.2	0.05	0.20
Salicylic acid	2-hydroxybenzoic acid	160.02	0.78	3.10
Tetracycline	Tetracycline	444.18	0.056	0.23
Tolazamide	1-[hexahydro-1H-azepin-1-yl]-3-[p-tolyl-sulfonyl] urea	311.4	0.04	0.16
Tolbutamide	1-butyl-3-[4-methyl benzynes sulfonyl] urea	270.4	0.92	3.70
Urea	Urea	60.06	20.63	82.50
Uric acid	2,6,8-trihydroxypurine	168.11	0.30	1.19

Some of the interferents tested occur naturally in the body, such as cholesterol or urea (although this is also found in skin treatments such as emollients for eczema), but most are substances taken to treat illness or other medical conditions. Some of these substances are more commonly administered medications than others, such as acetominophen (paracetamol), tetracycline (antibiotics), and ascorbic acid (vitamin C), whereas drugs such as levo-dopa used to treat Parkinson's disease, and methyl-dopa for blood pressure treatment, are only used by a small portion of the population. Figure 3.10 shows the detection of these potential interferents in 0.1 M NaOH by DPSV. The voltammetric responses are blank subtracted, and varied considerably as may be observed.

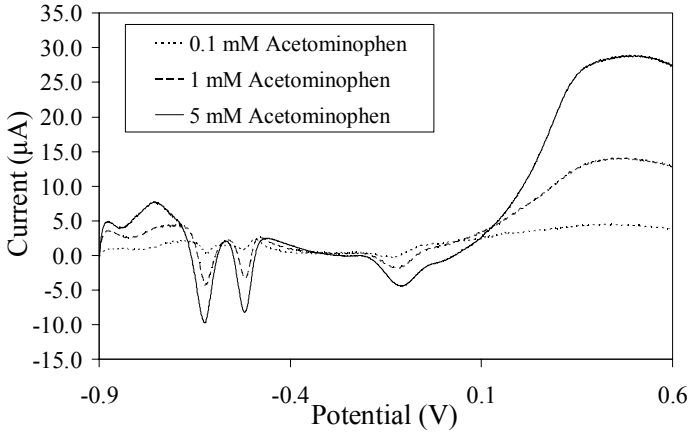
0.1 mM Acetominophen
1 mM Acetominophen
5 mM Acetominophen
Current (μA)
Potential (V)

(a)

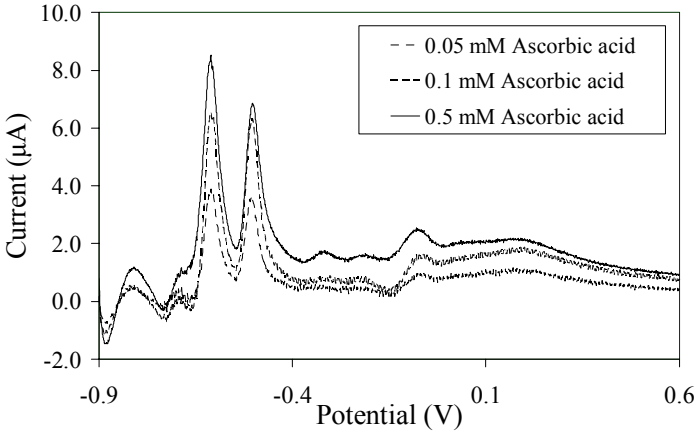
0.05 mM Ascorbic acid
0.1 mM Ascorbic acid
0.5 mM Ascorbic acid
Current (μA)
Potential (V)

(b)

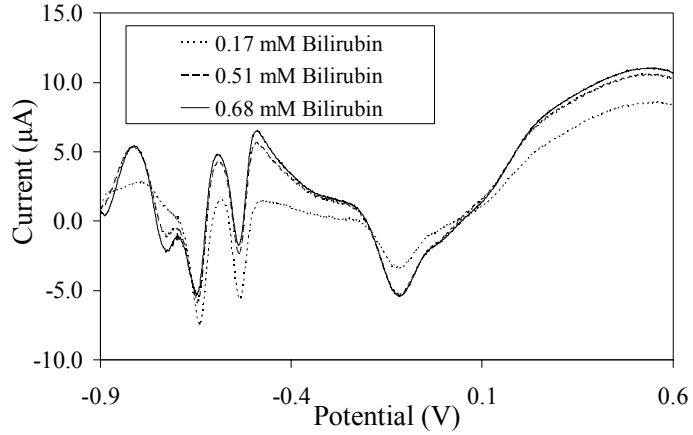
0.17 mM Bilirubin
0.51 mM Bilirubin
0.68 mM Bilirubin
Current (μA)
Potential (V)

(c)

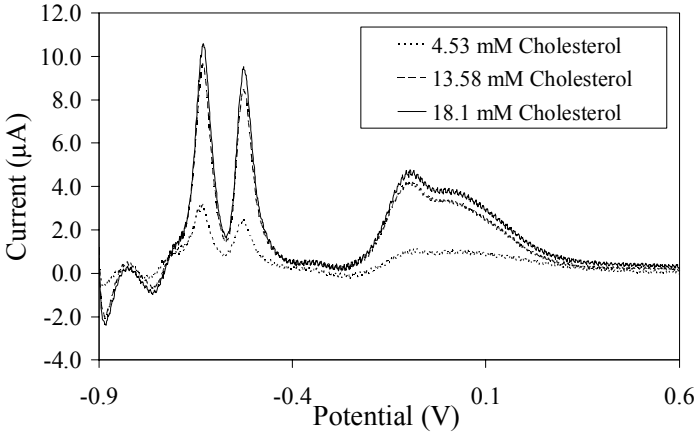
4.53 mM Cholesterol
13.58 mM Cholesterol
18.1 mM Cholesterol
Current (μA)
Potential (V)

(d)

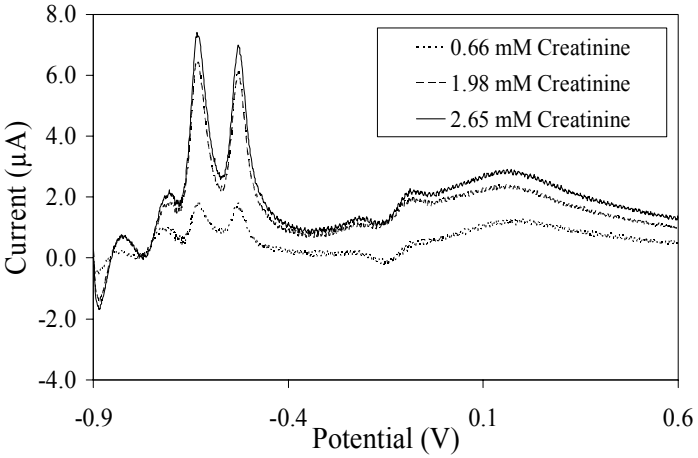
0.66 mM Creatinine
1.98 mM Creatinine
2.65 mM Creatinine
Current (μA)
Potential (V)

(e)

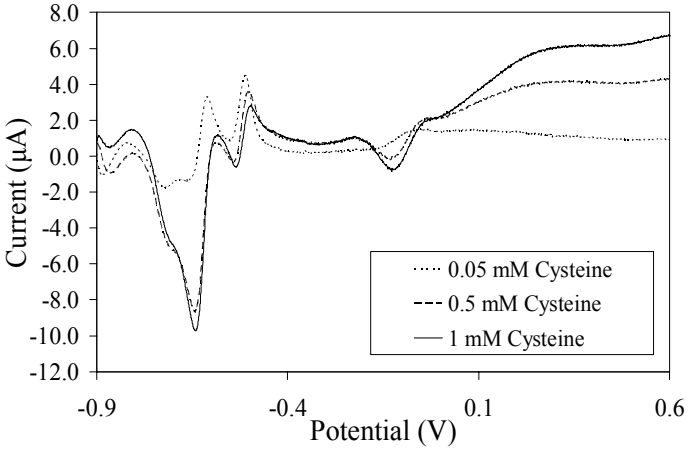
0.05 mM Cysteine
0.5 mM Cysteine
1 mM Cysteine
Current (μA)
Potential (V)

(f)

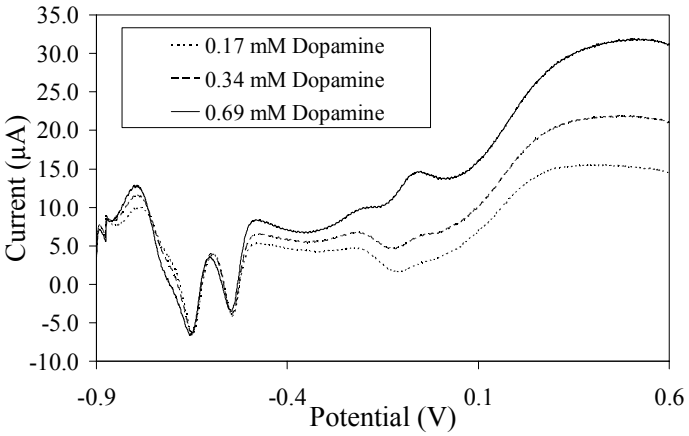
0.17 mM Dopamine
0.34 mM Dopamine
0.69 mM Dopamine
Current (µA)
Potential (V)

(g)

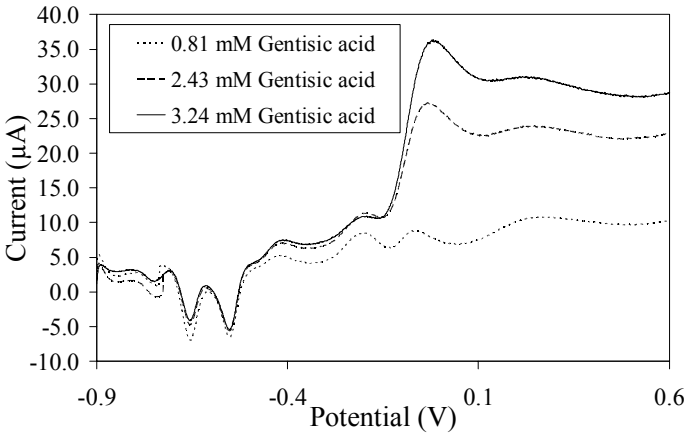
0.81 mM Gentisic acid
2.43 mM Gentisic acid
3.24 mM Gentisic acid
Current (µA)
Potential (V)

(h)

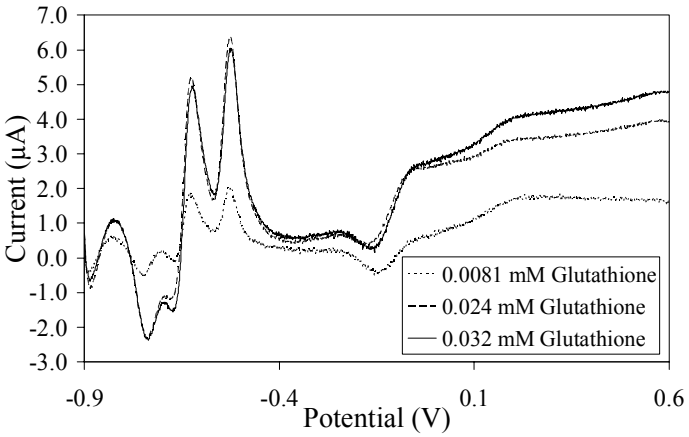
0.0081 mM Glutathione
0.024 mM Glutathione
0.032 mM Glutathione
Current (µA)
Potential (V)

(i)

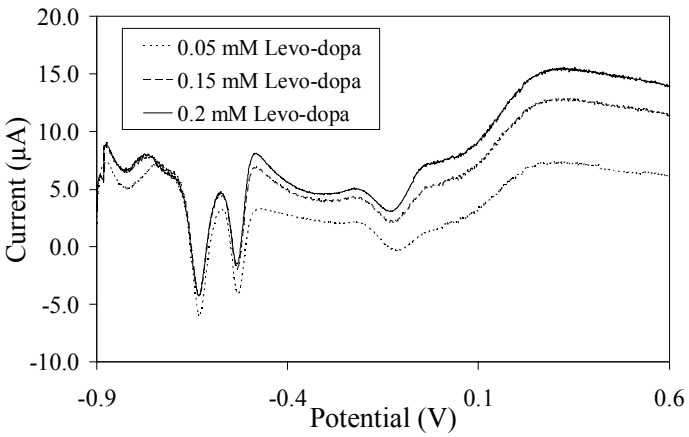
0.05 mM Levo-dopa
0.15 mM Levo-dopa
0.2 mM Levo-dopa
Current (µA)
Potential (V)

(j)

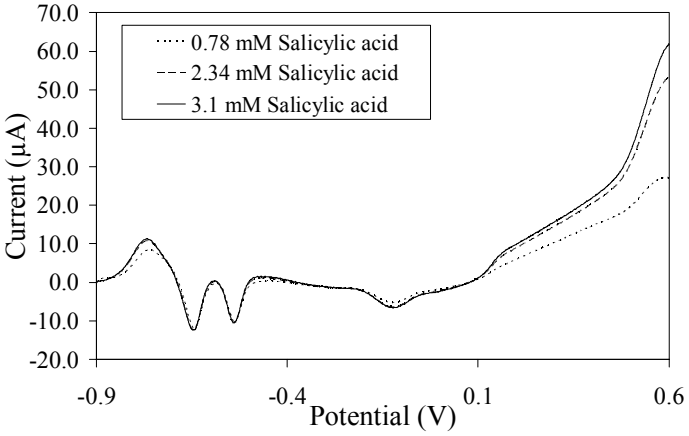
0.78 mM Salicylic acid
2.34 mM Salicylic acid
3.1 mM Salicylic acid
Current (µA)
Potential (V)

(k)

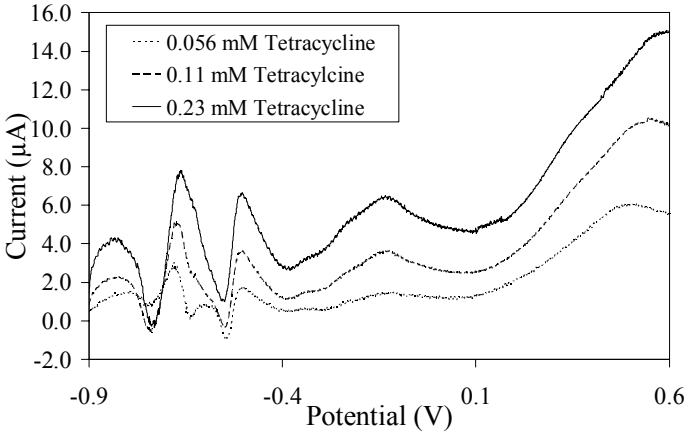
0.056 mM Tetracycline
0.11 mM Tetracylcine
0.23 mM Tetracycline
Current (µA)
Potential (V)

(l)

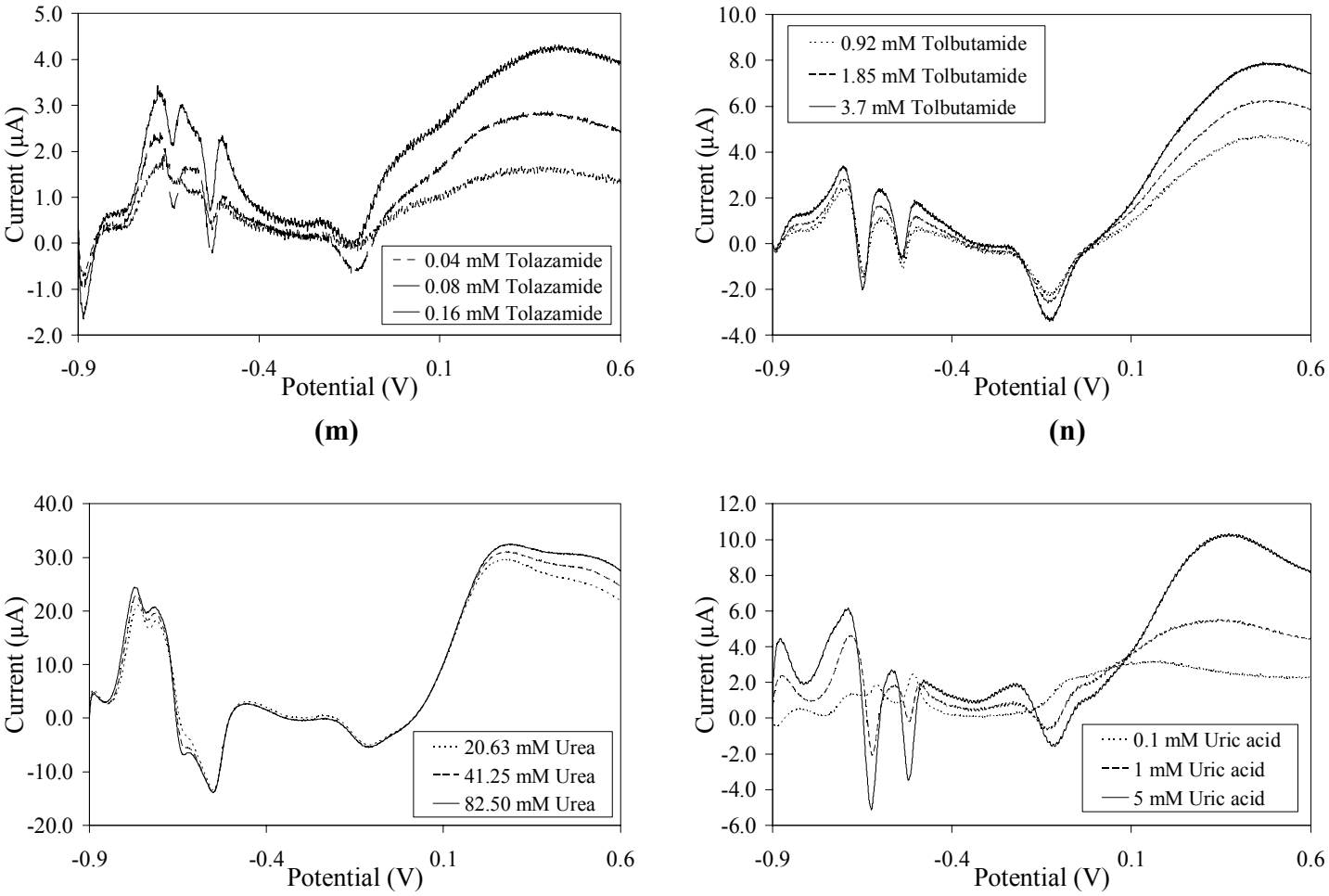

Figure 3.10: *DPSV responses (blank subtracted) for: (a) Acetominophen (b) Ascorbic acid (c) Bilirubin (d) Cholesterol (e) Creatinine (f) Cysteine (g) Dopamine (h) Gentisic acid (i) Glutathione (j) Levo-dopa (k) Salicylic acid (l) Tetracycline (m) Tolazamide (n) Tolbutamide (o) Urea (p) Uric acid, , in 0.1 M NaOH at a platinum working electrode vs. Ag/AgCl reference.*

It was evident that many of these species are electroactive and may cause interference problems, therefore it was necessary to run DPSV of ethanol, glucose and H_2O_2 in 0.1 M PBS in the presence of the most common and problematic of the interferent species, in order to determine their effect on the scan data. Solutions representing the higher concentrations found in the body of ascorbic acid (0.17 mM), acetaminophen (1.32 mM), cysteine (1 mM), uric acid (1.19 mM) and urea (82.5 mM) were made up in 0.1 M PBS

containing 5 mM ethanol. Each of these were measured by DPSV and compared to a DPSV scan of 5 mM ethanol in 0.1 M PBS alone (Figure 3.11). This process was repeated for glucose and H_2O_2. All five species have interfered with the normal DPSV scan for 5 mM ethanol to varying degrees. Ascorbic acid caused the current to increase but a similar current versus potential profile was maintained. Cysteine, acetaminophen and urea significantly altered the profile of the overall voltammetric response. The presence of uric acid yielded a slight increase in current, also yielding an additional peak at around -0.5 V.

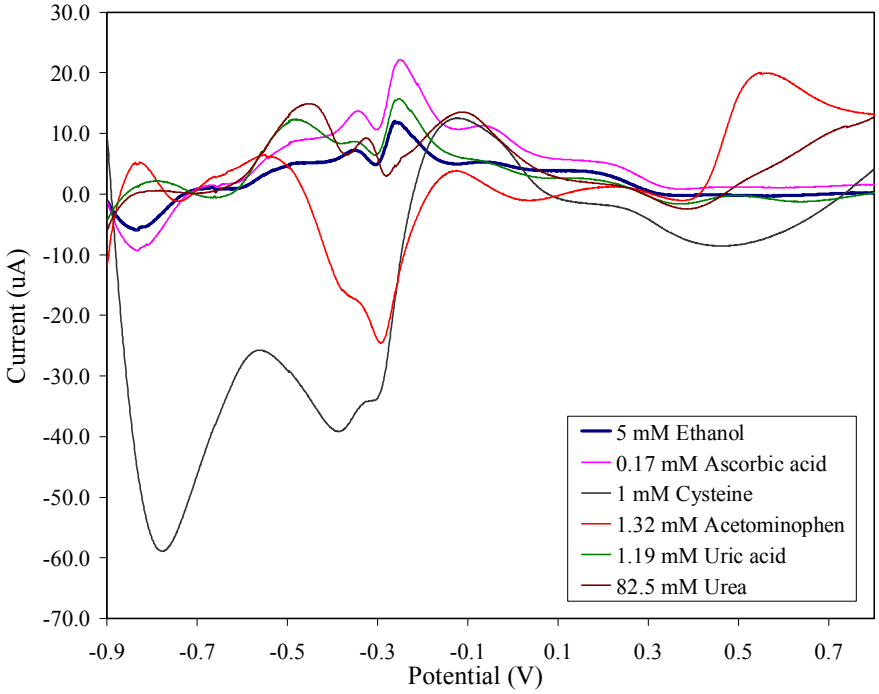

Figure 3.11: *DPSV (blank subtracted) of interferents in 0.1M PBS (blank)containing 5 mM ethanol.*

Figure 3.12 shows the effects of the species on the DPSV scan of 5 mM glucose in 0.1 M PBS. As with ethanol, all five species tested had an effect. Ascorbic acid had the least effect, causing the current to decrease slightly at the -0.25 V and -0.8 V peaks but remained a similar shape scan. Cysteine, acetaminophen and urea significantly altered the shape of

the voltammograms. Uric acid decreased the current slightly at the -0.25 V peak region and increased current in the -0.5 V and -0.8 V region.

Figure 3.13 shows the effects of the species on the DPSV scan of 5 mM H_2O_2 in 0.1 M PBS. As for ethanol and glucose, cysteine had the most significant effect, altering the shape of the whole scan. Uric acid and ascorbic acid had the least affect, remaining a similar shape scan, but at a more negative current. Acetaminophen and urea had a similar shape but a less negative current in the ~-0.4 V peak area, and different shapes and currents over the remainder of the scan.

It seems that overall for DPSV of glucose, ethanol and H_2O_2, ascorbic acid has the least significant effect, followed by uric acid. Cysteine has the most significant effect, followed by urea and acetaminophen. Therefore the presence of any of these species in a sample, will influence the voltammetric profile, making it more difficult to accurately predict concentrations of ethanol, glucose or H_2O_2. It may be possible to reduce the effect of some or all of these interferents by using a suitable membrane to exclude species based on size or charge, such as Nafion, which is negatively charged and repulses negatively charged acids such as ascorbic acid and uric acid. It should be noted that even commercially available self-test glucose biosensors are susceptible to the affects of acetominophen (Cartier, Leclerc, Pouliot *et al*, 1998). Also, if a patients medication is known, it may serve to aid complex volatmmogram interpretation.

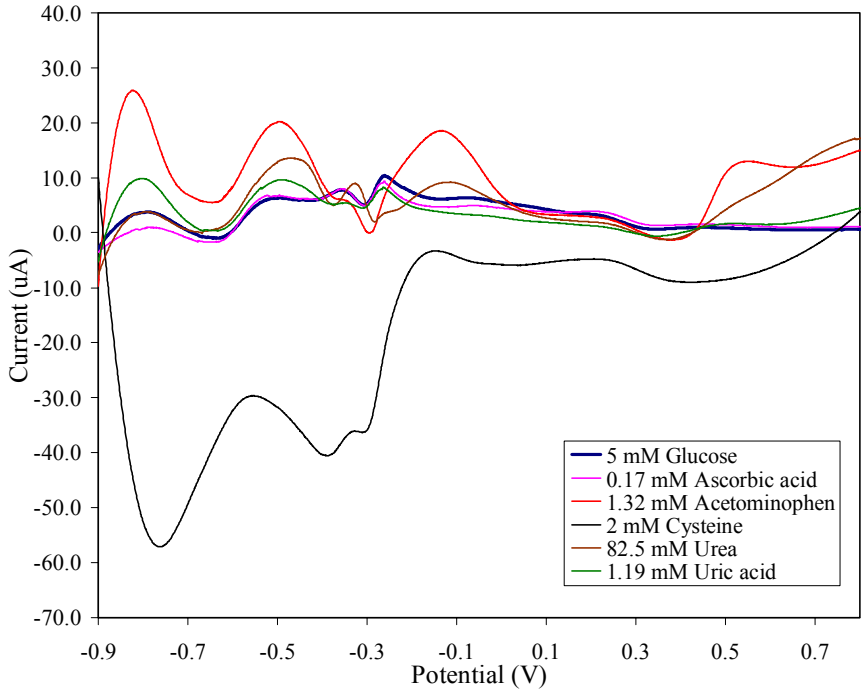

Figure 3.12: *DPSV of interferents in 0.1M PBS containing 5 mM glucose.*

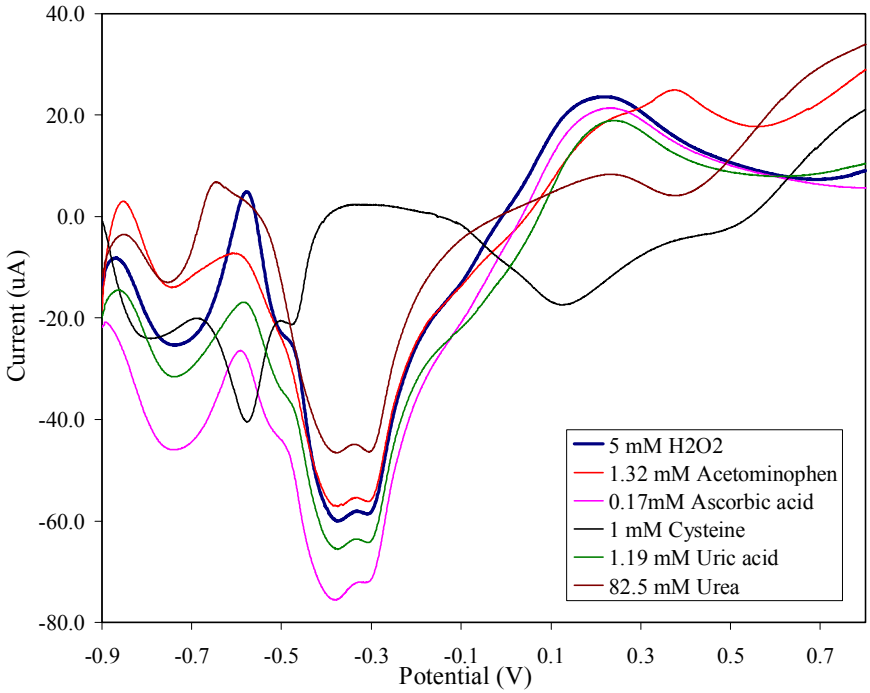

Figure 3.13: *DPSV of interferents in 0.1M PBS containing 5 mM H_2O_2.*

3.3.6 DPSV of glucose, ethanol and H_2O_2 in PBS

Having established a working system, each of the three identified markers glucose, ethanol and H_2O_2 were measured at different concentrations in 0.1 M PBS by DPSV. The data from triplicate measurements was averaged and used to identify peaks in the scans that could be used as a basis for the construction of a calibration curve.

Figure 3.14 illustrates the results for the measurement of 0.5 - 15 mM glucose in 0.1 M PBS. Three main peaks have been identified as possible sources from which to produce calibration plots. Peak one (-0.825 V) becomes increasingly negative in current with increase in glucose concentration, while peaks two (-0.54 V) and three (-0.1 V) become more positive with each increase in glucose concentration.

From these peaks, a given peak height value could be taken, as indicated by the red lines, or the peak area measured using Autolab software. Ratios between peak areas may also prove important indicators.

The DPSV scans for 0.5 to 10 mM ethanol can be seen in Figure 3.15. Three peaks were identified. Peaks one (-0.8 V) and two (-0.36 V) become more negative in current with increase in ethanol concentration, whilst peak three (-0.14 V) increases in peak height and area with increasing ethanol concentration. Examination of the raw voltammetric data suggests that peak three would provide the least linear relationship between peak current and concentration.

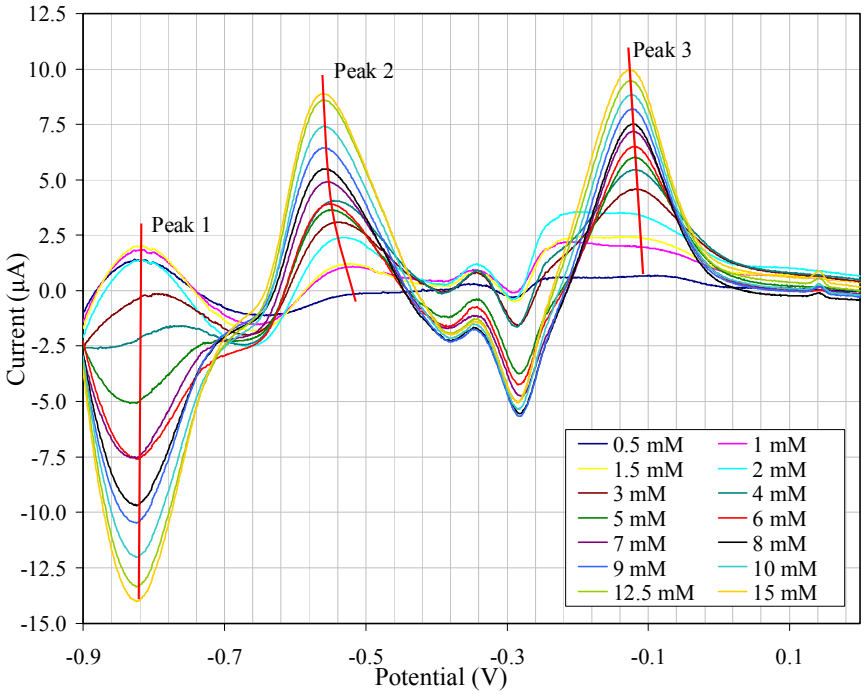

***Figure 3.14**: DPSV of glucose in 0.1M PBS at platinum working electrode vs. Ag/AgCl reference. Scans are blank subtracted averages of 3 scans.*

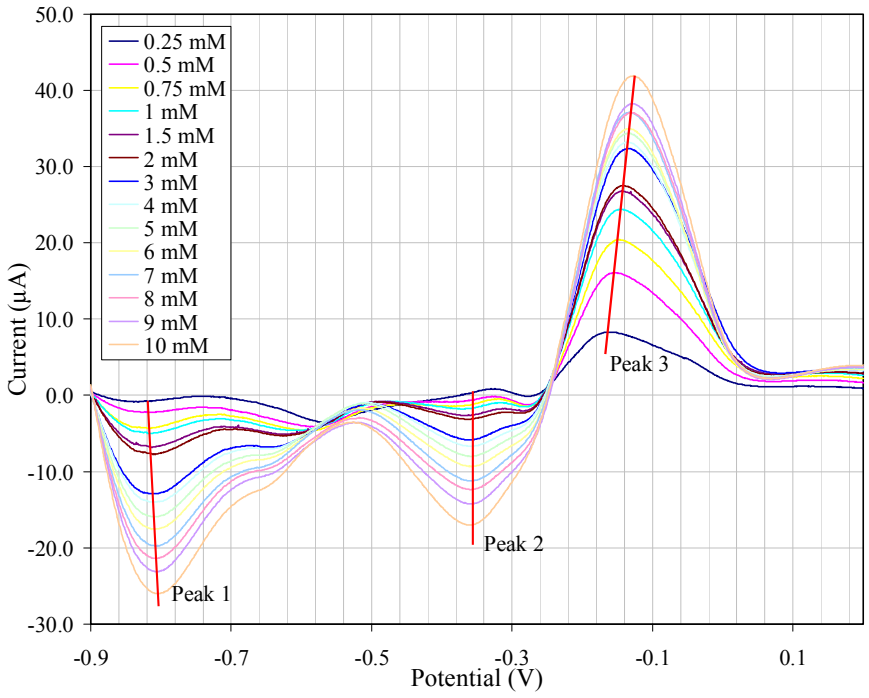

***Figure 3.15**: DPSV of ethanol in 0.1M PBS at platinum working electrode vs. Ag/AgCl reference. Scans are blank subtracted averages of 3 scans.*

Two oxidation peaks (-0.76 V and -0.34 V) were identified for H_2O_2 across the concentration range studied (0.25-10 mM), as illustrated in Figure 3.16. Both peaks exhibit more negative peak currents with increasing concentration. However, it can be seen that for peak one (-0.76 V) at concentrations less then 2 mM, this pattern is not followed. For peak two (-0.34 V), it can be seen that increase in peak size does not follow an entirely linear relationship until a concentration of 2 mM is exceeded.

Although patterns can be observed for averaged scans, the differences between scans of different concentrations were not very large, making it especially important to check the deviation that occurs with replicate scans. Therefore, a single concentration of ethanol (5 mM), glucose (5mM), and H_2O_2 (1 mM) in 0.1 M PBS were measured five times by DPSV, and the variation determined. As normal, electrodes and cells were cleaned between measurements, and each DPSV replicate was scanned ten times to establish blank equilibrium, and again for measurement equilibrium. Figure 3.17 displays that average of the five scans together with the standard deviation for each analyte.

The standard deviations were large, particularly for the glucose peak, which would make accurate prediction of concentration difficult in a sample containing, for example, elevated levels of ethanol. The major cause of this problem lies with the baseline (blank), since despite establishing a stable baseline for each measurement, the location of this baseline was found not to be reproducible between experiments. It is also clear that the analytes studied yielded peaks with similar potentials. Consequently, mixtures of these three analytes were examined to determine the effect of this factor on analyte determination.

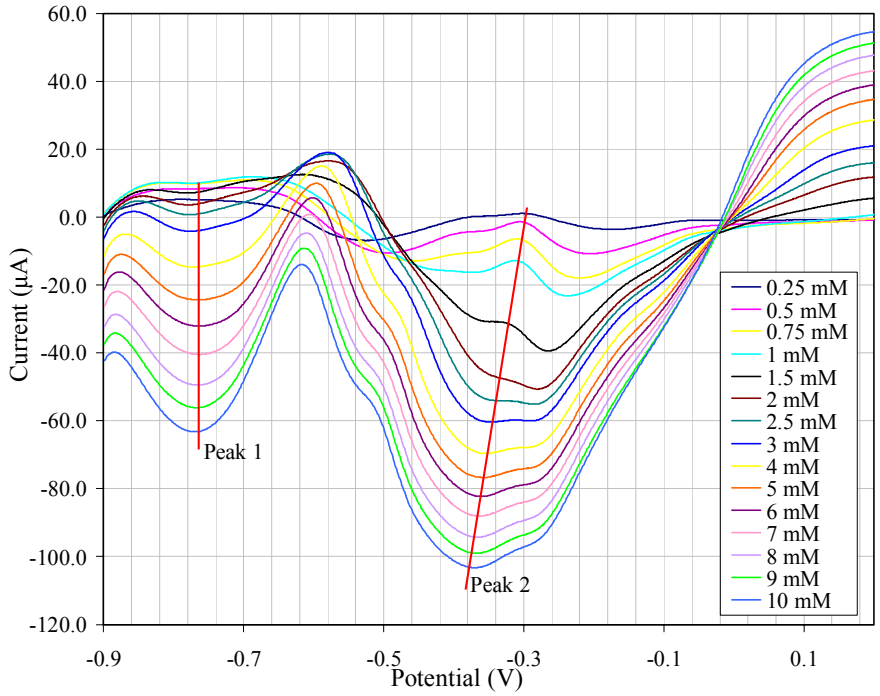

***Figure 3.16**: DPSV of H_2O_2 in 0.1M PBS at platinum working electrode vs. Ag/AgCl reference. Scans are blank subtracted averages of 3 scans.*

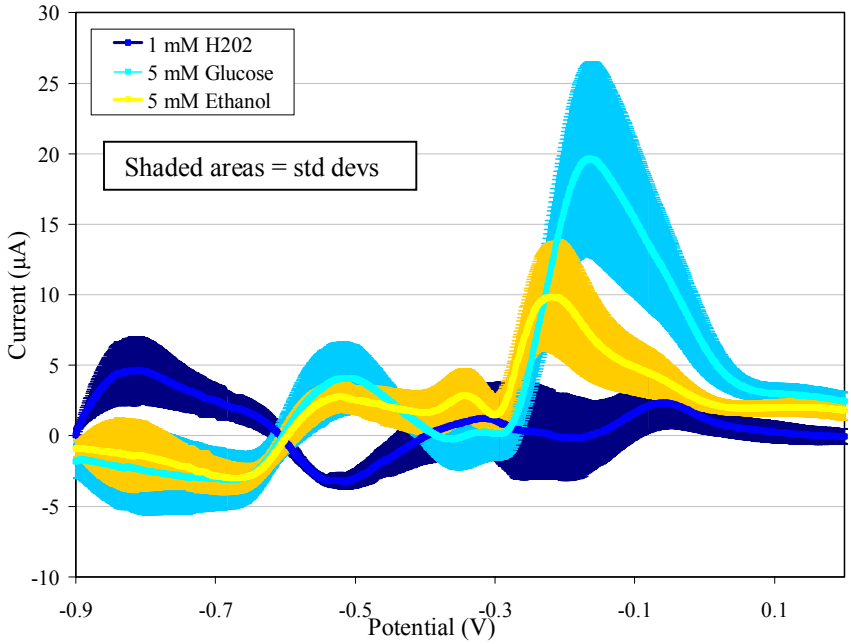

***Figure 3.17:** DPSV of 5 mM glucose, 5mM ethanol, 1mM H202 in 0.1 M PBS at platinum working electrode vs. Ag/AgCl reference. Scans are blank subtracted averages of 5 scans. Shaded areas represent +/- 1 standard deviation.*

3.3.7 DPSV of mixtures of glucose, ethanol and H_2O_2 in PBS

Solutions were prepared of combinations of the three selected target analytes in order to examine the resultant DPSV scans. The results of four combinations in 0.1 M PBS at a platinum working electrode vs. Ag/AgCl can be seen in Figure 3.18. By comparing the scans for ethanol and ethanol with glucose, it can be seen that the presence of glucose positively shifted the scan ~10 µA and added a broad peak between -0.6 and -0.9 V mirroring that present in the scan of glucose alone. H_2O_2 alone produces the most negative scan. The addition of ethanol to H_2O_2 shifted the scan positively between -0.9 and 0 V and negatively from 0 to 0.6 V. The same pattern is replicated to a greater extent with the presence of glucose with H_2O_2, and greater still with the presence of both glucose and ethanol with H_2O_2.

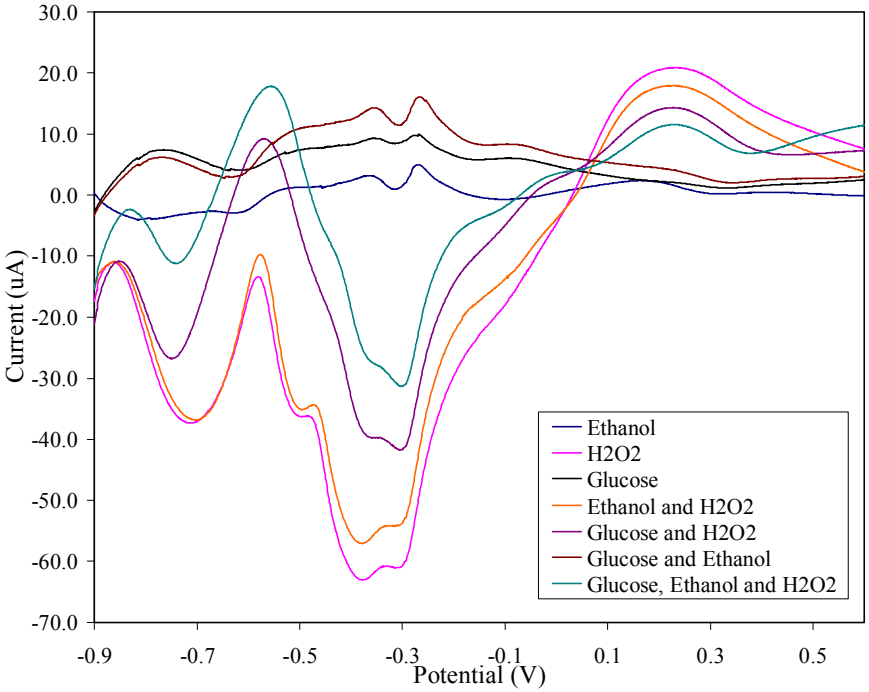

***Figure 3.18**: Blank subtracted DPSV scans of mixtures of 5mM ethanol, 5 mM glucose and 5 mM H_2O_2 in 0.1 M PBS at platinum working electrode vs. Ag/AgCl reference. n=3.*

Observation alone of Figure 3.18 has revealed that since the presence of either or both of glucose and ethanol in a solution containing H_2O_2 seems to yield voltammograms with a number of similar features. In an unknown sample, it would prove challenging, even with advanced statistical data treatment models, such as those employed by Bessant (1998), to determine whether the solution contains H_2O_2 alone, or one or both of glucose and ethanol. An unknown solution that does not contain H_2O_2, could be determined as containing ethanol alone, and not ethanol and glucose, by the absence of a peak from -0.6 to -0.9 V. A solution containing both glucose and ethanol may not be possible to determine from one containing glucose alone due to inter-analyte interference.

3.3.8 DPSV with screen printed electrodes

Despite the limitations of DPSV already uncovered, it was of interest to see whether the technique of DPSV could be performed using screen printed electrodes, since a portable device with disposable electrodes would be desirable for use with clinical material, and therefore the use of solid state electrode is therefore not practical. Two screen printed electrode assemblies were tested, both three electrode systems with a Ag/AgCl reference, but one type having a carbon working electrode, and the other a gold working electrode. Neither type was particularly successful, although the screen-printed gold electrode proved superior with respect to the voltammetric response profiles obtained. Figure 3.19 illustrates the problem encountered in establishing a stable baseline in 0.1 M PBS. The first eight blank scans are shown. Only a very minor change in the response profile was noted on addition of ethanol. The carbon design produced less of a distinctive peak for the baseline, which decreased further with the addition of ethanol (Figure 3.20).

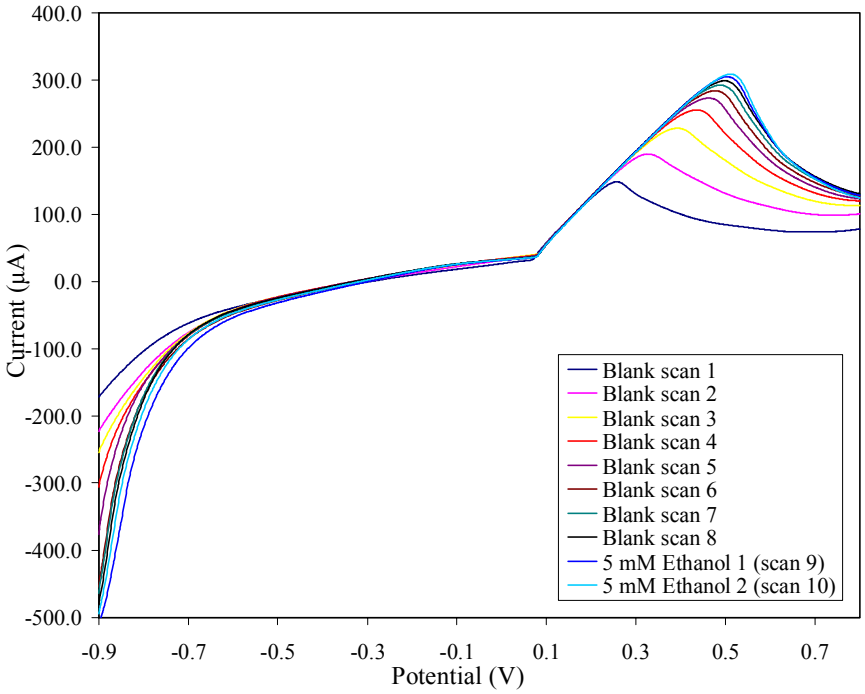

***Figure 3.19**: Aging effect of repeated DPSV scans in 0.1M PBS (blank) and 5 mM ethanol with a screen printed gold working electrode (vs. Ag/AgCl reference).*

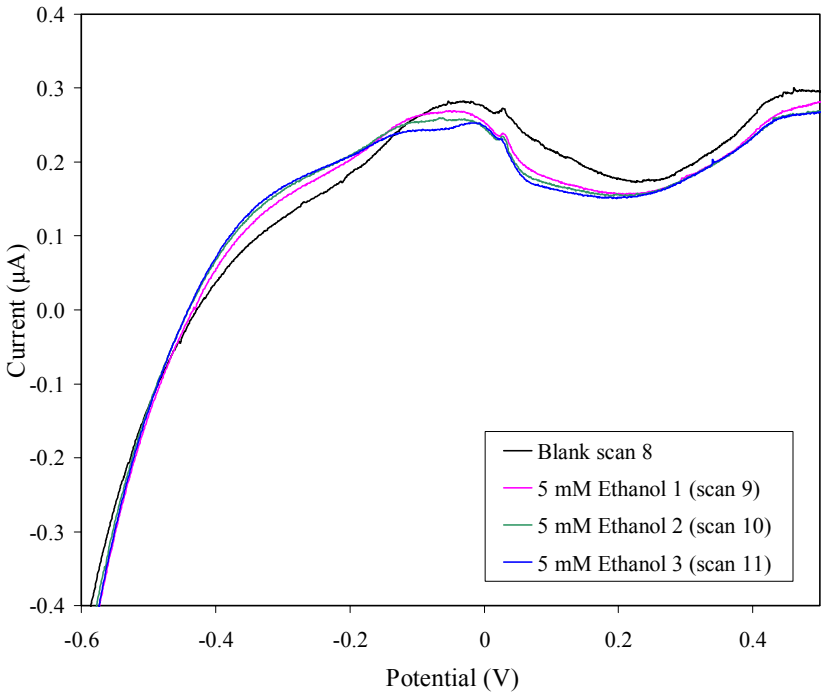

***Figure 3.20**: DPSV scans of 0.1 M PBS (blank) and 5 mM ethanol with a screen printed carbon working electrode (vs. Ag/AgCl reference).*

Therefore, neither of the two screen printed electrodes tested are suitable for DPSV, since the response profiles obtained illustrate that they are not sufficiently electrochemically sensitive to ethanol.

3.4 Conclusions

PAD was shown to be more sensitive than fixed-potential amperometry, thus illustrating the benefits of the cleaning pulse waveform, which was also employed in DPSV. The DPSV procedure employed was based on that used in earlier published work from this laboratory, for the determination of glucose, fructose and ethanol in complex solutions. Initial experiments were performed using the same experimental set-up and were found to concur with this earlier study (Bessant & Saini (1999)). Voltammograms of fructose and glucose, and of ethanol, methanol and propanol were created and examined. Gold and platinum solid-state working electrodes were compared, with platinum being found to be more favourable in this case. Possible electrochemical interfering species were also individually measured by DPSV in NaOH at clinically valid concentrations.

Following this, DPSV of ethanol, glucose and H_2O_2 was carried out in PBS in the presence of five of these species, selected according to their frequency of usage by the general population. All had an effect, cysteine being the most electrochemically active, followed by urea, acetaminophen, uric acid and ascorbic acid. Measurement of different concentrations of glucose, ethanol and H_2O_2 individually in PBS demonstrated clear peaks and relationships between peak heights and concentration. However, repeat measurements at one concentration for each analyte revealed high standard deviation values. DPSV of

mixtures of the three analytes illustrated potential difficulties in identifying individual components and concentrations of the analytes due to inter-analyte interference. A limited evaluation using carbon and gold screen printed electrodes found them to be of limited value for DPSV measurement of the selected analytes in the context of this study.

Given the problems highlighted in this initial study with: baseline reproducibility; large deviations (error); interfering species; identification in mixtures; and unsuitability of screen printed electrodes; it was decided that DPSV was not a suitable technique for the monitoring of wound biomarkers, and therefore not to progress the DPSV study further in favour of the biosensor array and odour analyser which held more promise after initial studies, and would be tested in surrogate wound fluid.

However, it is possible that incorporation of a negatively charged membrane such as Nafion may reduce interferent effects. Also, there is still some potential for the use of sophisticated data analysis, though this would be more difficult than anticipated due to the similarities in some voltammetric profiles. Also, little has been reported regarding DPSV of glucose and ethanol, and literature searches have not revealed any reports on DPSV of hydrogen peroxide, or of clinical interferents. Also, none of the reports have been based on measurements in PBS. Though a small section of work, no reports have been identified investigating the use of screen printed electrodes for the technique of DPSV. Therefore the work in this Chapter does hold the significant benefits of generating data and assessing the feasibility of this approach for clinical measurements.

4. Detection Using a Biosensor Array

4.1 Introduction

The objective of this Chapter, as outlined in Section 1.6, is to investigate whether a biosensor array may be used as a diagnostic tool in the early stages of wound healing, based on the detection of the bacterial metabolite ethanol, and the human markers glucose and hydrogen peroxide, within the wound fluid sample.

The suitability of a glucose biosensor, hydrogen peroxide biosensor and ethanol biosensor were investigated for the measurement of the selected biomarkers - glucose, hydrogen peroxide and ethanol respectively (outlined in Section 2.1), in 0.1M PBS, and secondly in model wound fluid. Since one of the main causes of complications in wound healing is bacterial, as discussed in Section 1.1.6, the direct detection of metabolic ethanol production by *S.aureus* with ethanol biosensor was also investigated. The effect of the presence of bacteria on the performance of the glucose and hydrogen peroxide biosensors was also tested. The effect of possible interferents such as ascorbic acid (vitamin C) was assessed for each of the three biosensors.

The objectives were achieved by screen printing a three electrode (carbon working, carbon counter, silver /silver-chloride reference) assembly (described in Section 4.2.3) which could be used as the basic starting point for each of three amperometric biosensors, with the exception of the glucose biosensor which had an additional layer, rhodinised carbon, printed onto the working electrode (reasons outlined in Section 4.3). The experimental programme followed for the biosensor work is illustrated in Figure 4.1:

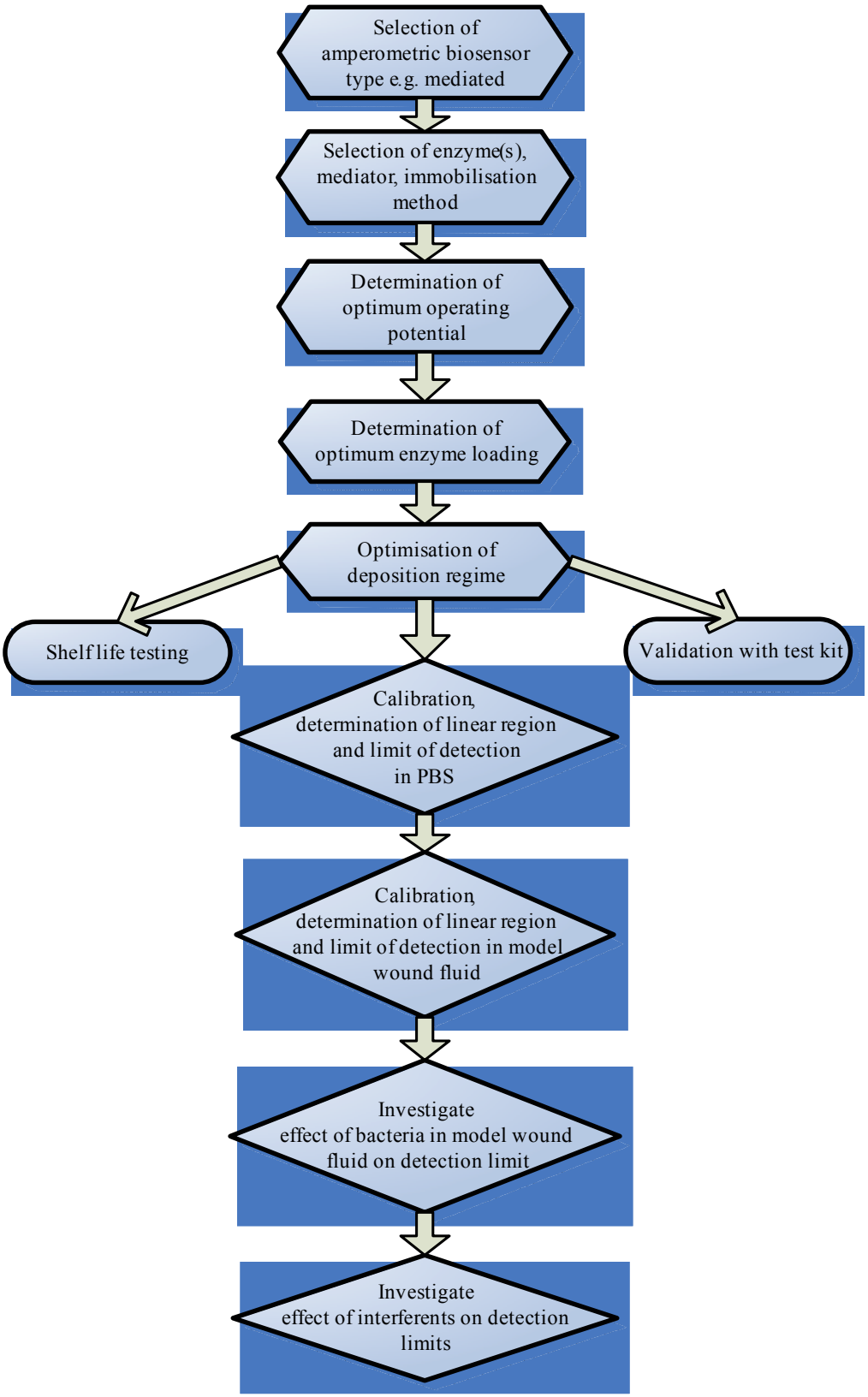

***Figure 4.1**: Flow diagram of biosensor development and testing stages*

The stages of Figure 4.1 are described in this chapter for each of the three biosensors. Model wound fluid was made by separating serum from blood, as described in 2.2.4, giving a surrogate wound fluid, based on the major component of wound fluid, namely serum.

4.2 Materials and Methods

4.2.1 Reagents

Aqueous solutions of phosphate buffer saline (Sigma, Poole, UK), ethanol (99.9% denatured HPLC grade, Aldrich, (Poole, UK), hydrogen peroxide (31.3% v/v assay ACS reagent, Sigma, Poole, UK), and glucose (reagent grade, Fisher, Loughborough, UK) were made using reverse osmosis water. Cellulose acetate MW 37,000 (Sigma, Poole, UK), and dimethylferrocene (Aldrich, Poole, UK) were prepared in acetone (Fisher, Loughborough, UK). Glucose oxidase (from *Aspergillus niger*, E.C. 1.1.3.4) was in the form of a freeze dried powder from Biozyme, Blaenavon, Wales. Horseradish peroxidase (from *Amoracia rusticana,* E.C. 1.11.1.7) was from Sigma (Poole, UK) in lyophilized powdered form. Buffered aqueous alcohol oxidase (from *pichia pastoris,* E.C. 1.1.3.13) and lyophilized powdered alcohol oxidase (from *Candida boidinii,* EC 1.1.3.13*)* were also from Sigma, (Poole, UK).

4.2.2 Instrumentation

Amperometric measurements were made using a PGSTAT10 multichannel (4 channel) Autolab illustrated in Figure 4.2 (Eco Chemie, Utrecht, The Netherlands), operated using GPES software (version 4.9). The biosensors were connected to the four channels of the Autolab using connectors made in-house using basic electronic components from Maplins,

UK. The connectors are known as FFC (Flat Flexible Cable) Connectors, using a 1.25mm pitch (Molex, part number 39-51-3084). They are mounted onto 'Veroboard', and then connect via 4mm plugs and sockets to the potentiostat, as illustrated in Figures 4.2 and 4.3. The wires were protected by heat shrink rubber, and the circuit board by PVC tape.

4.2.3 Measurement

Amperometric measurements were made using the 'Chrono methods > 0.1s' method of the GPES software. The interval time between points was 0.1 s, and measurements were made for a period of 150 s. The operating potentials for each of the biosensors are discussed later in the chapter.

4.2.4 Fabrication of screen-printed electrodes

Identical screen-printed 3-electrode assembly designs were used for each of the three biosensors, involving the successive deposition of ink layers. A DEK 248 printer (DEK, Weymouth, UK) incorporating screens with appropriate stencil designs (60 sensors per screen) were used for precision ink depositioning. The base material for electrode fabrication was 250 μm polyester sheeting (Cadillac Plastic, Swindon, UK) onto which was deposited successive ink layers. The hydrogen peroxide and ethanol sensors consisted of three deposition layers. The first of these was carbon ink 145R layer (MCA Services Ltd., Melbourn, Cambs. UK) - the base layer for all three electrodes; the second was a Ag/AgCl layer (MCA, UK) covering just the reference electrode; and the third an insulation layer – 242-SB epoxy-based blue protective coating ink (Agmet ESL, Reading UK). The electrodes were then heat-treated at 125°C for 1 h to cure the insulation shroud. The glucose sensor

had an additional layer applied before the insulation layer – rhodinised carbon (MCA, UK). Rhodinised carbon has been found to be a catalytic material with excellent properties for the oxidation of H_20_2, therefore one part rhodinised carbon 4a mixed with four parts 2.5% w/v hydroxyethyl cellulose in 0.1M phosphate buffer (pH 7.2) was screen-printed over the underlying working electrode (Kroger, Setford, & Turner (1998). The four layer assembly of the glucose sensor can be seen in Figure 4.4.

Figure 4.2: *Multichannel Eco Chemie Autolab and sensor connections*

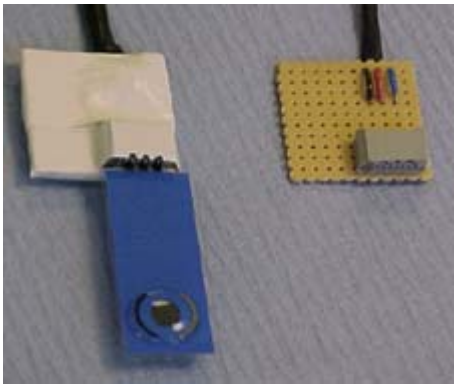

Figure 4.3*: Biosensor connection*

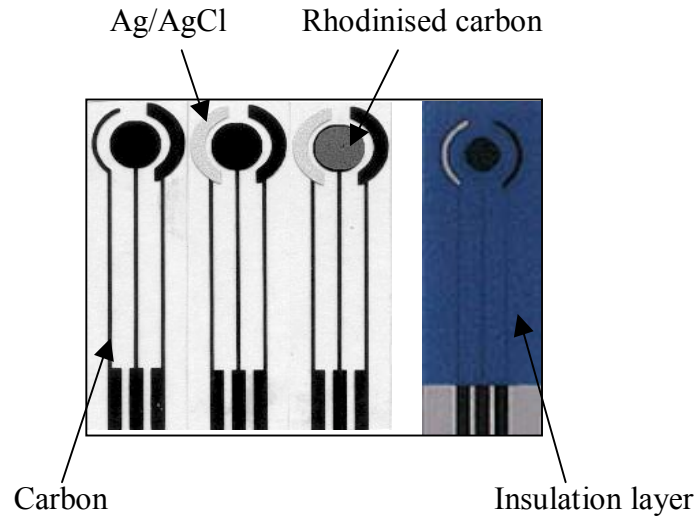

Figure 4.4*: Four layers of the screen printing process for three electrode assembly*

4.3 Glucose Biosensor

Following from screen printing the three electrode assembly with rhodinised carbon working electrode, the final stage of the glucose biosensor fabrication was the deposition of the enzyme glucose oxidase. The glucose biosensors made were based on the amperometric detection of H_2O_2 catalytically oxidised at the rhodinised carbon working electrode (Newman, White, Tothill *et al*, 1995). Several studies have reported the benefits of using rhodinised carbon in biosensor design, such as Turner, White, Schmid *et al* (1994), Kroger, Setford & Turner (1998), and Cullen, Jawaheer, White *et al* (2003). The enzyme glucose oxidase (GOx) (Biozyme, Blaenavon, Wales, UK) was acquired in the form of a freeze dried powder with 261.7 U/mg material, originating from *Aspergillus niger*. GOx from *A.niger* is a dimer of two identical subunits, each containing a tightly bound FAD molecule as cofactor, and is highly specific for ß-D-glucose. The glucose biosensor operating principle is depicted in Figure 4.5, where H_2O_2 was amperometrically detected at the rhodinised carbon working electrode poised at a suitable operating potential:

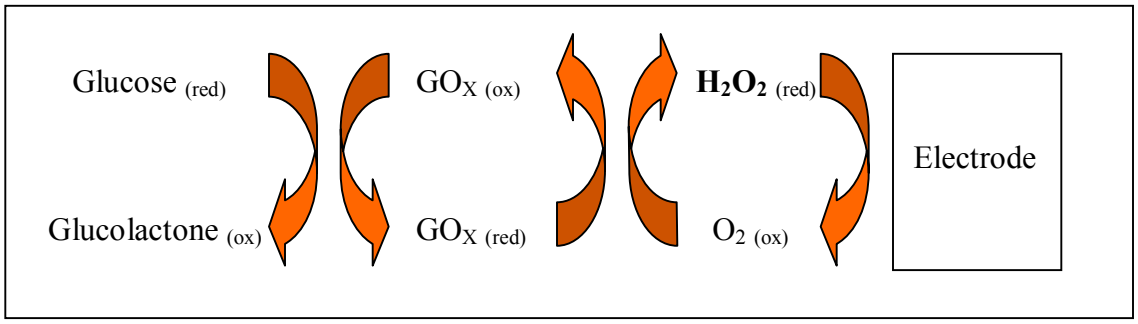

***Figure 4.5**: Glucose biosensor reaction scheme*

The GOx powder was dissolved in 0.1M PBS pH 7.2 to give the required activities for glucose determination in the context of this study. The work of Kröger, Setford & Turner (1998) was used as the basis for the optimisation of the glucose biosensor that follows.

4.3.1 Standard electrochemical measurement methodology

Although electrochemical theory activities for glucose determination in the context of this study suggests that amperometric measurements are best performed in stirred solutions, this is not practical, nor commonplace with commercially available screen-printed biosensor assemblies. It has also been shown previously with the sensors used in this study (Kröger, Setford & Turner, 1998) that it is not necessary to stir the measurement solution. Therefore, it was possible to carry out the experiments by pipetting a small droplet of test solution onto the sensor, covering the three electrodes. It was found that a volume of 150 µl was suitable.

Kröger, Setford & Turner (1998) also demonstrated that the background current for these sensors was consistently within a narrow range, and therefore, it was possible for glucose to be present in the measurement solution from the beginning. Using a four channel Autolab, one channel was used to measure the background current (blank), whilst the three remaining channels were used to simultaneously measure glucose in test solution. The sensors were equilibrated in the measurement solution and a current plateau was reached. A differential measurement was taken after 150 s (analyte current - background current = signal). An example can be observed in Figure 4.6, where H2O2 is measured at the rhodinised carbon working electrode. H_2O_2 was used for this example since H_2O_2 is the reaction product detected at the electrode surface in the glucose oxidase based system that follows.

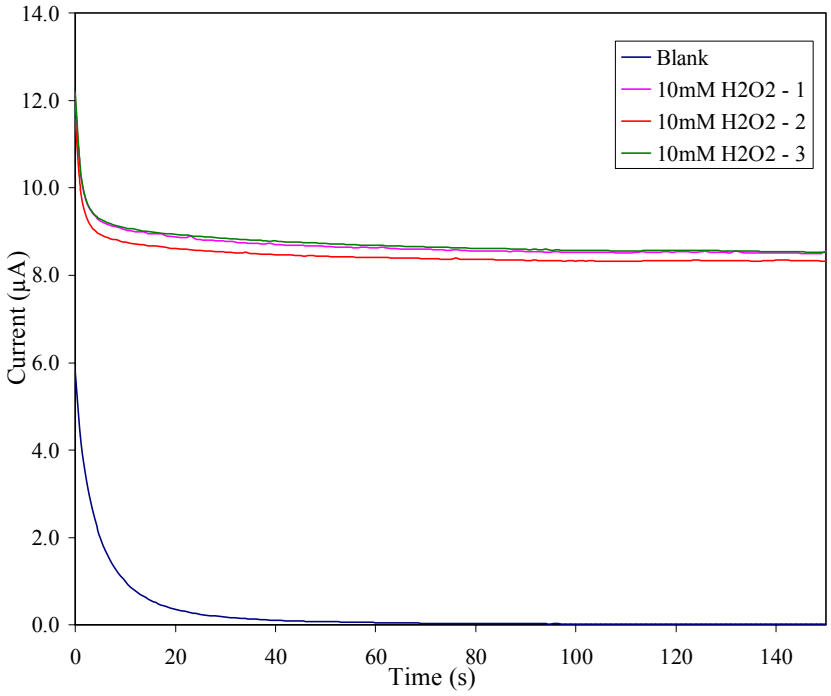

Figure 4.6: *Example amperometric measurement of H_2O_2 at rhodinised carbon working electrode vs. Ag/AgCl, at +300mV.*

4.3.2 Determination of optimum operating potential

The operating potential for the amperometric detection of GOx generated H_2O_2 at rhodinised carbon working electrodes has been reported in a number of publications as +300mV or +350mV vs. Ag/AgCl (White, Turner, Bilitewski *et al* 1994; Kröger, Setford, Turner, 1998; Cullen, Jawaheer, Rughooputh *et al* 2003).

To verify this, 10mM H_2O_2 was prepared in 0.1M PBS pH 7.2 for detection by the three electrode assembly in the absence of GOx. The current was measured at operating potentials from 100 to 600 mV, repeated in triplicate for each potential. The average current response to 10mM H_2O_2 at each potential, and the background current are shown in

Figure 4.7. The ratio between H_2O_2 current and background current (Figure 4.8) revealed the optimum potential to be in the region of +300mV to +350 mV.

The electrocatalytic activity of rhodinised carbon does indeed reduce the potential from that required using a standard carbon working electrode (typically >700mV), thus reducing the effect of interferences, as previously reported by Cullen, Jawaheer, Rughooputh *et al* (2003) for example. Therefore a potential of +300 mV was used for all future amperometric measurements of glucose using the screen printed three electrode system with rhodinised carbon working electrode.

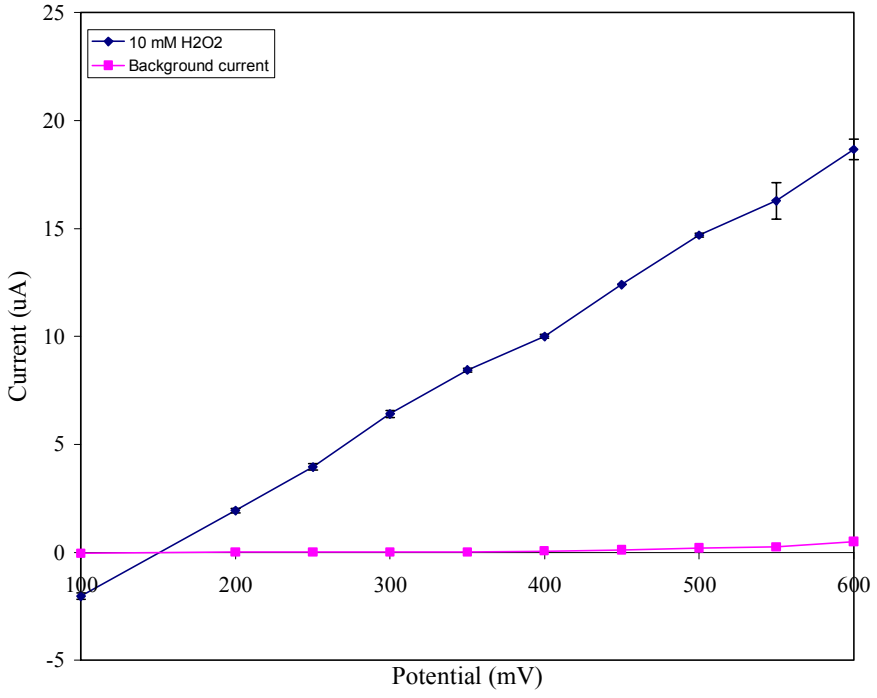

Figure 4.7: *Hydrodynamic voltammogram of background current and response towards 10 mM H_2O_2 in 0.1M PBS (pH7.2) at screen printed three electrode system with rhodinised carbon working electrode vs. Ag/AgCl. Error bars=SD, n=3.*

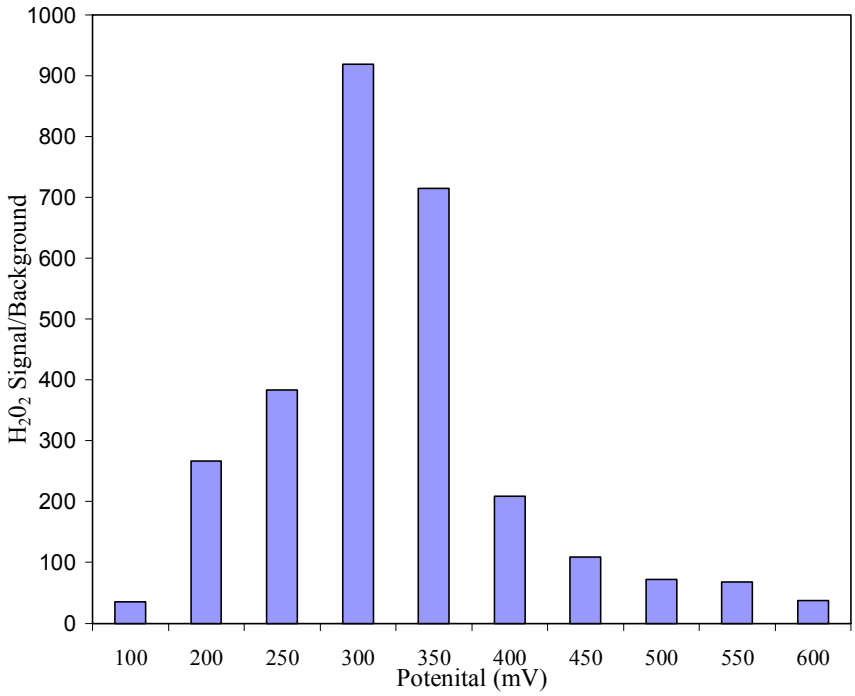

***Figure 4.8**: The signal to background ratio for rhodinised carbon three electrode system at 10 potentials in 10 mM H_2O_2 in 0.1M PBS pH7.2. n=3.*

4.3.3 Optimisation of glucose oxidase loading

To determine the optimum number of units of glucose oxidase required per sensor, a range of GOx loadings were tested in the range 0.5 to 4 U/sensor using a substrate solution of 10mM glucose in 0.1M PBS (pH 7.2) and at an operating potential of +300mV (n=3). The GOx preparations were applied to the rhodinised carbon electrode in a volume of 5 µl by pipette. The small volume and the porous nature of rhodinised carbon meant that immobilisation by an entrapment method or membrane was not necessary. The sensors were also designed for single use, and therefore the water solubility of the enzyme was of no concern. The signal: noise ratio was calculated for each enzyme loading (differential signal / standard deviation) and the optimum GOx loading found to be

1U/sensor. It can be seen in Figure 4.9 that the signal: noise value increases up to 1U, with no increase in response evident at higher enzyme loadings.

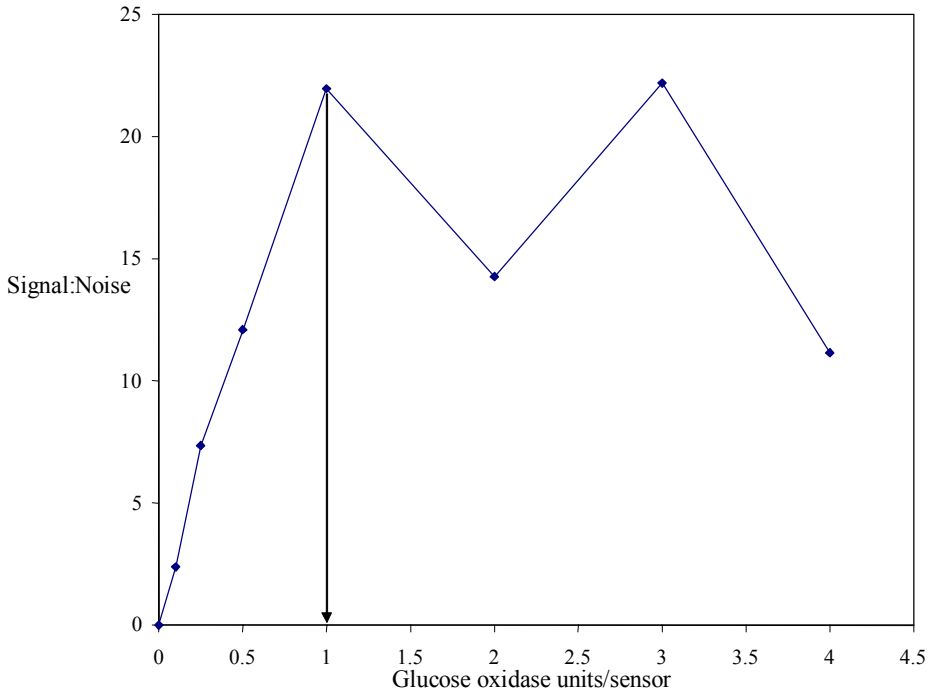

***Figure 4.9**: Signal to noise ratio for 7 glucose oxidase loadings on rhodinised carbon working electrode in 10mM glucose in 0.1M PBS pH7.2. n=3.*

4.3.4 Shelf life testing

In order to make glucose biosensors of sufficient batch size for large-scale testing, it was decided to investigate the shelf life of the biosensors. This is of course also an important factor to consider from a commercial point of view, where it could be many months between the time of production and the use of a sensor by the patient or physician.

Therefore, a batch of 100 glucose biosensors were prepared using 1 U GOx per sensor. The sensors were foil wrapped and stored in air tight glass jars containing one silica gel sachet

and stored at 4 °C. On the day of biosensor production (day 0), 500 µM glucose in 0.1M PBS was amperometrically measured with the biosensors in triplicate at +300 mV. This measurement was repeated regularly over a period of 77 days (sensors were not stored for a longer period than this during the project). The differential mean and standard deviations were calculated, as shown in Figure 4.10. After the first few days, the signal subsided by approximately 0.5 µA to a relatively stable value, averaging at 3.012 µA for the remaining 73 days, and showed no signs of significant further signal reduction.

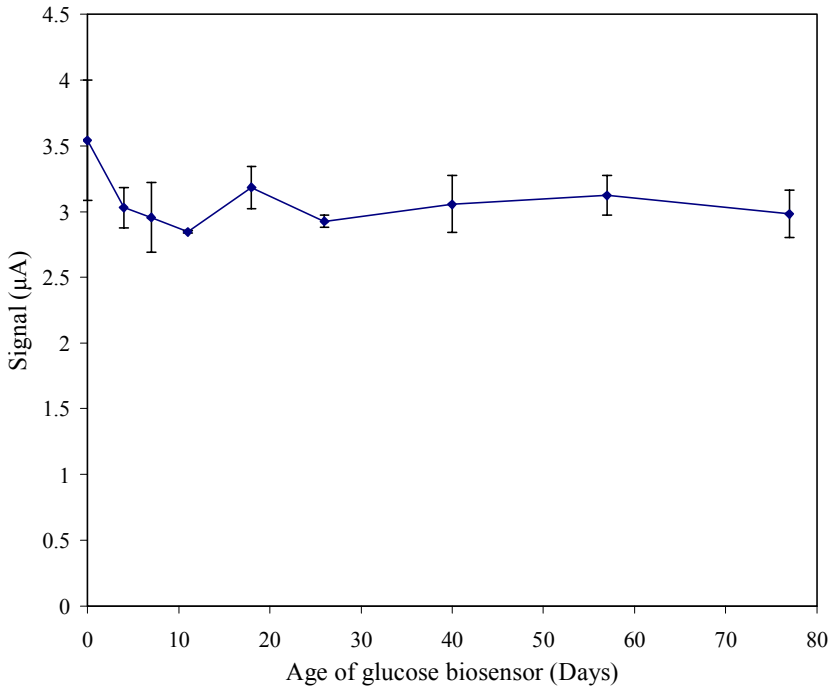

***Figure 4.10**: Shelf life testing of glucose oxidase glucose biosensor. Error bars are std dev, n=3.*

4.3.5 Determination of linear region and limit of detection

A batch of glucose biosensors containing 1 U GOx / sensor were prepared. Glucose concentrations from 50 μM to 7500 μM were prepared in 0.1M PBS pH7.2. Each concentration was determined amperometrically at +300mV (n=3). The resulting current values were averaged, blank subtracted and plotted vs. glucose concentration,. The mean background current was 0.0832 μA with a standard deviation of 0.0191 μA. The linear region was determined to be between 0 and 2500 μM, with the equation: y = 0.0006x and R^2 value of 0.994 (Figure 4.11).

The limits of detection (LOD) were determined as follows:

At 99.7% confidence: 3 x SD of blank = 0.0573

y = 0.0006*x therefore

0.0573 = 0.0006*(LOD)

LOD = 95.5 μM

At 95% confidence: 2 x SD of blank = 0.0382

y = 0.0006*x therefore

0.0382 = 0.0006*(LOD)

LOD = 63.67 μM

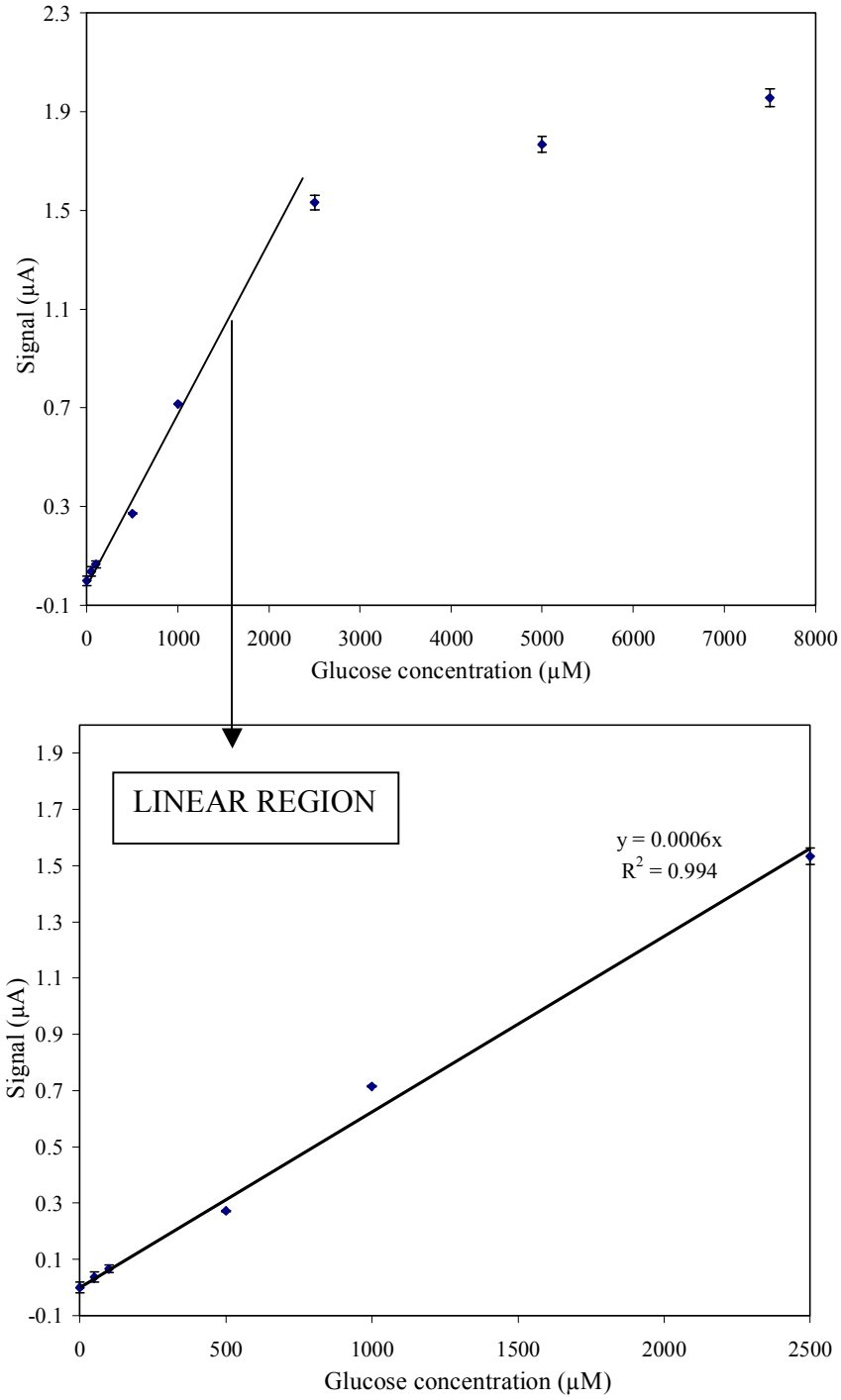

Figure 4.11: *Calibration of screen printed three electrode glucose biosensor and determination of linear region for detection of glucose in 0.1M PBS. Error bars are std dev, n=3.*

4.3.6 Detection of glucose in model wound fluid with glucose biosensor

Having established the glucose biosensor could detect glucose down to 99.5 μM (99.7% confidence) in 0.1 M PBS, the next stage was to detect glucose in serum, used as a model for wound fluid in this thesis. As mentioned in the introduction, monitoring the glucose levels in wound fluid may be one of a number of useful indicators as to whether a wound is healing properly.

To reduce sensor fouling and hence signal reduction, and to provide necessary electrolyte for electrochemical measurement, a single dilution step was required with 0.1M PBS to give a 1:1 v/v ratio of serum: PBS. It should also be noted that although a glucose value of 0 mM was ascribed to the 'blank' serum, the average blood glucose value of the donors was 4.8 mM. Therefore after the 1:1 dilution step, the background glucose level was in the region 2.4 mM, prior to spiking with glucose. However, as for measurements in PBS, readings were blank subtracted. Concentrations of glucose were prepared from 0.25 mM to 7.5 mM in the serum/PBS. Glucose was detected amperometrically at +300mV. The results are shown in Figure 4.12. The linear region of the calibration profile was determined to be from 0 to 2500 μM, as for glucose in PBS, with a limit of detection of 169.5 μM at 99.7% confidence, and 113 μM at 95% confidence. However, since 0 μM is really 2400 μM (due to presence of glucose before spiking), the linear curve may be extendable to ~ 4900 μM in a real situation, but may have slightly larger error bars. The detection limit was not quite as low as for the detection of glucose in PBS, and the error bars were noticeably larger, particularly from 3500 μM upwards. This was not unexpected, given the presence of more complex biological components in the sample, such as proteins and protein fragments.

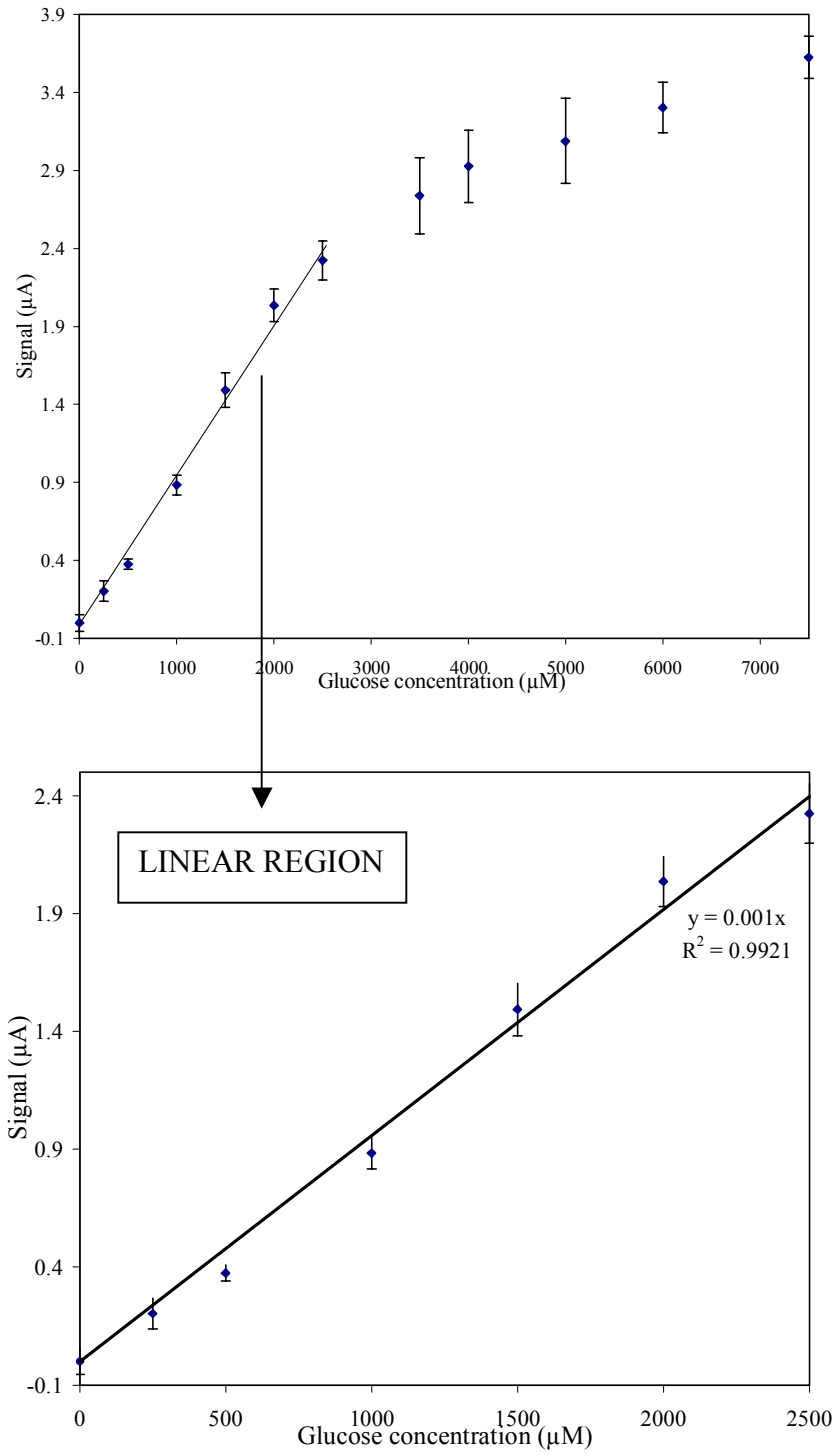

Figure 4.12: *Calibration of screen printed three electrode glucose biosensor and determination of linear region for detection of glucose in model wound fluid. Error bars are std dev, n=3.*

4.3.7 Validation with glucose BioAssay test kit

The results for the detection of glucose in serum with the glucose biosensors were validated using the glucose BioAssay test kit described in Chapter 2. Four solutions of 1:1 v/v serum: PBS were prepared containing unknown concentrations of glucose. The test kit procedure was followed as in Chapter 2 and the optical densities of the glucose containing 1:1 v/v serum: PBS solutions measured. The solutions were also measured amperometrically using the glucose biosensors, and the current values recorded converted into glucose values using the calibration graph in Figure 4.12. The test kit calibration graph (Figure 2.13) was used to convert the optical density values into glucose concentrations, tabulated in 4.1, and plotted against the glucose concentrations determined amperometrically (Figure 4.13).

Table 4.1: *Results of glucose biosensor validation by glucose BioAssay test kit*

BioAssay:

Glucose solution #	Optical density (630nm)	Glucose conc. (μM)
1	0.0404	1862
2	0.1072	4940
3	0.0740	3408
4	0.1328	6120

Biosensor:

Glucose solution #	Current (μA)	Glucose conc. (μM)
1	1.854	1854
2	3.056	4850
3	2.792	3400
4	3.321	6100

The glucose concentrations determined by the BioAssay method were very similar to those determined by the glucose biosensor, illustrated in Figure 4.13 with an R^2 value of 0.9998. Therefore the glucose biosensor could be considered a suitable rapid means of monitoring glucose in model wound fluid.

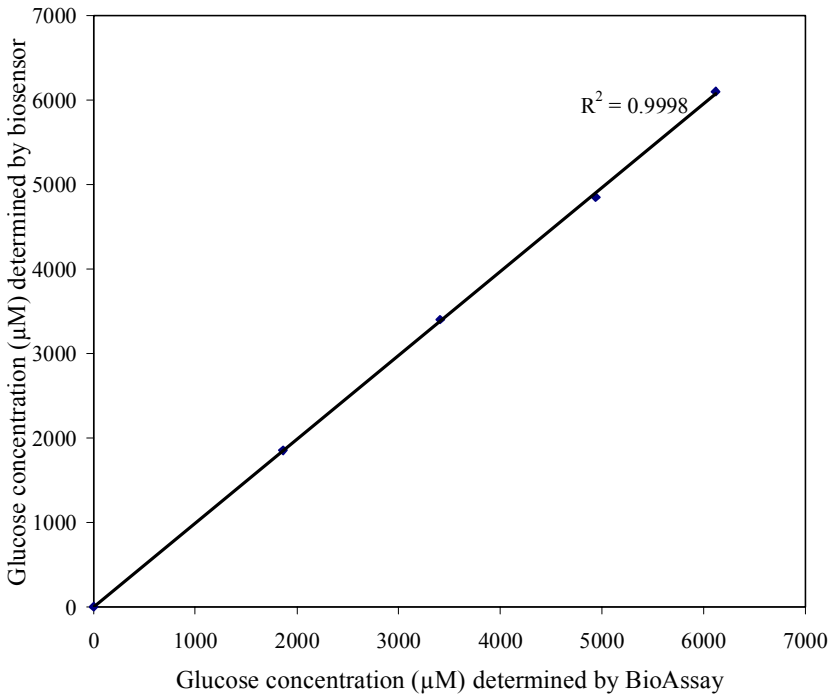

Figure 4.13: *Validation of glucose biosensor with BioAssay test kit*

4.3.8 Detection of glucose in model wound fluid containing S.aureus with glucose biosensor

The final test with the glucose biosensor again involved the detection of glucose in model wound fluid, but this time containing *S.aureus*, in order to test whether the presence of bacteria affects the performance of the biosensor. *S.aureus* was grown in serum to a cell density of 2 x 10^8 CFU/ml. This was then used to prepare known glucose concentrations as before, which were measured at +300 mV in triplicate with the glucose biosensors. Differential means and standard deviations were calculated shown in Figure 4.14 versus concentration. The linear region was similar to detecting in serum without *S.aureus*, from 0 to 2000 μM. The blank standard deviation was 0.051 μA, with a limit of detection of 146 μM at 95% confidence and 218.77 μM at 99.7% confidence. At 99.7% confidence, this is

49 µM higher than in *S.aureus* free serum. Therefore it would appear that the presence of bacteria does have a limited effect on glucose biosensor performance.

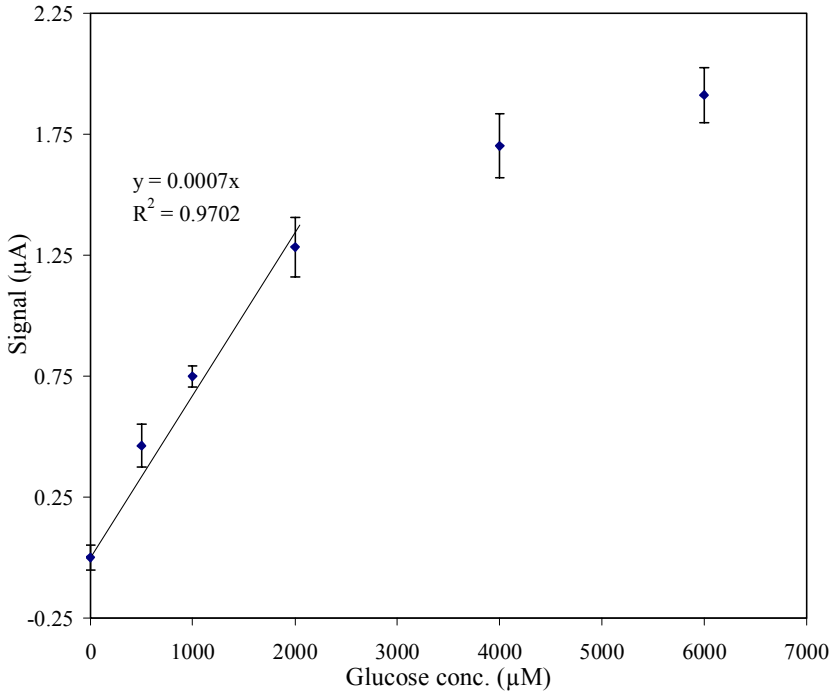

***Figure 4.14**: Calibration of screen printed three electrode glucose biosensor and determination of linear region for detection of glucose in model wound fluid containing 2 x 10^8 CFU/ml S.aureus. Error bars are std dev, n=3.*

4.3.9 Interferent testing

As already mentioned in Chapter 3, a problem in the development of new sensor technologies is that of interfering species, particularly ascorbic acid (vitamin C) and acetaminophen (paracetamol), which commonly interfere with commercial home blood glucose monitoring kits. Therefore, five common interfering species were tested for their affect on the measurement of 5 mM glucose in 0.1 M PBS with glucose biosensors. The results are summarised in Figure 4.15. As normal, results are blank subtracted averages of three replicates, and error bars are +/- standard deviation.

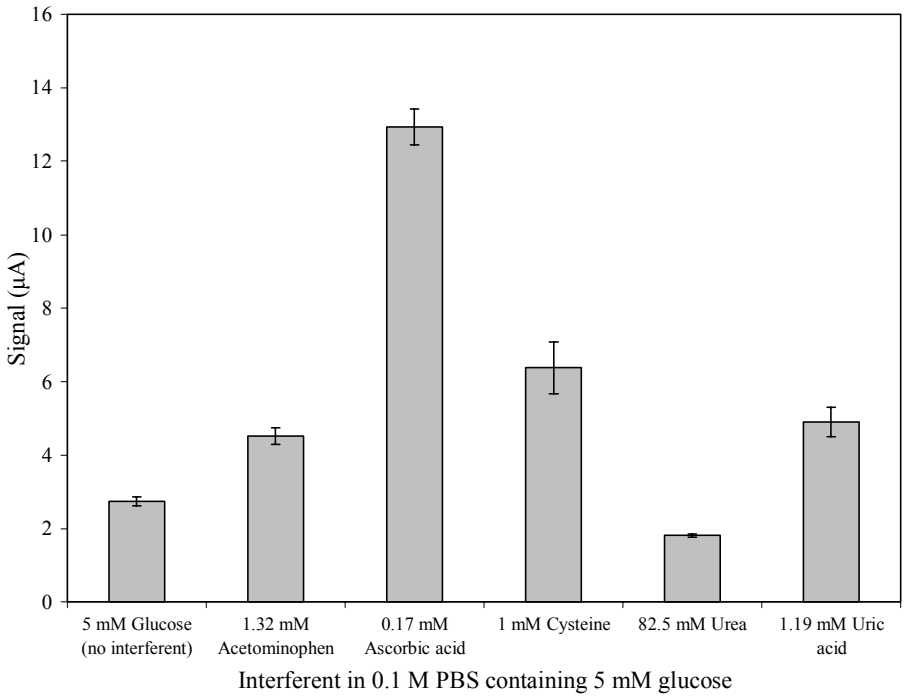

Figure 4.15: *Affect of interferents on the measurement of 5 mM glucose in 0.1 M PBS with glucose biosensor. Error bars are std dev, n=3.*

The levels of interferents tested were the highest concentrations of the ranges reported in Table 3.1, and therefore represent worst case scenarios. Ascorbic acid had by far the largest affect on the signal, increasing it by >4x the normal level. This was followed by cysteine, which ~ doubled the signal. Acetominophen and uric acid had a similar smaller affect, and urea had the opposite affect by decreasing the signal slightly. Clearly all have had some affect, but ascorbic acid seems to pose the largest problem. These effects are either because the interferents are electroactive at the operating potential of the biosensor, or they interfere with the electrode signal though reaction with the analyte (McGrath, Iwuoha, Diamond, *et al*, 1995). Some of these effects could be reduced or removed by incorporation of a perm-selective layer (Palmisano, Centonze, Guerrieri, *et al*, 1993; Centonze, Guerrieri, Malitesta, 1992; Garjonyte & Malinauskas, 2000) or by incorporation of a compensator electrode

(which has no enzyme and measures the background current of the solution which can be subtracted from the measurement by the enzyme electrode, assuming effects are additive)

4.3.10 Conclusions: Glucose biosensor

A rhodinised carbon three electrode assembly glucose biosensor was successfully fabricated, optimised and tested in 0.1M PBS and model wound fluid. The limit of detection was determined to be 170 μM at 99.7% confidence in model wound fluid with a single dilution step. Ascorbic acid was identified as a key interferent, greatly increasing the signal. The biosensor was tested in model wound fluid containing bacteria and validation with BioAssay test kit was also successful. It was concluded that the glucose biosensor approach is a suitable means of monitoring glucose in wound fluid and may form a useful component of a wound fluid biosensor array.

4.4 Hydrogen peroxide biosensor

The second of the three biosensor systems studied was a hydrogen peroxide (H_2O_2) biosensor. Hydrogen peroxide biosensors have been widely investigated, and there are many different variations of sensor construction. H_2O_2 biosensors were also fabricated 'in-house'. which gave the benefit of having full control over every parameter of the construction and operation of the biosensor. For the purposes of this study, i.e. to investigate the amperometric detection of hydrogen peroxide in model wound fluid, a mediated enzyme reaction was chosen (a so-called 'second generation' biosensor). Use of a mediated system overcame problems associated with direct (non-mediated) detection of H_2O_2, notably the need for higher operating potentials which increases the likelihood of interference problems. The enzyme used was horseradish peroxidase (HRPx) (E.C.

1.11.1.7) sourced from *Amoracia rusticana* (Sigma, UK). It was supplied as a liquid with a specific activity of 224U/mg, and stored in the freezer at -20 °C. HRPx is isolated from horseradish roots and belongs to the ferroprotoporphyrin group of peroxidases. HRPx is a single chain polypeptide containing four disulfide bridges and is a glycoprotein containing 18% carbohydrate. HRPx has been widely used in conjunction with electrochemical transduction for the detection of hydrogen peroxide (Moody, Saini & Setford, 2001; Wang & Wang, 2004; Kulys & Schmid, 1991; Johansson, Jonsson-Pettersson, Gorton *et al*, 1993).

The use of 1,1'-dimethylferrocene (DMFc) as a mediator (i.e. a non-physiological small redox mediator that shuttle electrons between the reduced enzyme prosthetic group and the electrode) in a HRPx biosensor has been investigated by Kulys & Schmid (1991) and Moody, Saini & Setford (2001) and found to be superior to other commonly used alternative mediators such as tetrathiafulvalene and potassium hexacyanoferrate. Therefore, the biosensor was developed using DMFc as the mediator. DMFc is a relatively stable dark red crystalline solid with limited water solubility. The reaction is illustrated in Figure 4.16.

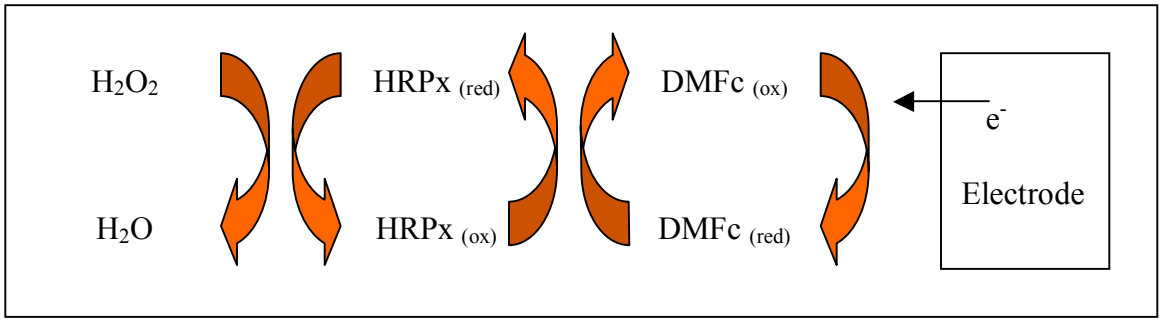

Figure 4.16: *Reaction scheme on the carbon working electrode of the dimethylferrocene mediated horseradish-peroxidase H_2O_2 biosensor*

In this work, the working electrode was coated with a membrane. Membranes serve a number of functions in biosensor applications. For example, a membrane may serve as a protective layer to prevent interfering species from reaching the electrode surface, by size exclusion or by charge repulsion. A membrane may also prevent soluble enzymes or mediators such as DMFc, initially physically immobilised on the transducer surface from desorbing and affecting the biosensor response. A membrane may also act as an additional diffusion barrier between the transducer-immobilised bioligand on the electrode surface and bulk solution, thus extending the dynamic range of the device (Johansson, Jonsson-Pettersson, Gorton *et al*, 1993). A range of membrane materials such as nylon and cellulose nitrate, and polymers have been investigated for use in biosensor construction. A popular choice of polymer is Nafion, a highly negatively charged perfluorated polymer. Nafion, by virtue of its negative charge, allows the passage of cations and repels anionic species, and can be used either alone or in combination with other polymer materials such as cellulose acetate (Wang & Wu, 1995). The use of electrochemically deposited polymers such as polypyrrole, polyphenylenediamine, polyaniline and polyphenol as permselective layers in the construction of biosensors is also commonplace, and has been recently reviewed by Emr & Yacynych (2005).

Cellulose acetate can be formulated to create size exclusion membranes, the size of pore being dictated by the particular molecular weight of the cellulose acetate used and the drying regime applied. Cellulose acetate is ideal for use in biosensor construction, since in solution form it can be dip coated, pipette deposited, or ink jet printed, making it amenable

to a range of mass production processes. It is also relatively cheap, easy to handle, and has been used successfully in a number of studies involving the electrochemical measurement of hydrogen peroxide (Ward, Jansen, Anderson *et al*, 2002; Cullen, Jawaheer, Rughooputh *et al*, 2003; Moody, Saini & Setford, 2001). Therefore cellulose acetate was selected for use with the hydrogen peroxide biosensor.

4.4.1 Determination of optimum operating potential

The basic electrochemical methodological approach used during the glucose biosensor development was also used for the H_2O_2 biosensor. To determine the optimum operating potential at which to operate the biosensor, staircase amperometry was performed across the potential range -100 mV to -500 mV (100 mV steps) using 3 mM H_2O_2 in 0.1M PBS (all tests in triplicate). The average current at each potential for 3 mM H_2O_2 and the blank controls (background) were calculated. The ratio between the H_2O_2 generated current and background current revealed the optimum operating potential to be -300 mV. Therefore this potential was used for all future amperometric measurements with the H_2O_2 biosensor. This concurs with the work of Moody, Saini & Setford (2001).

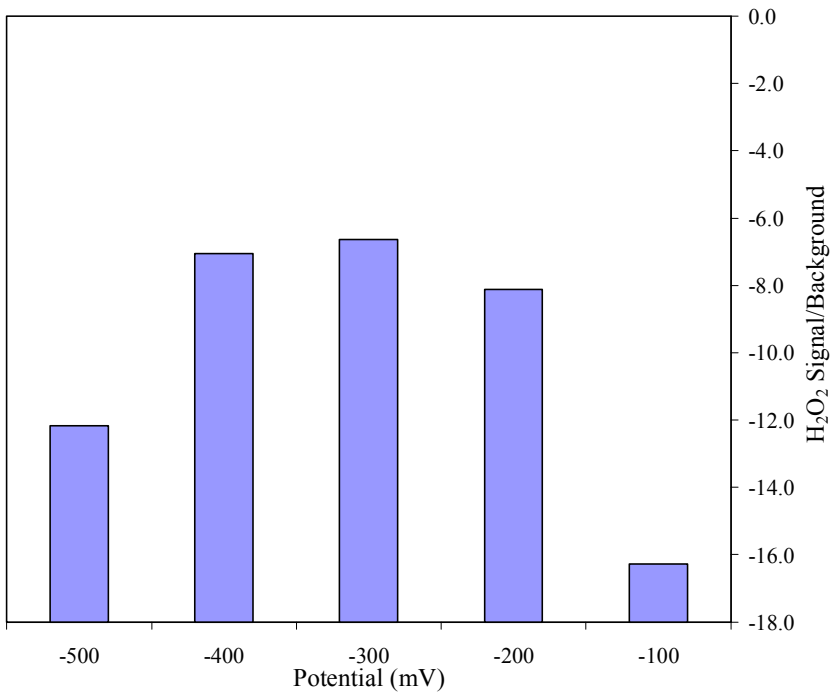

Figure 4.17: *The signal to background ratio for carbon three electrode system at 5 potentials, in 3 mM H_2O_2 in 0.1M PBS pH7.2. n=3.*

4.4.2 Application of horseradish peroxidase, dimethylferrocene and cellulose acetate

Initially, HRPx, DMFc and cellulose acetate (CA) were applied to the carbon working electrode, according to the procedure of Moody, Saini & Setford (2001). HRPx was made to 5U/µl in 0.1M PBS pH 7.2, DMFc to 12.5 g/L in acetone, and CA to 20g/L in acetone. The following volumes were applied to the working electrode:

HRPx (5U/µl) 5 µl

DMFc (12.5 g/L) 4 µl

CA (20 g/L) 4 µl

These volumes were applied together in a single solution deposition of 13 µl. In making a batch of sensors, the three components were pre-mixed by pipette action in a tube in order to provide a suitable batch size. However, it was found that preparing too large a volume at

one time, for example to make 100 sensors, resulted in acetone evaporation during the depositioning procedure, resulting in poor sensor repeatability. It also proved difficult to maintain a homogeneous mixture during the depositioning step, due to immiscibility between the aqueous and solvent phases, also contributing to sensor irreproducibility. Therefore a method was developed whereby a volume sufficient for the production of 60 sensors was prepared, but aliquotted into 10 microcentrifuge tubes. Therefore one tube contained enough mix for 6 sensors, and while depositing the mix to 6 sensors, the remaining 9 tubes remained capped thereby preventing evaporation until opened. This also improved the uniformity of the mixture, and hence reduced inter batch variation. Once prepared, sensors were allowed to dry at room temperature overnight, and then foil wrapped and stored in an air tight glass jar 'bocal canette' (Luminarc, France), with a silica gel sachet inside to absorb moisture.

4.4.3 Shelf life testing

Shelf life tests were carried out on the H_2O_2 biosensors for the same reasons given in Section 4.3.4 for the glucose biosensors. A batch of 100 H_2O_2 biosensors was made as described in Section 4.4.2. The sensors were foil wrapped and stored in air tight glass jars (Luminarc, France) containing one silica gel sachet and stored at 4 °C. On the day of biosensor production (day 0), 100 μM H_2O_2 in 0.1M PBS was amperometrically measured with the biosensors in triplicate at -300 mV. This measurement was repeated regularly over a period of 77 days, since the sensors were not stored for a longer period than this during the project. The differential mean and standard deviations were calculated, and are shown

in Figure 4.18. The largest reduction in signal took place between day 0 and day 4. This was followed by minimal signal reduction for the remaining 73 days.

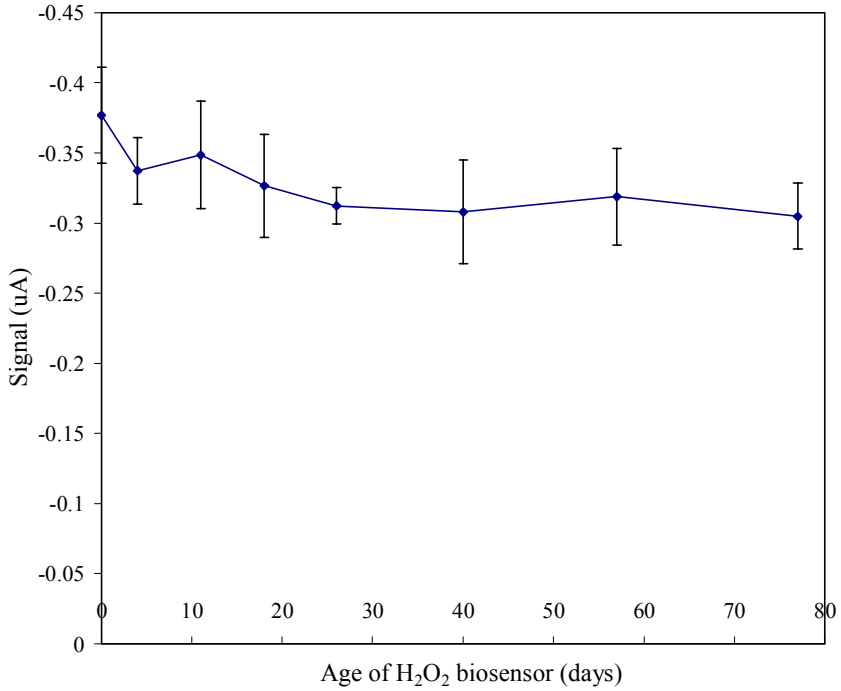

***Figure 4.18**: Shelf life testing of H_2O_2 biosensor. Error bars = std dev, n=3.*

4.4.4 Determination of linear region and limit of detection

A batch of H_2O_2 biosensors were made as described in Section 4.4.2. H_2O_2 concentrations of 5-2000 µM were prepared in 0.1M PBS pH7.2. Each concentration was amperometrically determined at -300 mV in triplicate. The resulting current values were averaged and blank subtracted and plotted *vs*. H_2O_2 concentration (error bars = standard deviation). The results for H_2O_2 solutions of 0- 200 µM and the linear region 0 to 25 µM with equation y = -0.011x and R^2 value of 0.975are shown in Figure 4.19. The background standard deviation was 0.0138 µA. The limit of detection was determined to be 3.8 µM at 99.7% confidence (2.5 µM at 95% confidence).

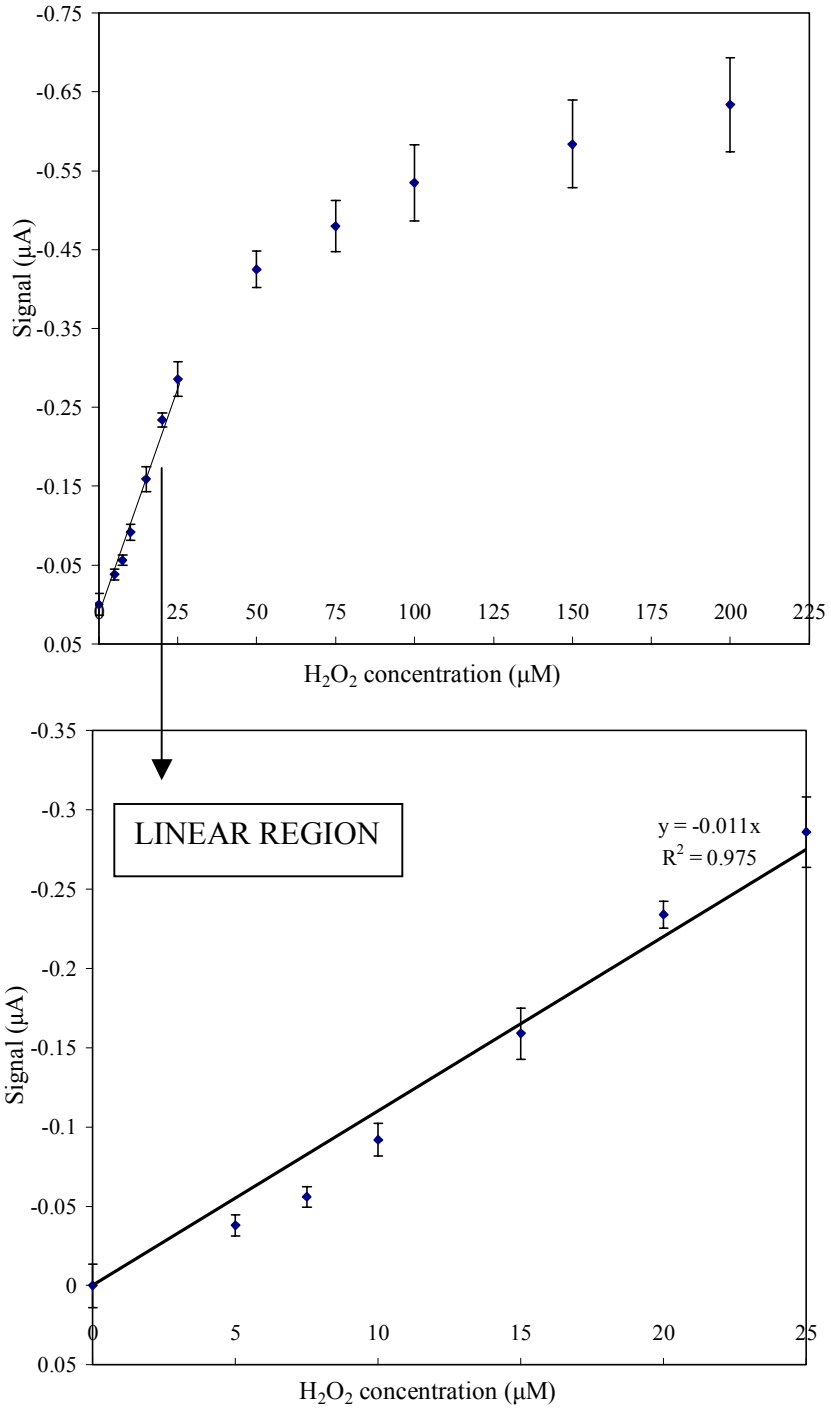

Figure 4.19: *Calibration of screen printed three electrode H_2O_2 biosensor and determination of linear region for detection of H_2O_2 in 0.1M PBS. Error bars are std dev, n=3.*

4.4.5 Validation with Checkit H_2O_2 test kit

The results for the detection of H_2O_2 in PBS with the hydrogen peroxide biosensors were validated using the Lovibond H_2O_2 Checkit test kit described in Section 2.2.7. Four solutions were prepared containing unknown concentrations of H_2O_2 in 0.1M PBS. The test kit instructions were followed as described in Section 2.2.7, to determine the concentrations of the four solutions. The solutions were also measured amperometrically using the H_2O_2 biosensors, and the currents recorded converted into H_2O_2 values using the calibration graph in Figure 4.19. The H_2O_2 concentrations in Table 4.2 determined by each method are plotted in Figure 4.20, where it can be seen that an R^2 value of 0.997 demonstrates the reliability of the H_2O_2 biosensor.

Table 4.2: *Results of H_2O_2 biosensor validation by H_2O_2 Checkit test kit*

Test kit:

H_2O_2 solution #	Checkit reading (mg/l)	H_2O_2 conc. (μM)
1	0.20	5.80
2	0.50	14.70
3	0.70	20.60
4	0.85	25.00

Biosensor:

H_2O_2 solution #	Signal (μA)	H_2O_2 conc. (μM)
1	-0.06655	6.05
2	-0.1672	15.20
3	-0.22902	20.82
4	-0.27852	25.32

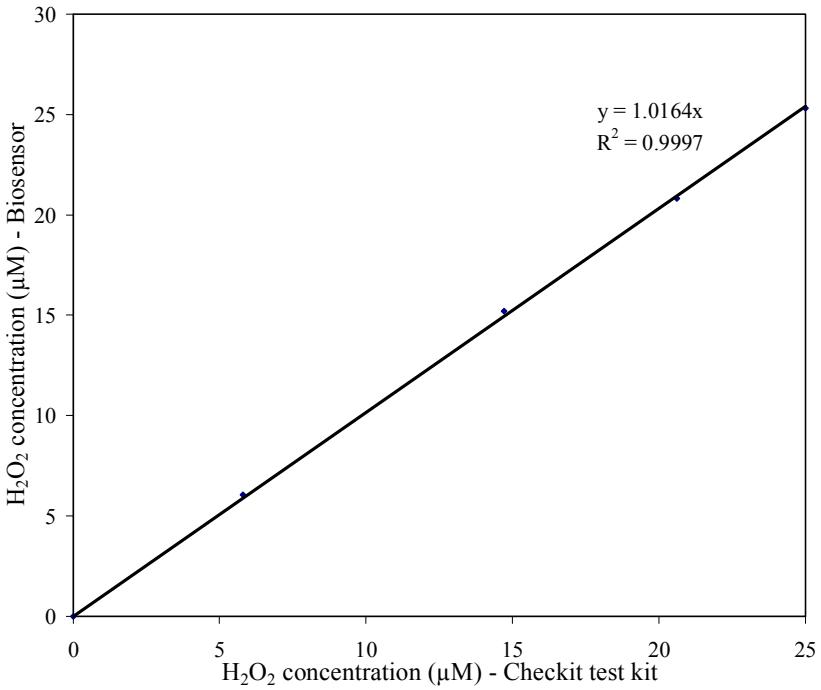

Figure 4.20: *Validation of H_2O_2 biosensor with Checkit test kit*

4.4.6 Detection of H_2O_2 in model wound fluid with hydrogen peroxide biosensor

Having established the hydrogen peroxide biosensor could detect H_2O_2 down to 3.8 µM (99.7% confidence) in 0.1 M PBS, the next stage was to detect H_2O_2 in 90:10 v/v serum in 0.1M PBS, as was also performed for the glucose biosensor in Section 4.3.8.

Concentrations of H_2O_2 were prepared from 200 µM to 2000 µM in the 90:10 v/v serum: PBS and determined amperometrically as before. The results are shown in Figure 4.21. The linear portion of the response profile was determined to be 0-1000 µM, a four-fold increase in comparison to the PBS data, ($y = -0.0028x$: R^2 value of 0.9846). The standard deviation of the blank was 0.007865 µA, and the limit of detection was found to be 8.5 µM at 99.7% confidence (6 µM at 95% confidence), similar to the limits found in PBS, having increased from 3.8 µM to 8.5 µM at 99.7% confidence.

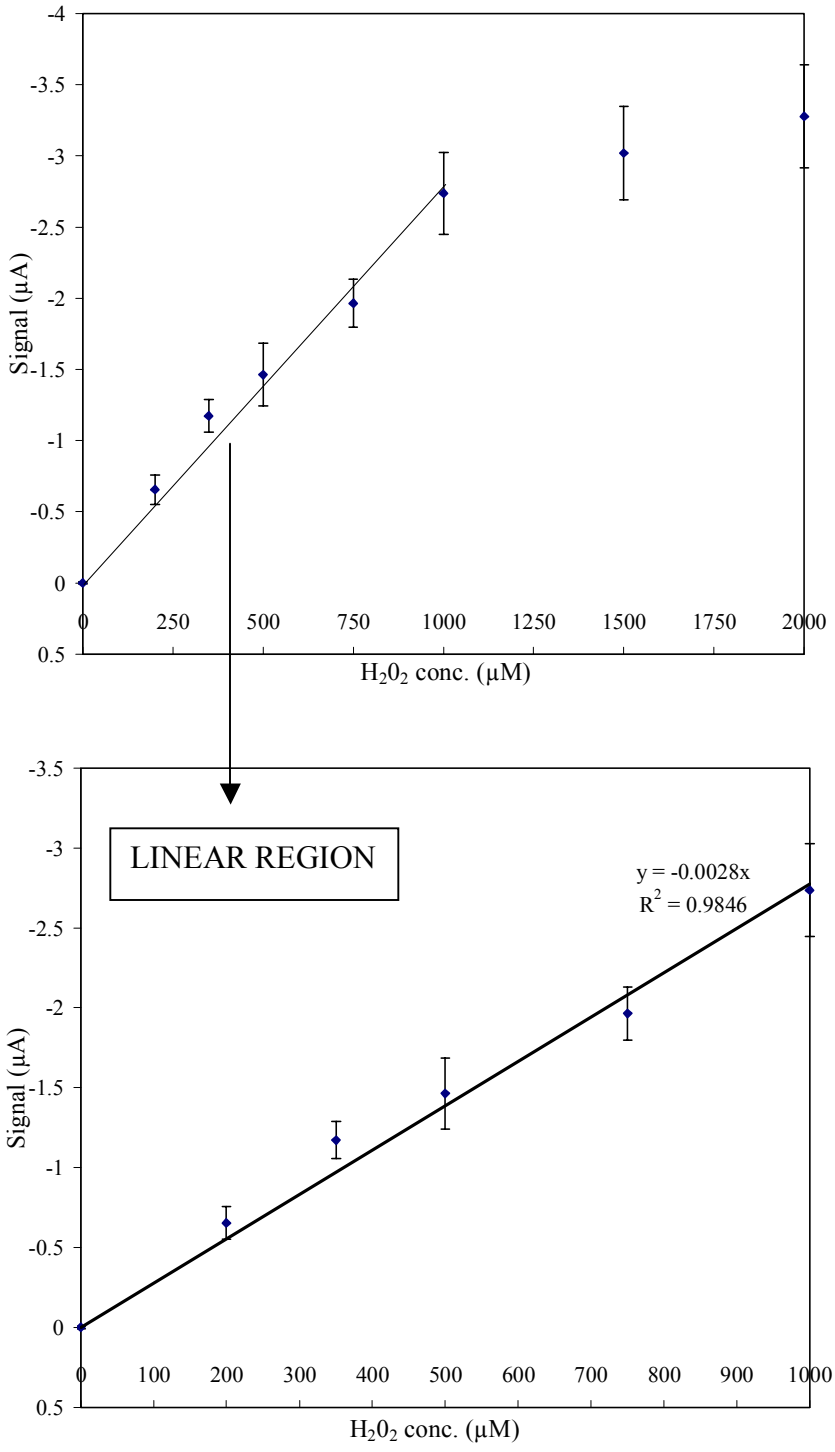

Figure 4.21: *Calibration of screen printed three electrode H_2O_2 biosensor and determination of linear region for detection of H_2O_2 in model wound fluid. Error bars are std dev, n=3.*

4.4.7 Detection of H_2O_2 in model wound fluid containing S.aureus with H_2O_2 biosensor

As with the glucose biosensor tests, the final test with the hydrogen peroxide biosensor again involved the detection of H_2O_2 in model wound fluid, but this time containing *S.aureus* to test whether the presence of bacteria affects the performance of the biosensor. *S.aureus* was grown in serum to a cell density of 2×10^8 CFU/ml. This was then used to prepare known H_2O_2 concentrations in 0.1M PBS from 250 to 2000 μM, which were measured at -300 mV in triplicate with the H_2O_2 biosensors. Differential means and standard deviations were calculated and plotted versus concentration as shown in Figure 4.22. The linear range of the sensor was equivalent to that obtained for H_2O_2 in serum without *S.aureus* (0-1000 μM). The blank standard deviation was measured at 0.0897 μA, with a limit of detection of 9.6 μM at 99.7% confidence (6.4 μM at 95% confidence), less than 2 μM higher than in *S.aureus* free serum, indicating that the presence of bacteria does not significantly effect biosensor performance.

4.4.8 Interferent testing

As done so for the glucose biosensor, five common interfering species were tested for their affect on the measurement of 0.5 mM H_2O_2 in 0.1 M PBS with H_2O_2 biosensors. The results are summarised in Figure 4.23. As normal, results are blank subtracted averages of three replicates, and error bars are +/- standard deviation.

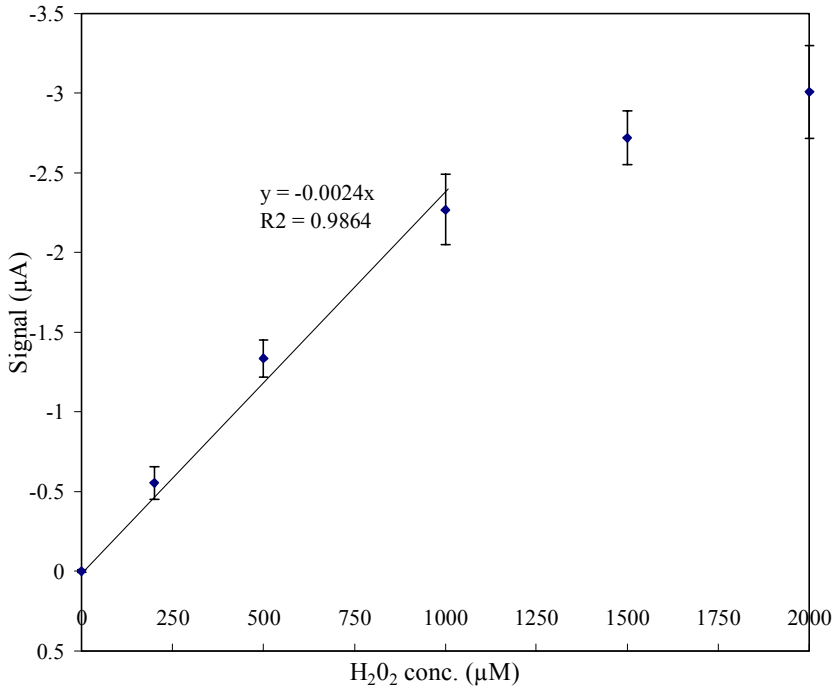

Figure 4.22: *Calibration of screen printed three electrode H_2O_2 biosensor and determination of linear region for detection of H_2O_2 in model wound fluid containing 2 x 10^8 CFU/ml S.aureus. Error bars are std dev, n=3.*

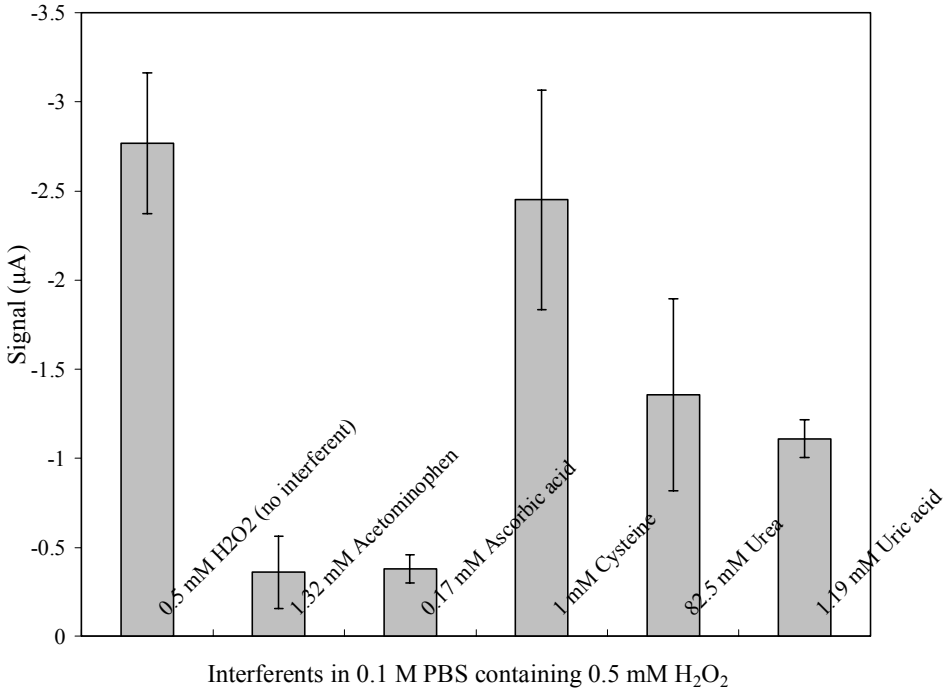

Figure 4.23: *Affect of interferents on the measurement of 0.5 mM H2O2 in 0.1 M PBS with H_2O_2 biosensor. Error bars are std dev, n=3.*

Inversely to the glucose biosensor (except for urea), the interferents reduced rather than increased the signal by differing amounts. Acetominophen and ascorbic acid had the greatest effect reducing the signal by ~7 times. The least effect was given by cysteine. Urea and uric acid approximately halved the signal. This is because they are electroactive at the same potential as H_2O_2, and are therefore adding to the reduction signal. As mentioned for the glucose biosensor, the incorporation of a compensator electrode could help to alleviate this.

4.4.9 Conclusions: H_2O_2 biosensor

A mediated three electrode H_2O_2 biosensor was fabricated and optimised in 0.1M PBS spiked with H_2O_2. Testing of the biosensor in model wound fluid with a single dilution step revealed the limit of detection to be 8.43 μM. The biosensor was tested in model wound fluid in the presence of bacteria, which had no significant effect. Interferent effects were tested where acetominophen and ascorbic acid were found to exhibit the most significant affects on signal. Validation using a Checkit enzyme based colorimetric test kit was successful. Although without data on the levels of H_2O_2 in the body one cannot be certain that the levels are detectable, but as a concept, a hydrogen peroxide biosensor could successfully be used to monitor H_2O_2 in wound fluid down to a level of approximately 8.4 μM. To take this further, real sample testing would be required.

4.5 Ethanol biosensor

The third biosensor was designed for the detection of ethanol in 0.1M PBS and model wound fluid. Many analytical methods have been developed for the measurement of ethanol, including chemical, colorimetric, chromatographic and refractive index methods.

However, although these methods are precise and reliable, they are relatively complex and time consuming, and also require expensive instrumentation and training of operators. Much research has been directed towards overcoming these disadvantages by use of the biosensor approach, particularly those based on electrochemical transduction.

Two enzymes, alcohol oxidase (AOx) and alcohol dehydrogenase (ADH) have been extensively used in ethanol biosensor studies (Lee, Kim, Lee *et al*, 1999; Sprules, Hartley, Wedge *et al*, 1996). ADH based biosensors require the co-enzyme nicotinamide adenine dinucleotide (NAD^+). However, the NAD^+ also needs to be able to diffuse to the enzyme active site without becoming irreversibly entrapped or otherwise linked (Fonseca, Azevedo, Prazeres *et al*, 2004). AOx is an oligomeric enzyme consisting of eight identical sub-units arranged in quasi-cubic arrangement, each containing a strongly bound co-factor, flavin adenine dinucleotide (FAD) (Vonck & van Bruggen, 1990). It is produced by methylotrophic yeasts, commonly *Hansenula, Pichia,* and *Candida.* AOx has been used extensively in ethanol biosensors from each of these three yeast sources (Gorton, Heller, Vijayakumar *et al*, 1996; Patel, Meier, Cammann *et al*, 2001, Kulys & Schmid, 1991). AOx irreversibly oxidises short chain alcohols to the corresponding aldehyde, using molecular oxygen as the electron acceptor. The reaction can be followed by either monitoring decrease in O_2 tension or the increase in H_2O_2 concentration.

$$RCH_2OH + O_2 \xrightarrow{AOx} RCHO + H_2O_2$$

Sensors based on O_2 measurement have the advantage of minimal electrochemical interference in real samples. However, response values are relatively low with high background signals, giving poorer detection limits when compared to H_2O_2 measurement

approaches. Furthermore, the dependence on oxygen can reduce sensor accuracy and reproducibility, since O_2 levels vary from sample to sample (Bott, 1998). Therefore H_2O_2 detection is the more commonly used and preferred method. H_2O_2 sensors have a greater dynamic range and wider linear range, but as previously mentioned for the H_2O_2 biosensor (Section 4.2), first generation sensors based on direct detection of H_2O_2 require an elevated detection potential, increasing the likelihood of electrochemical interference in real samples, for example from electroactive ascorbic acid or acetaminophen. Therefore, in a similar manner to that employed for the H_2O_2 biosensor developed for this study, an alternative direct detection route was employed. Options included: modifying the electrode with an electrocatalyst (such as that used for the glucose biosensor – see Section 4.3); using an alternative electron acceptor to O_2; to regenerate the oxidised form of FAD, (a rarely used method); use of a mediator (second generation biosensor) such as ferrocene, (although a literature search yielded no such mediator for AOx; use of a bienzyme system such as the many examples where HRPx is used to catalyse the electro-reduction of H_2O_2 at reduced potentials, either directly or by use of a mediator. The latter option of a bienzyme system using HRPx and AOx has been utilised successfully by a number of groups for ethanol detection, including Kulys & Schmid, (1991); Gorton, Heller, Vijayakumar *et al*. (1996).

After careful consideration, and based on the success of the HRPx sensor approach, a mediated bienzyme (HRPx and AOx) system was chosen using DMFc as the mediator. Having already developed a H_2O_2 biosensor utilising HRPx and DMFc, the simple addition of AOx to the deposition medium resulted in the relatively straightforward development of a mediated bienzyme ethanol biosensor.

4.5.1 Operating potential

Since the ethanol biosensor had a similar operating procedure as for the H_2O_2 biosensor, namely the current generated from the reduction of the oxidised form of the DMFc mediator at a carbon working electrode, the same operating potential of -300 mV (vs. Ag/AgCl reference electrode) was employed.

4.5.2 Determination of optimum alcohol oxidase loading

Two sources of AOx were investigated: *Candida boidinii* and *Pichia pastoris,* both purchased from Sigma (Poole, UK). AOx from *C.boidinii* was supplied with a specific activity of 13.6U/mg protein and AOx from *P.pastoris* with 23U/mg protein, both as a liquid stored at -20 °C. The optimum number of units of AOx per sensor was determined for both sources. A range of AOx loadings were prepared and applied to the working electrode at the same time as the HRPx, DMFc and CA as a total deposition volume of 15 µl, with the AOx fraction accounting for 2 µl of the total depositioning volume (as described by Moody, Setford, Saini, 2001). A 2mM volume of ethanol in 0.1M PBS (pH 7.2) was determined amperometrically at -300mV (n=3). The signal: noise ratio was calculated for each enzyme loading by determining the ratio of the differential signal versus standard deviation for each AOx source. The optimum loading for AOx from *C.boidinii* and *P.pastoris* was found to be 1.25 U/sensor and 1.15 U/sensor respectively, as illustrated in Figure 4.24 (a) and (b). The optimum number of units of AOx/sensor was similar for both sources, but AOx from *C.boidinii* was approximately twice as expensive, and also less widely available, both of which are important issues when considering possible production issues. Therefore AOx from *P.pastoris* was selected to prepare subsequent batches of ethanol biosensors, at an enzyme loading of 1 U/sensor.

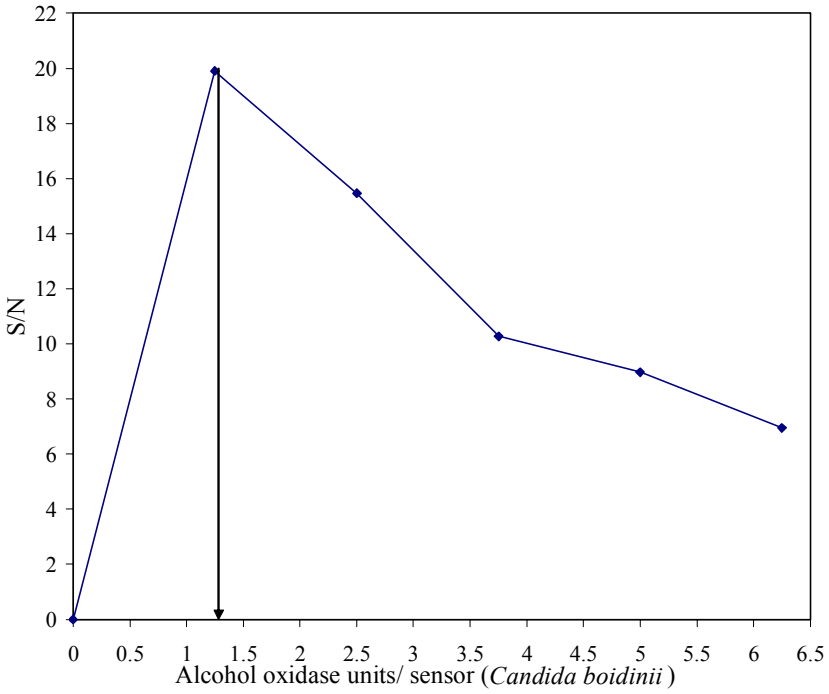

(a)

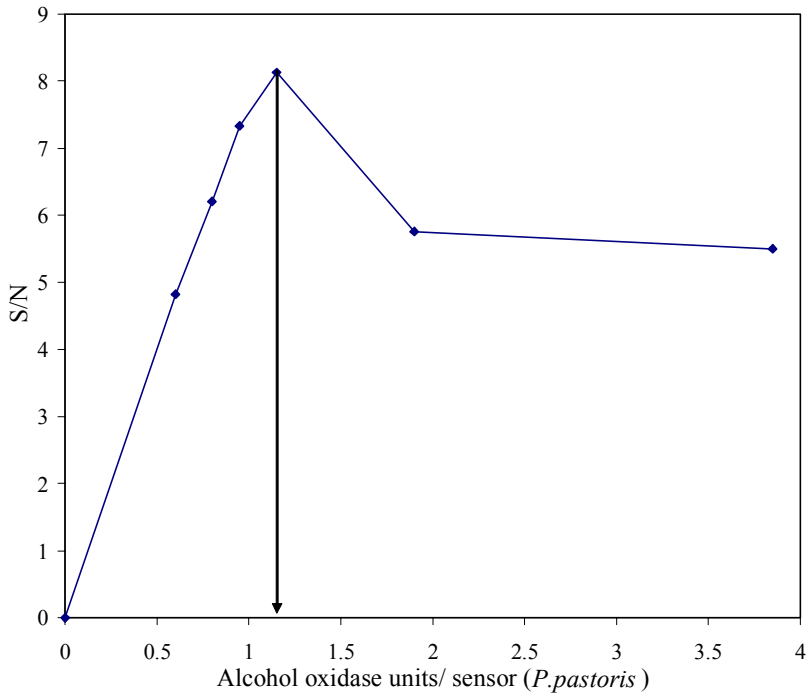

(b)

Figure 4.24*: Signal: noise ratios for alcohol oxidase loadings of bi-enzyme mediated system in 2mM ethanol in 0.1M PBS pH7.2. (a) C.boidinii and (b) P.pastoris. n=3.*

4.5.3 Deposition of horseradish peroxidase, alcohol oxidase, dimethylferrocene and cellulose acetate

As with the H_2O_2 sensors, deposition modification was required to increase uniformity and reduce sensor losses. The batch volume made was split up into microcentrifuge tubes, as described for the H_2O_2 sensors. However a reduction in deposition volume was also required. A volume of 15µl/ sensor resulted in spread beyond the working electrode film on a high percentage of sensors. Therefore, the depositioning volume was reduced which eliminated the solution-spread problem. Accordingly, the concentration of DMFc was raised from 12.5 to 25mg/ml thereby reducing the volume of DMFc per sensor from 4 to 2 µl and hence the overall deposition volume to 13 µl.

4.5.4 Shelf life testing

Shelf life tests were carried out on the ethanol biosensors for the same reasons given in Section 4.3.4. A batch of 100 ethanol biosensors was made as described in Section 4.5.3. The sensors were foil wrapped and stored in air tight glass jars containing one silica gel sachet and stored at 4 °C. On the day of biosensor production (day 0), 1000 µM ethanol in 0.1 M PBS was determined amperometrically in triplicate. This measurement was repeated regularly over a period of 77 days, since the sensors were not stored for a longer period than this during the project. The differential mean and standard deviations were calculated and are shown in Figure 4.25. The largest reduction in signal took place between day 0 and day 4, as observed for the glucose and H_2O_2 biosensors. Following this initial reduction, the signal stabilised to an average of -0.90 µA for the remaining 73 days of the test.

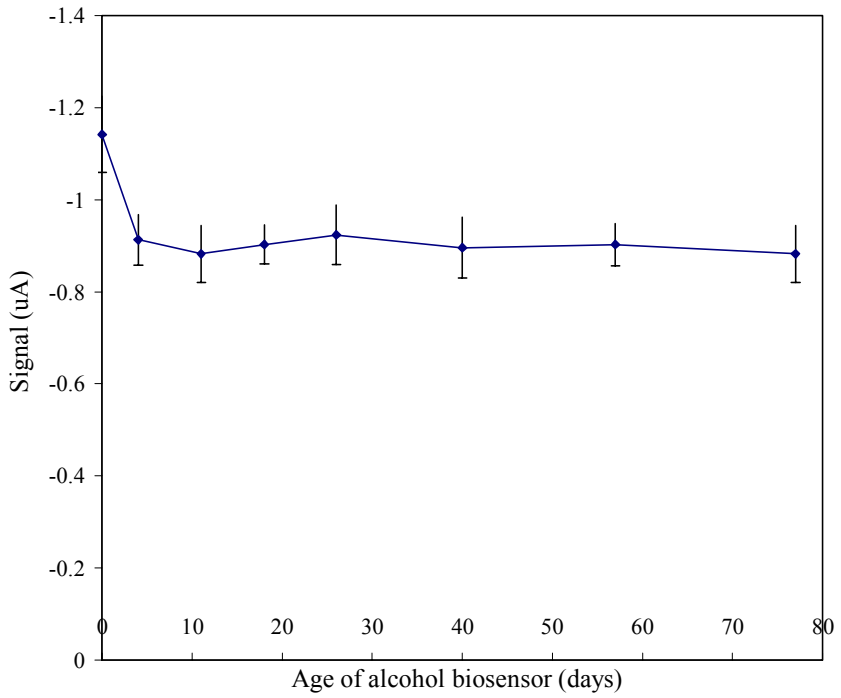

Figure 4.25: *Shelf life testing of alcohol biosensor. Error bars = std dev, n=3.*

4.5.5 Determination of linear region and limit of detection

A batch of ethanol biosensors was prepared as described in Section 4.5.3. Ethanol concentrations of 25-10,000 µM were prepared in 0.1M PBS pH7.2. Each concentration was determined amperometrically (n=3). The resulting currents were averaged and blank subtracted (signal) and plotted vs. ethanol concentration, with error bars. The background standard deviation was 0.0366 µA. The linear region was determined to be between 0 and 750 µM, yielding the equation: $y = -0.0011x$ with an R^2 value of 0.9946, as illustrated in Figure 4.26. The limit of detection was determined to be 99.8 µM at 99.7% confidence (66.5 µM at 95% confidence).

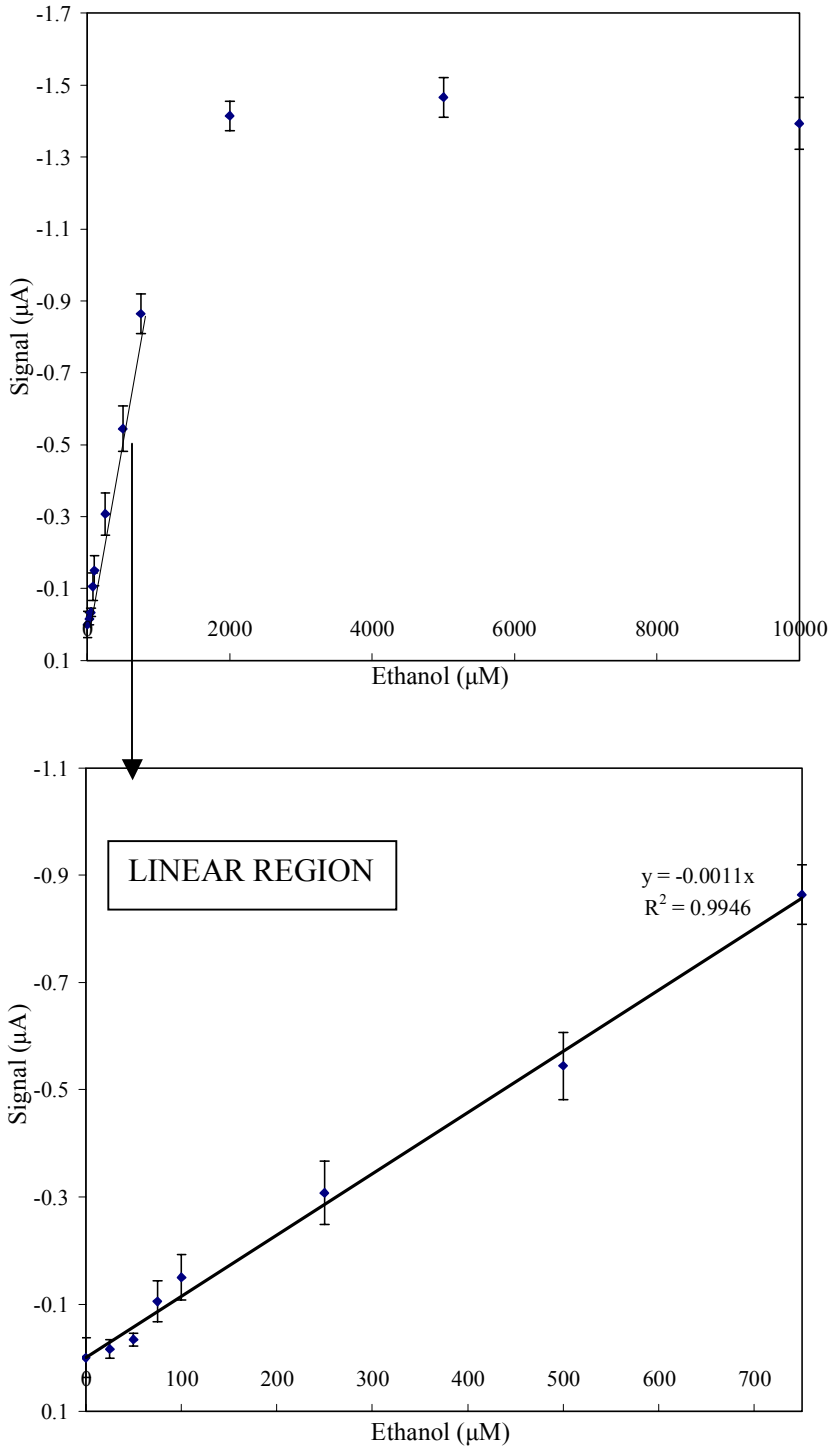

Figure 4.26: *Calibration of screen printed three electrode ethanol biosensor and determination of linear region for detection of ethanol in 0.1M PBS. Error bars are std dev, n=3.*

4.5.6 Validation

A test kit was not available for the detection of ethanol in solution in the range required. However, since the ethanol biosensor is ultimately based on the determination of hydrogen peroxide at the working electrode and utilises the same HRPx enzyme loading and mediator as for the hydrogen peroxide biosensor, it is not unreasonable to assume that the ethanol biosensor has a similar operational capability.

4.5.7 Further ethanol biosensor development – membranes and deposition regime

Before commencing work on the detection on ethanol in simulated wound fluid, further development work on the ethanol biosensor was carried out. To reduce the possible effects of interferents and proteinacious material present in serum, a range of membranes were investigated. Variations in the deposition of the enzymes, DMFc, CA and of Nafion were also investigated. The aim was to improve the linear range and the limit of detection of the sensor, by reducing inter-batch variation and hence noise. Table 4.3 below lists the membranes investigated.

***Table 4.3**: Membranes tested on ethanol biosensor*

Manufacturer	Membrane name	Membrane pore size (um)
Pall, Portsmouth, UK	Biodyne A	0.2
Pall, Portsmouth, UK	Biodyne A	0.45
Pall, Portsmouth, UK	Biodyne A	1.2
Pall, Portsmouth, UK	Immunodyne ABC	0.45
Whatman, Loughborough, UK	Cellulose nitrate	0.2
Whatman, Loughborough, UK	Cellulose nitrate	0.45
Whatman, Loughborough, UK	Cellulose nitrate	3
Whatman, Loughborough, UK	Cyclopore polycarbonate	0.4
Sterlitech, Kent, WA, USA	Nylon	0.45
Millipore, Watford, UK	Nylon	0.45
Spectrum, Loughborough, UK	Spectra membrane	MWCO 6-8k

A batch of ethanol biosensors were made according to the single deposition method described in Section 4.5.3. The membranes were cut into 1 cm squares, and placed on the sensor such that they covered the three electrodes (pre-dosed with enzyme, DMFc and CA) and secured using PVC tape. The amperometric procedure was initiated and 100 µl of 1:1 v/v serum: PBS deposited onto the membrane and the electrode response allowed to equilibrate prior to addition of 100 µl of 5 mM ethanol in 1:1 v/v serum: PBS. Tests were performed in triplicate, and the differential signal and signal: noise determined.

The Whatman Cyclopore proved unsuitable, since upon application of the serum/PBS, the membrane proved relatively hydrophobic resulting in uneven sample spread, and the serum did not filter though to the sensor surface. The Spectrum spectra membrane could not be used since it disintegrated upon application of serum/PBS. For all of the remaining membranes tested, there was a general difficulty in achieving full contact between the sensor and the membrane, and retaining contact once serum had been applied. Figure 4.27 shows the signal: noise ratios obtained for each of the membranes incorporated into the ethanol biosensors.

Only two of the membranes improved the signal to noise ratio beyond that of using no membrane. These were both Biodyne A membranes of 0.2 µm and 0.45 µm pore size, with a signal to noise of 54.4 and 10.4 respectively. Using no membrane gave a signal to noise of 8.7, therefore using the 0.45 µm Biodyne membrane would not greatly improve the sensor performance (compared to the improvement that follows through deposition development).

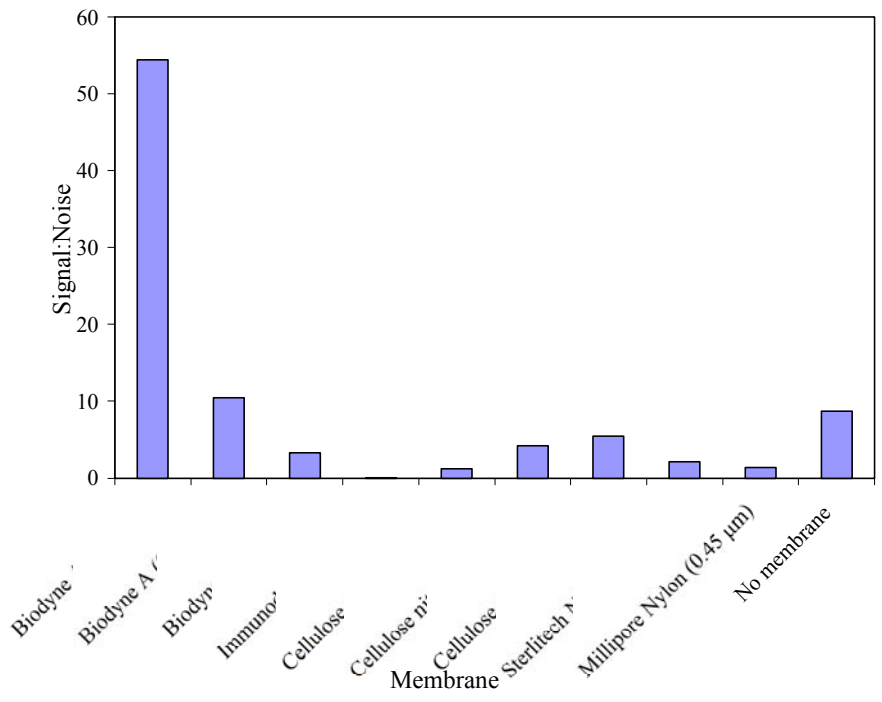

***Figure 4.27**: Comparison of signal: noise of ethanol biosensor using of a range of membranes.n=3.*

Given the difficulties associated with membrane integration into the sensor, the regime of applying AOx and HRPx enzymes, DMFc, and CA to the sensor, with the aim of improving the signal to noise ratio without the use of a membrane, was investigated further. Instead of applying all four components in one step, alternative depositioning regimes were examined, including the application of combinations of the reagents in seven variations of one, two or three layers, as shown in Table 4.4. The 13 µl deposition volume comprising two enzymes HRPx and AOx, and the CA immobilisation/diffusion layer were prepared, as described in Section 4.5.3. The same volumes per sensor also applied. A 5% v/v Nafion perfluorated resin aqueous dispersion (Aldrich, Poole, UK) was also investigated, at two drying temperatures to vary pore size. Except for the Nafion layers which were dried at 4°C and 50 °C, each layer was allowed to dry at room temperature before deposition of the next

layer. Each variation was made and deposited in replicates of six sensors (three for measurement, three for blank). 5 mM ethanol in 1:1 v/v serum: PBS was determined amperometrically to compare the formulations.

***Table 4.4**: Ethanol biosensor deposition parameters for the 4 biosensor reagents studied: AOx and HRPx enzymes, dimethylferrocene film, cellulose acetate and Nafion membrane materials. Numbers indicate layer number*

Combination	Enzymes	Enzymes + DMFc	Enzymes + DMFc + CA	DMFc + CA	5% Nafion Dried at 4 °C	5% Nafion dried at 50 °C	CA
1	1			2			
2	1			2	3		
3	1			2		3	
4		1			2		
5		1				2	
6			1				
7		1					2

.

The average signal, standard deviations and signal to noise ratio were calculated for each of the seven combinations, plotted in Figure 4.28. It can be seen clearly that combination number seven had by far the best signal to noise ratio of 19.1. This combination consisted of two deposition layers - layer one: HRPx, AOx and DMFc, and layer two: CA. The second best signal to noise was given by combination 6, the single deposition combination as used earlier in the chapter to detect ethanol in PBS, but was still considerably less than combination number 7. The addition of a Nafion layer increased the signal but had less favourable signal to noise ratios, possibly due to difficulty achieving a uniform and repeatable layer of nafion on the sensor surface. The very low signals and signal to noise witnessed for combinations 4 and 5, where a CA layer is absent, illustrate the importance of using CA as a diffusion layer on these sensors. Therefore, combination 7 was selected as the deposition regime of choice.

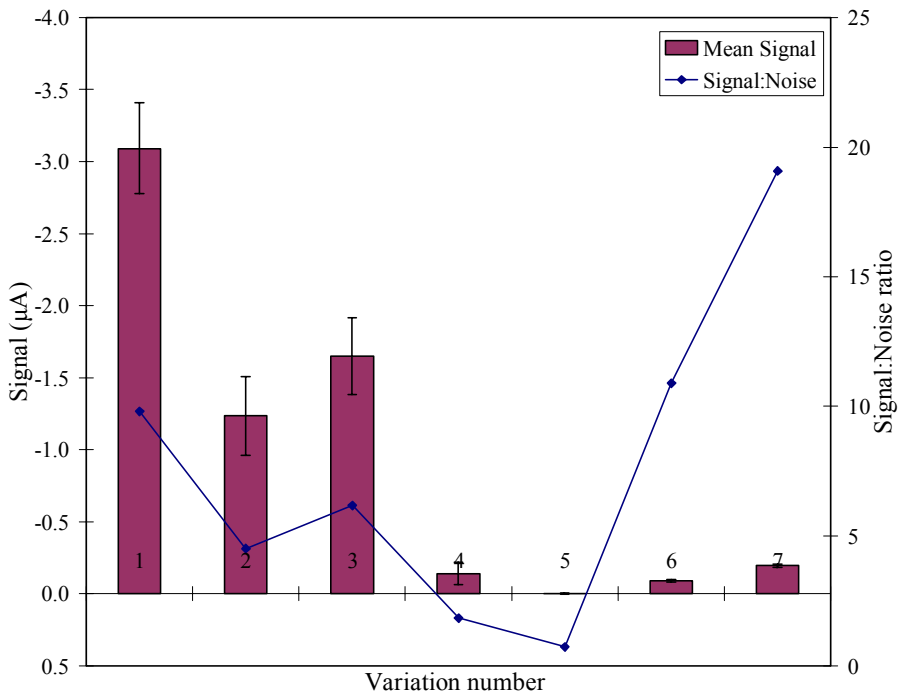

Figure 4.28: *Signal:noise ratio for the 7 deposition combinations of enzymes, dimethylferrocene, cellulose acetate and nafion used in alcohol biosensor construction. Error bars are std dev, n=3.*

Having decided to apply cellulose acetate as a separate second layer, a small investigation was carried out to determine whether application of CA by pipette action or dip coating was preferable. CA (20mg/ml) volumes of 0, 3 and 5 µl were applied to sensors by pipette action in replicates of six, and six sensors were also dip coated in CA. The sensors were then interrogated amperometrically using 5 mM ethanol in 1:1 v/v serum: PBS. The resulting average signals and signal to noise ratios were calculated and are shown in Figure 4.29. It can be seen that a far greater signal to noise ratio was present for the dip coated sensors, with a value of 238.0. This value far exceeded that produced when using the Biodyne A (0.2 µm) membrane, indicating that the dip coating route was superior to the pre-formed membrane depositioning approach, for the membranes studied in this work. CA was therefore applied by dip coating for all subsequent alcohol biosensor batches produced.

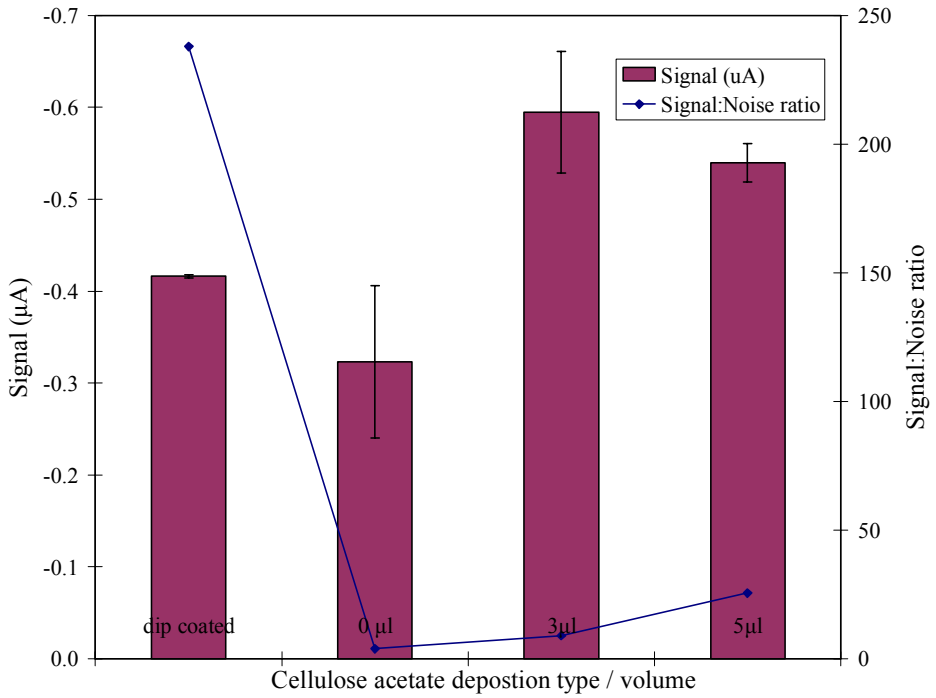

Figure 4.29: *Comparison of cellulose acetate application methods and volumes applied to alcohol biosensor. Error bars are std dev, n=3.*

4.5.8 Detection of ethanol in model wound fluid with ethanol biosensor

Having established that the alcohol biosensor had a limit of detection of 99.8 µM (99.7% confidence) in 0.1 M PBS using the single step reagent depositioning approach, the next stage of development was to examine the performance of the reformulated ethanol biosensors in 1:1 v/v serum: PBS, as performed for the glucose and hydrogen peroxide biosensors. A batch of ethanol biosensors was prepared using the new two layer deposition method, as described in Section 4.5.7

Concentrations of ethanol were prepared from 100-2000 µM in the 1:1 v/v serum: PBS. Ethanol was determined amperometrically at -300mV as before. Results are shown in Figure 4.30.

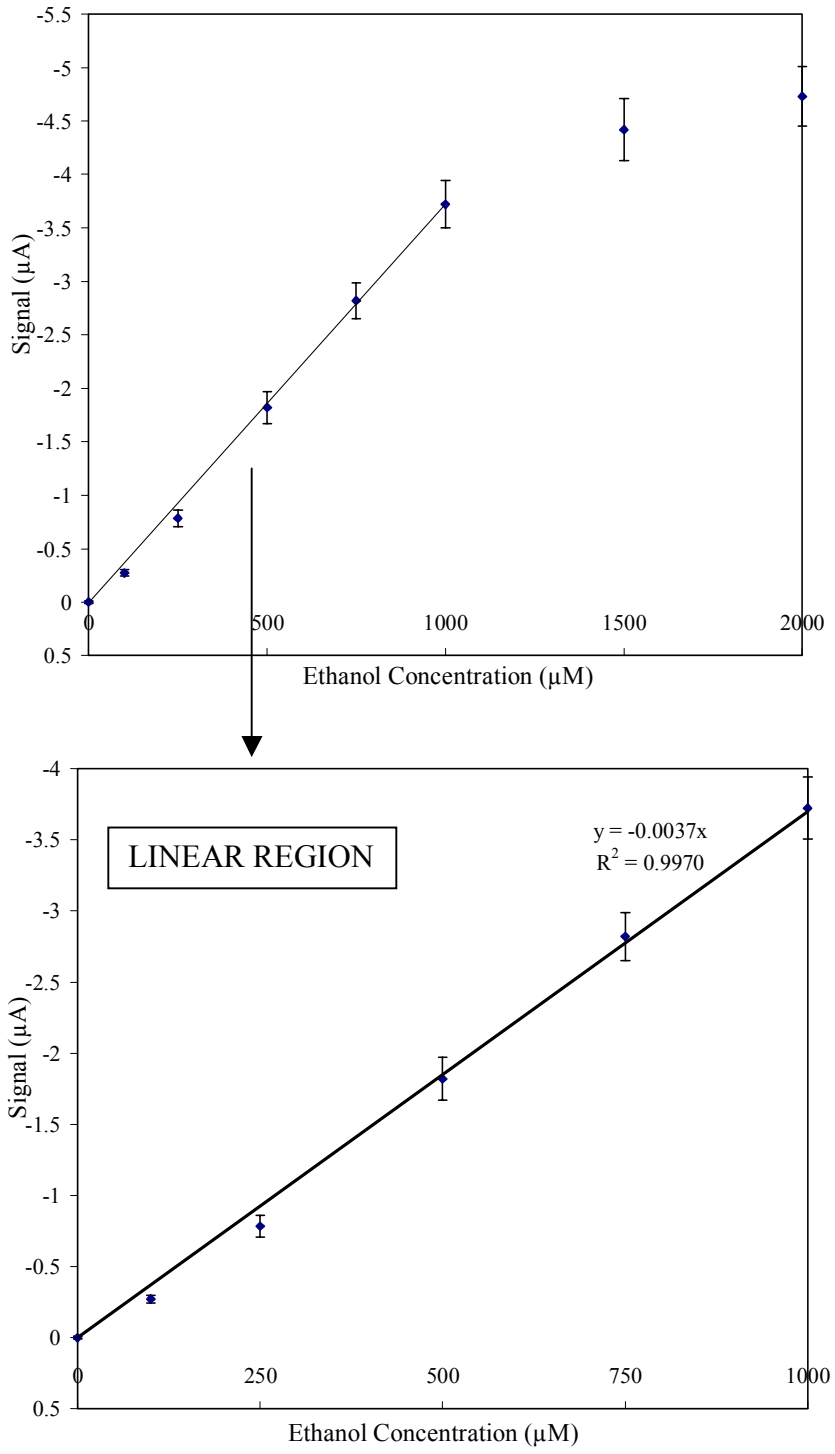

Figure 4.30: *Calibration of screen printed three electrode ethanol biosensor (2 layer deposition procedure, described in 4.5.7) and determination of linear region for detection of ethanol in model wound fluid. Error bars are std dev, n=3.*

The linear range of the sensor response was determined to be 0-1000 μM, 250 μM longer than in PBS alone, which were prepared by the single deposition formulation; (y = -0.0037x, R^2 value of 0.997). The standard deviation of the blank was found to be 0.0098 μA, yielding a limit of detection of 7.94 μM at 99.7% confidence (5.3 μM at 95% confidence), much lower than the limits found in PBS with the single deposition formulation (99.8 μM at 99.7% confidence).

4.5.9 Detection of S.aureus in model wound fluid with ethanol biosensor

Having established the biosensor could detect ethanol in diluted model wound fluid (1:1 v/v serum: PBS), it was next tested for its ability to detect bacteria in model wound fluid, by determining ethanol produced by metabolically active bacteria. However, as already mentioned in Section 2.3.1 only *S.aureus* would grow in serum alone. Attempting detection in serum supplemented with Dulbecco's modified Eagle's medium (DMEM) (as implemented in Chapter 5 for the odour analyser work), significantly interfered with the performance of the biosensor and thus this approach was not suitable. *S.aureus* alone was grown in serum (cultured as described in Section 2.2.5), and after a 1:1 dilution with 0.1 M PBS, was determined amperometrically (n=3) at five different cell densities. The average signals and standard deviations can be seen in Figure 4.31. The standard deviation of the blank was 0.02355 μA, and a linear biosensor response was observed over the range 0 to 4 x 10^8 CFU/ml (y = -0.0574x). The limit of detection was found to be 1.23 x 10^8 CFU/ml at 99.7% confidence (0.82 x 10^8 CFU/ml at 95% confidence). By using the mathematical relationship shown in Figure 4.30, the limit of detection in terms of the ethanol specific response was 19.0 μm at 99.7% confidence (12.7 μm at 95% confidence).

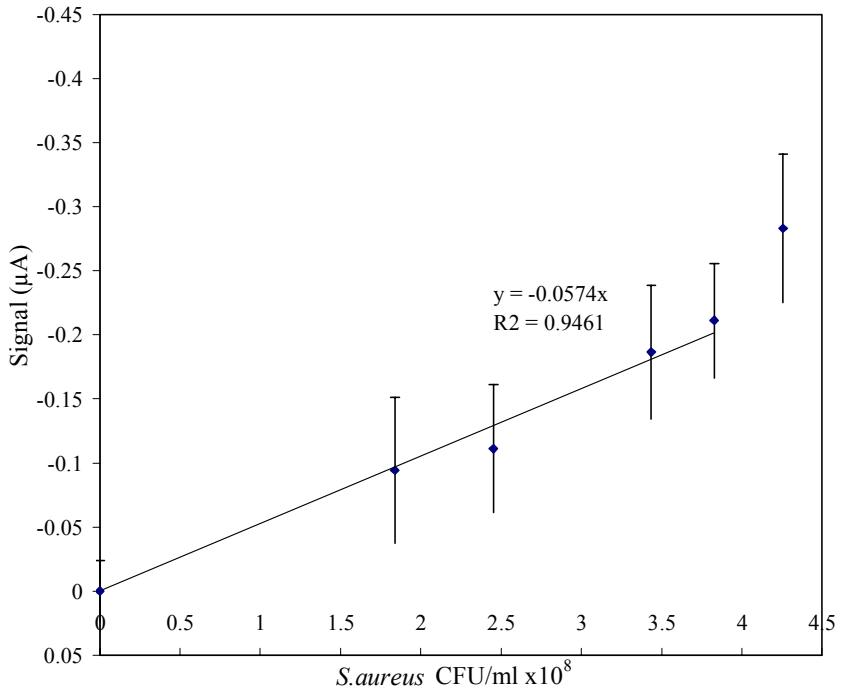

Figure 4.31: *Detection of metabolic ethanol production by S.aureus with screen printed three electrode alcohol biosensor in serum. Error bars are std dev, n=3.*

4.5.10 Interferent testing

As done so for the glucose and H_2O_2 biosensors, five common interfering species were tested for their affect on the measurement of 0.5 mM ethanol in 0.1 M PBS with ethanol biosensors. The results are summarised in Figure 4.32. Results are blank subtracted averages of three replicates, and error bars are +/- standard deviation.

The results are similar to those observed for the H_2O_2 biosensor, with acetominophen and ascorbic acid having the most significant affects on signal, and cysteine the least affect. However, the effects of urea and uric acid are not so severe. The change in signal is either because the species are electroactive at the same potentials as the analyte, or by electrode

fouling. These effects could be reduced by use of a perm-selective layer (Carelli, Centonze, De Giglio*, et al*, 2006; Hamdi, Wang, Monbouquette, 2005).

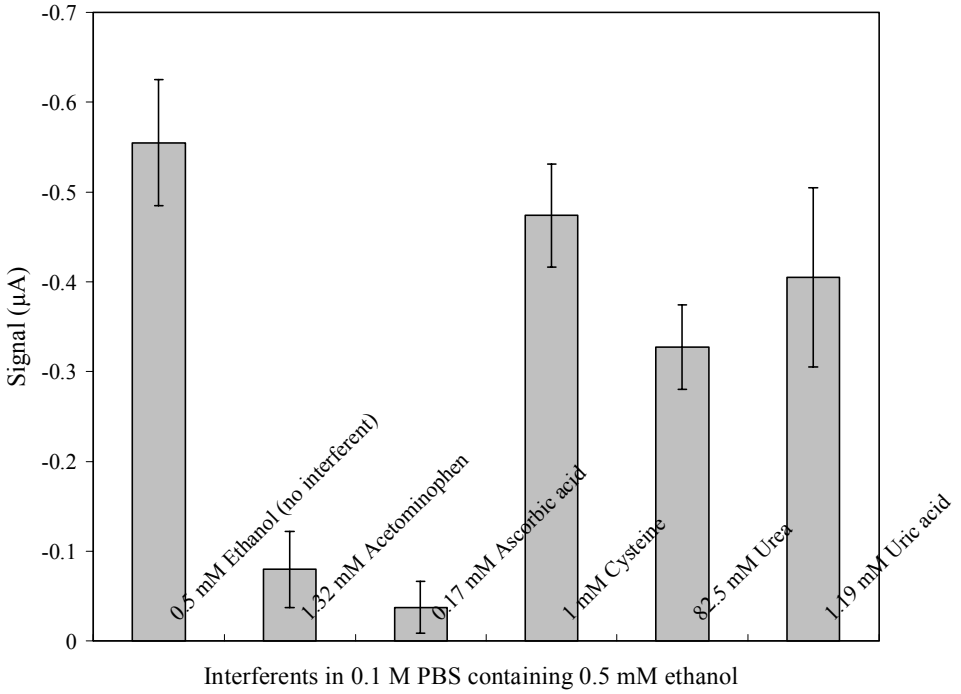

Figure 4.32: *Affect of interferents on the measurement of 0.5 mM ethanol in 0.1 M PBS with ethanol biosensor. Error bars are std dev, n=3.*

4.5.11 Conclusions: Ethanol biosensor

A bienzyme mediated ethanol biosensor was fabricated using a screen-printed three electrode assembly. AOx selection and optimisation determined that the optimum AOx loading was 1U/sensor using AOx isolated from *P.pastoris.* This enzyme was combined with HRPx and DMFc mediator. Cellulose acetate was found to be the most suitable immobilisation / diffusion layer when compared to Nafion and other membrane materials, with dip coating proving preferable to pipette application, with signal: noise values of 238.0 and 8.7 respectively. A detection potential of -300 mV was used for the detection of

H_2O_2 at the sensor surface. In model wound fluid with a single dilution step, the limit of detection for ethanol was 7.94 μM at 99.7% confidence. Direct detection of metabolically produced ethanol by *S.aureus* grown in model wound fluid by the ethanol biosensor, gave a limit of detection of 1.23×10^8 CFU/ml. This level does represent a significant bacterial count, since bacterial colonisation in wounds is considered problematic at levels of greater than 10^6 CFU/ml. Therefore, further biosensor refinement and optimisation is required in order to be used as an early warning system for bacterial invasion of a wound. However, this sensor does have potential to be used for monitoring further rises in bacterial colonisation, or indeed as part of a wound monitoring process where falls in ethanol production below a certain level could indicate reducing bacterial numbers and hence the success of a patient treatment regime.

4.6 Conclusions: Overall

The glucose, hydrogen peroxide and ethanol biosensors were all successful, detecting glucose, hydrogen peroxide and ethanol in surrogate wound fluid with a single dilution step, with limits of detection of 169.5 μM glucose, 8.43 μM hydrogen peroxide, and 7.94 μM ethanol respectively. The ethanol biosensor could detect *S.aureus* down to 1.23×10^8 CFU/ml, which could signal bacterial numbers falling below this level, possibly indicative of healing, or rising above a 'safe' level (i.e. $>10^6$ CFU/ml). Using the biosensor array, perhaps within a suite of diagnostic wound monitoring tests, a non-healing wound could be signalled to a busy physician more rapidly than it would otherwise be using conventional methods.

5. Bacterial Detection Using a Single Sensor Odour Analyser

5.1 Introduction

This Chapter aims to investigate whether a single sensor odour analyser may be used as a diagnostic tool in the early stages of wound healing, based on the detection of volatile bacterial metabolites and human markers of immune response within the localised wound environment.

Using a single sensor based odour analyser instead of an array of sensors, as present in commercially available electronic nose devices, has the advantages of reduced cost, and reduced complexity with respect to the sensor array. This is achieved by augmenting the volume of information gained from the sensor response by considering an increased number of sensor response curve features. Further information on the development of this machine can be found in the thesis of Lee-Davey (2004). There are many potentially influencing factors in the wound environment, for example: antiseptics and other antimicrobial agents; changing temperature of the wound environment; cell-derived molecules responsible for co-ordinating the healing process; medications taken by the patient, and though considered, could not all be investigated within the scope of this study. However, by separating serum from blood, as described in Section 2.2.4, it was possible to create a surrogate wound fluid, since the major component of wound fluid is serum. This enabled experimentation to be confined to the laboratory under a controlled environment in this preliminary feasibility study.

The objectives were limited to identifying whether the system could discriminate between those five bacterial species commonly associated with wound infection: *Staphylococcus aureus, Streptococcus pyogenes, Klebsiella pneumoniae, Escherichia coli* and *Pseudomonus Aeruginosa*. Tests were performed on individual cultures, then culture pairs, initially in broth and secondly in serum at fixed cell densities. By examining the headspace at constant cell densities, the differences detected may be more directly attributed to particular bacterial metabolic features, and not differences in cell numbers between bacteria. Detection and discrimination of the biological markers glucose, ethanol and H_2O_2 was also investigated. Headspace GC-MS (results presented in Section 2.3.3.) was used as the standard method as a basis for comparison.

Following odour analysis, discrimination of samples was based on principle component analysis (PCA), an unsupervised technique executed in Matlab. It requires the user to examine the data and select the principle components which provide the best virtual discrimination of samples, realised through plots of one principle component versus another. As described in Section 1.4.5.1, this technique reduces the dimensionality whilst retaining the variance of the original data, providing a relatively fast method of determining the success of the experiments at this developmental stage.

5.2 Materials and Methods

5.2.1 Odour analyser instrumentation

The odour analyser, developed by Lee-Davey (2004) at a basic level may be considered a relative of the traditional machine olfaction approach as exemplified by the so-called 'electronic nose'. However, instead of housing an array of sensors for odour detection, it uses just one - a single mixed metal-oxide semiconductor sensor (MMOS). MMOS sensors are designed for a range of applications, including air quality and volatile organic compounds (VOCs), and have found application in commercial systems, such as the Marconi eNOSE 5000 units. These sensors typically have a lifetime >5 years for some applications, repeatability, and a broad range - useful characteristics for the detection of multi component mixtures such as that of wound fluid.

G series CAP25 sensors from City Technologies Ltd, Portsmouth, UK, are *p*-type semi-conductors based on a chromium titanium oxide layer sandwiched between two electrodes. If the semiconductor is exposed to a reducing gas, oxygen is removed from the surface and thus gains electrons, leading to a positive (*p*) change in resistance. Further details of sensor operation can be found in Section 1.4.3 and from the supplier's website: www.citytech.co.uk.

The pattern of response from the sensor is dependent on the sensor operation temperature, which is 430 ± 50 °C. The sensor chamber is designed to be completely sealed and includes temperature control using a Peltier thermoelectric controller - TEC (Oven Industries Inc., PA, USA). This is connected to a temperature sensor (also within the chamber) and

microprocessor heat sink and fan (exterior). The chamber also contained an elongated path in order to equilibrate the volatilised sample at a uniform, desired temperature. An annotated photograph of the sensor chamber is given in Figure 5.1.

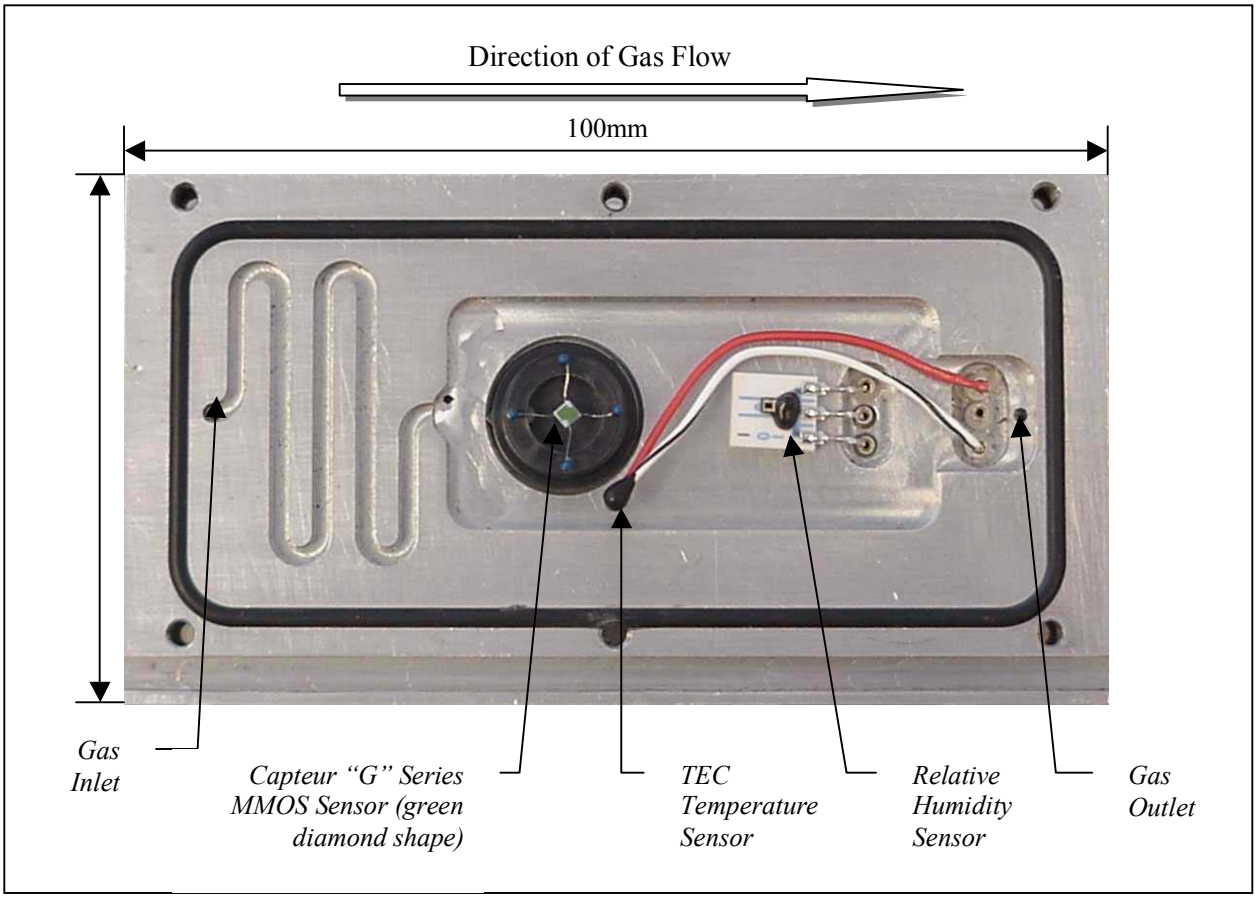

Figure 5.1: *The interior of the MMOS system sensor chamber, displaying the MMOS sensor, the relative humidity sensor, and the Peltier Thermoelectric Controller, temperature sensor.*

Resistance change is affected by humidity and water formation. At low temperatures, hydrogen gas may react with OH^- bonded to the surface of the sensor, however, by operating the sensor at an elevated temperature, a reduction in the negative effect of water is achieved. The sensor chamber also contains a sensor to monitor relative humidity

(Honeywell Inc., IL, USA). The program LabVIEW is used to vary system parameters and control the system. The system and sampling parameters employed are given in Table 5.1.

Table 5.1: *Odour analyser system parameters*

Parameter	**Value**
Bacterial sample volume (ml)	0.5
Injection volume (ml)	5
Sensor chamber temperature (°C)	30
Sample temperature (°C)	37
Carrier gas flow rate (ml/min)	150
Sensor baseline resistance (kΩ)	150
Sensor temperature (°C)	430

Achieving a stable baseline and response from an MMOS sensor is an important step to ensure repeatable sensor performance. Sensor sensitivity can be manipulated by increasing or decreasing the resistance baseline value and should be selected based on the particular nature of the samples to be analysed. Therefore, after sensor installation or replacement, the baseline resistance was adjusted to a final value of 150 KΩ after equilibration at the operating temperature for 24 hours to allow sensor stabilisation. The sensitivity of newly installed sensors was checked using 1.72 mM ethanol samples. This procedure was also carried out routinely to periodically check the performance of the sensor by comparing the response profile with that obtained when the sensor was first installed.

5.2.2 System operation

There are four stages to the sampling sequence:

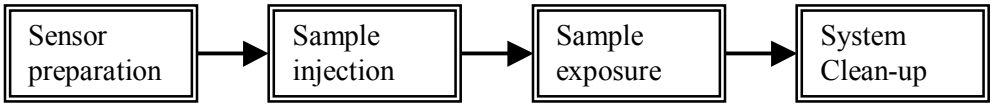

First the sensor must adjust and stabilise to any differences between the sampling and standby flow rates. Secondly, a fixed period of time (20 s) is allocated for sample injection. Following this, data is collected and recorded for analysis. Fourthly, there is a clean-up stage post analysis.

Figure 5.2 is a schematic representation of the odour analyser. The sensor manufacturer recommends a continuous air flow, even in standby mode, therefore the carrier gas zero grade air (BOC Ltd, Windlesham, UK) continually flowed over the sensor unit, allowing the baseline resistance pre and post analysis to stabilise. Flow control was maintained by a Mass Flow Controller (Brooks Instruments, PA, USA).

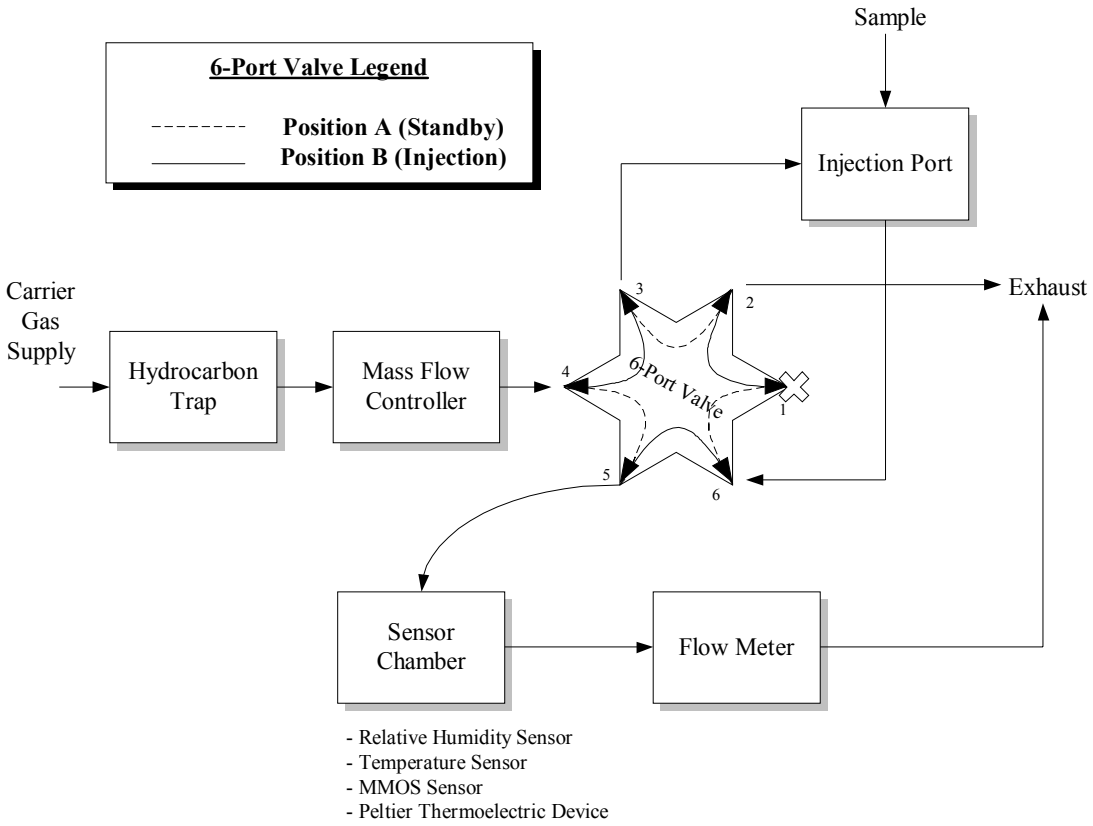

Figure 5.2: *Mode of operation of the single MMOS sensor odour analyser (Lee-Davey, 2004)*

In sampling mode, a headspace sample was injected into the sample port, and the six-port valve (Vici Valco Instruments Co., Houston, USA) switched so the zero grade air supply passes through the injection valve. This directed the headspace sample over the sensor surface in an undiluted "plug" and the sensor response was recorded over a period of 180 s. The response could be viewed in real-time using the LabVIEW software (National Instruments, Newbury, UK).

The sensor resistance response required data pre-processing in order to reduce noise. Therefore, post acquisition digital filtering was used, also conducted through LabVIEW, to automatically produce a noise-reduced sensor signal. Data from each analysis was recorded in the form of a tab separated spreadsheet, accessible through programs such as MS Excel and Mathworks Matlab for analysis. The parameters recorded in each file are listed below:

- Date and time of analysis
- Carrier gas flow rates in and out (ml/min)
- Relative humidity (%)
- MMOS sensor voltage (V)
- Sensor Resistance (Ω)
- Mean sensor resistance (Ω)
- Deviation from the sensor baseline resistance (%)
- Standard deviation of the mean resistance value (Ω)

After sample exposure there followed a system clean-up period of 600 s. Further information on the design of this system, including operation, configuration and calibration can be found in the thesis of (Lee-Davey, 2004).

5.2.3 Data Analysis

The second stage of the odour analysis procedure was that of data analysis, in this case by principle component analysis (PCA) of key response curve values using Matlab. PCA was considered a suitable chemometric technique for the validation of the odour analyser as a potential diagnostic tool, since there was little knowledge regarding the response of the sensor to various bacterial odours, and therefore an unsupervised learning technique (i.e. does not require a training data set) has obvious advantages. This technique is widely used as the analytical method of choice in the investigation of machine olfaction sensor responses. By using PCA, many variables could be considered simultaneously and with reduced dimensionality, making it easier to identify relationships between samples.

Individual features of the response curve recorded during sample analysis were used for PCA. Three distinct aspects to the response curve produced by the odour analyser MMOS sensor are immediately evident: a) the magnitude of the response curve, b) following a brief negative deviation from baseline resistance, a sharp rising slope rising to a maximum response value, and c) a decay slope as the sensor returned towards the baseline value. These three portions of the sensor response can be observed in Figure 5.3, in which a typical response to the headspace of a 1.72 mM (v/v) ethanol sample is shown.

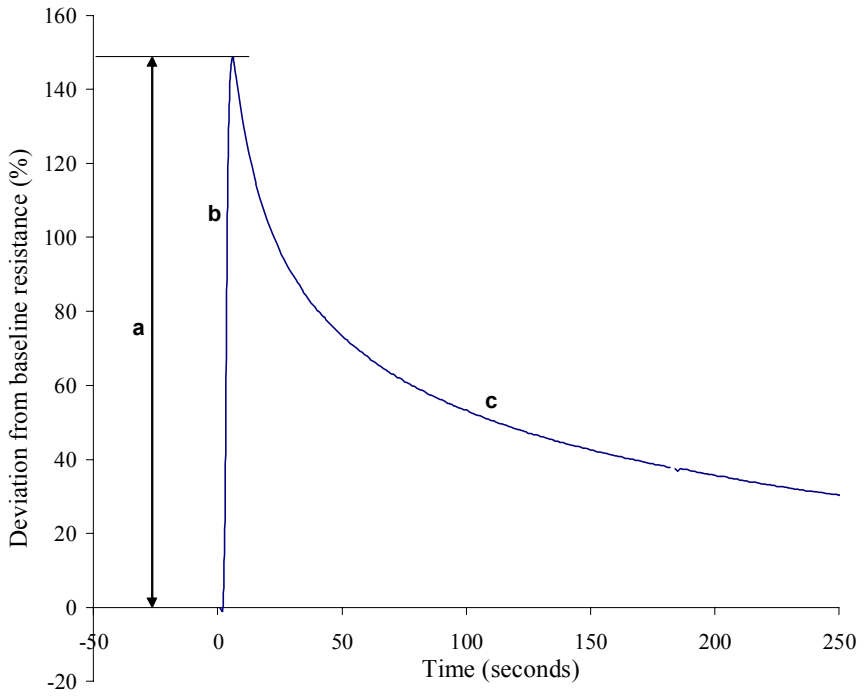

Figure 5.3: *A typical MMOS sensor response curve showing the three main characteristics: a) the magnitude of the response, b) the rising slope, c) the decay slope.*

Twenty seven distinct measurable parameters were extracted from the response curves. A list of the extracted features recorded from a sensor response curve can be found in Table 5.2. The curve features were obtained from the odour analyser output files using a program written in Matlab (*Allnostril*). Features of the samples were compiled into a matrix whereby principle component analysis could be conducted on the data using the '*pcagui*' function of the PLS Toolbox (Eigenvector Research Inc., Washington, USA) which ran as an 'ad-on' in Matlab. Once the PCA model loaded, it was possible to view the sample scores, eigenvalues, and to select the number of extracted features to apply to the model, which was usually the first eight.

Table 5.2: *The twenty seven components extracted from MMOS response curves.*

PC number	Extracted Components
1	Baseline resistance (Ω).
2	Maximum response (Ω).
3	Time of maximum response (s).
4	Signal to noise ratio (Ω).
5	Noise ratio (%).
6	Last value logged (%).
7	Minimum value (%).
8	Ratio of baseline resistance to maximum response.
9	Peak width (s).
10	Maximum gradient.
11	Time of maximum gradient (s).
12	Gradient of minimum to maximum slope.
13	Rising slope.
14	Area under the entire curve.
15	Area to maximum response value.
16	Area of peak width.
17	Area from maximum response to the end of file.
18	Decay curve half life (s).
19	Decay curve one third life (s).
20	Decay curve two third life (s).
21	Ratio of maximum response to half life.
22	Ratio of maximum response to one third life.
23	Ratio of maximum response to two third life.
24	Ratio of maximum response to last value logged.
25	Gradient of the logarithm linear curve of the decay slope.
26	Constant of the logarithm linear curve of the decay slope.
27	Coefficient of determination of the logarithm linear curve of the decay slope.

5.2.4 Preparation of non-bacterial samples

Aqueous solutions of phosphate buffer saline (Sigma, Poole, UK), ethanol (99.9% denatured HPLC grade, Aldrich, Poole, UK), hydrogen peroxide (31.3% v/v assay ACS reagent, Sigma, Poole, UK), and glucose (reagent grade, Fisher, Loughborough, UK) were prepared in reverse osmosis water.

5.2.5 Preparation of bacterial samples

Bacteria were grown up in glass 'universal' vials (Fisher, Loughborough, UK) containing 5 ml of the growth media stated for each study (tryptone soy broth (TSB) or yeast peptone dextrose (YPD) sterilized by autoclaving). For studies where serum or 90:10 v/v serum: Dulbecco's modified Eagles medium (DMEM) was used, the bacteria were grown in 40 ml clear plastic vials supplied sterile from Fisher, Loughborough, UK. All inoculations and sampling was carried out in a type 2 laminar flow cabinet with aseptic technique. The bacteria were cultured at 37 °C in a Gallenkamp orbital incubator at 140 rev/min.

By referring to the growth curves generated for each bacteria in the different media used (Section 2.3.1), it was possible to determine the number of bacteria at a given time by measuring optical density at 600nm. It was therefore possible to keep a constant bacterial count (± 0.05 abs reading) for headspace measurements, when required.

5.2.6 Sample injection

It was found that 1 ml was a suitable sample volume for analysis of the marker analytes ethanol, glucose and H_2O_2. However, for bacterial samples because the deviation in baseline resistance in analysis was often very large, the time required for the sensor to restabilise to its baseline value was much longer, and therefore a sample volume of 0.5 ml was used in order to reduce the time required for the baseline signal to restabilise after analysis, whilst still eliciting a sufficiently large sensor response.

Before analysis, all samples were held at 37°C in a water bath for 15 minutes to equilibrate, unless otherwise stated. Each sample was held in a 20 ml glass vial (Sigma, Poole, UK) and capped with air-tight aluminium pressure release seal caps pre-fitted with silicone septa (Sigma, Poole, UK). After equilibration, 5 ml of headspace was withdrawn from the vial and injected into the odour analyser system using a 5 ml gas tight syringe from SGE International PTY Ltd., Ringwood, Australia. Samples were processed randomly with replicate tests being performed as stated for each study.

5.3 Results and Discussion

5.3.1 Effect of sample preparation temperature and pH on odour analyser response

It was important to assess the impact of certain variables on the response produced by the odour analyser before studies involving bacterial samples and marker analytes were performed. Therefore initial studies on the key experimental parameters of sample preparation temperature and pH were performed, since temperature has been reported as having a major influence on headspace generation (Lee-Davey, 2004).

Using 1 ml of 4.31 mM ethanol in H_2O as the test sample, the effect of sample preparation temperature was tested by varying the water bath temperature for each sample from 19 °C to 43 °C for the 15 minute equilibration period prior to headspace sampling. Figure 5.3 (a) shows the direct response produced by the MMOS sensor in response to the headspace from 4.31 mM ethanol equilibrated at different temperatures. The clear increase in deviation from baseline resistance is depicted in Figure 5.4 (b) as a linear relationship.

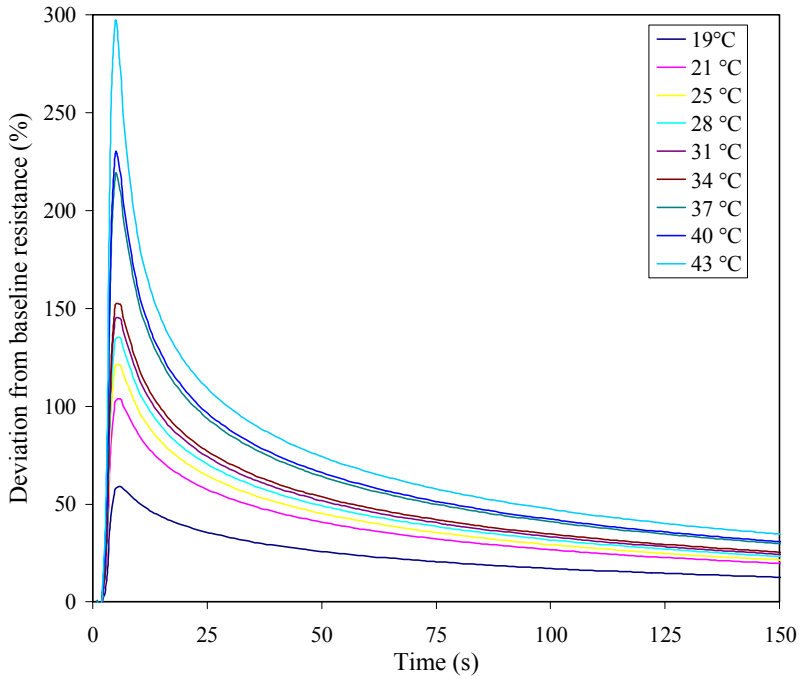

(a)

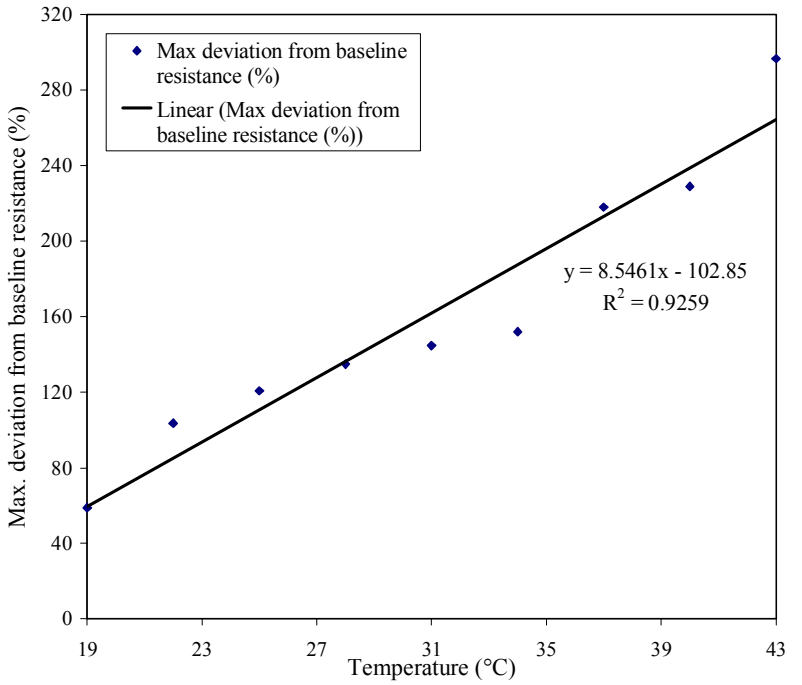

(b)

Figure 5.4: *Detection of 4.31 mM ethanol in water held at different temperatures before odour analyzer injection. (a) Deviation in baseline resistance with time. (b) Linear relationship between temperature and maximum deviation in baseline resistance.*

From this study it was clear that temperature has a large effect on MMOS response, which concurs with the findings on Lee-Davey (2004). It was therefore essential to maintain consistency in sample preparation temperature, and sensor operation temperature.

The effect of pH was tested by analysis of 0.1M phosphate buffer saline at pH values 6, 7 and 8 in triplicate, selected to cover the values either side of normal physiological pH (pH7.2), with an equilibration temperature of 37 °C. The direct responses from the odour analyser can be seen in Figure 5.5 (a). Figure 5.5 (b) was produced by taking the greatest positive and negative deviations from baseline resistance. A slightly non-linear relationship is apparent, but no significant effect was observed with pH change. Work that followed on marker analytes was carried out at pH 7.2 since this is the normal pH of human serum.

5.3.2 Detection of ethanol, glucose and H_2O_2 in PBS

Although the biological markers ethanol, glucose and H_2O_2 are not detected individually by the odour analyser in the bacterial studies that follow, it was of interest to determine whether the odour analyser was capable of detecting and/or discriminating between them. It also provides some basis to compare the odour analyser system with the biosensor array based system, which is able to detect these individual components.

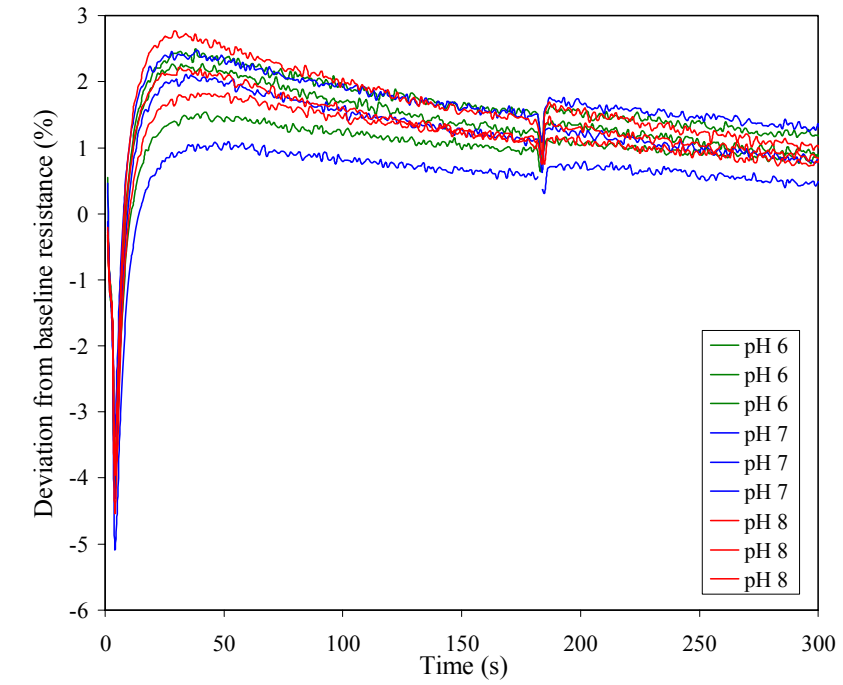

(a)

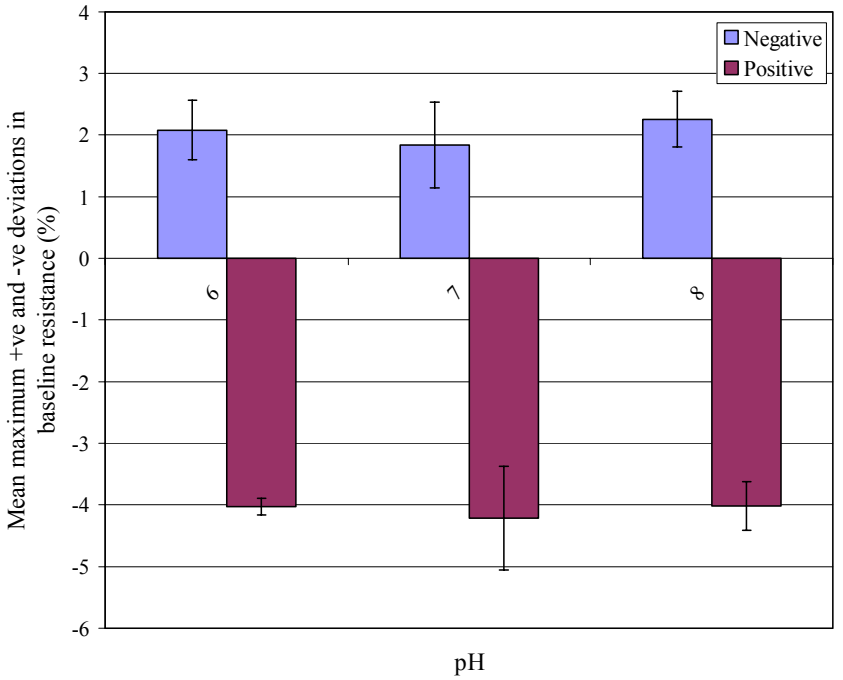

(b)

Figure 5.5: *Odour analyser detection of 0.1M PBS of different pH values. (a) Deviation from baseline resistance with time. (b) Mean maximum positive and negative deviations in baseline resistance with pH.*

Therefore, samples of ethanol at 2 and 20 mM, H_2O_2 at 0.1 and 1mM, and glucose at 2 and 10mM were prepared in 0.1M PBS for analysis. Each concentration of each analyte were tested in triplicate randomly at two equilibration temperatures, 25°C and 37°C, followed by PCA analysis. The circles around the clusters on the PCA plots were added by hand after PCA analysis in Matlab, and are there for illustrative purposes to highlight clustering for all graphs that follow. The PCA scores-plot results presented in Figure 5.6 (a) and (b) depict the lower concentration values of the three analytes studied at an equilibration temperature of 25°C for PC1 vs. PC2 and PC1 vs. PC3 respectively. These scores-plots illustrate overlapping between the glucose and 0.1 M PBS (blank) samples, although the virtual separation was much better than expected, due to the low volatility of glucose and H_2O_2. The circles around the points are for illustrative purposes only, of clustering. Ethanol, being a more volatile species, was clearly discriminated from the other analytes which exhibited much lower volatilities and hence response profile similarities. Figure 5.7 (a) and (b) shows that at the same temperature, but with higher concentrations of these analytes, the virtual separation is improved.

By raising the sample equilibration temperature to 37°C, even at the lower concentrations studied, the marker analytes were more clearly separated as illustrated in Figure 5.8 (a) and (b). Higher concentrations at 37°C are shown in Figure 5.9 (a) and (b). Spatial separation of the analyte groups at this temperature does not appear to be significantly different between the two concentrations studied.

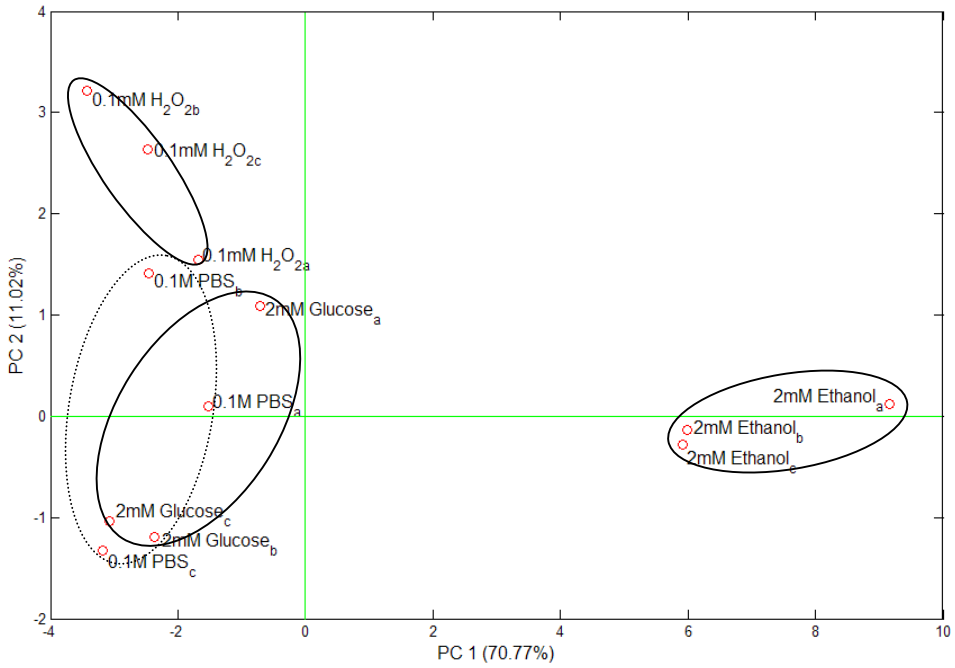

(a)

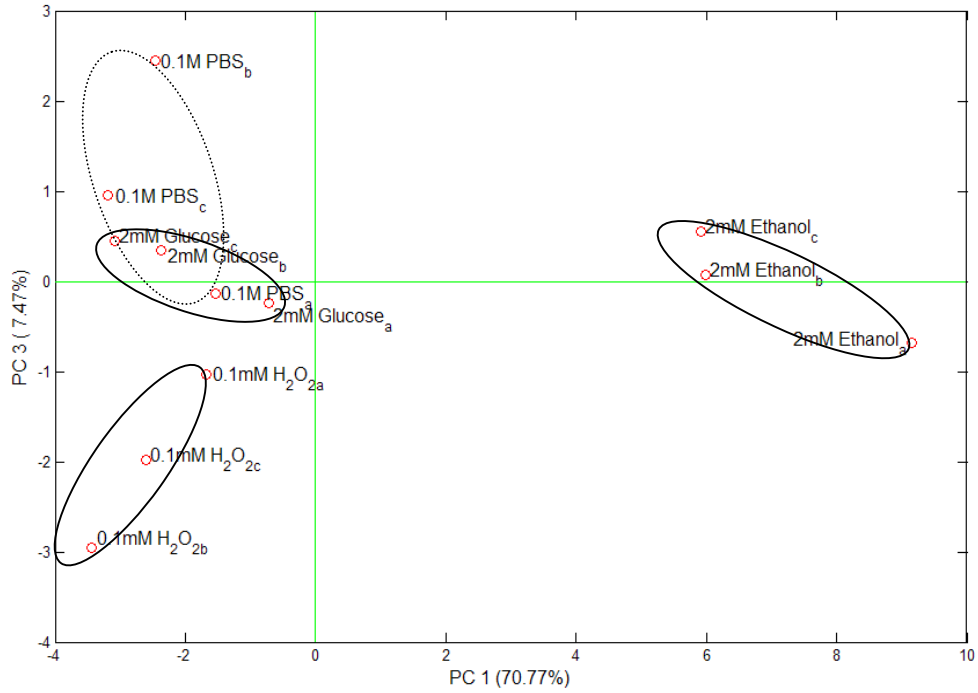

(b)

Figure 5.6: *Discrimination by PCA analysis of odour analyser detection of low concentration marker analytes with a pre-sampling temperature of 25°C. (a) PC1vPC2. (b) PC1vPC3*

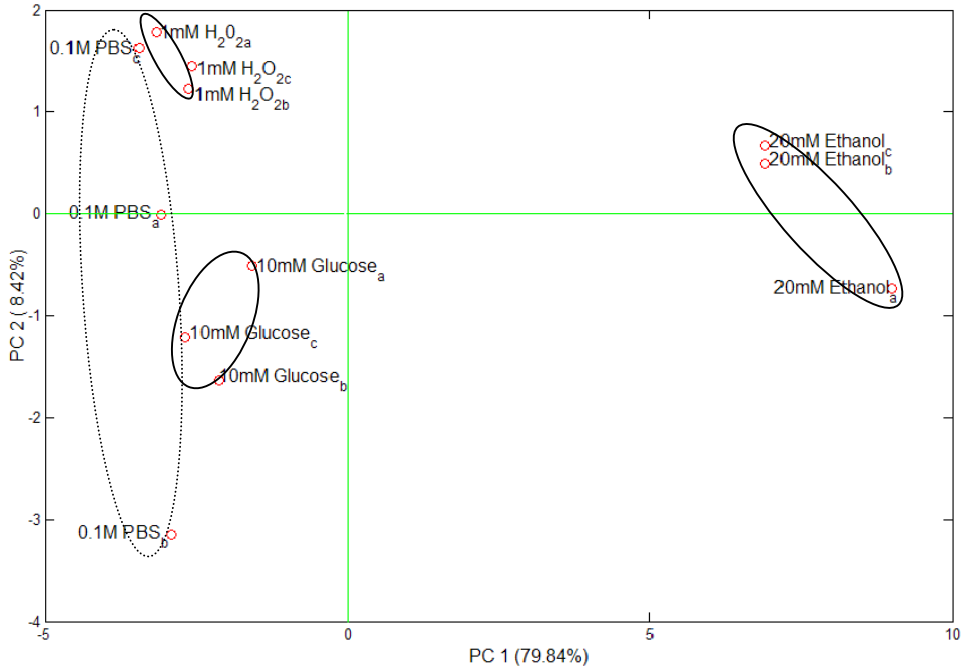

(a)

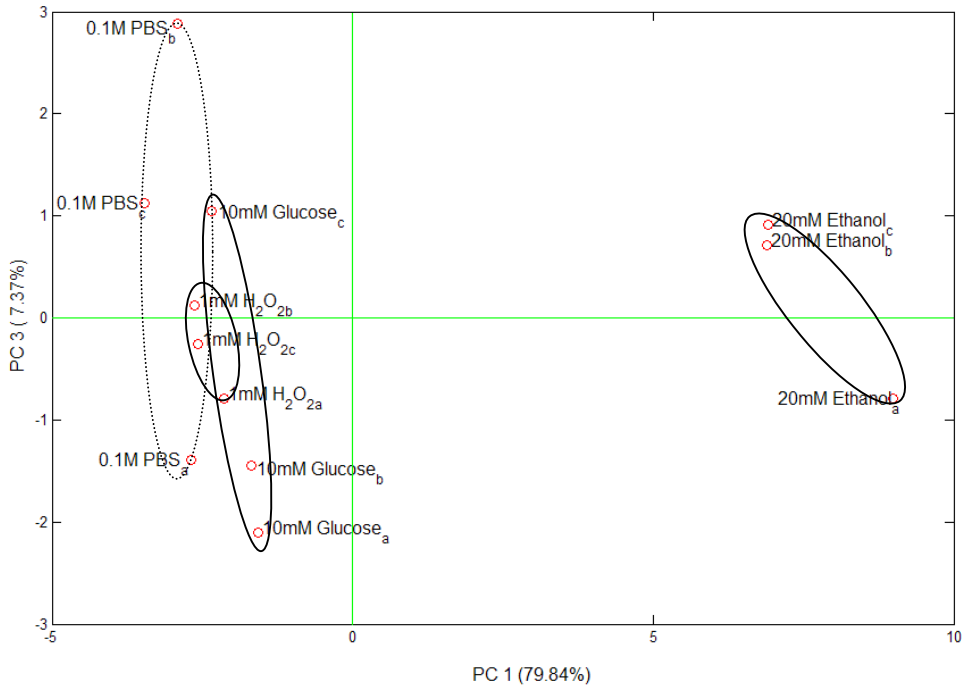

(b)

Figure 5.7: *Discrimination by PCA analysis of odour analyser detection of higher concentration marker analytes with a pre-sampling temperature of 25°C. (a) PC1vPC2. (b) PC1vPC3*

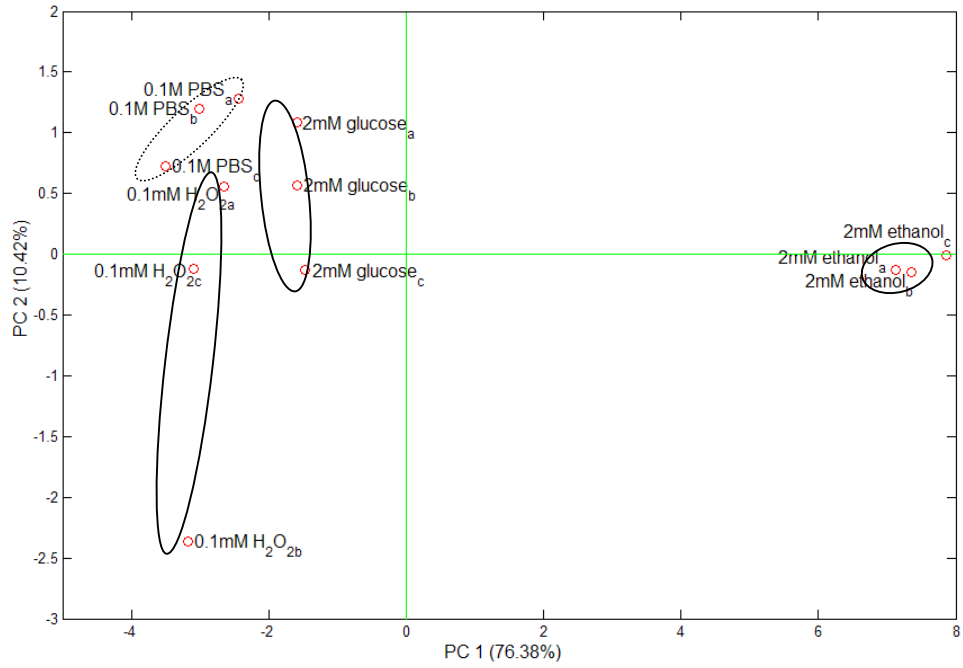

(a)

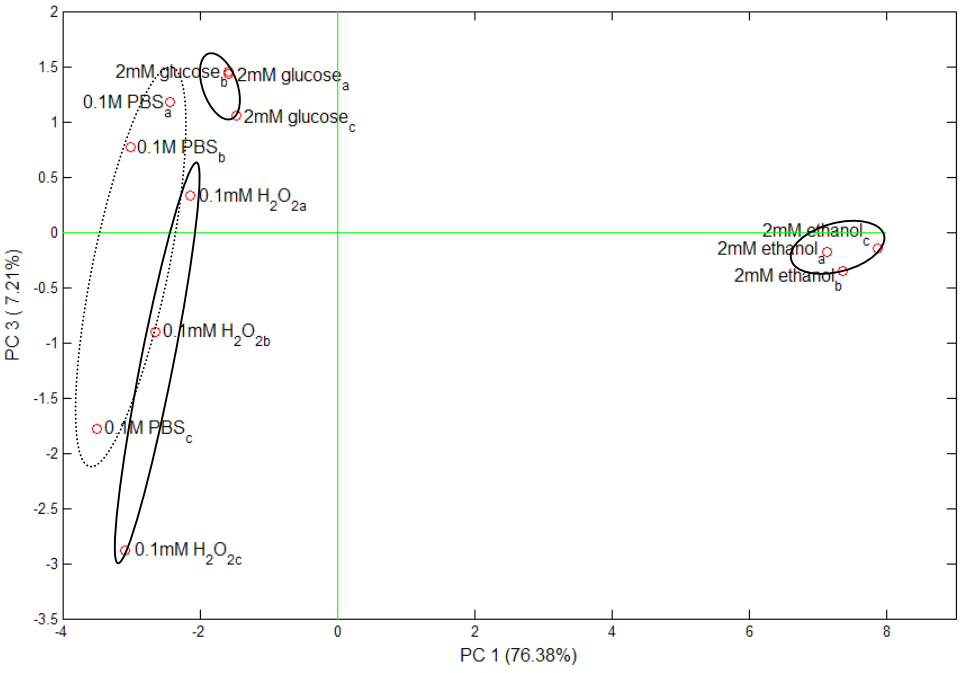

(b)

Figure 5.8: *Discrimination by PCA analysis of odour analyser detection of low concentration marker analytes with a pre-sampling temperature of 37°C. (a) PC1vPC2. (b) PC1vPC3*

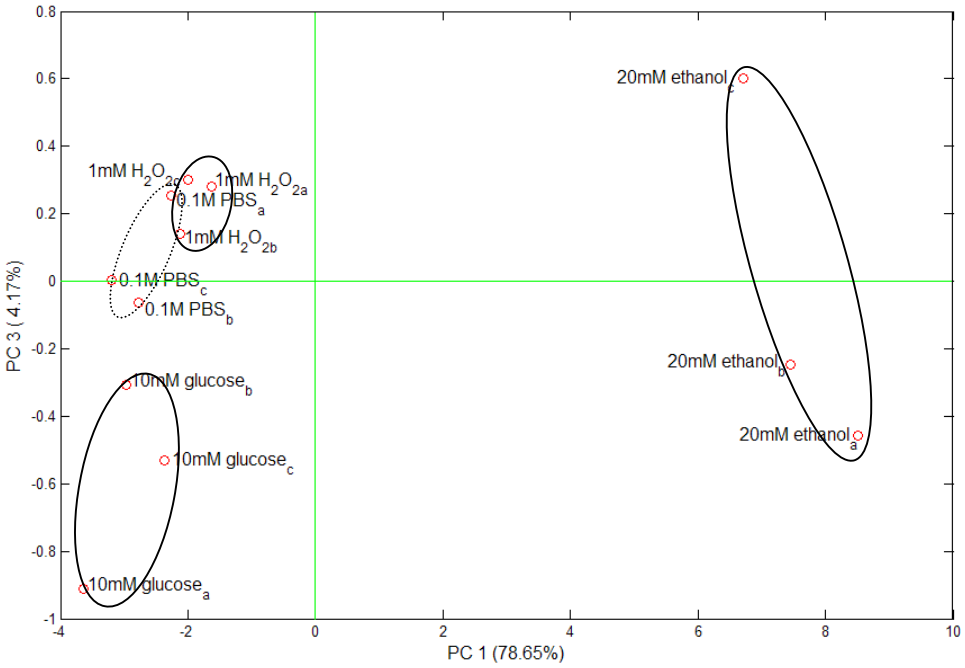

(a)

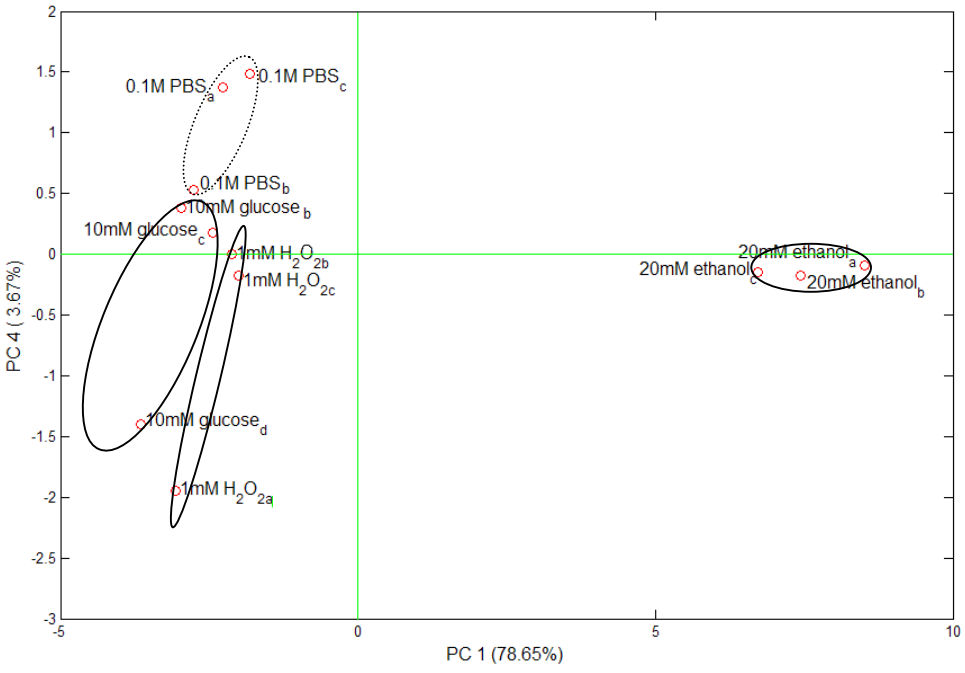

(b)

Figure 5.9: *Discrimination by PCA analysis of odour analyser detection of higher concentration marker analytes with a pre-sampling temperature of 37°C. (a) PC1vPC3. (b) PC1vPC4*

5.3.3 Detection of ethanol in serum

Since the main metabolite produced and detected by the bacteria being used in this thesis was ethanol, as confirmed by headspace GC-MS in Section 2.3.3, the ability of the odour analyser to detect different concentrations of ethanol was investigated. Ethanol solutions of 1, 5, 10 and 20 mM were prepared in serum, as a model for wound fluid (see Section 1.6). Random tests for each of these concentrations were performed in triplicate.

Figure 5.10 (a) shows the direct deviation in baseline resistance produced by the odour analyser. The triplicate mean maximum value from these deviations was used to produce Figure 5.10 (b) which illustrates a linear relationship between ethanol concentration and maximum deviation in baseline resistance. Therefore, the device is suited to the determination of ethanol, and potentially to other similar metabolic markers in wound fluid.

Since the odour analyser would not be used to detect each of the marker components separately in this application, the work that follows has focused on the detection and discrimination of five bacteria commonly isolated from wounds.

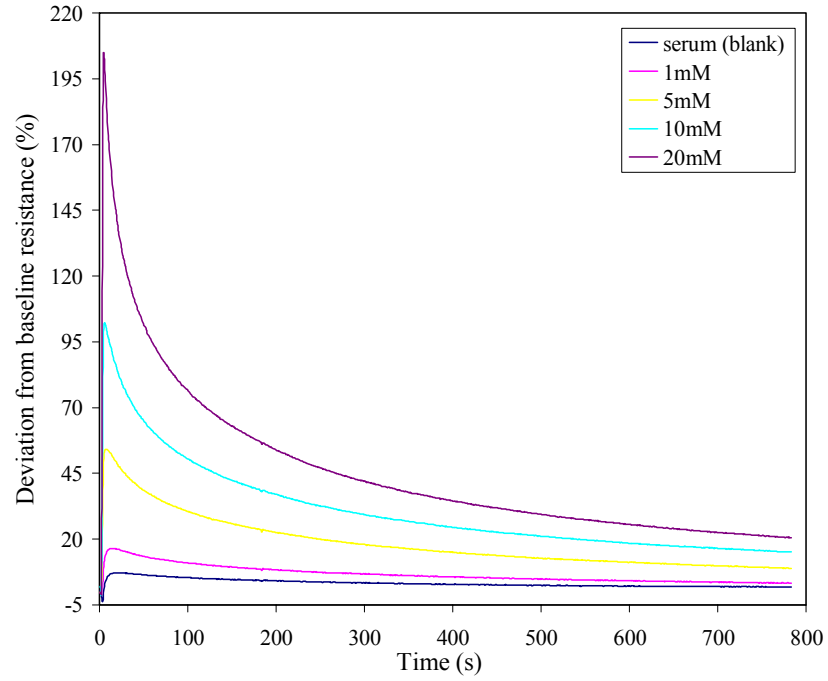

(a)

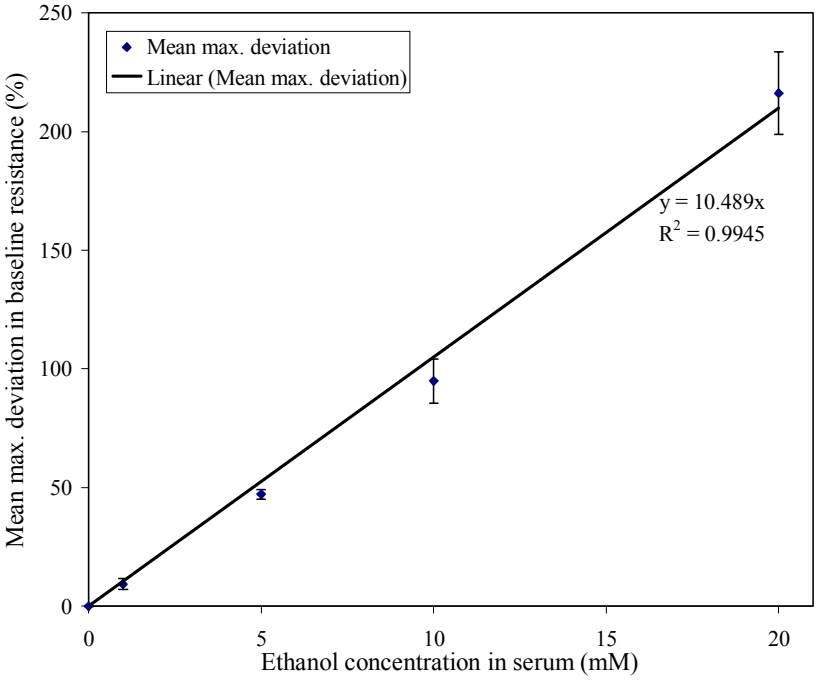

(b)

Figure 5.10: *Odour analyser detection of 0 to 20 mM ethanol in serum. (a) Deviation in baseline resistance with time, (b) Linear relationship between ethanol concentration and mean maximum deviation in baseline resistance.*

5.3.4 Detection of Staphylococcus aureus at different stages of growth

In order to ascertain whether the odour analyser was able to detect differences in growth phases of bacteria, a small proof of concept study was carried out. *Staphylococcus aureus* was grown in TSB at 37 °C, and headspace analysis carried out at the start (inoculation), lag, exponential and stationary phases of growth, determined by optical density readings and referral to bacterial growth figures in Section 2.3.1. The use of growth curves is illustrated in Figure 5.11, where the arrows indicate the times of odour analysis of *S.aureus* for this study.

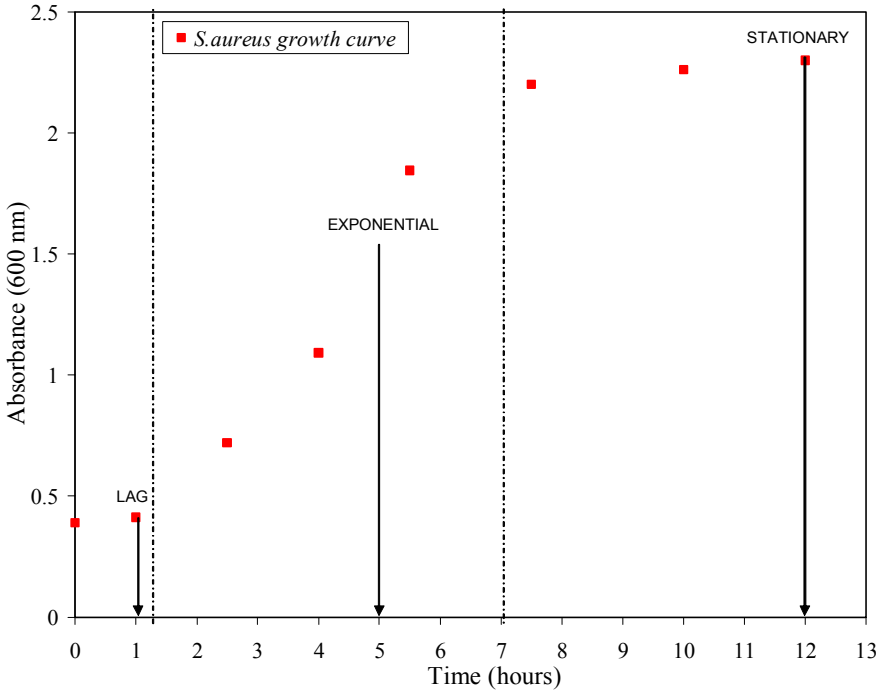

Figure 5.11: *Illustration of the use of S.aureus growth curve to determine growth phase. Arrows indicate time of odour analysis for this study.*

Figure 5.12 shows the deviations in baseline resistance that occurred at each of these stages. As expected, the deviation increased with the length of time the bacteria had been

growing, most probably due to the accumulation of volatile metabolic products such as those listed in Table 1.4, with accumulation in cell mass. Volatile metabolic profiles may also change with growth phase, with the production of volatile secondary metabolites as the cultures mature in the stationary phase. This is also true of spoilage bacteria isolated from milk (Haugen, Rudi, Langsrud, *et al*, 2006), and in cheese maturation (Marilley & Casey, 2004). Since the odour analyser was capable of detecting differences in concentration of bacteria, further studies on the detection of wound bacteria were carried out.

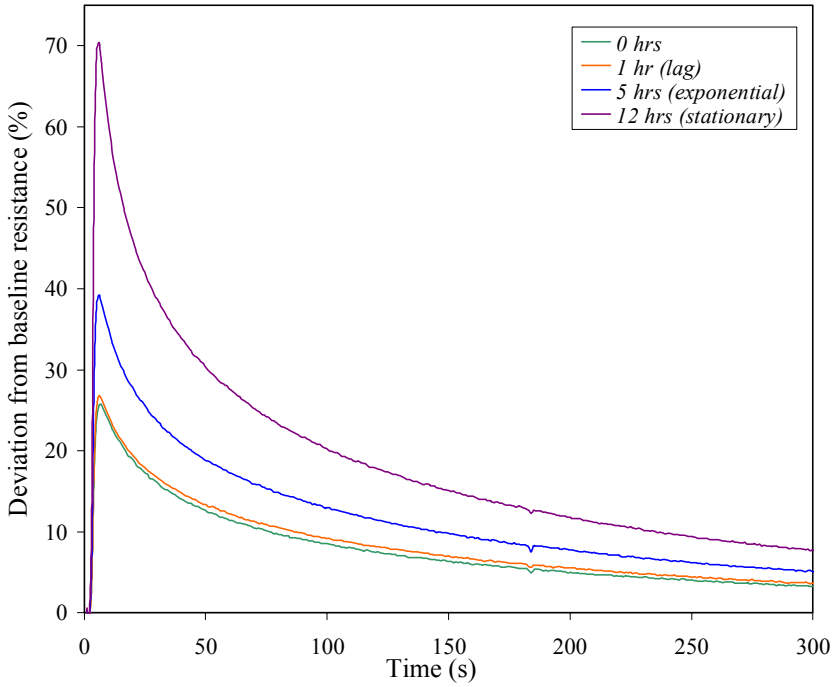

Figure 5.12: *Deviation in baseline resistance with time for odour analyser detection of S.aureus from 0 to 12 hrs growth at 37 °C in TSB.*

5.3.5 Detection of five species of bacteria grown in broth and discrimination using PCA analysis

In this study five of the most commonly isolated wound bacteria were grown and subject to headspace analysis using the odour analyser. The bacteria were grown up in YPD broth, a

more basic broth, in order to more closely represent the nutrients found in wound fluid. Each type of bacteria was analysed in replicates of four randomly. The bacterial broths headspace was analysed after 6 hours (exponential phase) and 24 hours (stationary phase). The data recorded was again analysed by PCA as before. The abbreviations used in the PCA plots that follow are tabulated below. 'Blank' refers to growth media alone which was also tested.

Table 5.3: *Bacteria abbreviations used in PCA plots*

Bacteria name	**Abbreviation used in graphs**
Staphylococcus aureus	SA
Streptococcus pyogenes	SP
Escherichia coli	EC
Klebsiella pneumoniae	KP
Pseudomonus aeruginosa	PA

Depending on the study, different principle components provided better discrimination between samples. The results of the best combinations of principle components for 6 hours growth are illustrated in Figure 5.13 (a) and (b) and in Figure 5.14 (a) and (b) for 24 hours.

PCA analysis provided good discrimination after both 6 hour and 24 hour incubation, although the virtual separation between each bacterial set appeared more distinct after 24 hours, where tighter clustering is evident. At both analysis times there was clear distinction between all cultures and the 'blank' samples. It therefore seems reasonable to conclude that under this set of conditions, the odour analyser is capable of discriminating between these five bacteria commonly isolated from wounds.

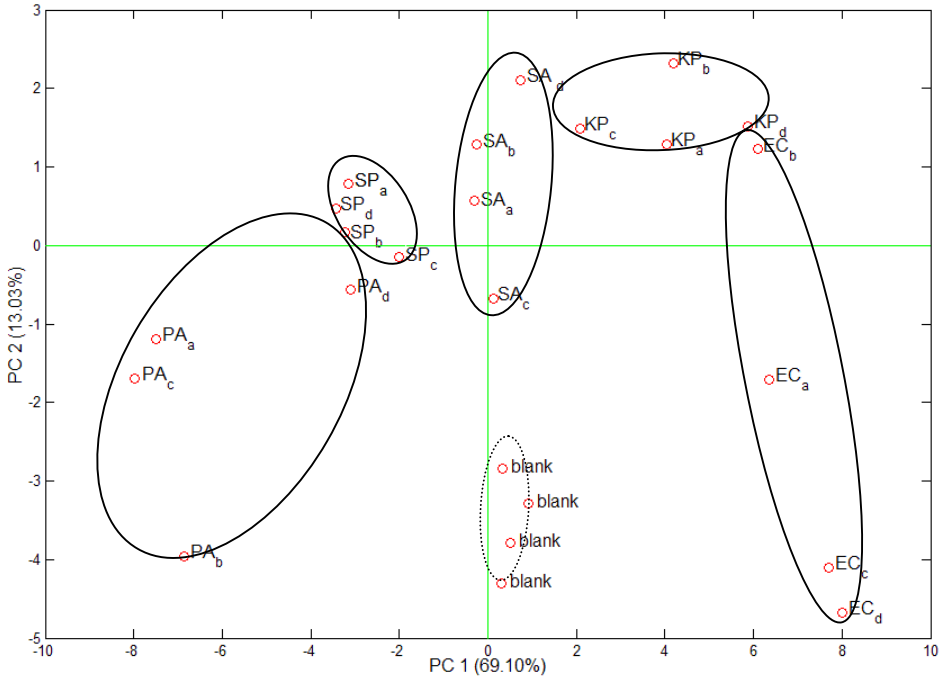

(a)

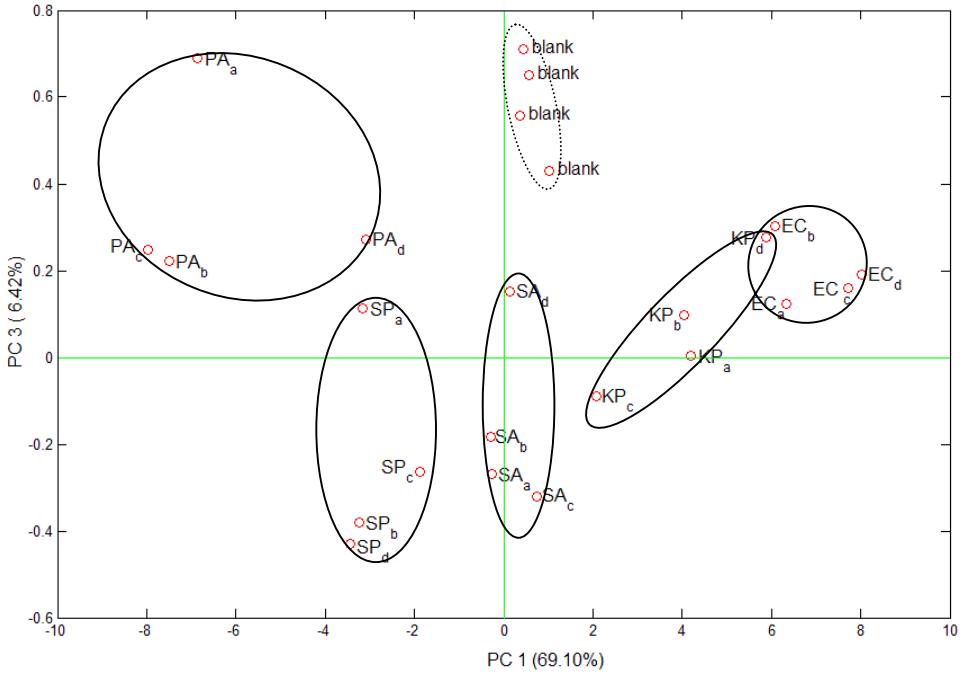

(b)

Figure 5.13: *Discrimination by PCA analysis of odour analyser detection of Pseudomonus aeruginosa, Streptococcus pyogenes, Escherichia coli, Staphylococcus aureus and Klebsiella pneumoniae, after 6 hrs growth in YPD broth (a) PC1vPC2. (b) PC1vPC3.*

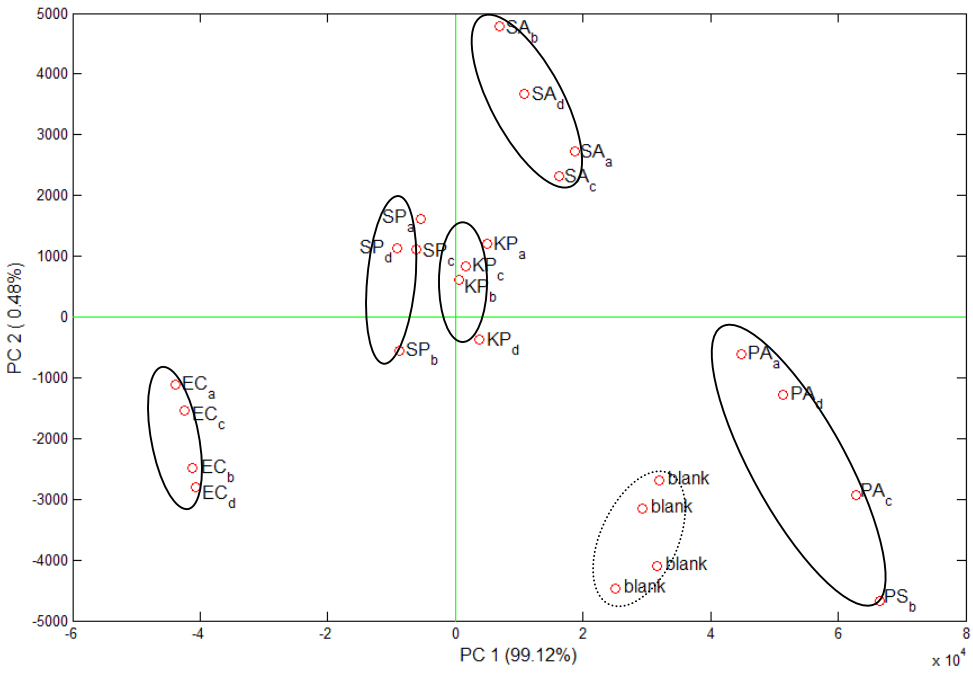

(a)

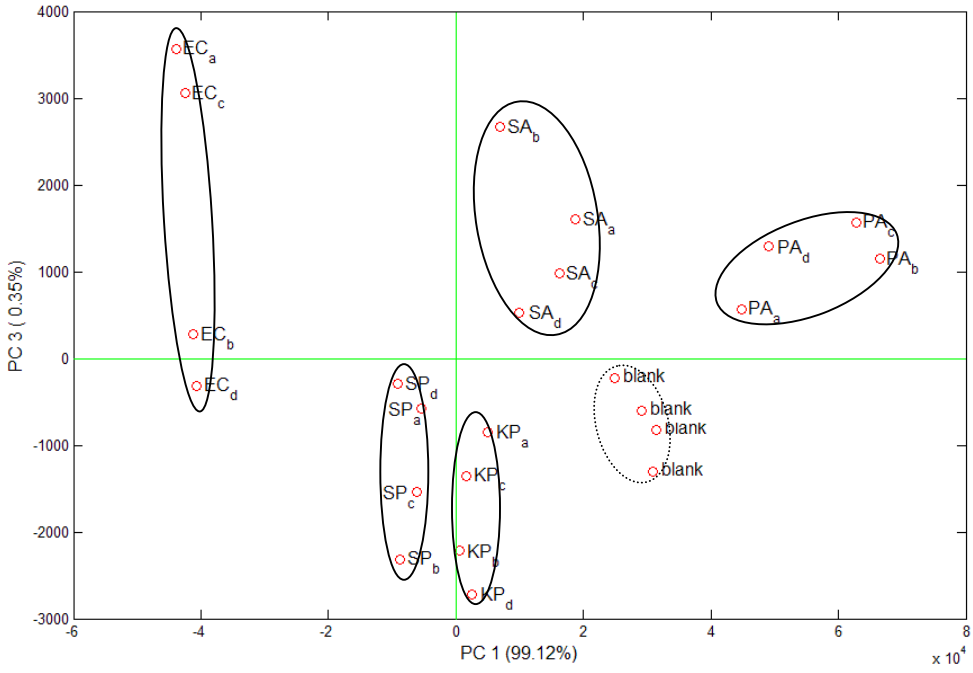

(b)

Figure 5.14: *Discrimination by PCA analysis of odour analyser detection of Pseudomonus aeruginosa, Streptococcus pyogenes, Escherichia coli, Staphylococcus aureus and Klebsiella pneumoniae, after 24 hrs growth in YPD broth (a)PC1vPC2, (b) PC1vPC3.*

5.3.6 Detection of five species of bacteria grown in serum and discrimination using PCA analysis

Following the positive findings of the detection of bacteria in broth, the tests performed in the following study aimed to more accurately represent wound fluid samples, and hence more accurately reflect the 'real-world' situation. As previously stated, serum was used as the model for wound fluid in this thesis. It was found however that only *S.aureu*s would grow in serum alone. It was established that by supplementing the serum with DMEM, which is itself a minimal medium, all five bacteria would grow. After looking at different ratios of serum:DMEM, it was found that 10% v/v DMEM in serum was a sufficient supplement, without considerably altering the wound fluid model. Therefore the bacteria were grown in a 90:10 v/v serum:DMEM mix.

Instead of keeping growth time constant, in this study CFU/ml was kept constant. Therefore, differences detected by the odour analyser combined with PCA analysis were based on differences in headspace content, and hence the volatile metabolic signatures of each bacteria, and not numbers of bacteria (since the bacteria grow at different rates). However, it should be noted that in a 'real' situation, cell densities would vary depending on the levels of growth, which itself may depend on the type of wound, and if more than one bacterial species was present, it is likely that one species would be more prevalent than another. For this study, bacteria were grown in replicates of five, and their headspace sampled at $1.5x10^8$ CFU/ml. Cell densities were determined by checking optical density regularly and referral to the bacterial growth figures shown in Section 2.3.1.

Figure 5.15 demonstrates that virtual separation of the five bacteria and serum is possible using the odour analyser. All bacterial clusters are well discriminated from the serum cluster. *E.coli* has clustered around the centre of the plot, therefore having values closer to 0 for PC1 and PC3. *S.aureus* and *K.pneumoniae* are located relatively closely, and are both tightly clustered.

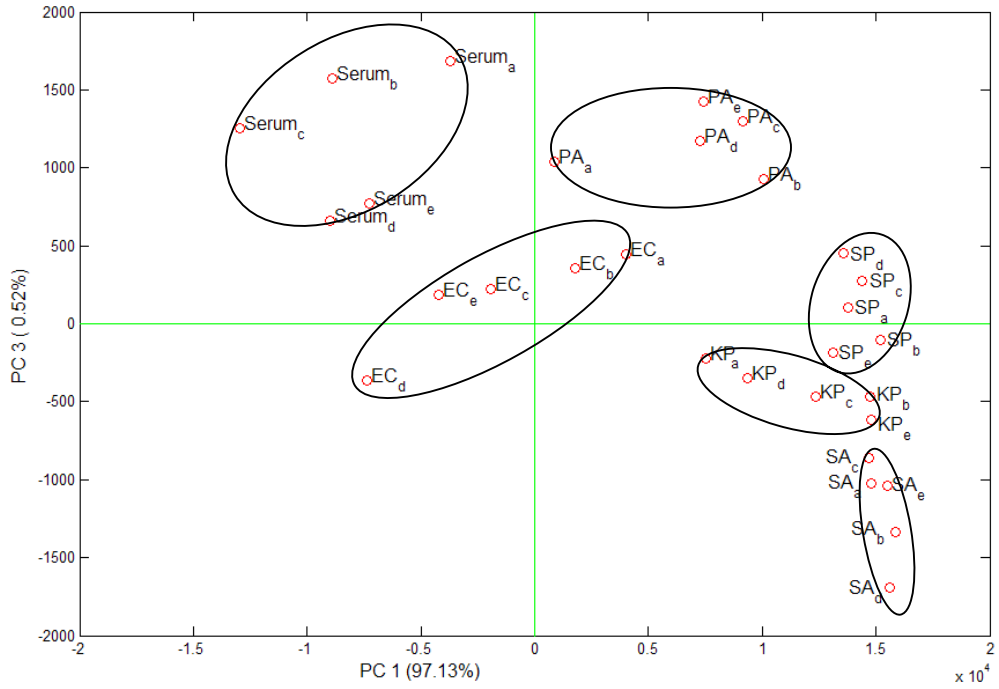

Figure 5.15: *Discrimination by PCA analysis of odour analyser detection of 1.5x10^8 CFU/ml Pseudomonus aeruginosa, Streptococcus pyogenes, Escherichia coli, Staphylococcus aureus and Klebsiella pneumoniae grown in 90:10 v/v serum: DMEM.*

The average maximum deviations in baseline resistance with corresponding standard deviations for each bacterial population grown in the serum culture, and the culture blank are shown in Table 5.4. *S.aureus* produced the greatest change in resistance, followed by *S.pyogenes, K.pneumoniae, P.aeruginosa*, and *E.coli*.

Table 5.4: *Maximum deviations in baseline resistance of odour analysis of $1.5x10^8$ CFU/ml bacteria grown in 90:10 v/v serum:DMEM*

Bacteria	Mean max. deviation (%)	Std dev.
S.aureus	13.123	0.502
S.pyogenes	11.757	0.354
K.pneumoniae	10.853	1.628
P.aeruginosa	8.007	1.147
E.coli	5.539	0.777
Serum (blank)	4.303	0.274

Although a quantitative comparison cannot be made, this order correlates with that detected by headspace GC-MS analysis under the same conditions (Section 2.3.3). During GC-MS analysis, the ethanol peak produced for each bacteria could be quantified using the standard curve produced. However, since only an ethanol peak was detected this was not sufficient to discriminate between bacteria. With the odour analyser, it is not possible to quantify the amount of ethanol in the headspace of the bacterial sample because of the broad specificity of the sensor used (essential for the single sensor olfactory device to function). The sensor responds to many more metabolites in the headspace than ethanol, and with the aid of PCA has demonstrated an ability to discriminate between those bacteria most commonly found to infect wounds.

5.3.7 Examination of paired bacterial cultures grown in serum

Having established that the odour analyser could discriminate between the five selected bacteria at a fixed cell density, the study was further advanced by examining paired samples of bacteria, since there is usually more than one main bacterial culture present in a typical wound fluid. Therefore each possible paired combination of the five bacteria were

grown separately to a cell density of $1.5x10^8$ CFU/ml, combined, and tested according to the methods outlined in the preceding Sections. Again, it should be noted that in a 'real' situation, it is unlikely that different bacteria would be present at the same cell densities, and that this is an artificial population mix. It is evident from Figure 5.16 that some overlapping is evident following PCA analysis. Serum was clearly discriminated from the bacterial preparations, although with a relatively broad clustering.

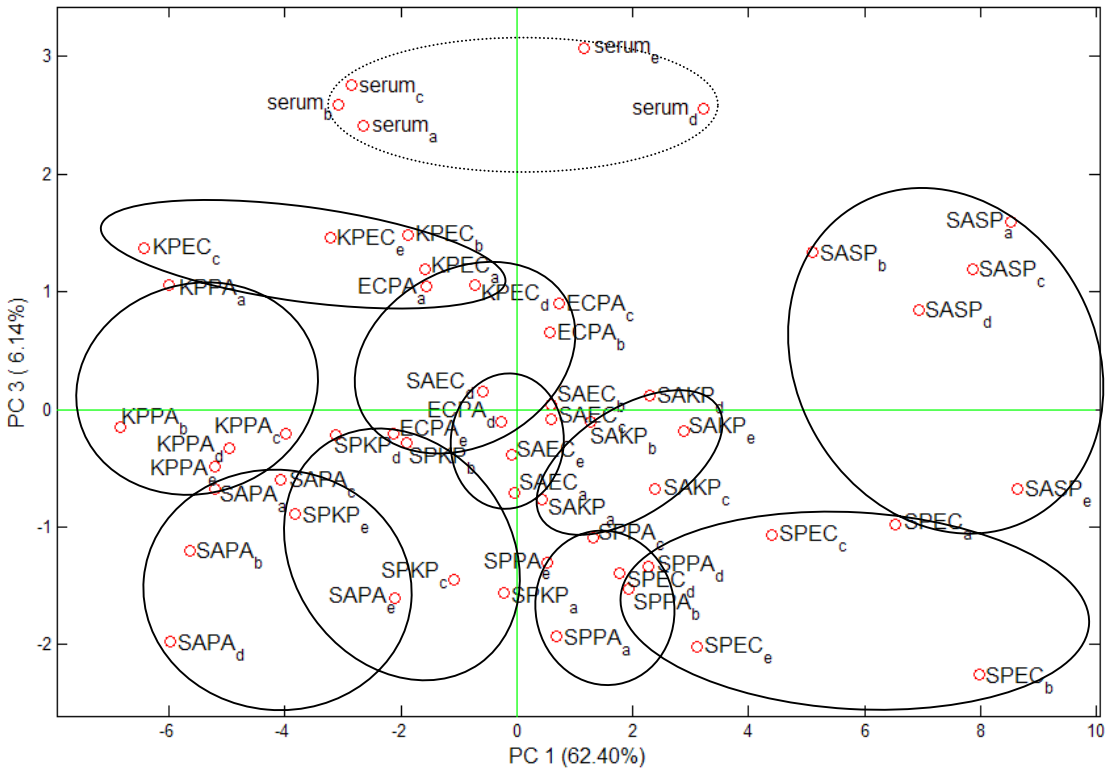

KPEC: *K.pneumoniae* + *E.coli*	ECPA: *E.coli* + *P.aeruginosa*
KPPA: *K.pneumoniae* + *P.aeruginosa*	SAKP: *S.aureus* + *K.pneumoniae*
SAPA: *S.aureus* + *P.aeruginosa*	SPPA: *S.pyogenes* + *P.aeruginosa*
SPKP: *S.pyogenes* + *K.pneumoniae*	SPEC: *S.pyogenes* + *E.coli*
SAEC: *S.aureus* + *E.coli*	SASP: *S.aureus* + *S.pyogenes*

Figure 5.16: *Discrimination by PCA analysis (PC1vPC3) of odour analyser detection of pairs of bacteria at $2x10^8$ CFU/ml grown in 90:10 v/v serum:DMEM at 37 °C*

Where significant overlapping was evident, it was usual for one of the bacterial species to be present in both overlapping pairs, for example in the overlapping of SPPA (*S.pyogenes* and *P.aeruginosa*) and SPEC (*S.pyogenes* and *E.Coli*), where *S.pyogenes* is common to both, and therefore similarities in volatile metabolic signatures may be produced. Clearly, discrimination of the paired bacteria has not been as successful as for individual bacteria, but nevertheless, some bacterial combinations can be clearly differentiated, such as the SASP and SPEC combinations suggesting that the approach can provide some useful diagnostic information. If we compare Figure 5.16 of mixed bacteria and Figure 5.15 of single bacteria (both compare PC1 and PC3), some similarities of cluster location are evident. SA and SP clusters are located in the bottom right corner of the plot in Figures 5.15 and 5.16, and both SA and SP are prevalent in pairs in the bottom right quadrant. Similarly, EC is located centrally in Figure 5.15, and finds itself located centrally in two of its four pair combinations in Figure 5.16.

5.3.8 Detection of different cell concentrations of S.aureus grown in serum

The aim of the final study was to investigate whether the odour analyser was able to detect differences in *S.aureus* cell density when grown in serum (un-supplemented), at a range of bacterial cell densities as present in the wound environment. *S.aureus* was grown up in serum alone under normal growth conditions. Three cell densities: $5x10^6$, $8x10^7$, and $2.25x10^8$ CFU/ml were randomly tested in replicates of five with the odour analyser. Figure 5.17 of PC1v3 illustrates that a distinction between clusters based on cell density is evident.

It appears that the odour analyser is able to detect cell densities at least as low as $5x10^6$ CFU/ml which is the level at which bacterial colonisation becomes problematic in bacterial infection of wounds (Smith & Thomson, 1994). It may be that the odour analyser is able to detect below this level, but lower levels were not tested. This level of bacteria is not visible to the eye when growing bacteria in a broth or serum, and cannot be detected by conventional methods such as spectroscopy where the optical density is measured, or by GC-MS.

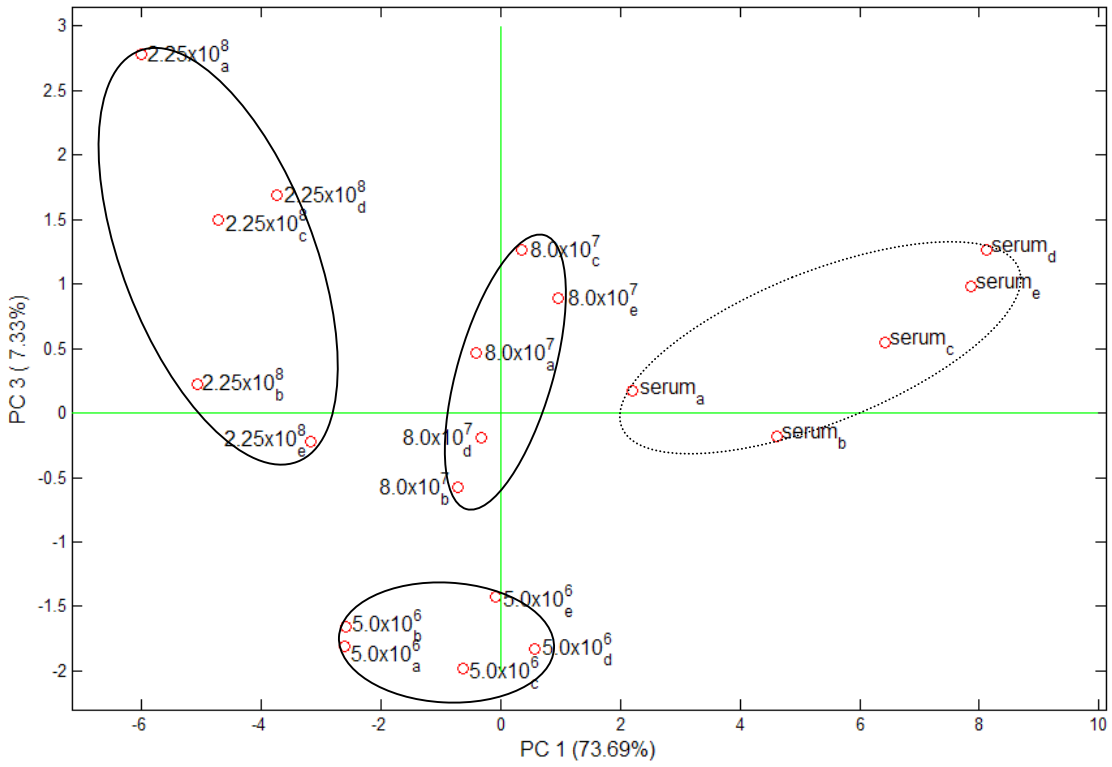

Figure 5.17: *Discrimination by PCA analysis (PC1vPC3) of odour analyser detection of three cell densities of S.aureus grown in serum at 37 °C.*

Some work has been carried out investigating the possibilities of using an electronic nose device in a hospital environment as a diagnostic tool (Gardner, Dutta, Morgan *et al*, 2005),

no public-access literature has been identified in which an odour analysis study has been successful in determining the differences in numbers of *S.aureus* (or other bacteria) with which to compare these results. However, Haugen, Rudi, Langsrud, *et al* (2006) have reported using a gas sensor array to detect milk spoilage bacteria down to 10^4 CFU/ml after 7 hours of growth.

5.4 Overall Chapter conclusions

The single sensor odour analyser combined with the discriminatory powers of PCA analysis was found to be capable of detecting and discriminating between three marker analytes, and five wound bacteria. It was able to detect differences in ethanol concentration in serum. Discrimination between individual bacteria was illustrated, and partial discrimination of paired bacteria was possible. It was also found that *S.aureus* could be detected down to a cell density of $5x10^6$ CFU/ml. Although there is much interest in the areas of combating hospital acquired infections, early detection, and electronic nose technology, literature searches have not revealed any other investigations of the use odour analysis to detect and discriminate these five bacteria, or differences in numbers of bacteria, in a wound environment. The results from these studies are very encouraging. Further research and development into this single sensor based system may potentially lead to a near patient monitoring system whereby a wound could be monitored and provide regular feedback and early warning of infection or other causes of non-healing. The system may also potentially be used for monitoring a variety of other infections and diseases, by detecting the odours from bodily fluids, such as urine or sputum.

6. General Discussion

6.1 Conclusions

Three possible wound monitoring concepts, with the potential to be integrated into wound dressings, or for near patient monitoring applications, have been investigated. The overall conclusions in the context of the initial objectives (Section 1.6) are discussed below:

1) From reviewing the literature, serum was identifed as a suitable model for wound fluid in which to investigate the three concepts. Serum samples were obtained from human volunteer whole blood samples which were spun down and the serum fraction obtained.

2) Three biomarkers indicative of healing/non-healing were identified though literature searches. These were: glucose – reported to increase from the non-healing to healing phase of a wound; H_2O_2 – increased generation in surgical wounds as a result of phagocytosis by mammalian polymorphonuclear leukocytes and monocytes reported; ethanol - since it is produced metabolically by certain pathogenic bacteria commonly isolated from wounds.

3) From literature searches, *S.aureus, K.pneumoniae, E.coli, P.aeruginosa,* and *S.pyogenes*, were determined to be five key bacteria commonly isolated from wound infections (Table 1.4). Laboratory strains were obtained, and growth characteristics determined in each of the different growth media examined.

4) Dual Pulse Staircase Voltammetry (DPSV) was investigated for its feasability as a technique for the monitoring of wounds, by detecting the biomarkers glucose,

ethanol and H_2O_2 in PBS. Scans of the individual analytes demonstrated distinctive peaks exhibiting, non-linear relationships with concentration. Limitations were discovered regarding repeatability and inter-analyte interference in mixtures of the three biomarkers, due to similar peak potentials. This study represents the first detailed study on the performsance of DPSV for determination of metabolites in biological fluids. Although a great deal of useful information was generated using this technique, it was decided not to progress this work further due to the complexity of the voltammograms obtained and issues regarding deconvolution of voltammograms obtained from analyte mixtures.

5) A biosensor array was constructed from three biosensors each consisting of a screen printed three electrode assembly of carbon (w.e), carbon (c.e.) and Ag/AgCl (ref) as the basal layer. The glucose biosensor also incorporated rhodinised carbon within the working electrode to allow reduction in the operating potential required to oxidise the enzymatic hydrogen peroxide by-product to +300 mV (vs Ag/AgCl). The optimal sensor performance was obtained using 1U of glucose oxidase per biosensor. The limit of detection was found to be 169.5 μM glucose (99.7% confidence) in surrogate wound fluid with a single dilution step.

The hydrogen peroxide biosensor utilised 25U/sensor of horseradish peroxidase with 12.5 mg/ml dimethylferrocene mediator, a cellulose acetate diffusion layer, and operated at a potential of -300 mV relative to the reference electrode. The limit

of detection in surrogate wound fluid with a single dilution step was found to be 8.43 μM (99.7% confidence).

The ethanol biosensor was constructed with the same components as the hydrogen peroxide biosensor, except that it also used 1U/biosensor of alcohol oxidase, giving a mediated bi-enzyme system. Following optimisation of the deposition procedure, the limit of detection in surrogate wound fluid with a single dilution step was determined to be 7.94 μM (99.7% confidence). Direct detection of ethanol from metabolically active *S.aureus* in surrogate wound fluid, (with a single dilution step) yielded a limit of detection of 1.23×10^8 CFU/ml at 99.7% confidence, and 19 μM in terms of ethanol specific response.

All three biosensors were successful, and subject to further study, could be suitable for the monitoring of a wound, either alone or within a suite of diagnostic tests. Although the alcohol biosensor could only detect *S.aureus* down to 1.23×10^8 CFU/ml, it could still provide useful diagnostic information. It could signal bacterial numbers falling below this level, possibly indicative of healing, or rising above a 'safe' level (i.e. $>10^6$ CFU/ml), which would only take a matter of hours, and would in all likelihood still signal a non-healing wound to a busy physician more rapidly than would otherwise be observed.

6) Investigation of the single sensor odour analyser as a 'near patient' wound monitoring system found it to be capable of detecting and discriminating between

three biomarkers, glucose, ethanol and H_2O_2, and detecting differences in ethanol concentration in surrogate wound fluid, when combined with principle components analysis. Discrimination between individual bacteria and partial discrimination of paired bacteria was illustrated, in broth and surrogate wound fluid. It was also found that *S.aureus* could be detected down to a cell density of $5x10^6$ CFU/ml in surrogate wound fluid, lower than that found for the biosensor concept.

The odour analyser concept was particularly successful, and has the potential to be used as a 'near patient' monitoring system for patients with wounds, and perhaps other infections or diseases by 'sniffing' samples such as urine, sputum or other excreted or exhaled body fluid.

7) Headspace GC-MS was used to detect volatiles in the headspace of five bacterial preparations grown in surrogate wound fluid. A slightly higher concentration of ethanol was detected in *S.aureus* and *S.pyogenes* than *K.pneumoniae, E.Coli* and *P.aeruginosa*. Levels detected were at a concentration suitable for measurement by other means, such as sensor technology or odour analysis. This data was verified further using Alcohol Draeger tubes to detect alcohol in the headspace of bacteria grown in surrogate wound fluid.

8) Hydrogen peroxide and glucose test kits were used successfully to validate the biosensor data.

6.2 Suggestions for Future Work

Literature searches have revealed much interest in the area of hospital acquired infections, most notably: in the prevention of infection after an operation; reducing further antibiotic resistance of bacteria; exploring alternative treatments; the development of technologies to monitor the progress of wound healing, in particular using electronic nose technology.

The results from the odour analyser work in Chapter 5 are very encouraging. Further research and development into this single sensor based odour analyser system may potentially lead to a 'near patient' monitoring system for bacterial infection of wounds. Suggestions for further work with the single sensor odour analyser follow:

1) Test system with clinical samples of wound fluid.
2) Investigate detection limits for the four other bacteria used in Chapter 5 (i.e. *E.coli, S.pyogenes, K.pneumoniae, P.aeruginosa*) in supplemented surrogate wound fluid (to enable bacterial growth).
3) Investigate ways of improving limit of detection, such as the use of different growth media to increase production of volatile metabolic products.
4) Investigate discrimination and detection limits of other commonly isolated wound bacteria, such as *Enterobacter, Serratia, Enterococcus, Proteus* individually and in combinations.
5) Investigate whether the system can discriminate between different strains of *S.aureus*, such as methicillin resistant *S.aureus*, coagulase negative *S.aureus*, and methicillin susceptible *S.aureus.*

6) Investigate suitable supervised learning pattern recognition techniques, and train and calibrate the system so that it can classify unknown odours as known ones that have been learnt.

7) The system could be investigated for its use in the diagnosis of urinary tract infections, by examining its ability to discriminate the bacteria commonly isolated from UTI infections: *E.coli* and *P.mirabilus.*

8) The system could also be investigated for its potential as a diagnostic tool for diabetes, by 'sniffing' breath odour.

Though DPSV was concluded to be an unsuitable electrochemical technique for monitoring wounds, the following suggestions are made:

1) Integration of a suitable membrane such as Nafion may improve repeatability, and reduce interference effects.

2) Investigation of less complex mixtures.

The biosensor array holds potential either alone, or as part of a suite of tests, to monitor the levels of three biomarkers present in the wound environment. The work in this thesis could be continued as follows:

1) Investigate ways to improve the bacterial limit of detection, e.g. by using other size exclusion techniques not studied in this thesis.

2) Investigate whether other possible biomarkers could be measured using biosensor technology, e.g. C-reactive protein, lactate, albumin.

7. List of References

1) Abdel-Hamid I, Atanasov P, Ivnitski D, Wilkins E (1999), Review. Biosensors for detection of pathogenic bacteria., *Biosensors and Bioelectronics* 14: 599-624

2) Ablaza VJ, Fisher J. (2003) Wound care via telemedicine: the wave of the future. 1-6.

3) Aldringer S, Labows jr JN, Zechman JM (1986), Characterisation of pathogenic bacteria by automated headspace concentration-gas chromatography., *journal of chromatography* 377: 49-57

4) Alegret S, Albareda-Sirvent M, Merkoci A (2000), Configurations used in the design of screen-printed enzymatic biosensors. A review, *Sensors and Actuators B* 69: 153-163

5) Bachinger T, Riese U, Eriksson R, Mandenius CF (2000), Monitoring cellular state transitions in a production-scale CHO-cell process using an electronic nose, *Journal of Biotechnology* 76: 61-71

6) Bamberg R, Sullivan K, Conner-Kerr T (2002), Diagnosis of wound infections:Current culturing practices of US wound care professionals, *Wounds* 14: 314-327

7) Barchiesi F, D'errico MM, Del Prete MS, Giacometti A, Petrelli E, Scalise G, Schimizzi AM (2000), Epidemiology and microbiology of surgical wound infections, *Journal of Clinical Microbiology* 38: 918-922

8) Bard AJ, Faulkner LR (2001), *Electrochemical methods: Fundamentals and applications*, John Wiley and Sons, Inc.,

9) Bartlett JG, Gorbach SL, Mayhew JW, Onderdonk AB, Thadepalli H (1976), Rapid diagnosis of anaerobic infections by direct gas liquid chromatography of clinical specimens, *The Journal of Clinical investigation* 57: 478-484

10) Bennett N, Burslem F, Gibson J, Macauley S, Murphy G, Schultz G, Stacey MC, Trengrove NJ (1999), Analysis of the acute and chronic wound environments: the role of proteases and their inhibitors, *Wound Repair and Regeneration* 7: 442-452

11) Bertotti M, Kosminsky L, Matos RC, Tabacniks MH (2003), Electrochemical codeposition of platinum and molybdenum oxides: Formation of composite films with distinct electrocatalytic activity for hydrogen peroxide, *electroanalysis* 15: 733-738

12) Bessant C. (1998) Virtual separation and simultaneous electrochemical measurement of aliphatic compounds. Ref Type: Thesis/Dissertation

13) Bessant C, Saini S (1999), Simultaneous determination of ethanol, fructose and glucose at an unmodified platinum electrode using artificial neural networks, *Analytical Chemistry* 71: 2806-2813

14) Biomerieux. (2002) API, bacterial identification. www.biomerieux.com

15) Blasco R, Murphy MJ, Sanders MF, Squirrell DJ (1998), Specific assays for bacteria using phage mediated release of adenylate kinase., *Journal of Applied Microbiology* 84: 661-666

16) Blixt Y, Borch E (1999), Using an electronic nose for determining the spoilage of vacuum-packaged beef, *International Journal of Food Microbiology* 46: 123-134

17) Bott AW (1998), Electrochemical methods for the determination of glucose, *Current Separations* 17: 25-31

18) Burton RW, Hohn DC, Hunt TK, Ponce B (1977), Antimicrobial systems of the surgical wound, *The American Journal of Surgery* 133: 597-600

19) Cai Y, Liu J, Shi Y, Liang L, Mou S (2005), Determination of several sugars in serum by high-performance anion-exchange chromatography with pulsed amperometric detection, *Journal of chromatography A* 1085: 98-103

20) Carelli D, Centonze D, De Giglio A, Quinto M, Zambonin PG (2006), An interference-free first generation alcohol biosensor based on a gold electrode modified by an overoxidised non-conducting polypyrrole film, *Analytica Chimica Acta* 565: 27-35

21) Carlsson J (1972), Simplified gas chromatographic procedure for identification of bacterial metabolic products, *Applied Microbiology* 25: 287-289

22) Cartier LJ, Leclerc P, Pouliot M, Nadeau L, Turcotte G, Fruteau-de-Laclos B (1998), Toxic Levels of Acetaminophen Produce a Major Positive Interference on Glucometer Elite and Accu-chek Advantage Glucose Meters, *Clinical chemistry* 44: 893-894

23) Centonze D, Guerrieri A, Malitesta C, Palmisano F, Zambonin PG (1992), Interference-free glucose sensor based on glucose-oxidase immobilized in an overoxidized non-conducting polypyrrole film, *Analytical and Bioanalytical Chemistry* 342: 729-733

24) Cheng J, Jandik P, Avdalovic N (2003), Use of disposable gold working electrodes for cation chromatography-integrated pulsed amperometric detection of sulfur containing amino acids, *Journal of chromatography A* 1:

25) Christenson A, Dock E, Gorton L, Ruzgas T (2004), Direct heterogeneous electron transfer of theophylline oxidase, *Biosensors and Bioelectronics* 20: 176-183

26) Ciosek P, Wroblewski W (2006), The analysis of sensor array data with various pattern recognition techniques, *Sensors and Actuators B: Chemical* 114: 85-93

27) Clement MV, Halliwell B, Long LH (2000), Hydrogen peroxide in the body, *FEBS Letters* 486: 10-13

28) Clough G, Noble M (2003), Microdialysis - A model for studying chronic wounds, *Lower Extremity Wounds* 2: 233-239

29) Cohen IK, McCoy BJ (1983), Wound Healing, in *Biochemistry and Physiology of the Skin*, ed. Goldsmith LA, Oxford University Press,

30) Coloe PJ (1978), Head-space gas liquid chromatography for rapid detection of *Escherichia coli* and *Proteus mirabilis.*, *Journal of Clinical Pathology* 31: 365-369

31) Cullen DC, Jawaheer S, Rughooputh SDDV, White SF (2003), Development of a common biosensor format for an enzyme based biosensor array to monitor fruit quality, *Biosensors and Bioelectronics* 18: 1429-1437

32) Cutting K (1994), Detecting infection, *Nursing Times* 90: 60-62

33) Cuzzell J, Krasner D (1995), Wound dressings, in *Clinical wound Management*, ed. Clarke DL, Drummond AE, and Dyer JJ, Slack Inc., p 131-144

34) D'Amico A, Di Natale C (2001), A contribution on some basic definitions of sensors properties, *IEEE Sensors Journal* 1: 189

35) Deng L, Tan H, Xu Y, Nie L, Yao S (1996) In-situ continuous detection of bacteria on the surface of solid medium with a bulk acoustic wave-impedance sensor. *Enzyme Microbial Technology* 21:258-264

36) Dermnet. Methicillin resistant staphylococcus aureus.
Ref Type: Electronic Citation

37) Dickinson TA, White J, Kauer JS, Walt DR (1998), Current trends in 'artificial-nose' technology, *Tibtech* 16: 250-258

38) Dobberpuhl DA, Johnson DC (1995), Pulsed electrochemical detection at the ring of a ring-disk electode applied to a study of amine adsorption at gold electrodes, *Analytical Chemistry* 67: 1254-1258

39) Dorey E (2005), MRSA: deadly superbug, *Chemistry and Industry* 18 April: 12-13

40) Edwards JG, Hartman NF, Schneider BH (1997), Interferometer: versatile integrated optic sensor for label-free, real-time quantification of nucleic acids, proteins, and pathogens., *Clinical chemistry* 43: 1757-1763

41) Emr SA, Yacynych AM (2005), The use of polymer films in amperometric biosensors, *electroanalysis* 7: 913-923

42) Evans P, Persaud KC, Pisanelli AM (1996), Medical diagnostics and health monitoring., UMIST/Osmetech plc,

43) Feng G, Zhang X-E, Zhang Z-P, Zhang X-M (1998), Simultaneous determination of maltose and glucose using screen-printed electrode system, *Biosensors and Bioelectronics* 13: 333-339

44) Fisher B, Fram P, Thomas S, Waring M (1998), Odour absorbing dressings: A comparative study, *World Wide Wounds*

45) Fonseca LP, Azevedo AM, Prazeres MF, Cabral MS (2004), Ethanol biosensors based on alcohol oxidase, *Biosens Bioelectron* 21: 235-247

46) Freinkel RK (1983), Carbohydrate metabolism of epidermis, in *Biochemicstry and physiology of the skin*, ed. Goldsmith LA, Oxford University Press,

47) Fry DE (2003), Surgical Site Infection: Pathogenesis and Prevention, *www.medscape.com*

48) Fung YS, Mo SY (1995), Application of dual pulse staircase voltammetry for simultaneous determination of glucose and fructose, *electroanalysis* 7: 160-165

49) Fung YS, Mo SY (1996), Determination of ethanol in beer by flow injection dual-pulse staircase voltammetric detection, *The Analyst* 121: 369-372

50) Ganong WF (2003), *Review of Medical Physiology*, Lange Medical Books/McGraw-Hill,

51) Gardner JW. (1987) Pattern Recognition in the Warwick Electonic Nose. 8th International Congress of European Chemoreception Research Organisation. Ref Type: Conference Proceeding

52) Gardner JW, Bartlett PN (1994), A brief history of electronic noses, *Sensors and Actuators B* 18-19: 220

53) Gardner JW, Craven MA, Bartlett PN (1996), Electronic noses - development and future prospects, *Trends in Analytical Chemistry* 15: 486-493

54) Gardner JW, Bartlett PN (1999), *Electronic Noses - Principles and Applications*, Oxford University Press,

55) Gardner JW, Shin HW, Hines EL (2000), An electronic nose system to diagnose illness, *Sensors and Actuators B* 70: 19-24

56) Gardner JW, Dutta R, Morgan D, Baker N, Hines EL (2005), Identification of Staphylococcus aureus infections in hospital environment: electronic nose based approach, *Sensors and Actuators B* 109: 355-362

57) Garg S, Jovanovic L, Potts RO, Tamada JA, Tierney MJ (2000), Clinical evaluation of the GlucoWatch® biographer: a continual, non-invasive glucose monitor for patients with diabetes., *Biosensors and Bioelectronics* 16: 621-629

58) Garjonyte R, Malinauskas A (2000), Glucose biosensor based on glucose oxidase immobilized in electropolymerized polypyrrole and poly(o-phenylenediamine) films on a Prussian Blue-modified electrode, *Sensors and Actuators B: Chemical* 63: 122-128

59) Garrigues S, Talou T, Nesa D (2004), Comparative study between gas sensors arrays device, sensory evaluation and GC/MS analysis for QC in automotive industry, *Sensors and Actuators B: Chemical* 103: 55-68

60) Gibson TD, Prosser O, Hulbert JN (2000) Not to be sniffed at. *Microbiology Today* 27: 14-16

61) Gibson TD, Prosser O, Hulbert JN, Pavlou AK (2000) Electronic Noses: an inspired idea? *Chemistry and Industry* April 2000 (issue 8):287-289

62) Gibson TD, Prosser O, Hulbert JN, Marshall RW, Corcoran P, Lowery P, Ruck-Keene EA, Heron S (1997), Detection and simultaneous identification of microorganisms from headspace samples using an electronic nose, *Sensors and Actuators B* 44: 413-422

63) Gogia PP (1995), Physiology of wound healing, in *Clinical wound management*, ed. Drummond AE, Clarke DL, and Dyer JJ, Slack Inc., Thorofare, NJ, USA

64) Gorton L, Heller A, Vijayakumar AR, Csoregi E (1996), Alcohol biosensors based on coupled oxidase-peroxidase systems, *Analytica Chimica Acta* 327: 223-234

65) Gorton L, Mattos IL, Ruzgas T (2003), Sensor and biosensor based on prussian blue modified gold and platinum screen printed electrodes, *Biosensors and Bioelectronics* 18: 193-200

66) Gorton L, Karyakin A, Palleschi G, Ricci F, Ruzgas T, Yigsaw Y (2003), Investigation of the effect of different glassy carbon materials on the performance of prussian blue based sensors for hydrogen peroxide., *electroanalysis* 15: 175-182

67) Guyton AC, Hall JE (2000), *Textbook of Medical Physiology*, W.B.Saunders Company: A Harcourt Sciences Company, Philadelphia

68) Hamdi N, Wang J, Monbouquette HG (2005), Polymer films as permselective coatings for H2O2-sensing electrodes, *Journal of Electroanalytical Chemistry* 581: 258-264

69) Hampson JP (1996), The use of metronidazole in the treatment of malodorous wounds, *Journal of wound Care* 5: 421-425

70) Hansen T, Petersen MA, Byrne DV (2005), Sensory based quality control utilising an electronic nose and GC-MS analyses to predict end-product quality from raw materials, *Meat Science* 69: 621-634

71) Hart AL, Turner APF (1996), On the use of screen- and ink-jet printing to produce amperometric enzyme electrodes for lactate., *Biosensors and Bioelectronics* 11: 263-270

72) Haugen JE, Rudi K, Langsrud S, Bredholt S (2006), Application of gas-sensor array technology for detection and monitoring of growth of spoilage bacteria in milk: A model study, *Analytica Chimica Acta* 565: 10-16

73) Hayes DF, Rizvi N. (1999) A "breathalyser" for lung cancer ? The Lancet 353[5 June], 1897-1898.

74) Hayward NJ, Jeavons TH, Nicolson AJC, Thornton AG (1977), Development of specific tests for rapid detection of *Eschericia coli* and all species of *Proteus* in urine., *Journal of Clinical Microbiology* 6: 195-201

75) Hayward NJ (1983), Headspace gas-liquid chromatography for the rapid laboratory diagnosis of urinary tract infections caused by enterobacteria, *journal of chromatography* 274: 27-35

76) Heineman WR, Kissinger PT (1984), *Laboratory techniques in electroanalytical chemistry*, Marcel Dekker, New York

77) Holbrook KA (1983), Structure and function of the developing human skin, in *Biochemistry and physiology of the skin*, ed. Goldsmith LA, Oxford University Press,

78) Hughes S, Lawrence Meschi P, Johnson DC (1981), Amperometric detection of simple alcohols in aqueous solutions by application of a triple-pulse potential waveform at platinum electrodes, *Analytica Chimica Acta* 132: 1-10

79) Huycke MM, Sahm DF, Gilmore MS (1998), Multiple-drug resistant enterococci: the nature of the problem and an agenda for the future, *Emerging infectious diseases* 4: 239-249

80) Ikegami A, Kaneyasu M. (1985) Olfactory detection using integrated sensors. Proc.3rd Int.Conf.Solid-State Sensors and Actuators , 136-139.
Ref Type: Conference Proceeding

81) Im MJC, Hoopes JE (1970), Energy metabolism in healing skin wounds, *Journal of Surgical Research* 10: 459-464

82) James TJ, Hughes MA, Cherry GW, Taylor RP (2000), Simple biochemical markers to assess chronic wounds, *Wound Repair and Regeneration* 8: 264-269

83) Johansson K, Jonsson-Pettersson G, Gorton L, Marko-Varga G, Csoregi E (1993), A reagentless amperometric biosensor for alcohol detection in column liquid chromatography based on co-immobilized peroxidase and alcohol oxidase in carbon paste, *Journal of Biotechnology* 31: 301-316

84) Johnson DC, LaCourse WR (1990), Liquid chromatography with pulsed amperometric detection at gold and platinum electrodes, *Analytical Chemistry* 62:

85) Johnson DC, LaCourse WR (1991), Optimisation of waveforms for pulsed amperometric detection (p.a.d.) of carbohydrates following separation by liquid chromatography, *Carbohydrate Research* 215: 159-178

86) Johnson DC, Dobberpuhl D, Roberts R, Vandeberg P (1993), Review: Pulsed amperometric detection of carbohydrates, amines and sulfur species in ion exchange chromatography-the current state of research, *journal of chromatography* 640: 79-96

87) Johnson DC, Dobberpuhl D, Roberts R, Vandeberg P (1993), Review: Pulsed amperometric detection of carbohydrates, amines and sulfur species in ion exchange chromatography-the current state of research, *journal of chromatography* 640: 79-96

88) Jones PW, Taylor DM, Williams DR (2000), Analysis and chemical speciation of copper and zinc in wound fluid, *Journal of Inorganic Biochemistry* 81: 1-10

89) Kolb B, Ettre LS (1997), *Static headspace gas chromatography: theory and practice*, Wiley-VCH, Inc., New York

90) Krasner D, Kane D (1997), *Chronic wound care: a clinical source book for healthcare professionals*, Health management publications, inc., Wayne, PA

91) Kroger S, Turner APF (1997), Solvent-resistant carbon electrodes screen printed onto plastic for use in biosensors, *Analytica Chimica Acta* 347: 9-18

92) Kroger S, Setford SJ, Turner APF (1998), Assessment of glucose oxidase behaviour in alcoholic solutions using disposable electrodes, *Analytica Chimica Acta* 368: 219-231

93) Kulys J, Schmid RD (1991), Bienzyme sensors based on chemically modified electrodes, *Biosensors and Bioelectronics* 6: 43-48

94) LaCourse WR, Johnson DC, Rey MA, Slingsby RW (1991), Pulsed amperometric detection of aliphatic alcohols in liquid chromatography, *Analytical Chemistry* 63: 134-139

95) LaCourse WR, Johnson DC (1993), Optimisation of waveforms for pulsed detection of carbohydrates based on pulsed voltammetry, *Analytical Chemistry* 65: 50-55

96) LaCourse WR, Dasenbrock CO (1999), Pulsed electrochemical detection of sulfur-containing antibiotics following high performance liquid chromatography, *J Pharm Biomed Anal* 19: 239-52

97) Lamagna A, Reich S, Rodriguez D, Scoccola NN (2004), Performance of an e-nose in hops classification, *Sensors and Actuators B: Chemical* 102: 278-283

98) Larsson L, Mardh P-A, Odham G (1981), Head-space gas chromatography as a tool in the identification of anaerobic bacteria and diagnosis of anaerobic infections, *Scandinavian Journal of Infectious Diseases Suppl.* 26: 14-18

99) Lee-Davey J. (2004) Application of machine olfaction principles for the detection of high voltage transformer oil degradation. Ref Type: Thesis/Dissertation

100) Lee J-W, Yeo I-H (2001), Integrated pulsed amperometry for the analysis of organic compounds, *Microchemical Journal* 70: 173-177

101) Lee W-Y, Kim T-H, Lee K-S, Park J-K, Shin M-C, Yee H-J (1999), Determination of breath alcohol using differential-type amperometric biosensor based on alcohol dehydrogenase, *Analytica Chimica Acta* 390: 91

102) Magan N, Pavlou AK, McNulty C, Jones JM, Sharp D, Brown J, Turner APF (2002), Use of an electronic nose system for diagnosis of urinary tract infections, *Biosensors and Bioelectronics* 17: 893-899

103) Marilley L, Casey MG (2004), Flavours of cheese products: metabolic pathways, analytical tools and identification of producing strains, *International Journal of Food Microbiology* 90: 139-159

104) Marti MP, Busto O, Guasch J, Boque R (2005), Electronic noses in the quality control of alcoholic beverages, *TrAC Trends in Analytical Chemistry* 24: 57-66

105) Massart DL, Wu W, Guo Q, Boucon C, de Jong S (2002), Feature selection in principle component analysis of analytical data, *Chemometrics and Intelligent Laboratory Systems* 61: 123-132

106) McGrath MJ, Iwuoha EI, Diamond D, Smyth MR (1995), The use of differential measurements with a glucose biosensor for interference compensation during glucose determinations by flow injection analysis, *Biosensors and Bioelectronics* 10: 937-943

107) Monk PS (2001), *Fundamentals of electroanalytical chemistry*, Wiley,

108) Moody A, Saini S, Setford S (2001), Peroxidase enzyme sensor for on-line monitoring of disinfection processes in the food industry., *The Analyst* 126: 1733-1739

109) Murray BE (1998), Diversity amoung multi-drug resistant enterococci, *Emerging infectious diseases* 4: 1-13

110) Nake A, Dubreuil B, Raynaud C, Talou T (2005), Outdoor in situ monitoring of volatile emissions from wastewater treatment plants with two portable technologies of electronic noses, *Sensors and Actuators B: Chemical* 106: 36-39

111) Nanney LB, Wenczak B (1993), Correlation of transforming growth factor-alpha and epidermal growth factor receptor with proliferating cell nuclear antigen in human burn wounds, *Wound Repair and Regeneration* 1: 219-230

112) Neuburger GG, Johnson DC (1987), Comparison of the pulsed amperometric detection of carbohydrates at gold and platinum electrodes for flow injection and liquid chromatographic systems, *Anal Chem* 59: 203-4

113) Neuburger GG, Johnson DC (1987), Pulsed coulometric detection of carbohydrates at a constant detection potential at gold electrodes in alkaline media, *Analytica Chimica Acta* 192: 205-213

114) Newman JD, White SF, Tothill IE, Turner APF (1995), Catalytic materials, membranes and fabrication technologies suitable for the construction of amperometric biosensors, *Anal Chem* 67: 4594-4599

115) Newman JD, Turner APF (2005), Home blood glucose biosensors: a commercial perspective, *Biosens Bioelectron* 20: 2435-2453

116) O'Halloran MP, Pravda M, Guilbault GG (2001), Prussian Blue bulk modified screen-printed electrodes for H2O2 detection and for biosensors, *Talanta* 55: 605-611

117) Odland GF (1983), Structure of the skin, in *Biochemistry and physiology of the skin*, ed. Goldsmith LA, Oxford University Press,

118) Olafsdottir G, Nesvadba P, Di Natale C, Careche M, Oehlenschlager J, Tryggvadottir SV, Schubring R, Kroeger M, Heia K, Esaiassen M (2004), Multisensor for fish quality determination, *Trends in Food Science & Technology* 15: 86-93

119) Onkal-Engin G, Demir I, Engin SN (2005), Determination of the relationship between sewage odour and BOD by neural networks, *Environmental Modelling & Software* 20: 843-850

120) Owens GS, LaCourse WR (1997), Pulsed electrochemical detection of thiols and disulfides following capillary electrophoresis, *J Chromatogr B Biomed Sci Appl* 695: 15-25

121) Palmisano F, Centonze D, Guerrieri A, Zambonin PG (1993), An interference-free biosensor based on glucose oxidase electrochemically immobilized in a non-conducting poly(pyrrole) film for continuous subcutaneous monitoring of glucose through microdialysis sampling, *Biosensors and Bioelectronics* 8: 393-399

122) Panchagnula R, Pillai O, Nair VB, Ramarao P (2000), Transdermal iontophoresis revisited, *Current Opinion in Chemical Biology* 4: 468-473

123) Parks WC (1999), Matrix metalloproteinases in repair, *Wound Repair and Regeneration* 7: 423-432

124) Patel NG, Meier S, Cammann K, Chemnitius G-C (2001), Screen-printed biosensors using different alcohol oxidases, *Sensors and Actuators B: Chemical* 75: 101-110

125) Patlak J. (1999) Fluid compartments in the body. 1999. http://physioweb.med.uvm.edu/bodyfluids/ionic.htm

126) Paulsson N, Larsson E, Winquist F (2000), Extraction and selection of parameters for evaluation of breath alcohol measurement with an electronic nose, *Sensors and Actuators* 84: 187-197

127) Pearson H. (2002) Bacteria defy last-resort antibiotic. http://www.nature.com/nsu/020722/020722-11.html

128) Penza M, Cassano G, Tortorella F, Zaccaria G (2001), Classification of food, beverages and perfumes by WO3 thin-film sensors array and pattern recognition techniques, *Sensors and Actuators B: Chemical* 73: 76-87

129) Persaud K, Dodd GH (1982), Analysis of discrimination mechanisms of the mammalian olfactory system using a model nose, *Nature* 299: 352-355

130) Plotkin MJ, Shnayerson M. (2002) The Killer Bug. Fortune [30 Sept], 47-51.

131) Plowman R, Graves N, Griffin M (2000). The socio-economic burden of hospital acquired infection. London: Public Health Laboratory Service.

132) Prusak-Sochaczewski E, Luong JHT, Guilbault GG (1990). Development of a piezoelectric immunosensor for the detection of Salmonella typhimurium. *Enzyme Microbiol. Technol.* 12:173-177

133) Ragazzo-Sanchez JA, Chalier P, Chevalier D, Ghommidh C (2006), Electronic nose discrimination of aroma compounds in alcoholised solutions, *Sensors and Actuators B: Chemical* 114: 665-673

134) Ricci F, Palleschi G (2005), Sensor and biosensor preparation, optimisation and applications of Prussian Blue modified electrodes, *Biosensors and Bioelectronics* 21: 389-407

135) Saxena V, Malhotra BD (2003) Electrochemical Biosensors In: *Advances in Biosensors* 5:63-100. Elsevier Science

136) Schaller E, Bosset JO, Escher F (1998), ‘Electronic Noses’ and Their Application to Food, *Lebensmittel-Wissenschaft und-Technologie* 31: 305-316

137) Skoog D, West D, Holler F, Crouch S (2000), *Analytical Chemistry: An introduction*, Saunders College Publishing, Orlando

138) Slack R, Greenwood D (1992), *Medical Microbiology*, Churchill-Livingston,

139) Smith DJ, Thomson PD (1994), What is infection?, *The American Journal of Surgery* 167: 7S-11S

140) Sprules SD, Hartley IC, Wedge R, Hart JP, Pittson R (1996), A disposable reagentless screen-printed amperometric biosensor for the measurement of alcohol in beverages, *Analytical Chimica Acta* 329: 215-221

141) Surgical-tutor.org. Wound infection. 2002.

142) Tarnowski D, Korneniewski C (1996), Amperometric detection with membrane-based sampling for percent level determinations of ethanol, *Analytica Chimica Acta* 332: 111-121

143) Tarnowski DJ, Korzeniewski C (1996), Amperometric detection with membrane-based sampling for percent-level determinations of ethanol, *Analytica Chimica Acta* 332: 111-121

144) Tian Y, Mao L, Okajima T, Ohsaka T (2005), A carbon fiber microelectrode-based third-generation biosensor for superoxide anion, *Biosensors and Bioelectronics* 21: 557-564

145) Trengrove NJ, Langton SR, Stacey MC (1996), Biochemical analysis of wound fluid from non-healing and healing chronic leg ulcers, *Wound Repair and Regeneration* 4: 234-239

146) Turner APF, White SF, Schmid RD, Bilitewski U, Bradley J (1994), Investigations of platinized and rhodinised carbon electrodes for use in glucose sensors, *electroanalysis* 6: 625-632

147) Turner APF. (2005) Biosensors and Bioelectronics homepage. http://www.elsevier.com/wps/find/journaldescription.cws_home/405913/description#description.

148) Varma S, Shantilatha P, Mitra CK (2003), *Advances in biosensors: perspectives in biosensors*, JAI Press Inc, Conneticut p 1-36

149) Vonck J, van Bruggen EJ (1990), Electron microscopy and image analysis of two-dimensional crystals and single molecules of alcohol oxidase from *Hansenula polymorpha*, *Biochimica et Biophysica Acta (BBA) - Protein Structure and Molecular Enzymology* 1038: 74-79

150) Wang J, Wu H (1995), Highly selective biosensing of glucose utilizing a glucose oxidase + rhodium + Nafion(R) biocatalytic-electrocatalytic-permselective surface microstructure, *Journal of Electroanalytical Chemistry* 395: 287-291

151) Wang L, Wang E (2004), A novel hydrogen peroxide sensor based on horseradish peroxidase immobilised on colloidal Au modified ITO electrode, *Electrochemistry Communications* 6: 225-229

152) Ward WK, Jansen LB, Anderson E, Reach G, Klein JC, Wilson GS (2002), A new amperometric glucose microsensor: in vitro and short-term in vivo evaluation, *Biosensors and Bioelectronics* 17: 181-189

153) White SF, Turner APF, Bilitewski U, Schmid RD, Bradley J (1994), Lactate, glutamate and glutamine biosensors based on rhodinised carbon electrodes, *Analytica Chimica Acta* 295: 243-251

154) Wilkins WF, Hatman AD (1964), An electronic analog for the olfactory processes, *Ann.NY Acad.Science* 116: 608

155) Wold S, Esbensen K, Geladi P (1987), Principle components analysis, *Chemometrics and Intelligent Laboratory Systems* 2: 52

156) Xu S, Han X (2004), A novel method to construct a third-generation biosensor: self-assembling gold nanoparticles on thiol-functionalized poly(styrene-co-acrylic acid) nanospheres, *Biosensors and Bioelectronics* 19: 1117-1120

157) Yang YM, Yang PY, Wang XR (2000), Electronic nose based on SAWS array and its odor identification capability, *Sensors and Actuators B: Chemical* 66: 167-170